



Specification Compliance and Calibration

Data Book

Volume II

for

Solar Backscatter Ultraviolet

Spectral Radiometer Mod 2

(SBUV/2 Emu-Flight)

Document No. B6802-78

January 11, 1984

Prepared for

NATIONAL AERONAUTICS AND SPACE ADMINISTRATION

Goddard Space Flight Center

Greenbelt, Maryland 20771

in accordance with

Contract NAS 5-24600, Item 40C

BASD Approvals:

Prepared by:

George Morris

George Morris

SBUV/2 Test Engineer

William K. Fowler

William K. Fowler

UV Radiometry and Physicist

Del Nelson

Del Nelson

SBUV/2 Project Manager

R.T. McConaughey

R.T. McConaughey

SBUV/2 System Engineer



FOREWORD

This document is Volume II of a two volume data book. This volume contains the calibration data applicable to the Engineering-Flight Unit Serial Number 001 of the Solar Backscatter Ultraviolet Spectral Radiometer Mod 2 (SBUV/2). Reference to the Table of Contents will indicate the organization and contents of this volume.

This document was prepared per item 40C of Contract NAS 5-26400 between the Goddard Space Flight Center (GSFC), Greenbelt, Maryland, and the Ball Aerospace Systems Division (BASD), Boulder, Colorado.



LIST OF ILLUSTRATIONS (Continued)

<u>Figure</u>	<u>Title</u>	<u>Page</u>
4-37 thru 41	Sweep Mode	—
4-37	Irradiance Response Day 240, FEL #127, BaSO ₄ Diffuser.....	4-73
4-38	Radiance Response Day 240, FEL #127, BaSO ₄ Diffuser.....	4-74
4-39	Irradiance Response Sweeps sec 26 and sec 36.....	4-75
4-40	Irradiance Response sec 36 * 0.93 and sec 26 * 1.05.....	4-76
4-41	Radiance/Irradiance Calibration Constants.....	4-77
4-42 thru 50	Sweep Mode Calibration Constants Versus Wavelength Plots	4-78

9

10

11

12

13

14

15

16

17

18

19

20

21

Chapter 1

The first part of the book is devoted to the study of the properties of the function $f(x)$ defined by the equation $f(x) = x^2 + 1$. In this chapter, we shall prove that $f(x)$ is a strictly increasing function on the interval $(0, \infty)$. To this end, we shall use the definition of a strictly increasing function. Let x_1 and x_2 be any two numbers in the interval $(0, \infty)$ such that $x_1 < x_2$. Then, we have $x_2 - x_1 > 0$. Now, we shall show that $f(x_2) - f(x_1) > 0$. We have $f(x_2) - f(x_1) = (x_2^2 + 1) - (x_1^2 + 1) = x_2^2 - x_1^2 = (x_2 - x_1)(x_2 + x_1)$. Since $x_2 - x_1 > 0$ and $x_2 + x_1 > 0$, it follows that $f(x_2) - f(x_1) > 0$. Hence, $f(x)$ is a strictly increasing function on the interval $(0, \infty)$.

It is easy to see that $f(x)$ is also a strictly increasing function on the interval $(-\infty, 0)$.

Therefore, $f(x)$ is a strictly increasing function on the interval $(-\infty, \infty)$.

It is also easy to see that $f(x)$ is a strictly increasing function on the interval $(-\infty, \infty)$.

It is also easy to see that $f(x)$ is a strictly increasing function on the interval $(-\infty, \infty)$.

It is also easy to see that $f(x)$ is a strictly increasing function on the interval $(-\infty, \infty)$.

It is also easy to see that $f(x)$ is a strictly increasing function on the interval $(-\infty, \infty)$.

It is also easy to see that $f(x)$ is a strictly increasing function on the interval $(-\infty, \infty)$.



Section 1

WAVELENGTH CALIBRATION

1.1 METHOD

Spectral emission lines are generated using hollow cathode discharge tubes and the internal low pressure mercury arc. Wavelengths are identified from the MIT wavelength tables and are corrected for local atmospheric pressure and temperature. The instrument is operated in both the sweep mode and the position mode while looking at the sources, and detector response and grating position data are recorded. The centroid of the instrument profile of each narrow spectral line is taken as the grating position corresponding to the line wavelength. A sine curve of the form shown below is fitted to the data points.

$$\lambda = A_0 \sin A_1 (C + A_2),$$

where

λ = line wavelength (nm),

C = grating angle encoder readout at profile centroid

The following 12 spectral lines from the noted sources, corrected for Boulder's altitude, were used for the wavelength calibration:

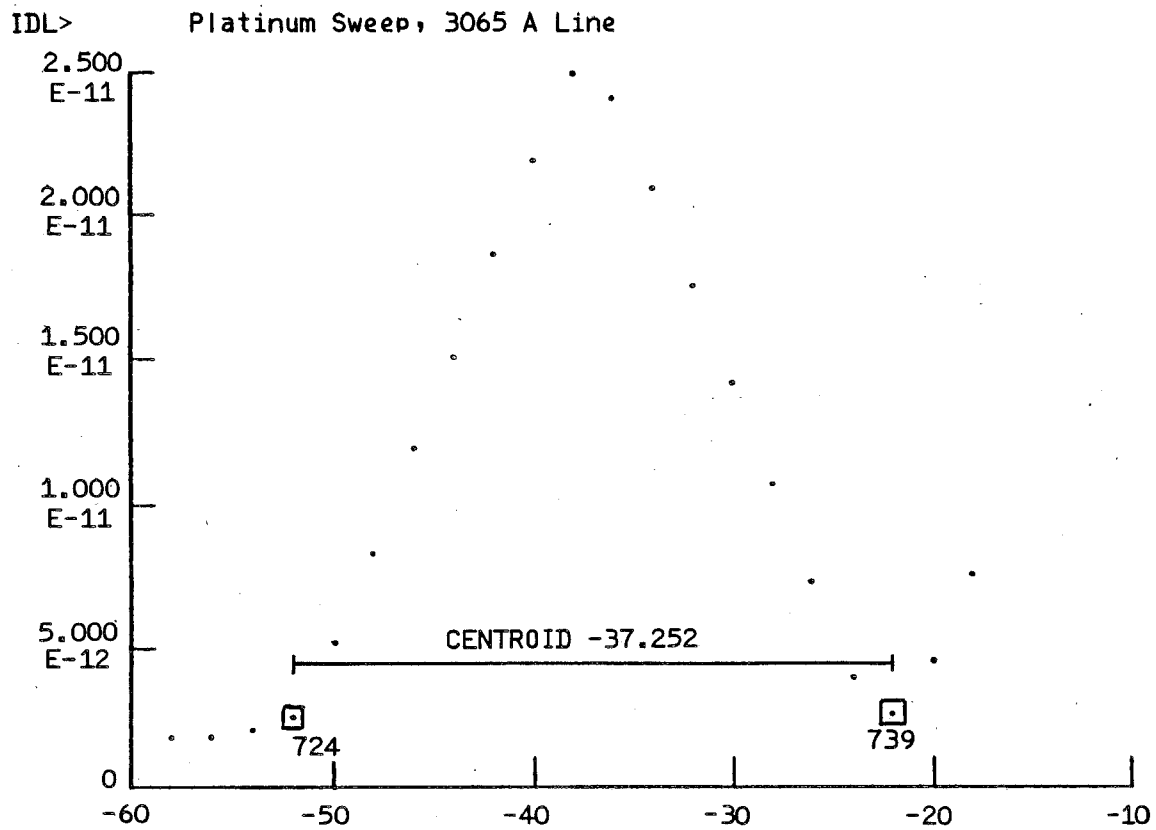
184.90 nm - Hg	283.04 nm - Pt	307.61 nm - Zn
202.56 nm - Zn	285.23 nm - Mg	324.77 nm - Cu
213.87 nm - Zn	299.81 nm - Pt	327.51 nm - Cu
253.67 nm - Hg	306.49 nm - Pt	404.68 nm - Hg

In position mode wavelength calibration, zero order location was used as the 13th point.

The resulting coefficients for the wavelength calibration are:



B6802-78

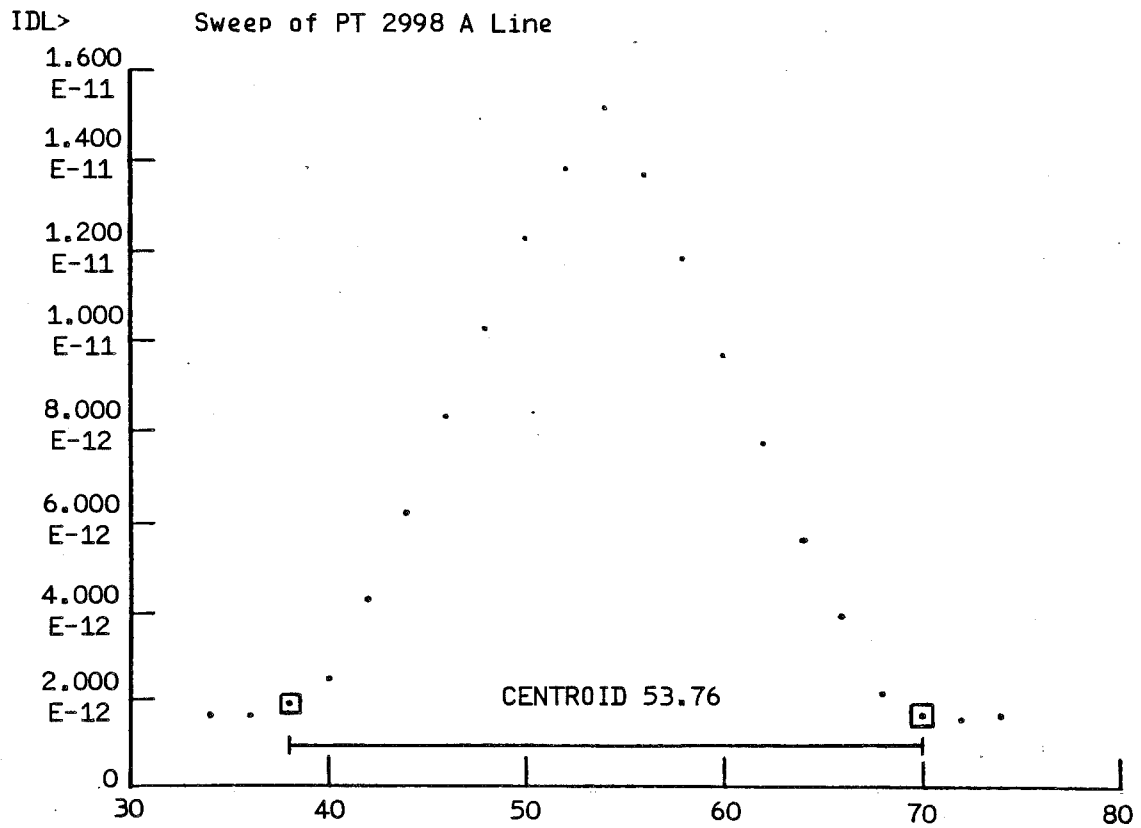


A/N 3990

Figure 1-2a



B6802-78



A/N 3990

Figure 1-2b

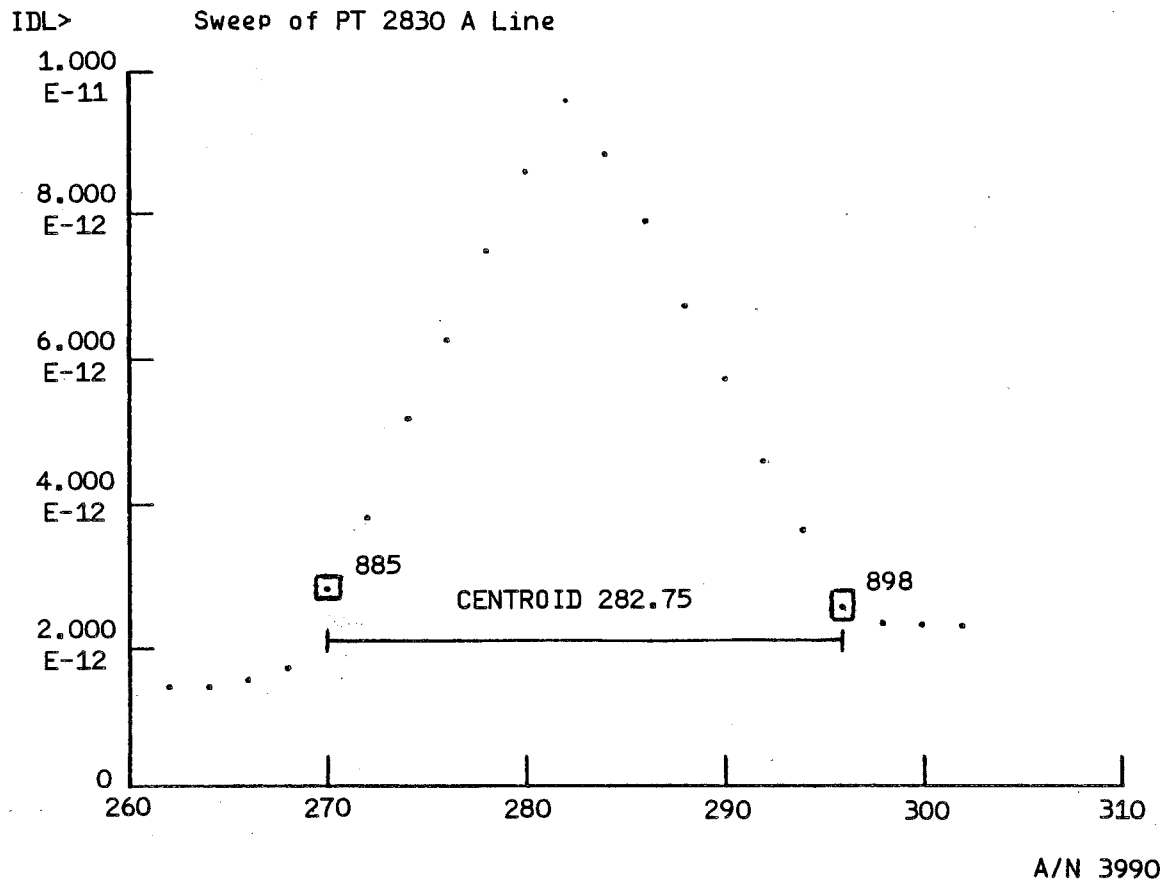


Figure 1-2c



B6802-78

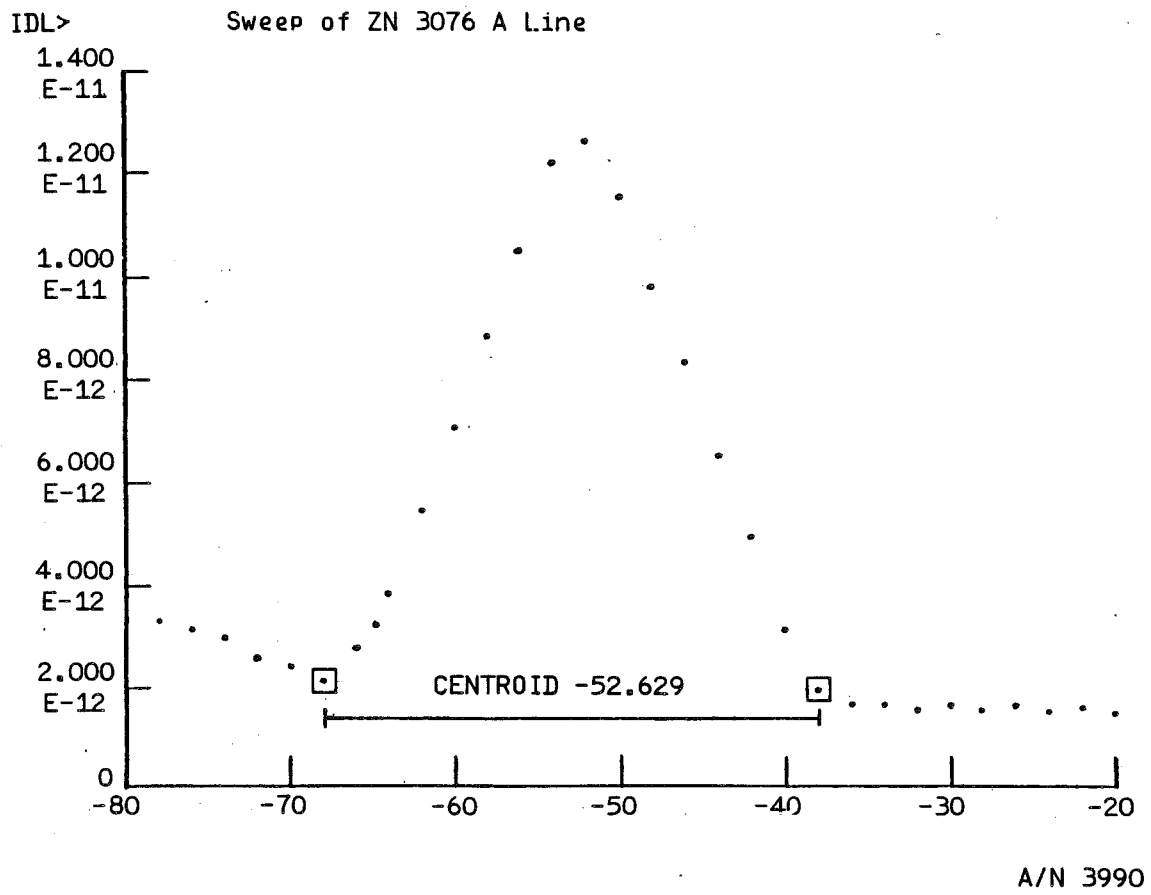
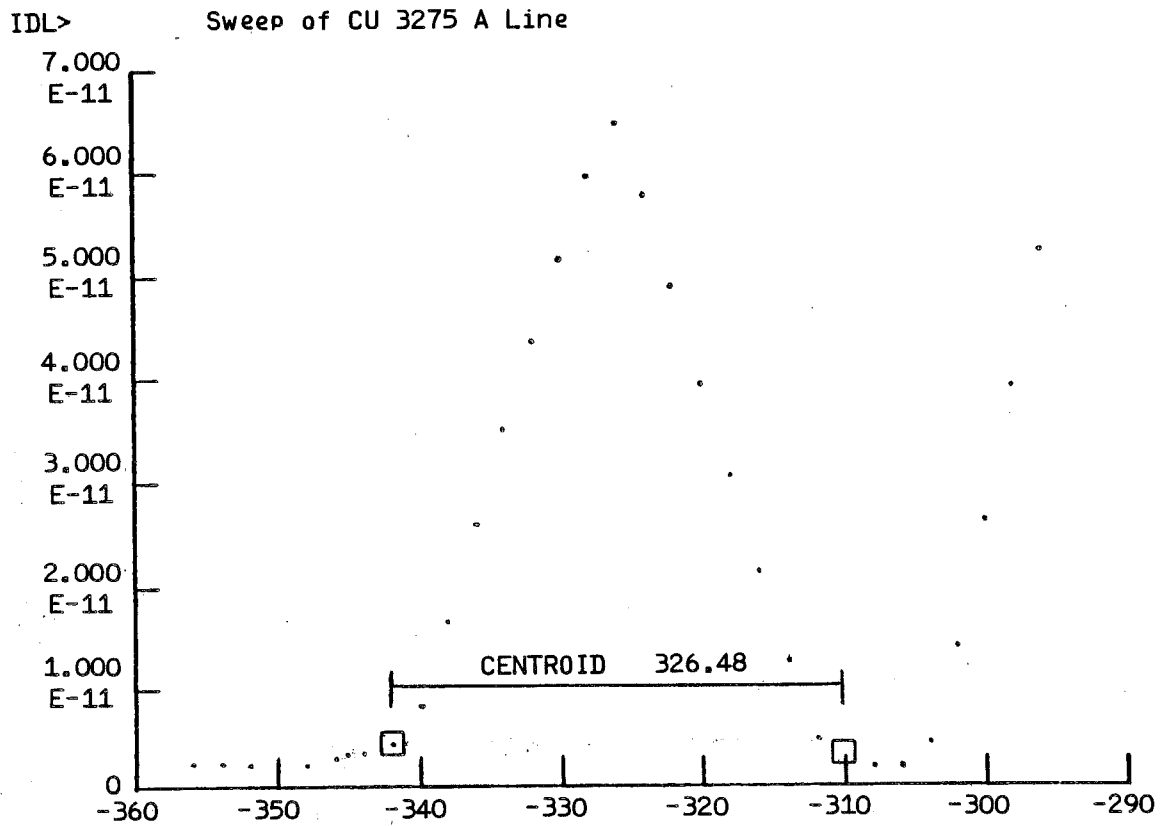


Figure 1-2d



B6802-78



A/N 3990

Figure 1-2g



B6802-78

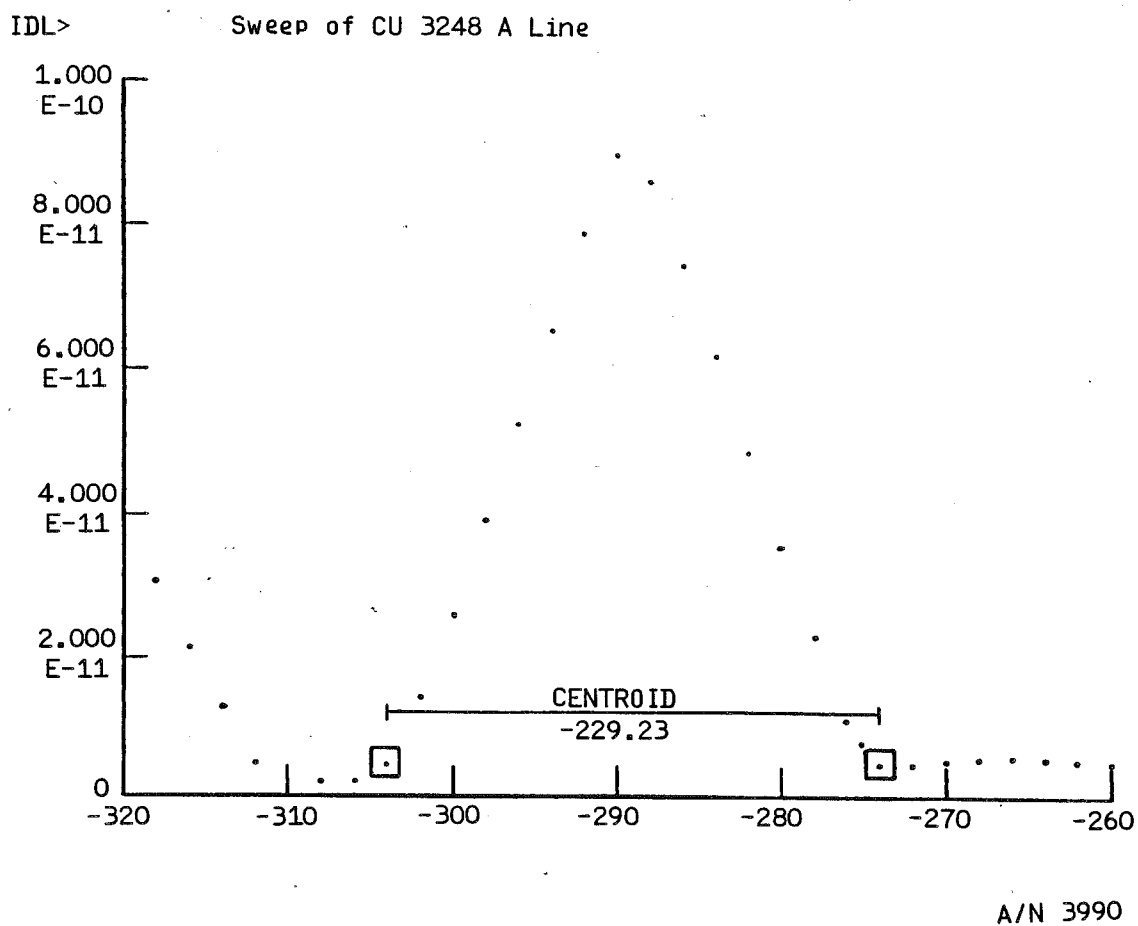
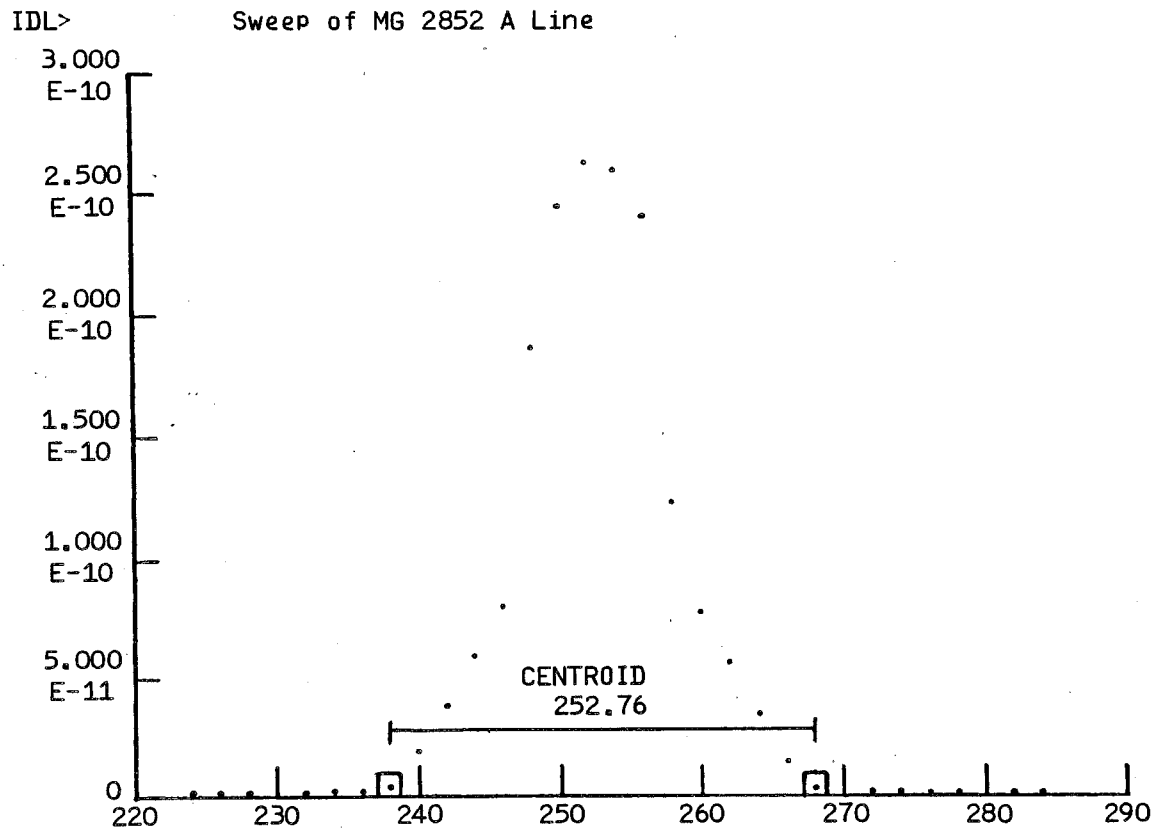


Figure 1-2h



A/N 3990

Figure 1-2i

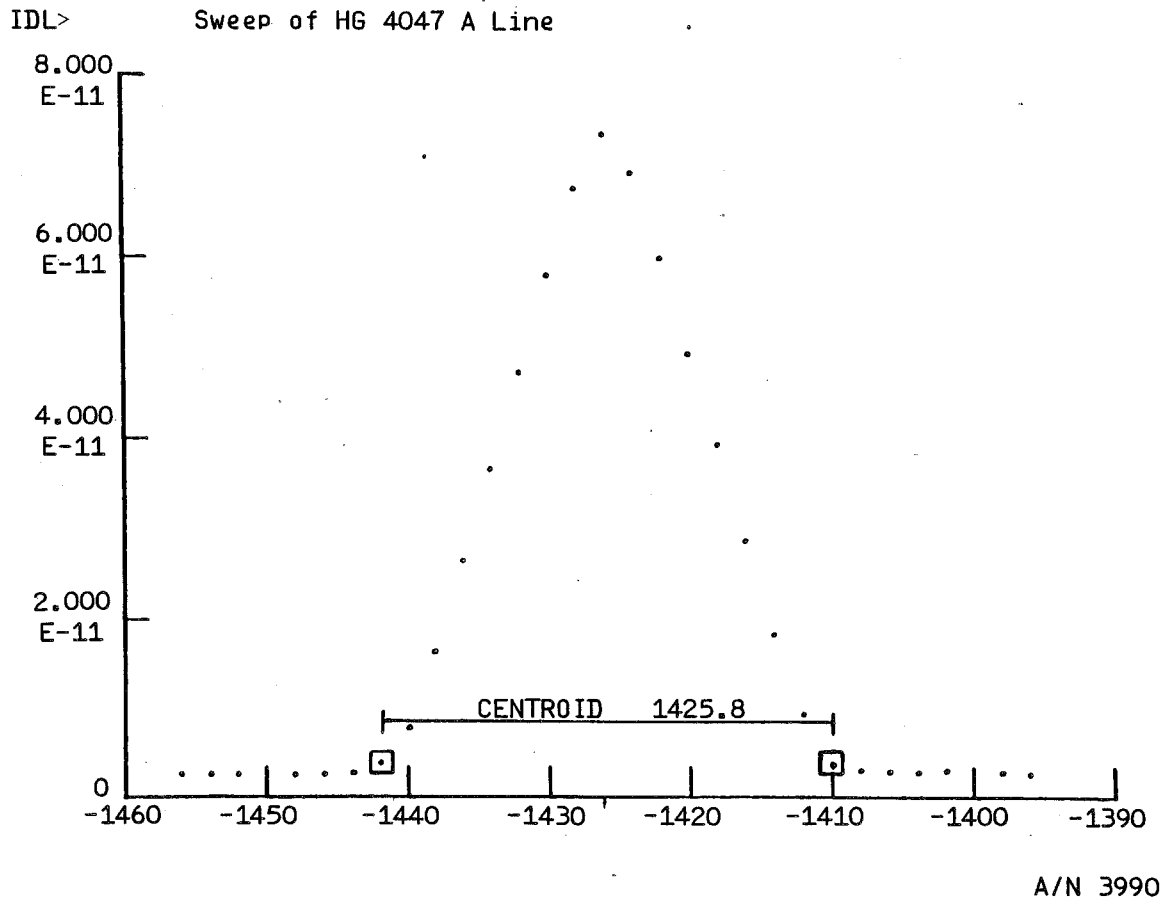


Figure 1-2j

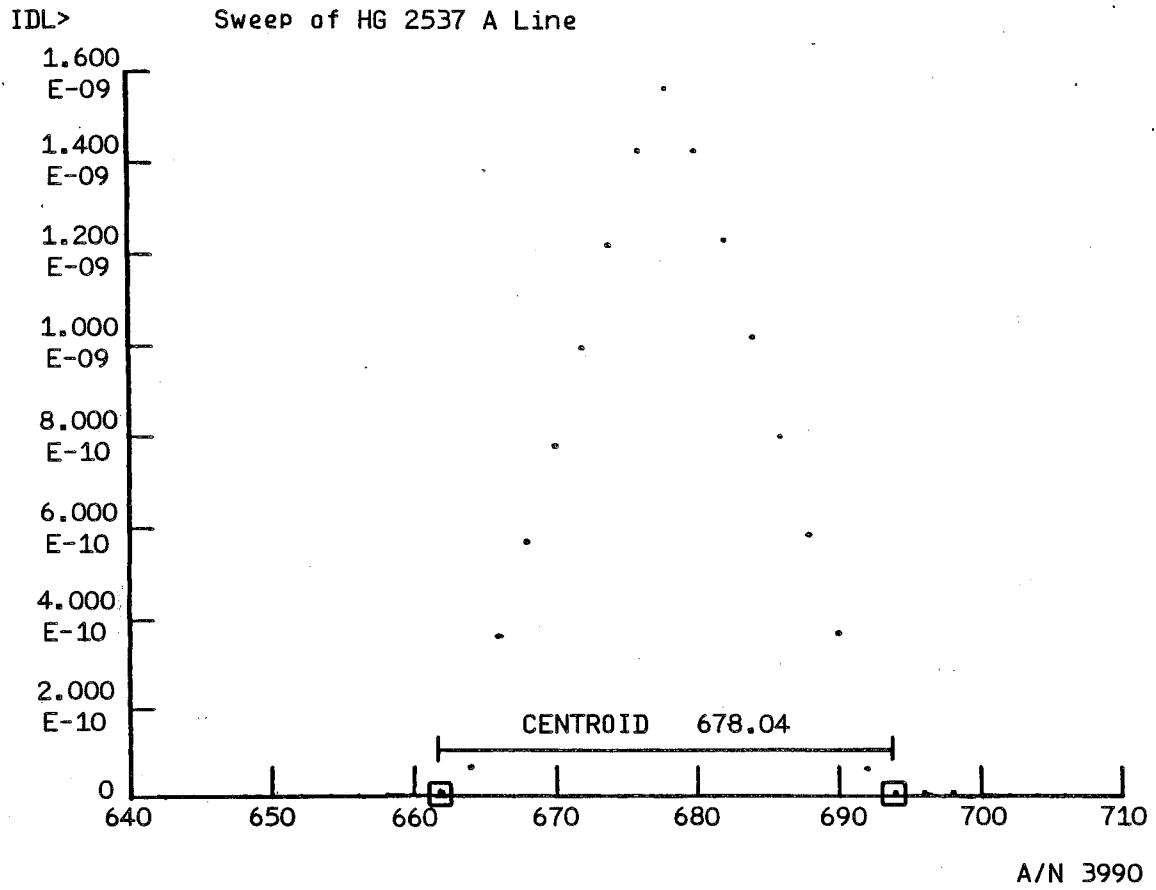


Figure 1-2k

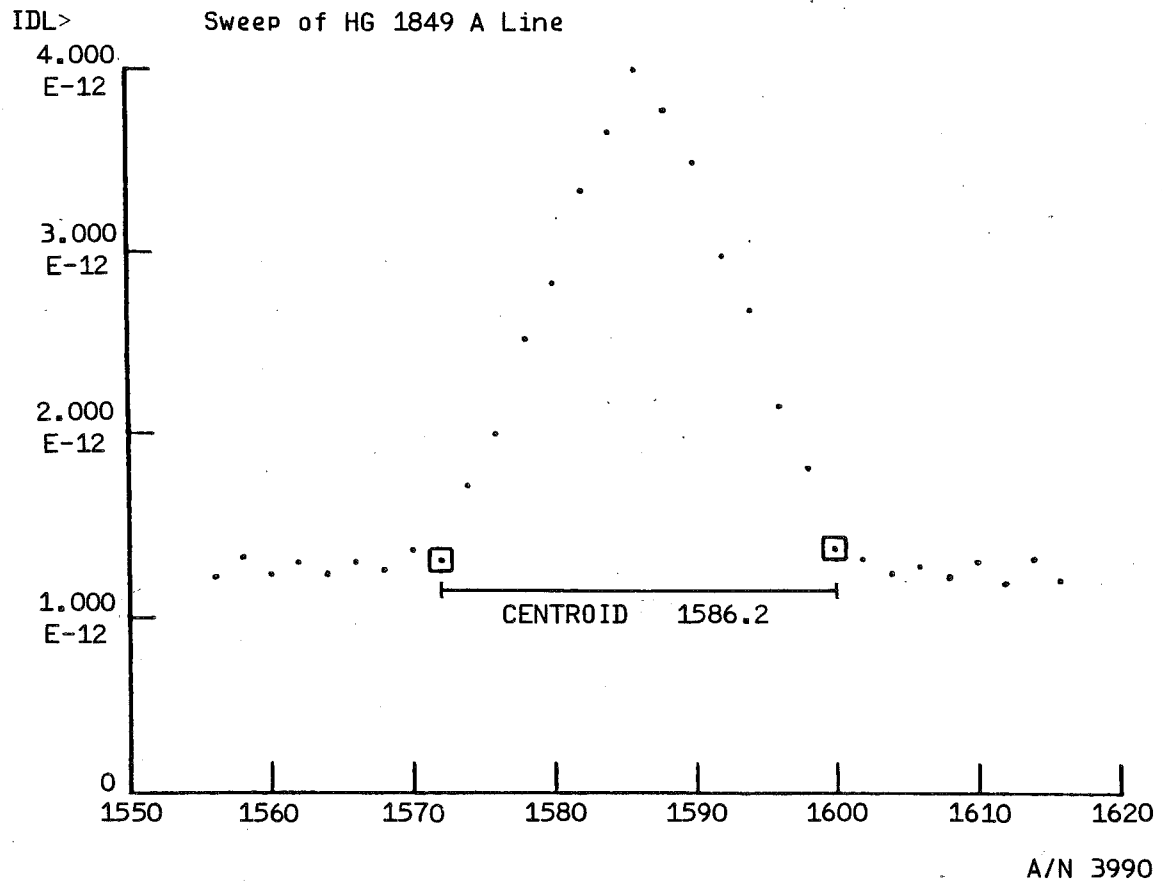


Figure 1-21



Figure 1-3 a

Sine Curvefit, Position Mode

```
IDL>YFIT=CURVEFIT(X,Y,W,A,SIGMAA)
FUNCTION CURVEFIT,X,Y,W,A,SIGMAA
IDL>PRINT,A,SIGMAA
      8196.0      -9.58732E-05      -3960.3
      8.18857E-03      8.27772E-07      30.744
IDL>D=Y-YFIT
IDL>FOR I=0,13 DO PRINT,X(I),Y(I) ,YFIT(I),D(I)
```

<u>Grating Position</u>	<u>Wavelength</u>		<u>Residual (Å)</u>
	<u>Actual</u>	<u>Curvefit</u>	
-37.880	3064.9	3065.3	-0.45874
54.320	2998.1	2998.0	0.10327
283.21	2830.4	2829.9	0.52441
-52.940	3076.1	3076.3	-0.24170
1207.1	2138.7	2138.4	0.27393
1355.2	2025.6	2025.8	-0.21765
-327.13	3275.1	3274.9	0.21436
-289.74	3247.7	3248.0	-0.25439
253.34	2852.3	2851.9	0.34326
-1426.3	4046.8	4047.1	-0.28979
678.57	2536.7	2536.4	0.25806
1586.7	1849.0	1849.1	-7.60498E-02
3960.0	0.00000E+00	0.25841	-0.25841

```
IDL>XFIT=-A(2)+(1/A(1))*ASIN(Y/A(0))
IDL>DY=Y-Y^U
IDL>DX=XIXFIT^U
IDL>DX=X-XFIT
IDL>FOR I=0,13 DO PRINT,Y(I),X(I),XFIT(I),DX(I)
```

<u>Wavelength</u>	<u>Grating Position</u>		<u>Residual (steps)</u>
	<u>Actual</u>	<u>Curvefit</u>	
3064.9	-37.880	-37.250	-0.62951
2998.1	54.320	54.179	0.14129
2830.4	283.21	282.50	0.71097
3076.1	-52.940	-52.609	-0.33136
2138.7	1207.1	1206.7	0.36145
2025.6	1355.2	1355.5	-0.28589
3275.1	-327.13	-327.43	0.29797
3247.7	-289.74	-289.39	-0.35254
2852.3	253.34	252.87	0.46597
4046.8	-1426.3	-1425.9	-0.42468
2536.7	678.57	678.23	0.34491
1849.0	1586.7	1586.8	-9.91211E-02
0.00000E+00	3960.0	3960.3	-0.32886



Figure 1-3 b

Sweep Mode

```

PFD FUNCT,X,A,F,PDER
Compiled FUNCT
IDL>YFIT=CURVEFIT(X,Y,W,A,SIGMA)
FUNCTION CURVEFIT,X,Y,W,A,SIGMA
CURVEFIT - Failed to converge
IDL>PRINT,A
      8196.0      -9.58926E-05      -3959.5
IDL>FOR I=0,13 DO PRINT,X(XI),Y(YI),W(WI)
      0      -514.03      3408.3      0.00000E+00
      1      -37.250      3064.9      1.0000
      2       53.770      2998.1      1.0000
      3       282.75      2830.4      1.0000
      4      -52.630      3076.1      1.0000
      5       1206.9      2138.7      1.0000
      6       1354.2      2025.6      1.0000
      7      -326.48      3275.1      1.0000
      8      -289.23      3247.7      1.0000
      9       252.71      2852.3      1.0000
     10      -1425.8      4046.8      1.0000
     11       678.00      2536.7      1.0000
     12       1586.2      1849.0      1.0000
     13       3960.5      0.00000E+00      0.00000E+00
IDL>YFIT=CURVEFIT(X,Y,W,A,SIGMA)
IDL>PRINT,A,SIGMA
      8196.0      -9.59017E-05      -3959.2
      2.58830E-02      2.61717E-06      101.67
IDL>DX=X-XFIT
*** Variable is not defined, Name= 'XFIT'. Error detected at:
LINE 0, ROUTINE $$MAIN$$,
IDL>DY=Y-YFIT
IDL>FOR I=0,13 DO PRINT,X(XI),Y(YI),YFIT(XI,DY(XI))
      -514.03      3408.3      3409.2      -0.91644
      -37.250      3064.9      3064.9      -4.29688E-02
       53.770      2998.1      2998.4      -0.32300
       282.75      2830.4      2830.2      0.21118
      -52.630      3076.1      3076.1      -6.25000E-02
       1206.9      2138.7      2138.3      0.37231
       1354.2      2025.6      2026.3      -0.70227
      -326.48      3275.1      3274.5      0.57788
      -289.23      3247.7      3247.7      1.63574E-02
       252.71      2852.3      2852.4      -0.10132
      -1425.8      4046.8      4047.0      -0.25708
       678.00      2536.7      2536.7      -5.39551E-02
       1586.2      1849.0      1849.1      -0.16602
       3960.5      0.00000E+00      -1.0203      1.0203
IDL>XFIT=-A(2)+(1/A(XI))*ASIN(Y/A(XI))
IDL>DX=X-XFIT
IDL>FOR I=0,13 DO PRINT,Y(YI),X(XI),XFIT(XI,DX(XI))
      3408.3      -514.03      -512.85      -1.1841
      3064.9      -37.250      -37.191      -5.90820E-02
      2998.1       53.770       54.211      -0.44118
      2830.4       282.75      282.46      0.28638
      3076.1      -52.630      -52.545      -8.53233E-02
      2138.7       1206.9       1206.4      0.49109
      2025.6       1354.2       1355.1      -0.92188
      3275.1      -326.48      -327.28      0.80246
      3247.7      -289.23      -289.25      2.31628E-02
      2852.3       252.71       252.85      -0.13741
      4046.8      -1425.8      -1425.4      -0.37646
      2536.7       678.00       678.07      -7.22656E-02
      1849.0       1586.2       1586.4      -0.21680
      0.00000E+00      3960.5      3959.2      1.2991

```

Weights set to zero;
wide, complex line,
zero order not observed
in sweep mode.

Final values of Coefficients

Residuals
Wavelength (Å)

Residuals
Grating Position (Steps)



Section 2

LINEARITY AND DYNAMIC RANGE

2.1 MEASUREMENT OF LINEARITY

The linearity of SBUV/2 is measured by illuminating it by two roughly equal light sources, first by one, next by the other, and then by both together. If the instrument responds linearly, the final response is the sum of the first two responses. To the extent that the instrument deviates from this behavior, it is non-linear. To cover the dynamic range, successively brighter sources are used, each roughly equal to the sum of its predecessors.

In practice, an FEL lamp is imaged at the entrance port of an integrating sphere by a concave mirror. Apertures at the mirror are exposed or masked to produce the various light levels. The dynamic range is extended by using neutral density filters.

Suppose that the instrument response to the first light level Φ_1 is S_1 and likewise for Φ_2 and S_2 . Since Φ_1 and Φ_2 are nearly equal, we assume linearity over such a small difference and state that:

$$\Phi_2 = \Phi_1 \left(\frac{S_2}{S_1} \right).$$

When we add the sources,

$$^2\Phi = \Phi_1 + \Phi_2 = \Phi_1 \left(1 + \frac{S_2}{S_1} \right)$$

(A preceding superscript $^m\Phi$ or mS denotes the sum of the light levels from Φ_1 to Φ_m .) In general,

$$^m\Phi = ^{m-1}\Phi \left(1 + \frac{S_m}{^{m-1}S} \right),$$



so each new light level can be calculated from the response of the instrument to the previous levels. If the instrument is linear, then $\frac{S}{\Phi}$ is constant over the dynamic range. The degree of change in the ratio with changes in Φ measures the non-linearities.

SBUV/2 has three gain ranges, so linearity is measured within each range, and the gain ratios are measured in the regions where the ranges overlap.

2.2 LINEARITY TEST RESULTS

The linearity test results are summarized in Table 2-2-1. The first three columns are the relative radiant flux levels Φ to which the instrument was exposed. The first column fluxes were produced using a neutral density filter of density 3.851 (ND4) the second of 2.000 (ND2); and the third with no filter (ND0). The fluxes are normalized between columns at midrange, indicated in the table by encircled values with connecting lines.

The second set of three columns lists the instrument responses in each range to the incident fluxes. The counts are "corrected" by subtracting the background count level, measured at each flux level while interrupting the direct light path.

The third set of three columns are the expected counts in the three ranges, calculated by assuming zero based linearity and arbitrarily choosing a gain coefficient (a_r) for that range. That is,

$$(\text{expected counts}) = a_r (\text{flux}).$$

The gains chosen were

$$a_1 = 281$$

$$a_2 = 2.76$$

$$a_3 = 0.0244$$



The last set of three columns list the percent differences between the measured and expected counts and represent the nonlinearity of the instrument. These values are plotted in Figure 2-2-1 for all three ranges. Above levels of a few hundred counts, ranges 1 and 3 are linear within 1%; range 2 is not. Figure 2-2-2 is a graph of the percent deviations from linearity of the response of range 2 versus relative radiant input. Below the 800 count level the response is linear. Above 800 counts, the response is about 1.5% too high for each doubling of flux, resulting in a cumulative nonlinearity of about 10% at the top of the dynamic range. The response data fits a power curve given by:

$$S = a_1 \Phi^{1.01985}$$

$$a_1 = 2.46582$$

to within $\pm 0.2\%$ over the range from 290 to 60,000 counts. Below 380 counts the response follows a linear curve,

$$S = a_0 \Phi$$

$$a_0 = 2.774$$

to within $\pm 0.35\%$.

Table 2-1
LINEARITY TESTS

RELATIVE FLUX LEVELS			MEASURED, CORRECTED INSTRUMENT COUNTS			EXPECTED COUNTS			% NON LINEARITY ZERO BASED		
ND 4	ND 2	ND 0	R 1	R 2	R 3	R 1	R 2	R 3	R 1	R 2	R 3
.993			260			281			-7.49		
2.038			599			577			-7.5		
4.073			1148			1153			-0.43		
8.392			2373	23.45		2376	23.45		-0.14	0	
16.85			4736	47.07		4736	47.10		0	0.32	
34.60			9706	96.55		9724	96.36		-0.186	0.19	
69.63			19588	194.7		19572	194.1		0.08	0.32	
	71.94		19979	198.6		19939	198.6		0.20	0	
138.2			38935	386.6		38844	385.1		0.23	0.39	
	144.3		40032	398		39987	398.4		0.11	-0.10	
281.4			79561	794		79092	784.5		0.59	1.22	
	290.0		80273	801		80346	800.6		-0.09	0.12	
559.4			*	1600			1558		2.69	2.69	
	591.7			1653			1633		1.19	1.19	
	1196										
	2450			3397	44.35		3302		2.89	2.89	
	4914			7045	43.81		6763		4.17	4.17	
		7.662×10^3		14358	125.3		13565	120.1	5.84	5.84	4.3
				21914	177.45		19681	186.7	11.34	11.34	-4.9
	9838			29117	262		27159	240.4	7.21	7.21	8.9
		14.91×10^3		44226	370		39371	363	12.33	12.33	1.8
	20220			60721	494		55817	494	8.79	8.79	0
		29.14×10^3		90199	712		79497	710	13.46	13.46	0.26
	40180			*	962			964	-0.20	-0.20	0.40
		59.39×10^3			1453			1447	0.40	0.40	0.16
		119.6×10^3			2919			2914	0.16	0.16	-0.24
		244.7×10^3			5948			5962	-0.24	-0.24	-0.09
		492.9×10^3			12001			12012	-0.09	-0.09	-0.09
		983.1×10^3			23936			23957	-0.09	-0.09	0
		1998×10^3			48685			48684	0	0	0
		3959×10^3			*						



B6802-78

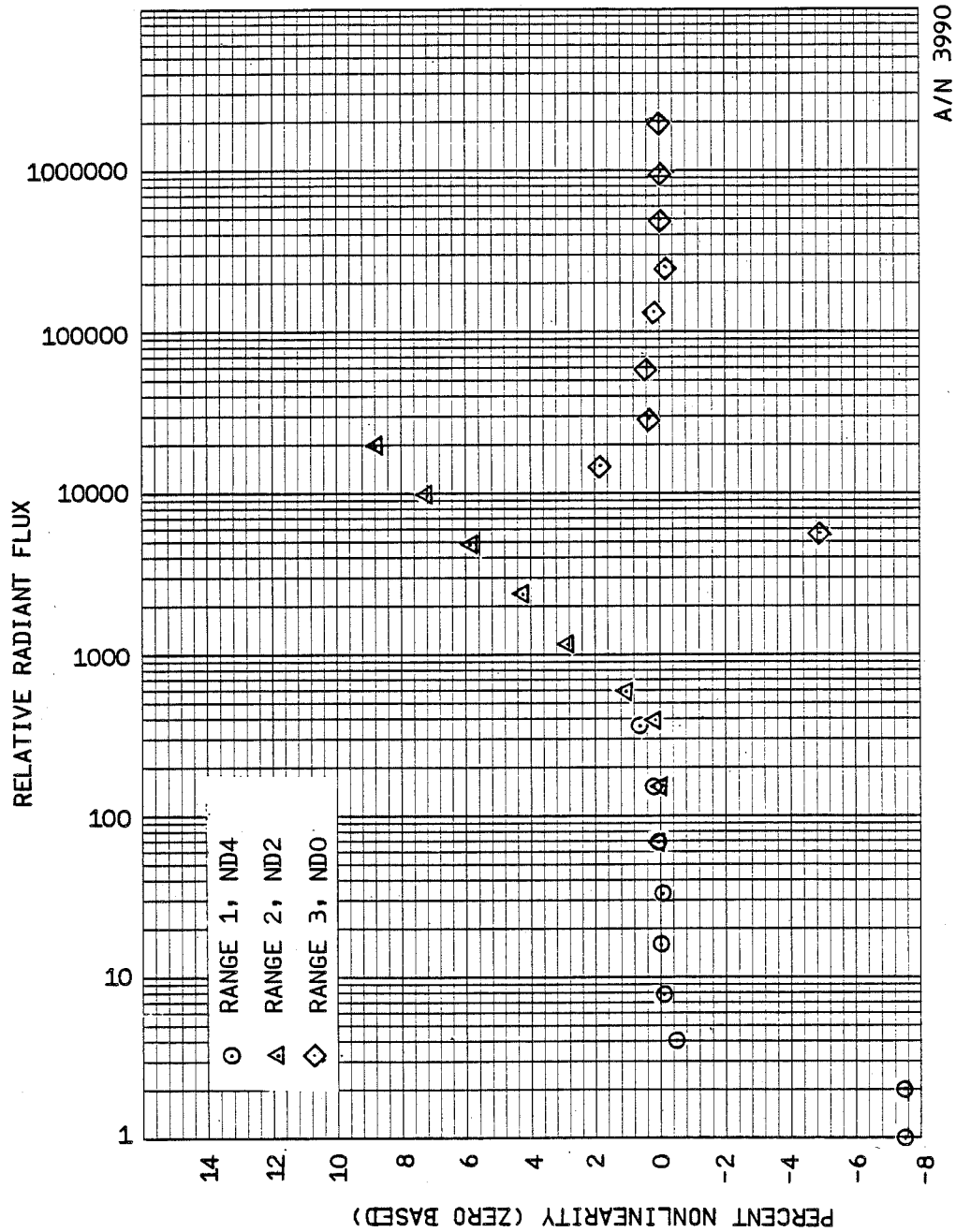


Figure 2-1 Non-linearities of the EMU/Flight Instrument

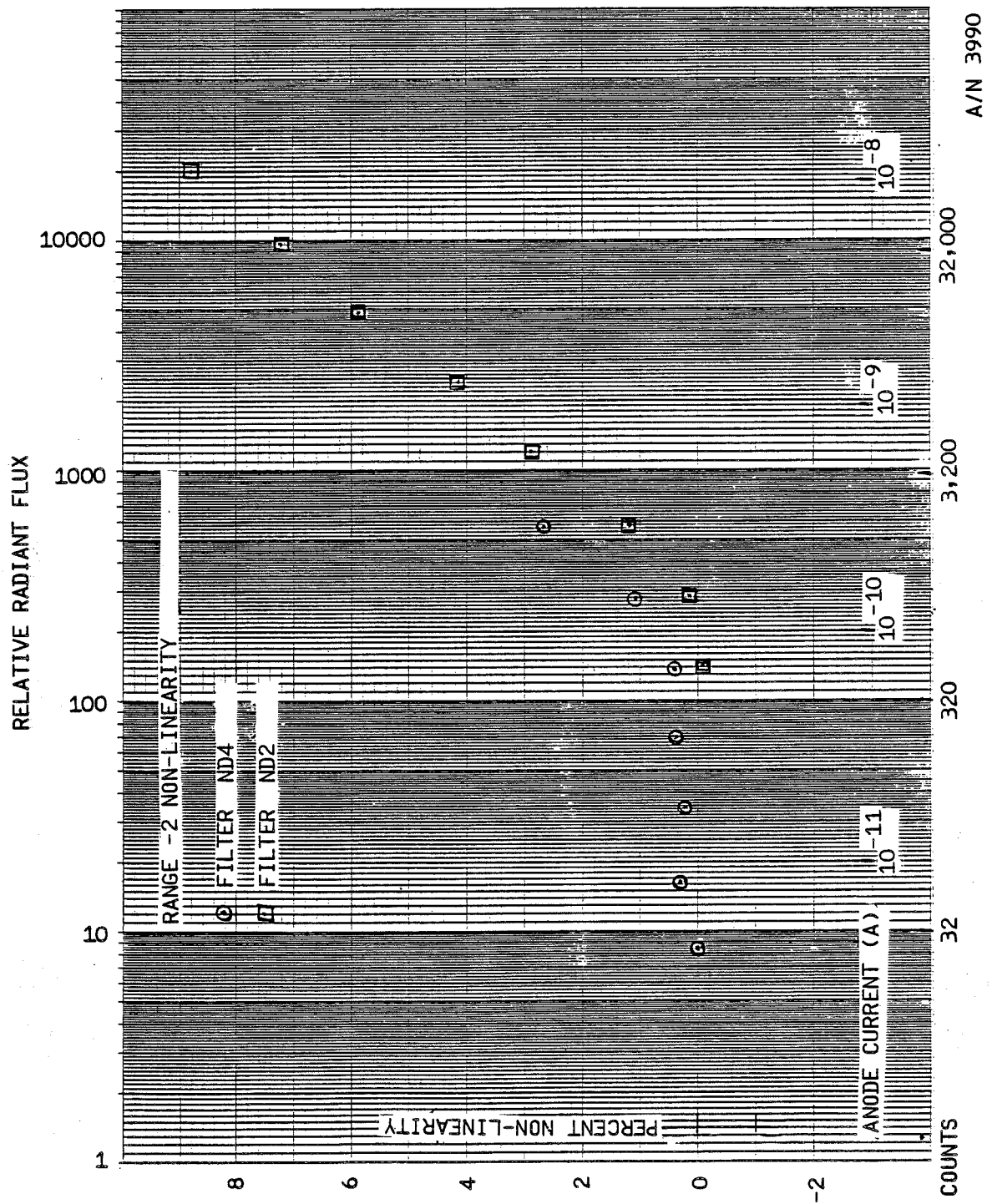


Figure 2-2 System and PMT Non-linearity



B6802-78

Section 3

NATIONAL BUREAU OF STANDARDS CALIBRATION

This section contains the calibrations by the National Bureau of Standards of Sources and Diffusers used for the Radiometric Calibration of SBUV/2.

3.1 FEL LAMPS

For further information refer to:

U.S. Department of Commerce
National Bureau of Standards
Report of Calibration
NBS Test No.: 28951 (P.O. No. 35519)



UNITED STATES DEPARTMENT OF COMMERCE
National Bureau of Standards
Washington, D.C. 20234

SEP 24 1981

In reply refer to: 534/226444-1
534/226444-2
534/226444-3
534/226444-4



RECEIVED

SEP 28 1981

FEDERAL

Ball Aerospace Systems Division
P. O. Box 1062, Bldr. Indust. Park
Boulder, Colorado 80306

Subject: Lamp Standards of Spectral
Irradiance

Order No.: 28951 dated September 4, 1981
and P. O. #35519

Gentlemen:

Enclosed are results of the tests which you requested in the above
reference. Please refer to the above file numbers in any later communi-
cation concerning these tests.

Sincerely,

Donald A. Miespacher
for

Klaus D. Mielenz, Acting Chief
Radiometric Physics Division
Center for Radiation Research

Material Tested:

Four Spectral Irradiance Standard Lamps

Enclosure:

Four Reports of Calibration
One Report "Type DXW Lamp Standards of Spectral Irradiance"
One Report "Type FEL Lamp Standards of Spectral Irradiance"
One Report "Revised Uncertainty Estimates for Spectral
Irradiance Calibrations"
NBS Technical Note 594-13

U.S. DEPARTMENT OF COMMERCE
NATIONAL BUREAU OF STANDARDS
WASHINGTON, D.C. 20234

REPORT OF CALIBRATION

of
One Standard of Spectral Irradiance

Supplied to:

Ball Aerospace Systems Division
P. O. Box 1062, Bldr. Indust. Park
Boulder, Colorado 80306

(See your order number 28951 dated September 4, 1981.)

1. Material

One 1000-watt quartz-halogen, type FEL, tungsten coiled-coil filament lamp has been supplied by the National Bureau of Standards as a standard of spectral irradiance and bears the designation F-124.

2. Calibration

The lamp was calibrated using the equipment and procedures described in the enclosed writeup, "Type DXW Lamp Standards of Spectral Irradiance." The preparation and operation of the type FEL lamp supplied for this calibration are described in the enclosure, "Type FEL Lamp Standards of Spectral Irradiance." Note particularly paragraph IV of this enclosure which describes the orientation of the test lamp.

3. Results

The results of this test are given in the attached Table 1. See also the enclosure, "Revised Uncertainty Estimates for Spectral Irradiance Calibrations."

For the Director,

Donald A. McSparron
for

Klaus D. Mielenz, Acting Chief
Radiometric Physics Division
Center for Radiation Research

NBS Test No.: 534/226444-1

P.O. No.: 28951 (P. O. #35519)

Date: September 22, 1981

TABLE 1

Spectral irradiance (W/cm^2) at 50 cm from lamp F-124 when operated on dc with the polarity as indicated on the attached identification plate.

λ (nm)	Lamp No. F-124 7.900 amps
250	0.1530
260	.2720
270	.4615
280	.7332
290	1.109
300	1.615
310	2.273
320	3.143
330	4.227
340	5.545
350	7.125
400	19.51
450	39.80
500	66.22
555	98.66
600	125.4
654.6	154.4
700	174.3
800	203.3
900	212.2
1050	202.9
1150	186.9
1200	178.5
1300	160.0
1540	119.1
1600	109.6

NBS Test No.: 534/226444-1

F-124 FIT

a= 44.5768 b=-4667.28 Apparent Blackbody Temperature- 3082.73

TERM	COEFFICIENT	STD. DEV.
1A=	-29.4262	7.66576
2B=	0.359997	0.0981992
3C=	-1.59729E-03	4.67766E-04
4D=	3.14923E-06	9.81707E-07
5E=	-2.32456E-09	7.65712E-10

STANDARD DEVIATION= 5.54185E-03

Wavelength	MEASURED Irradiance	PREDICTED Irradiance	% Difference
250	0.159549	0.159055	0.309623
260	0.282688	0.28514	-0.867387
270	0.479504	0.478042	0.304898
280	0.763172	0.759248	0.514169
290	1.15424	1.15044	0.329221
300	1.67576	1.68038	-0.275696
310	2.35499	2.37193	-0.719323
320	3.25803	3.25676	0.0389806
330	4.37849	4.36226	0.370675
340	5.73634	5.72271	0.237607
350	7.35955	7.37566	-0.218899
400	20.081	20.081	0

AVERAGE S.D.= 0.423349

Curve fit F-124 FEL lamp recalibration- August 1983

This table has been retyped at BASD for the purpose of legible reproduction.

U.S. DEPARTMENT OF COMMERCE
NATIONAL BUREAU OF STANDARDS
WASHINGTON, D.C. 20234

REPORT OF CALIBRATION

of
One Standard of Spectral Irradiance

Supplied to:

Ball Aerospace Systems Division
P. O. Box 1062, Bldr. Indust. Park
Boulder, Colorado 80306

(See your order number 28951 dated September 4, 1981.)

1. Material

One 1000-watt quartz-halogen, type FEL, tungsten coiled-coil filament lamp has been supplied by the National Bureau of Standards as a standard of spectral irradiance and bears the designation F-127.

2. Calibration

The lamp was calibrated using the equipment and procedures described in the enclosed writeup, "Type DXW Lamp Standards of Spectral Irradiance." The preparation and operation of the type FEL lamp supplied for this calibration are described in the enclosure, "Type FEL Lamp Standards of Spectral Irradiance." Note particularly paragraph IV of this enclosure which describes the orientation of the test lamp.

3. Results

The results of this test are given in the attached Table 1. See also the enclosure, "Revised Uncertainty Estimates for Spectral Irradiance Calibrations."

For the Director,

Donald A. Miesner
for

Klaus D. Mielenz, Acting Chief
Radiometric Physics Division
Center for Radiation Research

NBS Test No.: 534/226444-2

P.O. No.: 28951 (P. O. #35519)

Date: September 22, 1981

TABLE 1

Spectral irradiance (W/cm^2) at 50 cm from lamp F-127 when operated on dc with the polarity as indicated on the attached identification plate.

λ (nm)	Lamp No. F-127 8.000 amps
250	0.1578
260	.2818
270	.4795
280	.7664
290	1.162
300	1.692
310	2.387
320	3.302
330	4.446
340	5.835
350	7.511
400	20.65
450	42.18
500	70.30
555	105.0
600	133.5
654.6	164.6
700	185.9
800	217.1
900	227.0
1050	216.9
1150	199.9
1200	190.9
1300	171.4
1540	127.5
1600	116.7

NBS Test No.: 534/226444-2

Goniometric Mappings

The first three readings are measurements of the aligned position (0,0) at the beginning, middle, and end of the scan, expressed in volts (full scale). The table which follows is the voltage output at that particular rotation, divided by the average (0,0) readings.

Attached you will find goniometric scans of each of the lamps at $\pm 3^\circ$ by $\pm 5^\circ$ at λ 300 nm. In addition, I have included (i) a repeat run on F-128 (ii) F-131* at λ 654.575 nm; and (iii) a sample of the irradiance field of a frosted FEL type lamp.

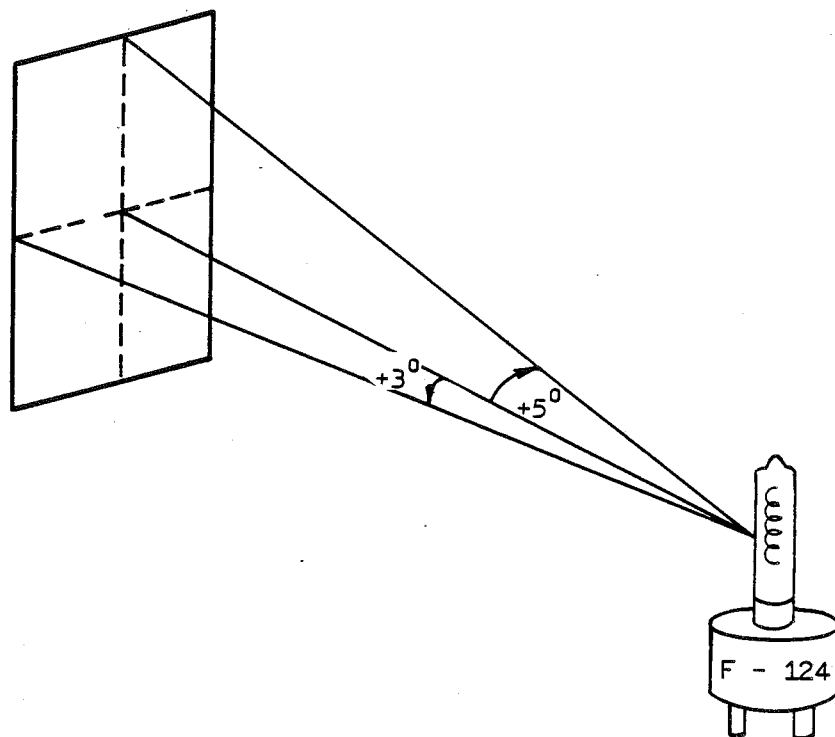
* NOTE: Calibration Lamp data from Lamps F-128 and F-131 is not included here since the lamps were not used in EMU-FLT calibration.

[Typed at BASD from hand-written NBS original]



B6802-78

FEL LAMP GONIMETRIC MAPPING



A/N 3990

(REDRAWN AT BASD FROM ORIGINAL NBS SKETCH FOR REPRODUCIBILITY)

GONIOMETRIC SCAN OF FEL-124 LAMP

***** F-124 *****

9/21/81

WAVELENGTH: 300 NM

+/- 3 DEGREES BY +/- 5 DEGREES

\$.995825 .992792

97.06	97.63	97.49	97.55	97.66	97.85	97.81
97.73	98.41	98.28	98.46	98.55	98.64	98.69
98.50	98.94	98.92	99.15	98.95	98.14	99.38
98.95	99.35	99.20	99.51	99.42	99.74	99.85
99.03	99.72	99.49	99.73	99.81	99.96	100.14
99.19	99.49	99.60	99.98	99.91	99.98	100.37
98.97	99.55	99.31	99.87	99.75	99.87	100.00
98.82	99.25	99.16	99.44	99.55	99.52	99.90
98.29	98.80	98.79	98.97	99.00	98.92	99.39
97.61	98.23	97.94	98.48	98.41	98.45	98.69
97.20	97.45	97.45	97.64	97.76	97.89	97.95

This table was retyped at BASD for the purpose of legible reproduction.

GONIOMETRIC SCAN OF FEL-127 LAMP

***** F-127 *****

9/18/81

WAVELENGTH: 300 NM

+/- 3 DEGREES BY +/- 5 DEGREES

1.02975

\$ 1.03125 1.0295

98.20	98.19	98.08	97.88	97.87	97.96	97.80
98.90	98.91	98.91	98.66	98.90	98.90	98.68
99.48	99.37	99.58	99.41	99.39	99.53	99.37
100.06	100.05	99.97	99.71	99.86	99.99	99.82
100.28	100.33	100.20	100.01	100.12	100.22	100.11
100.27	100.10	100.19	100.11	100.14	100.15	100.04
99.62	99.83	99.84	99.69	99.81	100.02	99.74
99.24	99.21	99.10	99.14	99.31	99.53	99.53
98.24	98.47	98.50	98.44	98.70	98.87	98.88
97.60	97.92	98.01	97.92	98.31	98.23	98.26
97.20	97.50	97.36	97.47	97.77	97.71	97.75

This table was retyped at BASD for the purpose of legible reproduction.



UNITED STATES DEPARTMENT OF COMMERCE
National Bureau of Standards
Washington, D.C. 20234

March 30, 1982

Mr. Bill Fowler
Ball Aerospace Systems Division
Box 1062
Boulder, CO 80306

Dear Mr. Fowler:

Enclosed you will find copies of the fits performed on your four FEL* lamps and a table generated for each lamp from 250 nm to 400 nm every 5 nm. The fit coefficients may be applied to the following equation:

$$E_{\lambda} = (A_0 + A_1\lambda + A_2\lambda^2 + \dots + A_4\lambda^4) \frac{e^{(a+b/\lambda)}}{\lambda^5} \quad (mW \cdot m^{-2} \cdot m^{-1})$$

where λ is nm/100

A_0 is term 0

A_1 is term 1

.

.

.

A_4 is term 4

If you have any questions, please contact me at (301) 921-3613.

Sincerely,

James H. Walker
Radiometric Physics Division
Center for Radiation Research

Enclosure

* Curvefits for FEL Lamps F-124 and F-127 are reproduced here as they are the only lamps used in EMU-FLT calibration.

F-124 FIT (WL/100)

a= 21.6494 b=-47.1039 Apparent Blackbody Temperature- 305452

TERM COEFFICIENT STD. DEV.

0	A=-32.4757	6.13651
1	B= 40.0895	7.86086
2	C=-17.96	3.74437
3	D= 3.56856	.785831
4	E=-.265161	0.061294

STANDARD DEVIATION= 4.41272E-3

Wavelength (nm/100)	MEASURED Irradiance		PREDICTED Irradiance	% Difference	
2.5	.152969	.152598	.152602	.242519	2.69513E-3
2.6	.271957	.273915	.273934	-.720082	7.09385E-3
2.7	.461516	.459792	.459858	.373643	1.44023E-2
2.8	.733209	.730407	.730504	.382117	.01322
2.9	1.10874	1.10808	1.10821	5.93498E-2	1.19631E-2
3	1.61469	1.61735	1.6175	-.164666	9.13962E-3
3.1	2.27269	2.28469	2.28513	-.528096	1.92848E-2
3.2	3.1426	3.13987	3.14008	8.68521E-2	6.80356E-3
3.3	4.22727	4.21301	4.21359	.337431	1.38988E-2
3.4	5.5449	5.53643	5.53699	.152831	1.02664E-2
3.5	7.125	7.14024	7.14075	-.213917	7.0655E-3
4	19.5106	19.5095	19.5112	5.78737E-3	8.60334E-3

AVERAGE S.D.= .337026

This table has been retyped at BASD for the purpose of legible reproduction.

F-127 FIT (WL/100)

a= 21.7316 b=-47.2151 Apparent Blackbody Temperature- 304733

TERM COEFFICIENT STD. DEV.

0	A=-33.1789	6.30721
1	B= 40.7713	8.08114
2	C=-18.194	3.85002
3	D= 3.60131	.808141
4	E=-.26619	6.30436E-2

STANDARD DEVIATION= 4.52306E-3

Wavelength (nm/100)	MEASURED Irradiance		PREDICTED Irradiance	% Difference	
2.5	.157776	.157325	.157331	.286055	3.71287E-3
2.6	.281788	.283909	.283931	-.752599	7.97783E-3
2.7	.479536	.478508	.478579	.214275	1.48106E-2
2.8	.766407	.762544	.762621	.504006	1.00286E-2
2.9	1.1616	1.15961	1.15973	.171425	1.06091E-2
3	1.6923	1.69573	1.69592	-.202761	1.09105E-2
3.1	2.3866	2.3993	2.39952	-.532141	8.98305E-3
3.2	3.3024	3.30065	3.3009	5.30782E-2	7.6279E-3
3.3	4.4464	4.43251	4.43337	.312479	1.95576E-2
3.4	5.8351	5.82926	5.82991	.100024	1.10922E-2
3.5	7.5112	7.52175	7.5235	-.140425	2.32531E-2
4	20.649	20.6487	20.6531	1.47792E-3	2.15041E-2

AVERAGE S.D.= .34545

This table has been retyped at BASD for the purpose of legible reproduction.



B6802-78

3.2 Mini Arcs

For further information refer to:

U.S. Department of Commerce
National Bureau of Standards
Report of Calibration

U.S. DEPARTMENT OF COMMERCE
NATIONAL BUREAU OF STANDARDS
WASHINGTON, D.C. 20234

February 22, 1982

REPORT OF CALIBRATION

VUV Spectral Irradiance of Argon Mini-Arc I

submitted by

Ball Aerospace Systems Division
P.O. Box 1062 Bldr Indust Pk
Boulder, Colorado 80306

An Argon mini-arc light source, labeled "I", was calibrated for spectral irradiance in the wavelength range 152 nm to 335 nm based upon the NBS argon mini-arc¹. The latter is a secondary standard of spectral radiance and had been calibrated previously at 40.00 Å with three primary radiometric radiance standards, the NBS wall-stabilized hydrogen arc² from 140 nm to 335 nm, a plasma blackbody-line radiator³ from 114.5 nm to 165.6 nm, and a tungsten strip lamp from 250 nm to 335 nm. The overlap of the wavelength bands of applicability of these three standards ensured consistency of the calibration base.

A brief description of the method used to transfer from a spectral radiance source (the NBS mini-arc) to a spectral irradiance source follows. The calibrated area of the NBS mini-arc is the central 0.3 mm diameter region where the discharge is approximately homogeneous. In order to use this radiance source to calibrate the irradiance of another source, the radiation of the NBS arc from outside the central 0.3 mm region must be blocked. This was done by the use of a set of two collimating apertures located between the arc and the spectrometer. (One aperture also served as the entrance aperture to the spectrometer.) The response of the spectroradiometer to the radiation from the region of the arc axis is then a relative measure of the sensitivity as a function of wavelength. For measuring the irradiance from the source to be calibrated, the aperture closest to the source was removed, so that the complete area of the unknown source was seen by the spectrometer. To account for slightly different solid angles of radiation entering the spectrometer from the two different sources, a diffuser was placed behind the spectrometer entrance aperture for both measurements.

The above measurements determine the irradiance of the unknown source from 160-330 nm, but only on a relative scale. To get an absolute scale, the irradiance of the unknown source is compared at 250 nm only to that of a calibrated FEL irradiance standard. For this measurement, an integrating sphere is used at the entrance aperture to

a double spectrometer. The double spectrometer is necessary for rejecting scattered radiation from outside the desired wavelength bandpass, especially from the tungsten FEL lamp. Both sources were placed 50 cm from the aperture of the integrating sphere.

The spectral irradiance of the mini-arc, in units of $\text{W cm}^{-2} \text{ nm}^{-1}$, is listed in Table 1 for an arc current of 40.00 A.

The values of spectral irradiance listed in Table 1 apply to the radiation emitted by the mini-arc light source through a sealing window. Also listed in Table 1 is the transmission of the MgF_2 ultraviolet window attached to the light source and that of an additional MgF_2 window. The spectral irradiance of the arc plasma itself is obtained by dividing the values given in Table 1 by the transmission of the appropriate window. The spectral irradiance of the light source using another window, for example window 2 is then obtained by multiplying the quotient by its transmission, for example

$$E_{\lambda}(\#2) = \frac{E_{\lambda}(\#1)}{T(\#1)} \times T(\#2) \quad \text{(where, for example, the arc was calibrated with window \#1)}$$

In this way damage to the arc window does not result in the loss of a calibrated light source. Also, it is possible through such substitution of a calibrated window, to periodically check for deterioration of the window due to, for example, condensation on the window of uv-photodissociated hydrocarbons in the vacuum system.

1. Calibration Conditions. A continuous flow of high purity (research grade) argon, with total gas cylinder impurities quoted to be less than 10 ppm (99.999% pure), was used to purge the arc source. The total flow was 5000 cc min^{-1} and was divided equally in a gas manifold and directed to the three input gas ports. The output ports vented directly into the laboratory. The pressure in the arc chamber was equal to the ambient pressure, measured to be 1.00 atm, or 760 mm Hg, $\pm 1\%$.

The arc was ignited by shorting out the anode (+) and cathode (-) with a tungsten strikingrod inserted into the arc channel. After ignition, the cathode was withdrawn from the arc axis by unscrewing the cathode holder exactly five rotations from its inwardmost position.

The current was measured using a calibrated shunt, leads, and digital voltmeter.

The optical conditions for which the calibration is appropriate are as follows:

a) The arc was aligned with its axis of symmetry along the optical path. The center arc plate of the arc was 50 cm from the

entrance aperture, which was 1mm x 2mm.

b) The spectrometer resolution was 0.8 nm.

c) A short gas cell is located between the mini-arc and the vacuum system. It is normally purged with high purity argon at atmospheric pressure. Thus, the mini-arc uv window is not exposed to vacuum system contaminants during a calibration.

2. Mini-Arc Characteristics and Goniometry. The mini-arc calibrated is a modified version of similar arcs previously calibrated. The modification resulted in approximately uniform radiation over a much larger solid angle than that characteristic of earlier mini-arcs. In addition, the ignition of the arc was greatly facilitated.

By measuring signals as the arc was rotated about its center, the irradiance was mapped over the major part of the solid angle irradiated by the arc. Measurements of the irradiance at 320 and 220 nm were taken at 1 degree increments for both θ and ϕ , where θ is the angle about a horizontal axis thorough the arc center and ϕ is the angle about a vertical axis (See Fig. 1) The results are given in Table 2 and in Fig. 2. Values in the table and figure are relative to the irradiance for $\theta = \phi = 0$, i.e. where the arc is aligned with the optical axis. The angular resolution for these measurements was ± 0.3 degrees for both θ and ϕ . The data at 320 and 220 nm showed no significant difference as far as relative signal vs angles θ and ϕ .

The irradiance of the mini-arc is a function of pressure. The values in Table 1 apply to an ambient pressure of 1 atm. The irradiance at other pressures is given by

$$L(p) = (1.2 p - 0.2) L(0)$$

where p is the pressure in atmosphere and $L(0)$ is the irradiance at 1 atm. This relation holds for all wavelengths.

Tests have shown that the MgF_2 window is the component most likely to cause a systematic change in the arc irradiance. Measurements on the NBS arc indicated a negligible change in the irradiance of the arc plasma itself after 24 hrs continuous operation. Window deterioration may arise from radiation damage or from vacuum system hydrocarbons. Some windows have shown a wavelength dependent change in transmission of a few percent after several hours use. Therefore, periodic checking of the window transmission is recommended, as described on page 1.

The ultraviolet continuum spectrum is interrupted by several atomic and ionic emission lines, mainly in the wavelength region from 114 nm to 135 nm. These lines arise from air and water vapor impurities in the argon gas cylinder, the gas handling system, and the outgassing

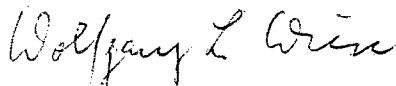
arc chamber. Table 3 lists the wavelengths where these lines occur for an arc current of 40 A and indicates the relative intensity of the lines relative to the argon continuum for a bandpass of 0.25 nm. Figure 3 is a strip chart recording of a photoelectric scan of the spectrum under these conditions. The width of the lines is instrument-limited in this case. High resolution measurements indicate that all the lines have a halfwidth of about 0.01 nm.

3. Uncertainties. The uncertainties are a function of wavelength, since three different primary standards were used in the calibration procedure. The uncertainties are summarized in Table 3.

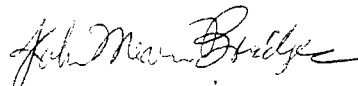
References

1. J.M. Bridges and W.R. Ott, Appl. Opt. 16, 367 (1977).
2. W.R. Ott, K. Behringer, and G. Gieres, Appl. Opt. 14, 2121 (1975).
3. G. Boldt, Space Sci. Rev. 11, 728 (1970).
4. H.J. Kostkowski, D.E. Erminy, and A.T. Hattenburg, in Advances in Geophysics, Vol. 14, p. 111 (Academic Press, New York, 1970).

For the Director,



Wolfgang L. Wiese, Chief
Atomic and Plasma Radiation
Division
Center for Radiation Research



John M. Bridges, Physicist
Atomic and Plasma Radiation
Division
Center for Radiation Research

Attachments.

Table 1. Calibrated spectral irradiance of Arc I in units of $\text{W cm}^{-2} \text{nm}^{-1}$. Values of the spectral irradiance are given for an arc current of 40.00 A, and at a distance of 50.0 cm from the center of the arc.

Wavelength (nm)	Spectral Irradiance with window #59 ($\text{W cm}^{-2} \text{nm}^{-1}$)	Transmission	
		Window #59	Window #61
335	8.22×10^{-7}	.920	.937
320	7.81×10^{-7}	.917	.936
310	7.39×10^{-7}	.915	.932
300	6.96×10^{-7}	.911	.931
290	6.49×10^{-7}	.902	.929
280	5.95×10^{-7}	.879	.922
270	5.52×10^{-7}	.871	.916
260	5.07×10^{-7}	.876	.910
250	4.63×10^{-7}	.886	.909
240	4.24×10^{-7}	.894	.910
230	3.74×10^{-7}	.894	.914
220	3.24×10^{-7}	.890	.911
210	2.76×10^{-7}	.890	.910
200	2.30×10^{-7}	.886	.904
190	1.81×10^{-7}	.873	.898
180	1.37×10^{-7}	.838	.891
170	1.03×10^{-7}	.797	.871
162	0.84×10^{-7}	.765	.851
152	0.65×10^{-7}	.719	.833

Table 2. Relative signal as a function of θ and ϕ , where θ and ϕ angles arc is rotated from optical axis. (See text and fig. 1).

θ (degrees)	-6	-5	-4	-3	-2	-1	0	1	2	3	4	5	6
6						.784	.841	.795					
5				.905	.949	.956	.956	.950	.934	.888			
4			.941	.968	.980	.984	.978	.972	.963	.950	.918		
3			.970	.990	.993	.995	.990	.989	.984	.972	.955		
2	.961	1.000	1.000	1.000	1.001	1.000	.998	.998	.992	.988	.975	.946	
1	.976	.997	.998	.998	1.000	.999	.999	.999	.997	.989	.979	.953	
0	.972	.995	.999	.999	.999	1.000	1.000	1.000	.998	.992	.984	.954	
-1	.966	.990	.999	.999	.999	1.000	1.002	1.000	.993	.988	.974	.946	
-2	.947	.981	.994	.999	.999	.999	1.001	1.000	.996	.989	.966	.941	
-3	.933	.973	.995	.995	.996	.997	.998	.996	.990	.977	.951	.914	
-4		.938		.965	.976	.987	.985	.977	.967	.949	.920		
-5				.936	.952	.959	.961	.956	.941	.922			
-6					.849	.902	.905	.897	.846				

ϕ (degrees) \longrightarrow

Table 3. Survey of emission lines present in the 40 A argon mini-arc spectrum. The spectrometer bandpass is 0.25 nm.

$\lambda(\text{nm})$	Element	Radiance of line peak relative to continuum
115.22	O I	1
116.79	N I	1
117.69	N I	0.3
118.94	C I	0.3
119.38	C I	1
119.99	N I	30
121.57	H I	100
124.33	N I	5
126.13	C I	2
127.75	C I	5
128.98	C I	1
130.22	O I	15
130.55	O I	10
131.07	N I	1
131.95	N I	0.5
132.93	C I	4
133.53	C II	8
135.58	C I	0.2
141.19	N I	0.7
143.19	C I	0.1
145.91	C I	0.1
146.33	C I	1
146.75	C I	0.1
148.18	C I	0.2
149.26	N I	4
149.47	N I	6
156.10	C I	4
157.50	Ar II	0.2
160.04	Ar II	0.2
160.35	Ar II	0.1
160.65	Ar II	0.05
165.72	C I	2
174.27	N I	1
174.53	N I	0.5
175.19	C I	0.1
187.31	Ar II	0.05
188.90	Ar II	0.1
193.09	C I	2
247.86	C I	0.05
328.0-334.0		0.1
336.5-342.5		0.15
334.5-347.0	Ar II and Ar I	0.1
348.5-350.5	(broadened lines)	0.05
353 and above		

Table 4. Uncertainties in mini-arc
spectral irradiance calibration.

Wavelength (nm)	
160-200	10%
200-330	6%

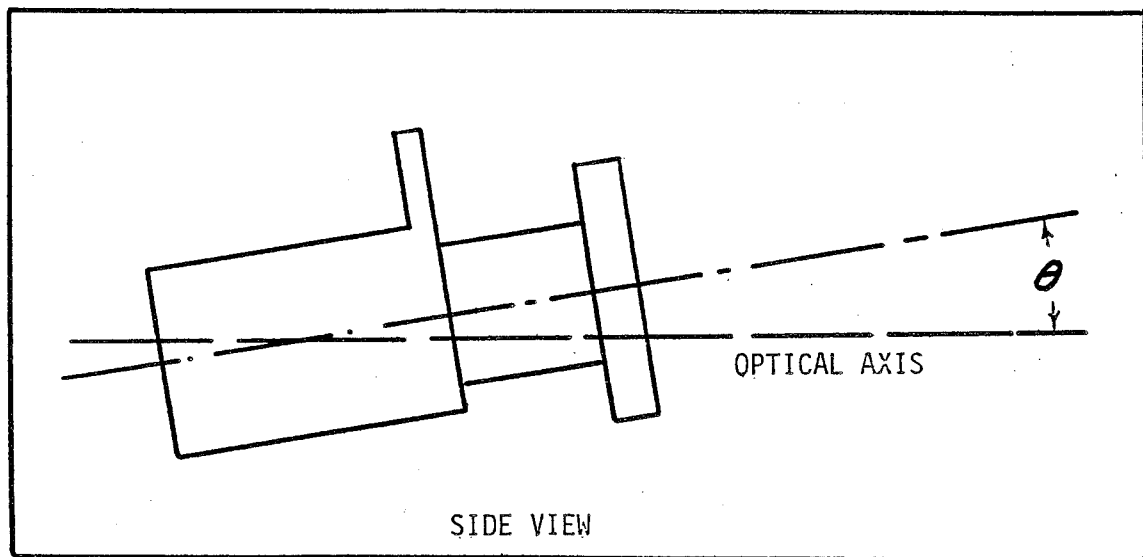
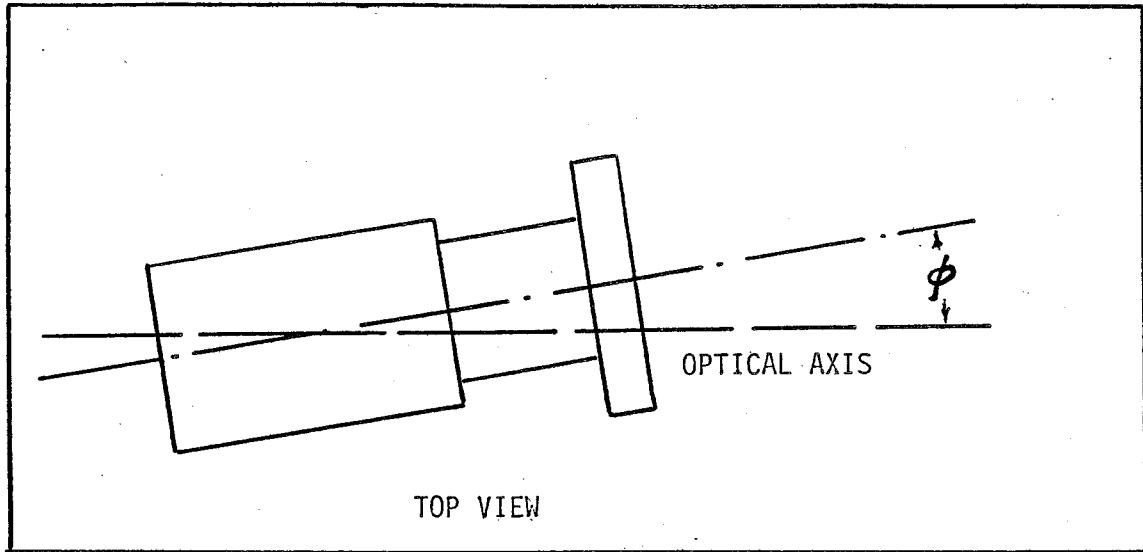


Figure 1. Diagrams defining θ and ϕ

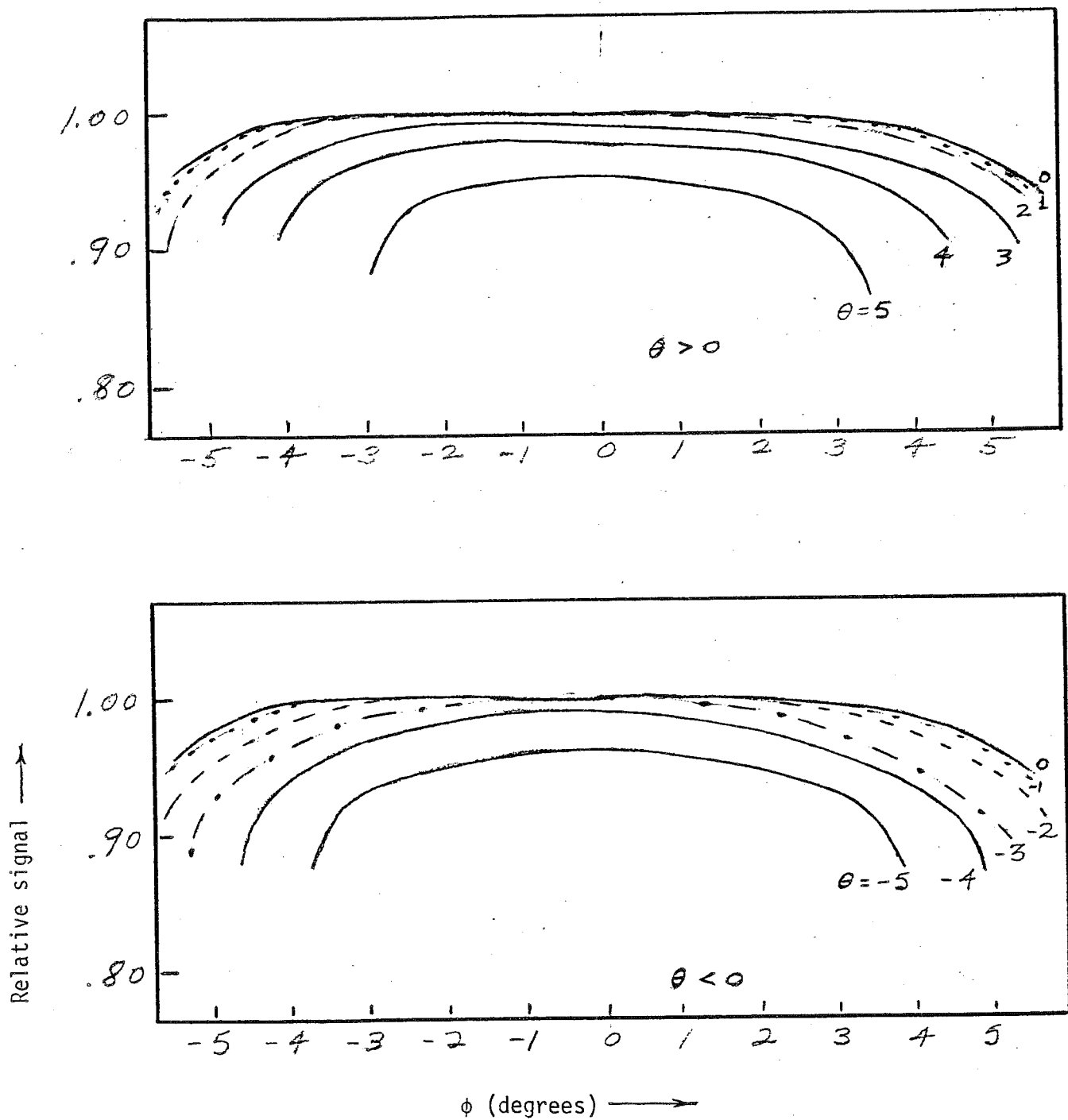


Figure 2. Relative signal vs ϕ , with θ as parameter, where θ and ϕ are angles arc is rotated from optical axis. (See text and Figure 1).

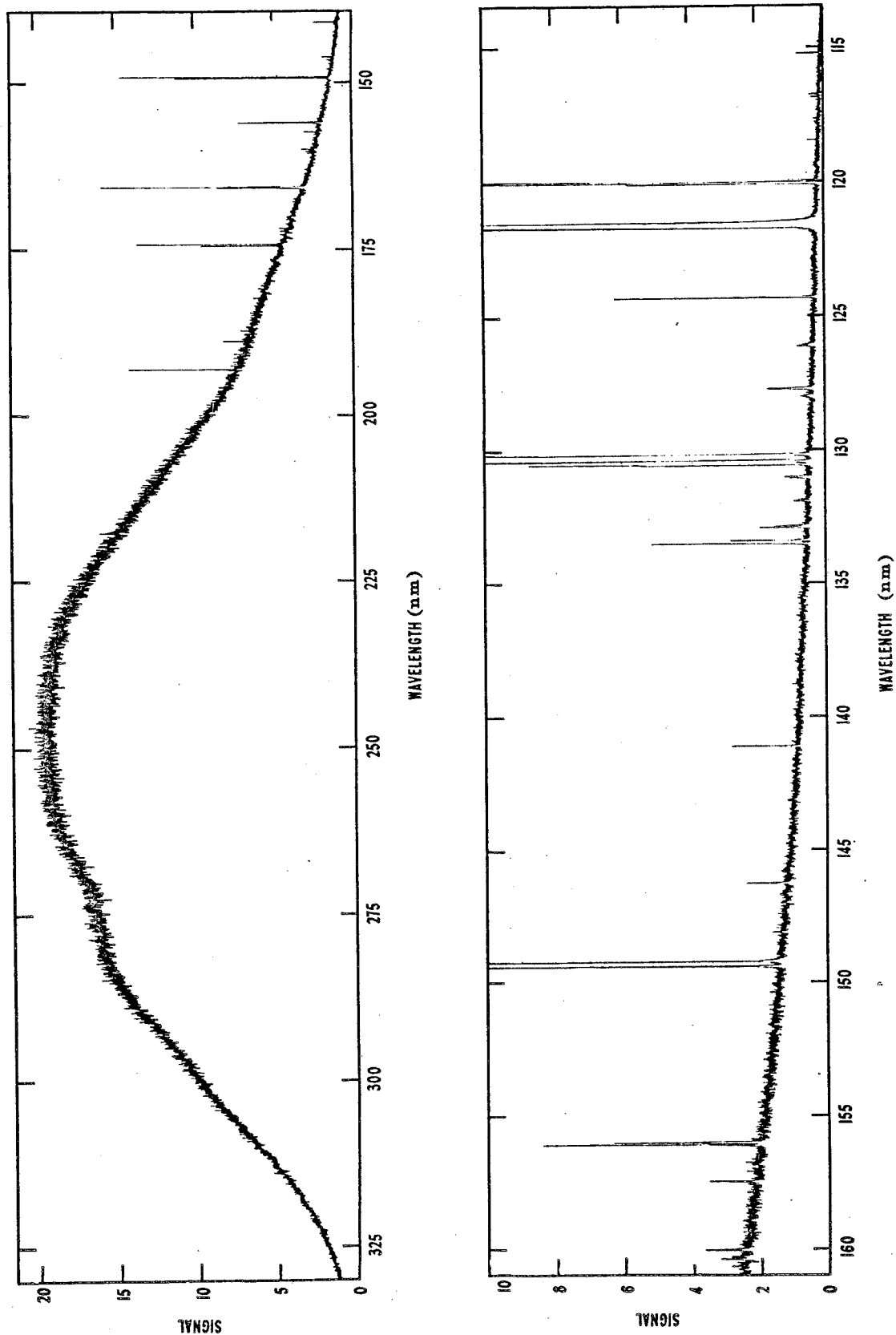


Figure 3. High resolution scan of the 40.00 A argon mini-arc spectrum. The decreasing signal above 250 nm is due to the use of a solar blind photomultiplier in the measurement system.



B6802-78

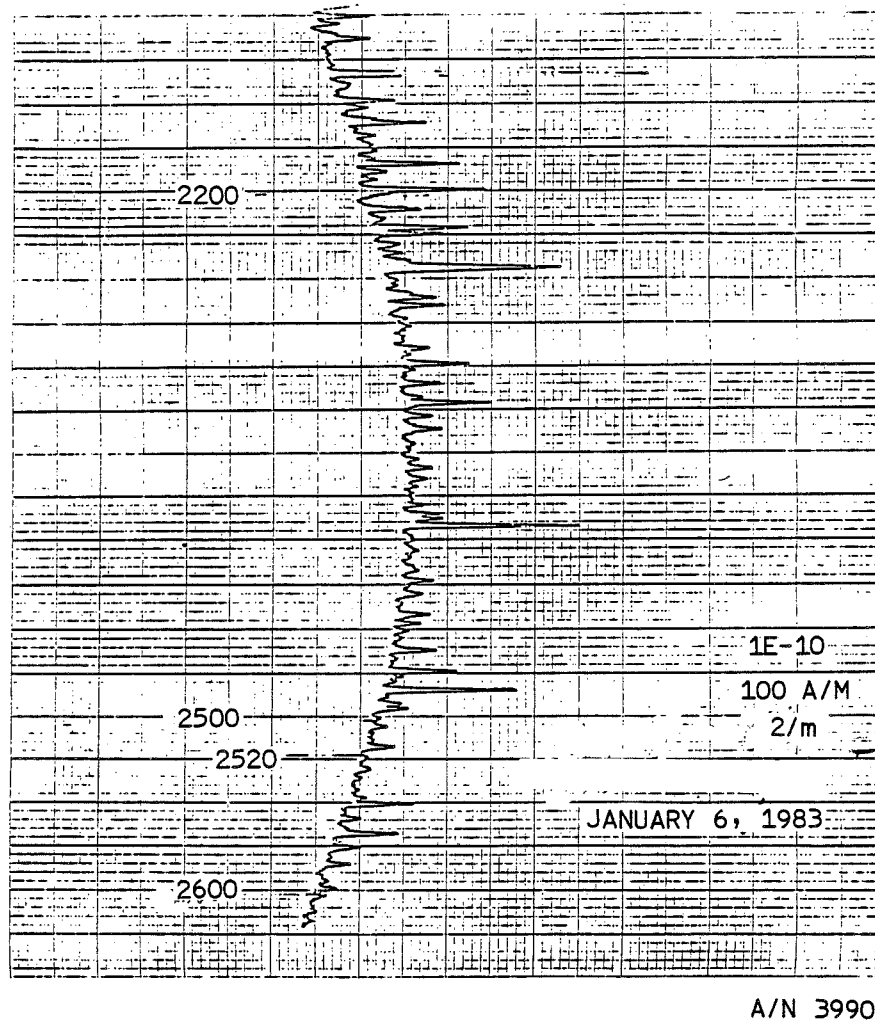
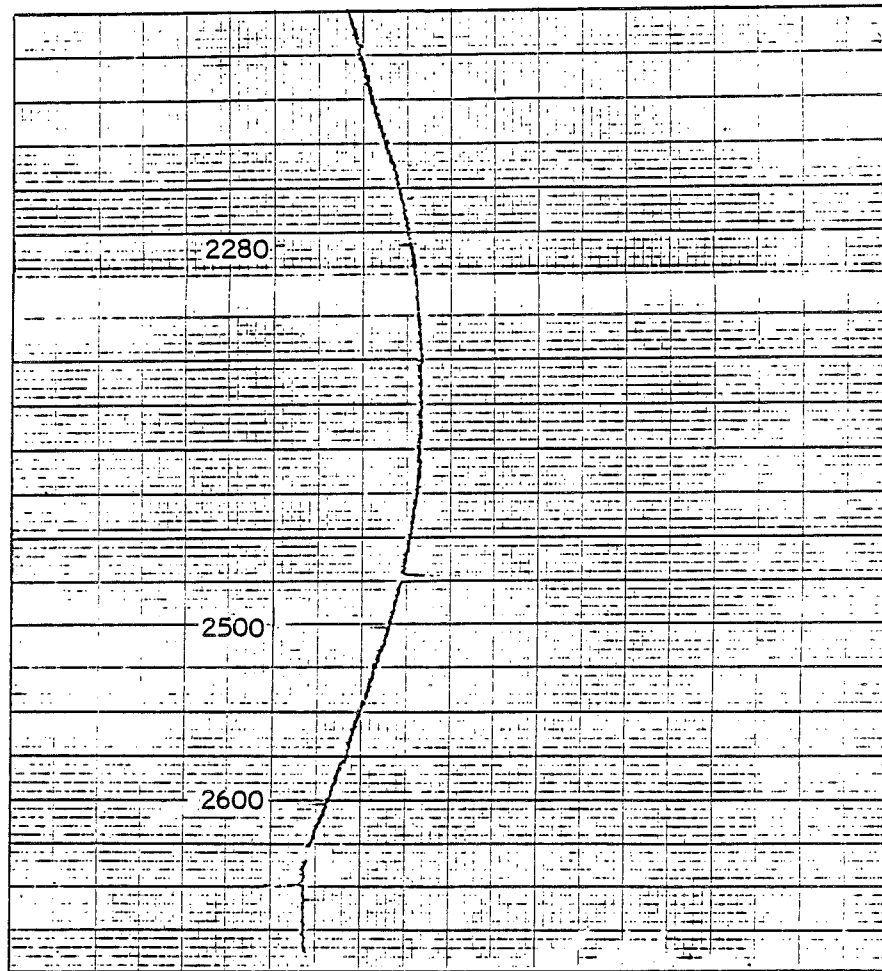


Figure 4 Emission Lines in Arcs as Calibrated in February 1982



A/N 3990

Figure 5 Emission Lines in Arcs as Calibrated in
January 1983



B6802-78

A/N 3990

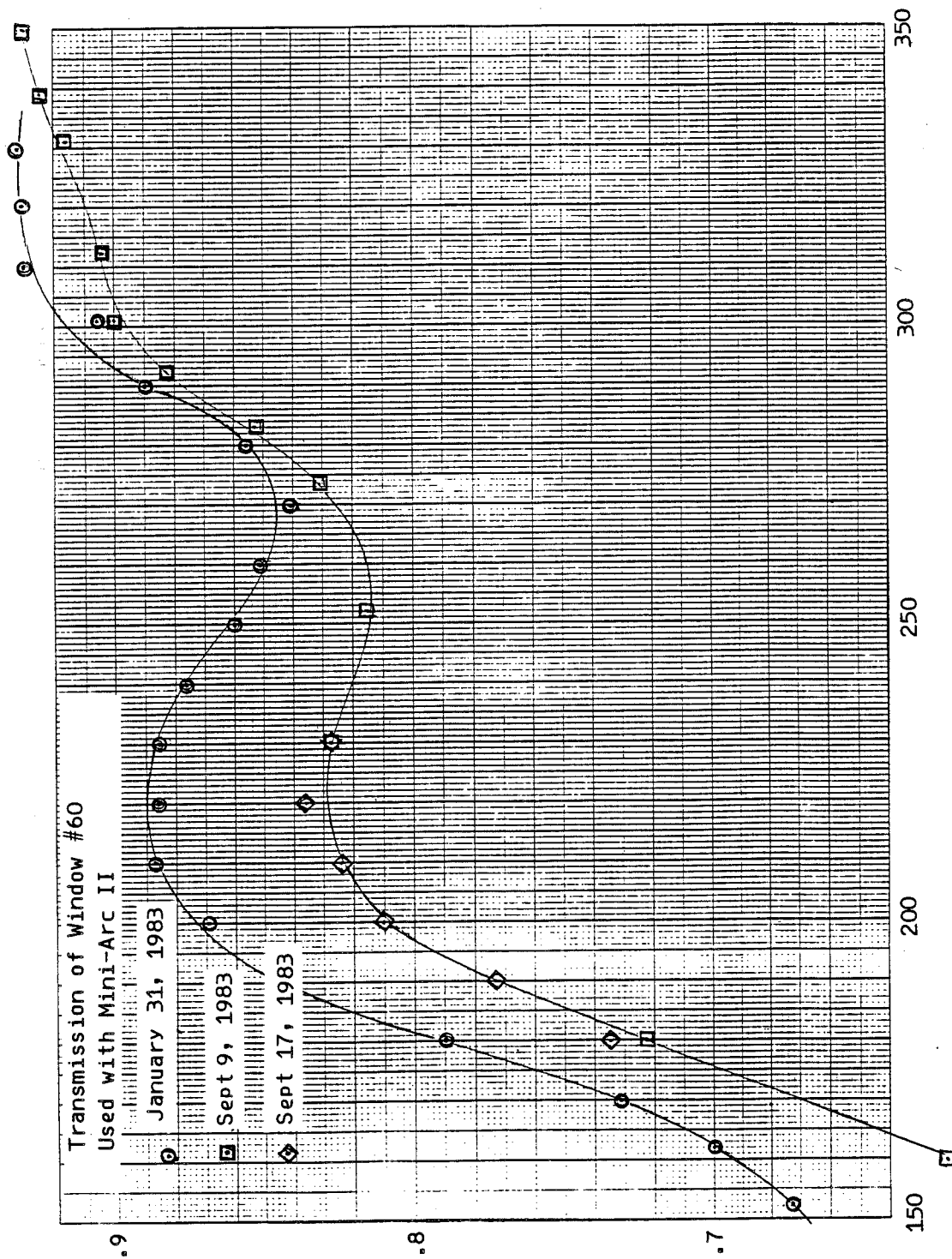


Table I. Calibrated spectral irradiance of Arc I in units of $W\text{ cm}^{-2}\text{ nm}^{-1}$. Values are given for an arc current of 40.00 A, and at a distance of 50.0 cm from the center of the arc.

Wavelength (nm)	Spectral Irradiance with window #59 $W\text{ cm}^{-2}\text{ nm}^{-1}$	Transmission, Window #59
335	8.66×10^{-7}	.923
320	8.29×10^{-7}	.919
310	7.71×10^{-7}	.919
300	7.37×10^{-7}	.915
290	6.79×10^{-7}	.898
280	6.13×10^{-7}	.870
270	5.67×10^{-7}	.858
260	5.19×10^{-7}	.860
250	4.80×10^{-7}	.873
240	4.36×10^{-7}	.885
230	3.87×10^{-7}	.888
220	3.32×10^{-7}	.886
210	2.73×10^{-7}	.880
200	2.34×10^{-7}	.869
190	1.92×10^{-7}	.854
180	1.39×10^{-7}	.816
170	0.987×10^{-7}	.772
162	0.748×10^{-7}	.750
152	0.537×10^{-7}	.711

Table II. Calibrated spectral irradiance of Arc II in units of $\text{W cm}^{-2}\text{nm}^{-1}$. Values are given for an arc current of 40.00 A, and at a distance of 50.0 cm from the center of the arc.

Wavelength (nm)	Spectral Irradiance with window #60	Transmission, Window #60
335	8.94×10^{-7}	.916
320	8.54×10^{-7}	.915
310	7.96×10^{-7}	.915
300	7.59×10^{-7}	.906
290	6.98×10^{-7}	.890
280	6.25×10^{-7}	.856
270	5.79×10^{-7}	.841
260	5.30×10^{-7}	.852
250	4.94×10^{-7}	.860
240	4.50×10^{-7}	.877
230	4.04×10^{-7}	.886
220	3.47×10^{-7}	.886
210	2.85×10^{-7}	.887
200	2.43×10^{-7}	.869
190	1.97×10^{-7}	.847
180	1.40×10^{-7}	.790
170	0.975×10^{-7}	.731
162	0.740×10^{-7}	.700
152	0.538×10^{-7}	.673

U.S. DEPARTMENT OF COMMERCE
NATIONAL BUREAU OF STANDARDS
WASHINGTON, D.C. 20234

February 22, 1982

REPORT OF CALIBRATION

VUV Spectral Irradiance of Argon Mini-Arc II

submitted by

Ball Aerospace Systems Division
P.O. Box 1062 Bldr Indust Pk
Boulder, Colorado 80306

An Argon mini-arc light source, labeled "II", was calibrated for spectral irradiance in the wavelength range 152 nm to 335 nm based upon the NBS argon mini-arc¹. The latter is a secondary standard of spectral radiance and had been calibrated previously at 40.00 Å with three primary radiometric radiance standards, the NBS wall-stabilized hydrogen arc² from 140 nm to 335 nm, a plasma blackbody-line radiator³ from 114.5 nm to 165.6 nm, and a tungsten strip lamp from 250 nm to 335 nm. The overlap of the wavelength bands of applicability of these three standards ensured consistency of the calibration base.

A brief description of the method used to transfer from a spectral radiance source (the NBS mini-arc) to a spectral irradiance source follows. The calibrated area of the NBS mini-arc is the central 0.3 mm diameter region where the discharge is approximately homogeneous. In order to use this radiance source to calibrate the irradiance of another source, the radiation of the NBS arc from outside the central 0.3 mm region must be blocked. This was done by the use of a set of two collimating apertures located between the arc and the spectrometer. (One aperture also served as the entrance aperture to the spectrometer.) The response of the spectroradiometer to the radiation from the region of the arc axis is then a relative measure of the sensitivity as a function of wavelength. For measuring the irradiance from the source to be calibrated, the aperture closest to the source was removed, so that the complete area of the unknown source was seen by the spectrometer. To account for slightly different solid angles of radiation entering the spectrometer from the two different sources, a diffuser was placed behind the spectrometer entrance aperture for both measurements.

The above measurements determine the irradiance of the unknown source from 160-330 nm, but only on a relative scale. To get an absolute scale, the irradiance of the unknown source is compared at 250 nm only to that of a calibrated FEL irradiance standard. For this measurement, an integrating sphere is used at the entrance aperture to a double

spectrometer. The double spectrometer is necessary for rejecting scattered radiation from outside the desired wavelength bandpass, especially from the tungsten FEL lamp. Both sources were placed 50 cm from the aperture of the integrating sphere.

The spectral irradiance of the mini-arc, in units of $\text{W cm}^{-2} \text{ nm}^{-1}$, is listed in Table 1 for an arc current of 40.00 A.

The values of spectral irradiance listed in Table 1 apply to the radiation emitted by the mini-arc light source through a sealing window. Also listed in Table 1 is the transmission of the MgF_2 ultraviolet window attached to the light source and that of an additional MgF_2 window. The spectral irradiance of the arc plasma itself is obtained by dividing the values given in Table 1 by the transmission of the appropriate window. The spectral irradiance of the light source using another window, for example window 2 is then obtained by multiplying the quotient by its transmission, for example

$$E_{\lambda}(\#2) = \frac{E_{\lambda}(\#1)}{T(\#1)} \times T(\#2) \quad \text{(where, for example, the arc was calibrated with window \#1)}$$

In this way damage to the arc window does not result in the loss of a calibrated light source. Also, it is possible through such substitution of a calibrated window, to periodically check for deterioration of the window due to, for example, condensation on the window of uv-photodissociated hydrocarbons in the vacuum system.

1. Calibration Conditions. A continuous flow of high purity (research grade) argon, with total gas cylinder impurities quoted to be less than 10 ppm (99.999% pure), was used to purge the arc source. The total flow was 5000 cc min^{-1} and was divided equally in a gas manifold and directed to the three input gas ports. The output ports vented directly into the laboratory. The pressure in the arc chamber was equal to the ambient pressure, measured to be 1.00 atm, or 760 mm Hg, $\pm 1\%$.

The arc was ignited by shorting out the anode (+) and cathode (-) with a tungsten striking rod inserted into the arc channel. After ignition, the cathode was withdrawn from the arc axis by unscrewing the cathode holder exactly five rotations from its inwardmost position.

The current was measured using a calibrated shunt, leads, and digital voltmeter.

The optical conditions for which the calibration is appropriate are as follows:

a) The arc was aligned with its axis of symmetry along the optical path. The center arc plate of the arc was 50 cm from the entrance

aperture, which was 1mm x 2mm.

b) The spectrometer resolution was 0.8 nm.

c) A short gas cell is located between the mini-arc and the vacuum system. It is normally purged with high purity argon at atmospheric pressure. Thus, the mini-arc uv window is not exposed to vacuum system contaminants during a calibration.

2. Mini-Arc Characteristics and Goniometry. The mini-arc calibrated is a modified version of similar arcs previously calibrated. The modification resulted in approximately uniform radiation over a much larger solid angle than that characteristic of earlier mini-arcs. In addition, the ignition of the arc was greatly facilitated.

By measuring signals as the arc was rotated about its center, the irradiance was mapped over the major part of the solid angle irradiated by the arc. Measurements of the irradiance at 320 and 220 nm were taken at 1 degree increments for both θ and ϕ , where θ is the angle about a horizontal axis thorough the arc center and ϕ is the angle about a vertical axis (See Fig. 1) The results are given in Table 2 and in Fig. 2. Values in the table and figure are relative to the irradiance for $\theta = \phi = 0$, i.e. where the arc is aligned with the optical axis. The angular resolution for these measurements was ± 0.3 degrees for both θ and ϕ . The data at 320 and 220 nm showed no significant difference as far as relative signal vs angles θ and ϕ .

The irradiance of the mini-arc is a function of pressure. The values in Table 1 apply to an ambient pressure of 1 atm. The irradiance at other pressures is given by

$$L(p) = (1.2 p - 0.2) L(0)$$

where p is the pressure in atmosphere and $L(0)$ is the irradiance at 1 atm. This relation holds for all wavelengths.

Tests have shown that the MgF_2 window is the component most likely to cause a systematic change in the arc irradiance. Measurements on the NBS arc indicated a negligible change in the irradiance of the arc plasma itself after 24 hrs continuous operation. Window deterioration may arise from radiation damage or from vacuum system hydrocarbons. Some windows have shown a wavelength dependent change in transmission of a few percent after several hours use. Therefore, periodic checking of the window transmission is recommended, as described on page 1.

The ultraviolet continuum spectrum is interrupted by several atomic and ionic emission lines, mainly in the wavelength region from 114 nm to 135 nm. These lines arise from air and water vapor impurities in the argon gas cylinder, the gas handling system, and the outgassing

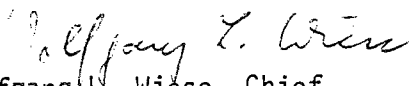
arc chamber. Table 3 lists the wavelengths where these lines occur for an arc current of 40 A and indicates the relative intensity of the lines relative to the argon continuum for a bandpass of 0.25 nm. Figure 3 is a strip chart recording of a photoelectric scan of the spectrum under these conditions. The width of the lines is instrument-limited in this case. High resolution measurements indicate that all the lines have a halfwidth of about 0.01 nm.

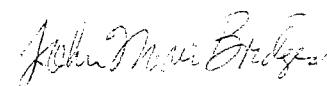
3. Uncertainties. The uncertainties are a function of wavelength, since three different primary standards were used in the calibration procedure. The uncertainties are summarized in Table 3.

References

1. J.M. Bridges and W.R. Ott, Appl. Opt. 16, 367 (1977).
2. W.R. Ott, K. Behringer, and G. Gieres, Appl. Opt. 14, 2121 (1975).
3. G. Boldt, Space Sci. Rev. 11, 728 (1970).
4. H.J. Kostkowski, D.E. Erminy, and A.T. Hattenburg, in Advances in Geophysics, Vol. 14, p. 111 (Academic Press, New York, 1970).

For the Director,


Wolfgang L. Wiese, Chief
Atomic and Plasma Radiation
Division
Center for Radiation Research


John M. Bridges, Physicist
Atomic and Plasma Radiation
Division
Center for Radiation Research

Attachments.

Table 1. Calibrated spectral irradiance of Arc II in units of $\text{W cm}^{-2} \text{ nm}^{-1}$. Values of the spectral irradiance are given for an arc current of 40.00 A, and at a distance of 50.0 cm from the center of the arc.

Wavelength (nm)	Spectral Irradiance with window #60 ($\text{W cm}^{-2} \text{ nm}^{-1}$)	Transmission	
		Window #60	Window #62
335	8.52×10^{-7}	.918	.938
320	8.09×10^{-7}	.916	.935
310	7.66×10^{-7}	.913	.931
300	7.22×10^{-7}	.912	.929
290	6.74×10^{-7}	.902	.924
280	6.18×10^{-7}	.877	.914
270	5.73×10^{-7}	.868	.904
260	5.26×10^{-7}	.874	.900
250	4.82×10^{-7}	.884	.904
240	4.42×10^{-7}	.889	.909
230	3.90×10^{-7}	.899	.912
220	3.38×10^{-7}	.896	.914
210	2.88×10^{-7}	.894	.912
200	2.39×10^{-7}	.886	.909
190	1.88×10^{-7}	.869	.904
180	1.42×10^{-7}	.836	.891
170	1.07×10^{-7}	.798	.872
162	$.882 \times 10^{-7}$.775	.860
152	$.694 \times 10^{-7}$.753	.850

Table 2. Relative signal as a function of θ and ϕ , where θ and ϕ angles are rotated from optical axis. (See text and fig. 1).

θ (degrees)	-6	-5	-4	-3	-2	-1	0	1	2	3	4	5	6
6						.689	.749	.692					
5				.855	.934	.953	.956	.946	.934	.856			
4			.908	.967	.975	.978	.978	.978	.966	.949	.911		
3	.884	.956	.988	.992	.992	.989	.989	.989	.981	.972	.956	.894	
2	.917	.970	.992	.994	.992	.992	.994	.991	.986	.981	.966	.939	
1	.850	.940	.987	1.005	1.000	1.000	1.000	.999	.999	.994	.983	.961	.840
0	.876	.957	.992	1.005	.997	1.001	1.000	1.000	1.002	1.000	.994	.975	.878
-1	.863	.955	1.006	1.012	1.010	1.001	1.003	1.005	1.001	.997	.990	.977	.886
-2		.932	.979	1.004	1.005	1.001	1.004	1.005	1.004	.995	.983	.949	
-3		.901	.956	.983	1.005	1.003	1.000	1.003	.999	.983	.963	.935	
-4			.924	.962	.985	.995	.990	.990	.990	.976	.951		
-5			.819	.910	.941	.966	.979	.966	.954	.933	.830		
-6				.665	.865	.910	.919	.914	.881	.666			

ϕ (degrees) \longrightarrow

Table 3. Survey of emission lines present in the 40 A argon mini-arc spectrum. The spectrometer bandpass is 0.25 nm.

$\lambda(\text{nm})$	Element	Radiance of line peak relative to continuum
115.22	O I	1
116.79	N I	1
117.69	N I	0.3
118.94	C I	0.3
119.38	C I	1
119.99	N I	30
121.57	H I	100
124.33	N I	5
126.13	C I	2
127.75	C I	5
128.98	C I	1
130.22	O I	15
130.55	O I	10
131.07	N I	1
131.95	N I	0.5
132.93	C I	4
133.53	C II	8
135.58	C I	0.2
141.19	N I	0.7
143.19	C I	0.1
145.91	C I	0.1
146.33	C I	1
146.75	C I	0.1
148.18	C I	0.2
149.26	N I	4
149.47	N I	6
156.10	C I	4
157.50	Ar II	0.2
160.04	Ar II	0.2
160.35	Ar II	0.1
160.65	Ar II	0.05
165.72	C I	2
174.27	N I	1
174.53	N I	0.5
175.19	C I	0.1
187.31	Ar II	0.05
188.90	Ar II	0.1
193.09	C I	2
247.86	C I	0.05
328.0-334.0		0.1
336.5-342.5		0.15
334.5-347.0	Ar II and Ar I	0.1
348.5-350.5	(broadened lines)	0.05
353 and above		

Table 4. Uncertainties in mini-arc
spectral irradiance calibration.

Wavelength (nm)	
160-200	10%
200-330	6%

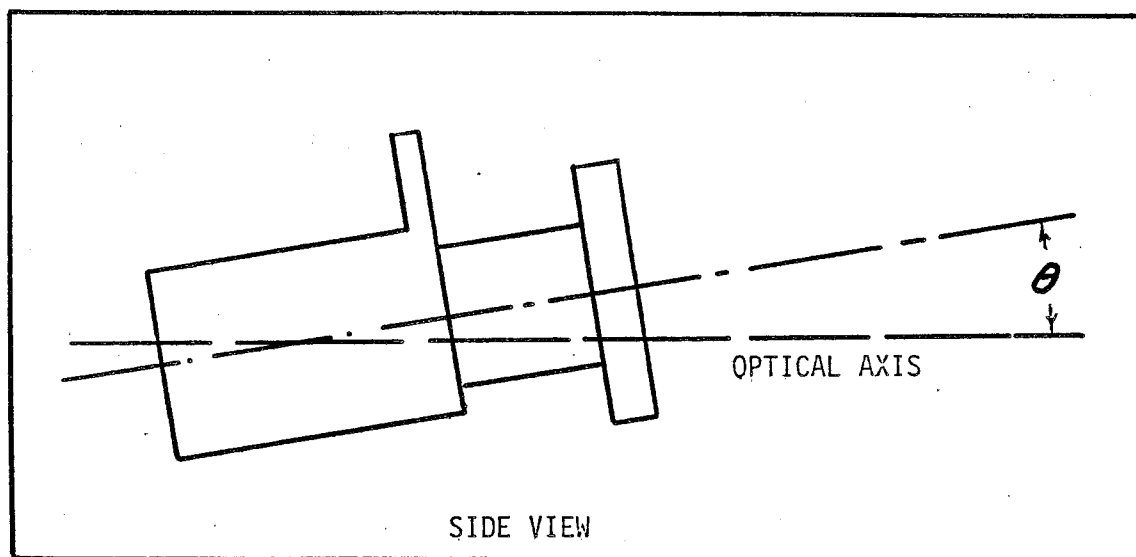
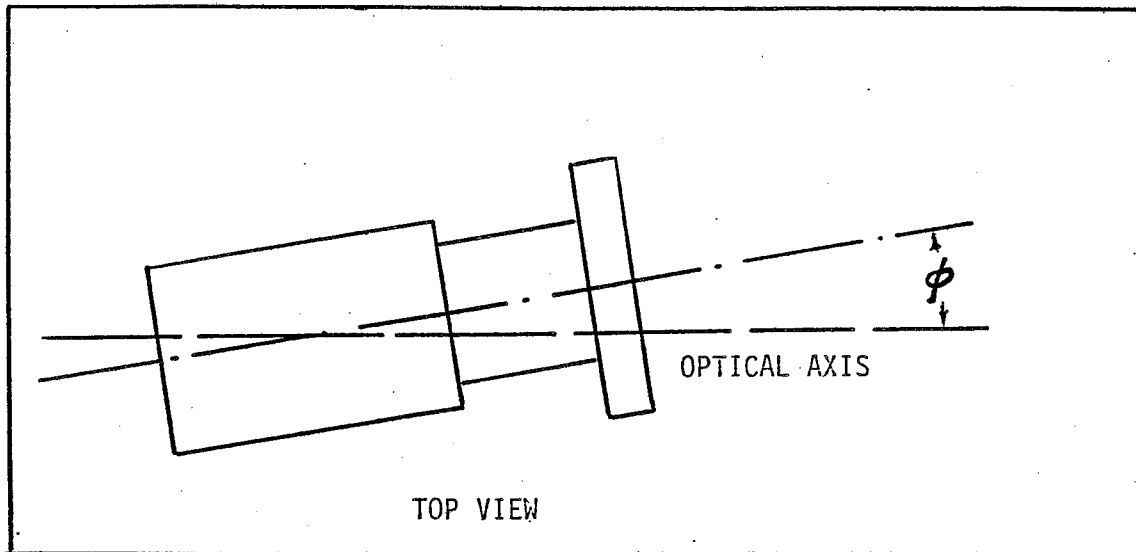


Figure 1. Diagrams defining θ and ϕ

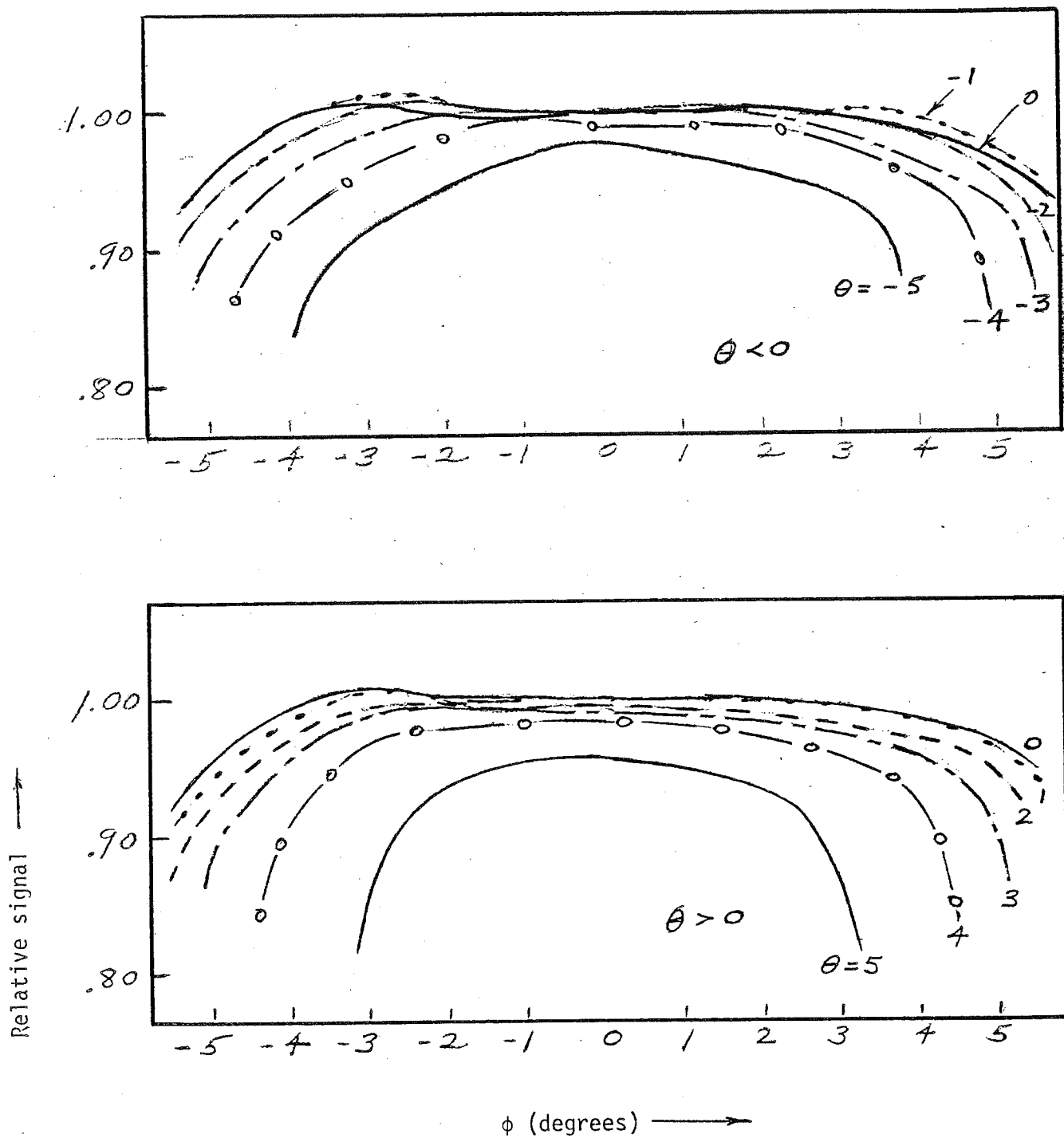


Figure 2. Relative signal vs ϕ , with θ as parameter, where θ and ϕ are angles arc is rotated from optical axis. (See text and Figure 1).

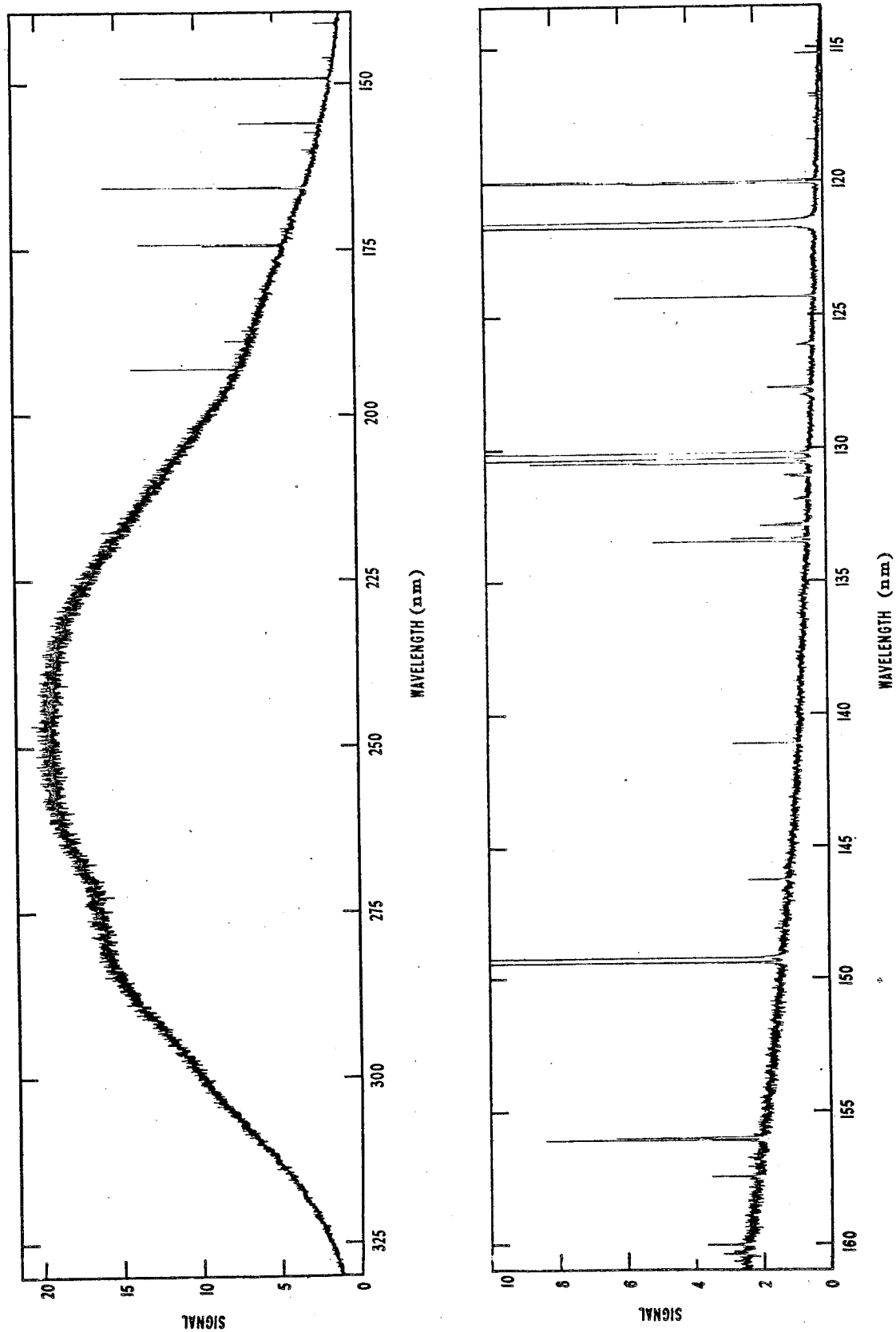


Figure 3. High resolution scan of the 40.00 Å argon mini-arc spectrum. The decreasing signal above 250 nm is due to the use of a solar blind photomultiplier in the measurement system.



B6802-78

The following arc window measurements were done
at BASD September 9 through 14, 1983
after completion of SBUV/2 calibration.



B6802-78

DATE: 9-9-83

WINDOW S/N 59

Wavelength nm	% Transmission
160.0	67.9
180.0	75.5
230.0	85.3
252.0	85.0
273.5	86.4
283.0	88.3
292.2	90.5
301.9	92.1
312.5	92.5
331.2	92.8
339.8	92.8
350.0	93.0
375.0	93.0
400.0	93.9



B6802-78

DATE: 9-9-83

WINDOW S/N 60

Wavelength nm	% Transmission
160.0	61.7
180.0	72.3
230.0	82.7
252.0	81.5
273.5	83.1
283.0	85.3
292.2	88.3
301.9	90.0
312.5	90.2
331.2	90.8
339.8	91.3
350.0	91.1
375.0	91.5
400.0	92.7



B6802-78

DATE: 9-12-83

WINDOW S/N 60

Wavelength nm	% Transmission
180.0	73.5
190.0	77.3
200.0	79.0
210.0	80.4
220.0	81.6
230.0	82.7



B6802-78

DATE: 9-12-83

WINDOW S/N 59

Wavelength nm	% Transmission
180.0	77.2
190.0	80.3
200.0	82.1
210.0	83.8
220.0	84.8
230.0	85.7



B6802-78

DATE: 9-14-83WINDOW S/N 59

After Cleaning

Wavelength nm	% Transmission
160	81.2
170	78.3
180	77.5
190	80.0
200	81.9
210	83.9
220	85.3
230	86.3
252	85.7
273.5	86.4
283	88.0
292.2	90.8
301.9	91.8
312.5	92.4
331.2	93.1
339.8	93.3
350.0	93.2
375.0	93.2
400	93.8



B6802-78

DATE: 9-14-83

WINDOW S/N 60

After Cleaning

Wavelength nm	% Transmission
160.0	74.6
170.0	78.5
180.0	76.0
190.0	79.0
200.0	80.7
210.0	82.5
220.0	84.3
230.0	84.8
252.0	83.1
273.5	83.8
283.0	86.1
292.2	89.1
301.9	90.6
312.5	91.2
331.2	92.0
339.8	92.3
350.0	92.2
375.0	92.2
400.0	92.8



B6802-78

3.3 CALIBRATION OF DEUTERIUM LAMPS

For a complete report refer to U.S. Department of Commerce National Bureau of Standards Report of Calibration

NBS Test No.: 534/226445-1

and

NBS Test No.: 534/226445-3



UNITED STATES DEPARTMENT OF COMMERCE
National Bureau of Standards
Washington, D.C. 20234

NOV 17 1981

In reply refer to: 534/226445-1
534/226445-2
534/226445-3

Ball Aerospace Systems Division
P. O. Box 1062
Boulder Industrial Park
Boulder, Colorado 80306

Subject: Deuterium Lamp Standard
of Spectral Irradiance

Order No.: 35519 dated September 4, 1981

Gentlemen:

Enclosed are results of the tests that you requested in the above reference. Please refer to the above file numbers in any later communication concerning these tests.

Sincerely,

Original signed by
Klaus D. Mielenz

Klaus D. Mielenz, Acting Chief
Radiometric Physics Division
Center for Radiation Research

Material Tested:

Three bi-post deuterium lamps

Enclosure:

Three Reports of Calibration
One Report "Deuterium Lamp Standards of Spectral Irradiance-1981"

U.S. DEPARTMENT OF COMMERCE
NATIONAL BUREAU OF STANDARDS
WASHINGTON, D.C. 20234

REPORT OF CALIBRATION

of

One Deuterium Lamp Standard of
Spectral Irradiance

Supplied to

Ball Aerospace Systems Division
P. O. Box 1062
Boulder Industrial Park
Boulder, Colorado 80306

(See your Purchase Order No. 35519 dated September 4, 1981.)

1. Material

One deuterium lamp potted in a black anodized medium bi-post base has been supplied by NBS for this calibration. The lamp designation, YE-939 is painted on the ceramic insulator on the side of the lamp anode shield.

2. Calibration

The lamp was calibrated using the equipment and procedures described in the enclosed report, "Deuterium Lamp Standards of Spectral Irradiance-1981". Note particularly paragraph III of this enclosure, which describes the orientation and operation of a test lamp.

3. Results

The results of this test are given in the attached Table 1. See also paragraph IV of the enclosure for a discussion of the uncertainty of the reported values.

For the Director,

Original signed by
Klaus D. Mielenz

Klaus D. Mielenz, Acting Chief
Radiometric Physics Division
Center for Radiation Research

NBS Test No.: 534/226445-1

Date: November 17, 1981

Page 1 of 2

REPORT OF CALIBRATION
Ball Aerospace Systems Division

TABLE 1

Spectral Irradiance of Lamp No. YE-939 at a distance of 50.0 cm for a current of 300 mA when operated as outlined in paragraph III of the attached report, "Deuterium Lamp Standards of Spectral Irradiance-1981".

WAVELENGTH (nm)	SPECTRAL IRRADIANCE (W/cm ³)
200	0.463
210	.449
220	.434
230	.415
240	.391
250	.331
260	.281
270	.242
280	.206
290	.176
300	.150
310	.130
320	.112
330	.098
340	.086
350	.077

NBS Test No.: 534/226445-1

Date: November 17, 1981

Page 2 of 2

U.S. DEPARTMENT OF COMMERCE
NATIONAL BUREAU OF STANDARDS
WASHINGTON, D.C. 20234

REPORT OF CALIBRATION

of

One Deuterium Lamp Standard of
Spectral Irradiance

Supplied to

Ball Aerospace Systems Division
P. O. Box 1062
Boulder Industrial Park
Boulder, Colorado 80306

(See your Purchase Order No.35519 dated September 4, 1981.)

1. Material

One deuterium lamp potted in a black anodized medium bi-post base has been supplied by NBS for this calibration. The lamp designation, YE-959 is painted on the ceramic insulator on the side of the lamp anode shield.

2. Calibration

The lamp was calibrated using the equipment and procedures described in the enclosed report, "Deuterium Lamp Standards of Spectral Irradiance-1981". Note particularly paragraph III of this enclosure, which describes the orientation and operation of a test lamp.

3. Results

The results of this test are given in the attached Table 1. See also paragraph IV of the enclosure for a discussion of the uncertainty of the reported values.

For the Director,

Original signed by
Klaus D. Mielenz

Klaus D. Mielenz, Acting Chief
Radiometric Physics Division
Center for Radiation Research

NBS Test No.: 534/226445-2

Date: November 17, 1981

Page 1 of 2

REPORT OF CALIBRATION
Ball Aerospace Systems Division

TABLE 1

Spectral Irradiance of Lamp No. YE-959 at a distance of 50.0 cm for a current of 300 mA when operated as outlined in paragraph III of the attached report, "Deuterium Lamp Standards of Spectral Irradiance-1981".

WAVELENGTH (nm)	SPECTRAL IRRADIANCE (W/cm ³)
200	0.506
210	.481
220	.455
230	.425
240	.394
250	.328
260	.275
270	.234
280	.198
290	.168
300	.143
310	.123
320	.107
330	.094
340	.083
350	.074

NBS Test No.: 534/226445-2

Date: November 17, 1981

U.S. DEPARTMENT OF COMMERCE
NATIONAL BUREAU OF STANDARDS
WASHINGTON, D.C. 20234

REPORT OF CALIBRATION

of

One Deuterium Lamp Standard of
Spectral Irradiance

Supplied to

Ball Aerospace Systems Division
P. O. Box 1062
Boulder Industrial Park
Boulder, Colorado 80306

(See your Purchase Order No.35519 dated September 4, 1981.)

1. Material

One deuterium lamp potted in a black anodized medium bi-post base has been supplied by NBS for this calibration. The lamp designation, YE-964 is painted on the ceramic insulator on the side of the lamp anode shield.

2. Calibration

The lamp was calibrated using the equipment and procedures described in the enclosed report, "Deuterium Lamp Standards of Spectral Irradiance-1981". Note particularly paragraph III of this enclosure, which describes the orientation and operation of a test lamp.

3. Results

The results of this test are given in the attached Table 1. See also paragraph IV of the enclosure for a discussion of the uncertainty of the reported values.

For the Director,

[Signature]
Klaus D. Mielenz

Klaus D. Mielenz, Acting Chief
Radiometric Physics Division
Center for Radiation Research

NBS Test No.: 534/226445-3

Date: November 17, 1981

REPORT OF CALIBRATION
Ball Aerospace Systems Division

TABLE 1

Spectral Irradiance of Lamp No. YE-964 at a distance of 50.0 cm for a current of 300 mA when operated as outlined in paragraph III of the attached report, "Deuterium Lamp Standards of Spectral Irradiance-1981".

WAVELENGTH (nm)	SPECTRAL IRRADIANCE (W/cm ³)
200	0.508
210	.485
220	.461
230	.432
240	.401
250	.336
260	.283
270	.242
280	.204
290	.174
300	.149
310	.128
320	.112
330	.098
340	.087
350	.077

NBS Test No.: 534/226445-3

Date: November 17, 1981



3.4 DIFFUSERS

For a complete report refer to U.S. Department of Commerce National Bureau of Standards Report of Calibration NBS Test No.: 534/97D-83.



UNITED STATES DEPARTMENT OF COMMERCE
National Bureau of Standards
Washington, D.C. 20234

DCT 18 1983

In reply refer to: 534/97D-83

Ball Aerospace Systems Division
Attn: William Fowler
P. O. Box 1062
Boulder, Colorado 80306

Subject: 6°/Hemispherical Reflectance
and Bidirectional Reflectance
Distribution Function (BRDF)
of 8 BaSO₄ Diffuser Plates and
1 Aluminum Diffuser Plate

Order No.: Reference Letter Dated Sept. 9,
1983 from SBUV/2 Technical
Officer, NASA/GSFC Metsat
351-3450, signed by F. G.
Cunningham.

Gentlemen:

Enclosed are results of the test which you requested in the above
reference. Please refer to the above file number in any later communication
concerning this test.

Sincerely,

Klaus D. Mielenz

Klaus D. Mielenz, Chief
Radiometric Physics Division
Center for Radiation Research

NBS Cost Center 5342600

Enclosure:

One Report of Test
NBS Monograph 160
NBS Tech. Note 594-11
1 reprint
1 figure
8 tables

U.S. DEPARTMENT OF COMMERCE
NATIONAL BUREAU OF STANDARDS
WASHINGTON, D.C. 20234

REPORT OF TEST

for
6°/Hemispherical Reflectance Factor
and
Bidirectional Reflectance Distribution Function (BRDF)
of
8 BaSO₄ Diffuser Plates
and
1 Aluminum Diffuser Plate

Submitted by

Ball Aerospace Systems Division
Attn: William Fowler
P. O. Box 1062
Boulder, Colorado 80306

(Reference Letter dated Sept. 9, 1983 from SBUV/2 Technical Officer, NASA/GSFC Metsat Project/480, Cost Center No. 531-3450, signed by F. G. Cunningham.)

1. Purpose

The purpose of this test is to measure: (1) the 6°/hemispherical reflectance factor of 8 BaSO₄ diffuser plates and 1 aluminum diffuser plate, and (2) the bidirectional reflectance distribution function (BRDF) of selected BaSO₄ diffusers and the aluminum diffuser. The conditions of illumination and viewing for the BRDF measurements are illustrated in Figure 1. A complete definition of BRDF is given in a copy of NBS Monograph 160 accompanying this test. A complete description of the NBS reference spectrophotometer for diffuse reflectance and the NBS reference specular reflectometer that were used for the measurements reported in this test are given in references 1 and 2.

2. Materials

The materials submitted for measurement and the dates on which they were measured are listed below for the 6°/hemispherical and the BRDF measurements. The results of the measurements are listed in the indicated tables.

NBS Test No.: 534/97D-83

Date: October 3, 1983

Specimen ID		6°/Hemispherical	BRDF
BaSO ₄ (2"x2")	No. 1	Aug. 19 (table 2)	Sept. 2 (table 5)
"	" 2	Aug. 19 (table 2)	
"	" 3	Aug. 18 (table 1)	
" (3"x4")	" 1	Aug. 19 (table 2)	
"	" 2	Aug. 19 (table 2)	Sept. 7 (table 6)
"	" 3	Aug 18 (table 1) Sept. 20 (table 3)	Sept. 1 (table 4) Sept. 14 (table 7)
" (12"x12")	" 3	Aug. 18 (table 1)	
"	" B	Sept. 20 (table 3)	
Aluminum (3"x4"	No.5083	Sept. 20 (table 3)	Sept. 14 (table 8)

3. Measurements of 6°/Hemispherical Reflectance Factor

Measurements of 6°/hemispherical reflectance factor were made by means of the NBS reference spectrophotometer for diffuse reflectance (see reference 1). The spectral passband was 10 nm. Measurements were made at the 12 requested wavelengths (see wavelength listing in Tables 1 through 3) with the sample beam incident on the specimens at 6° from the normal. The specular component of the reflected sample beam is included in the measurement of 6°/hemispherical reflectance factor. The sample beam illuminates an area of 12 mm by 18 mm in the center of the specimen.

Three specimens of freshly prepared pressed Halon powder are measured before and after the test specimens. These measurements and the absolute (reflectance relative to a perfect diffuser) of the Halon are used in the data reduction to adjust the measured reflectances of the test specimens to the absolute reflectance scale (see reference 3). The 6°/hemispherical reflectance factor for the test specimens is reported in Tables 1 through 3.

4. Measurements of Bidirectional Reflectance Distribution Function (BRDF)

Measurements of BRDF for the geometrical conditions specified in Figure 1 were made by means of the NBS Reference Specular Reflectometer and NBS Reference Spectrophotometer for Diffuse Reflectance (see references 1 and 2).

NBS Test No.: 534/97D-83

Date: October 3, 1983

Measurements were made at each specified wavelength and angle of viewing for two polarizations. Because of the low signal levels associated with this type of reflectance measurement, a step-down technique was used in order to expand the lower range of the photometric scale for the specimen measurement. This was accomplished through the use of a specular black glass of approximately 4% specular reflectance. The absolute reflectance of the black glass was determined by direct techniques for measuring specular reflectance. Measurements of the test specimens were then made relative to the black glass for each specified wavelength, angle of viewing, and polarization. The ratio of the reflected radiance of the test specimens to the incident irradiance was later computed, using the black glass reflectance data to establish the absolute scale for the BRDF reflectance values of the test specimens. The data for the two polarizations were averaged. The results of the data reduction are listed in Tables 4 through 8.

5. Specification of the Detector Limiting Aperture Solid Angle and Projected Solid Angle

The average solid angle and average projected solid angle of the limiting aperture of the detector were determined for each viewing angle by measurement of the distance of the limiting aperture from the specimen plane and the diameter of the aperture. Since the illuminated area of the specimen is not a point source it was necessary that the average solid angle and average projected solid angle of the illuminated area be determined for purposes of computing the BRDF values. When the radiation beam with $\pm 25^\circ$ collimation is incident on the specimen at the specified 70 degrees, the illuminated area is 36 by 18 mm. The distance from the center of the illuminated area to the center of the limiting aperture of the detector is 480 mm. The diameter of the limiting aperture is 34.79 mm. The average solid angle and average projected solid angle of the illuminated area measured from the center of the limiting aperture were determined by dividing the illuminated area into 648 1-mm square areas and computing the solid angle at the center of each 1-mm square area. These calculations were made for each specified angle of viewing. The average values from the array are as follows:

<u>Viewing Angle</u>	<u>Average Solid Angle (Steradians)</u>	<u>Average Projected Solid Angle (Steradians)</u>
-22°	.004118	.003818
-25°	.004118	.003732
-28°	.004119	.003636
-31°	.004119	.003531
-34°	.004120	.003415

NBS Test No.: 534/97D-83

Date: October 3, 1983

6. Uncertainties

The values of 6°/hemispherical reflectance factor listed in Tables 1 through 3 are believed to be uncertain by no more than ± 0.005 (1/2 percent). This uncertainty is based on the variation in reflectances of the freshly prepared pressed Halon specimens and on the random errors in the measurements. Errors due to test specimen nonuniformity have not been assessed.

Several uncertainties in the measurement process contribute to a final uncertainty of ± 0.01 for the BRDF results reported in Tables 4 through 8. An uncertainty of ± 0.0037 in the BRDF is introduced through the step-down technique in which the black glass specular reflectance is used. Uncertainty in the distance of the limiting aperture from the specimen plane contributes an uncertainty of ± 0.0013 . Another uncertainty of ± 0.0010 exists for the measured diameter of the limiting aperture. In addition to these, there is a random error that contributes another ± 0.0040 to the uncertainty.

7. References

- (1) Venable, W. H. Jr., Hsia, J. J., Weidner, V. R., "Development of an NBS reference spectrophotometer for diffuse reflectance and transmittance", Nat. Bur. Stand. U. S. Tech. Note 594-11, 47 pp. (1976).
- (2) Weidner, V. R., Hsia, J. J., "NBS specular reflectometer-spectrophotometer", Appl. Opt. 19, 1268-1273, (1980).
- (3) Weidner, V. R., Hsia, J. J., "Reflection properties of pressed polytetrafluoroethylene powder", J. Opt. Soc. Am. 71, 856-861, (1981).

Prepared by:

Victor R. Weidner

Victor R. Weidner
Radiometric Physics Division
Center for Radiation Research

Approved by:

Jack J. Hsia

Jack J. Hsia
Radiometric Physics Division
Center for Radiation Research

NBS Test No.: 534/97D-83

Date: October 3, 1983

Enclosures: NBS Monograph 160
NBS Tech. Note 594-11
1 reprint
1 figure
8 tables

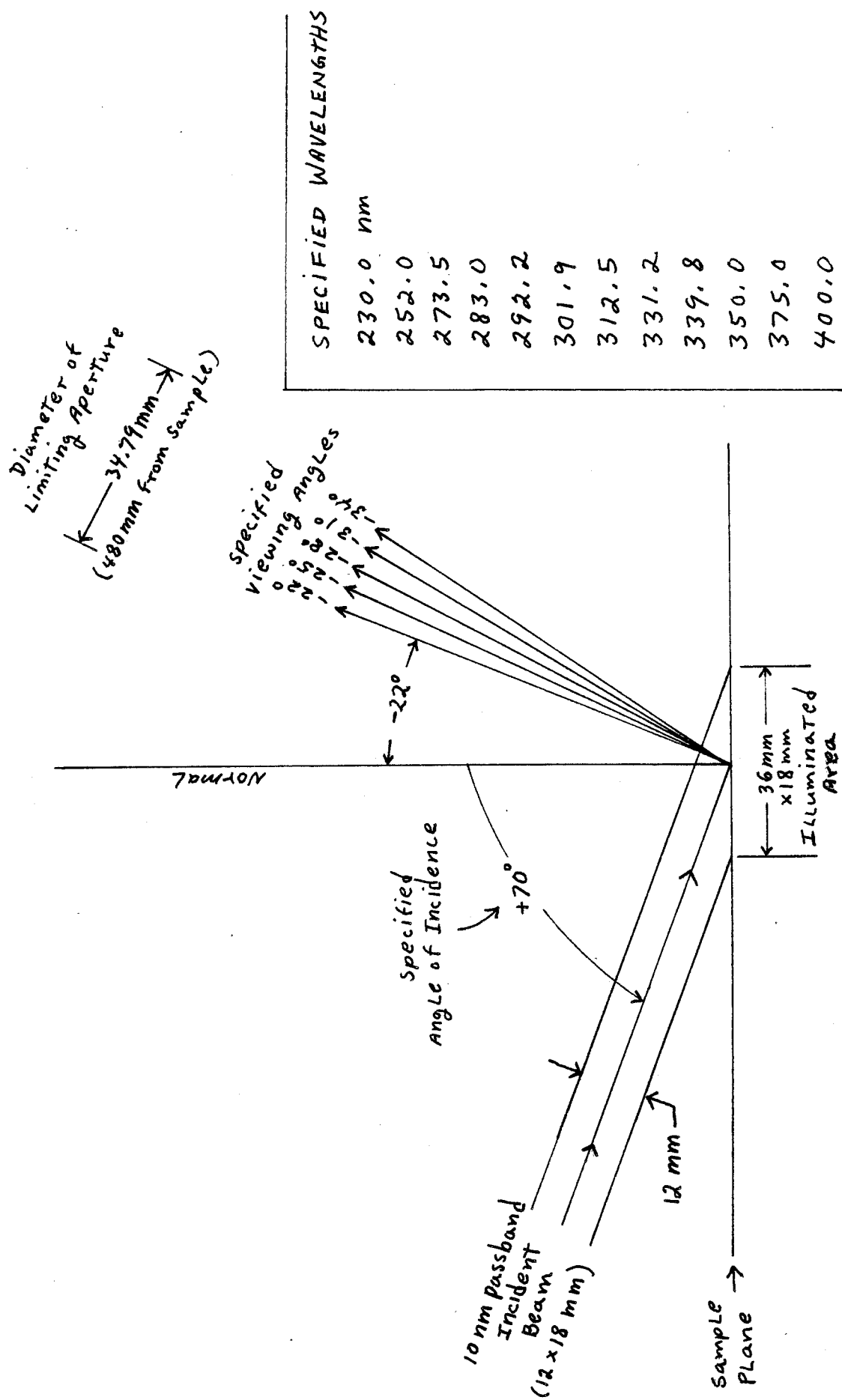


FIGURE 1

Table 1

6°/hemispherical Reflectance Factor of Three BaSO₄ Specimens Measured Aug. 18, 1983

Wavelength (nm)	BaSO ₄ 2"x2" No. 3	BaSO ₄ 3"x4" No. 3	BaSO ₄ 12"x12" No. 3
230	0.9002	0.8937	0.9000
252	.9203	.9159	.9207
273.5	.9312	.9282	.9342
283	.9308	.9279	.9368
292.2	.9335	.9312	.9407
301.9	.9397	.9374	.9454
312.5	.9457	.9429	.9484
331.2	.9512	.9484	.9532
339.8	.9531	.9503	.9547
350.	.9551	.9527	.9564
375	.9562	.9528	.9579
400	.9565	.9545	.9585

NBS Test No.: 534/97D-83

Table 2

6°/hemispherical Reflectance Factor of Four BaSO₄ Specimens Measured Aug. 19, 1983

<u>Wavelength (nm)</u>	<u>BaSO₄ 2"x2" No. 1</u>	<u>BaSO₄ 2"x2" No. 2</u>	<u>BaSO₄ 3"x4" No. 1</u>	<u>BaSO₄ 3"x4" No. 2</u>
230	0.9046	0.9000	0.8002	0.9101
252	.9236	.9204	.8765	.9273
273.5	.9203	.9225	.8910	.9106
283	.9227	.9221	.8970	.9218
292.2	.9192	.9216	.9142	.9088
301.9	.9243	.9283	.9297	.9064
312.5	.9451	.9440	.9446	.9402
331.2	.9523	.9529	.9543	.9465
339.8	.9519	.9542	.9574	.9409
350	.9518	.9558	.9590	.9419
375	.9611	.9597	.9606	.9593
400	.9500	.9547	.9567	.9457

NBS Test No.: 534/97D-83

Table 3

6°/hemispherical Reflectance Factor of Two BaSO₄ Specimens and One Aluminium Diffuser Specimen Measured Sept. 20, 1983

<u>Wavelength (nm)</u>	<u>BaSO₄ 3"x4" No. 3</u>	<u>BaSO₄ 12"x12" (plate B)</u>	<u>Aluminum Diffuser 3"x4" No. 5083</u>
230	0.8864	0.9072	0.4046
252	.9094	.9317	.4372
273.5	.9186	.9195	.4607
283	.9204	.9387	.4676
292.2	.9213	.9284	.4752
301.9	.9283	.9248	.4838
312.5	.9367	.9530	.4871
331.2	.9468	.9562	.4968
339.8	.9492	.9495	.5017
350	.9515	.9525	.5055
375	.9524	.9659	.5104
400	.9548	.9577	.5145

NBS Test No.: 534/97D-83

Table 4

Bidirectional Reflectance Distribution Function of BaSO₄ (3"x4" No. 3)
 Measured Sept. 1, 1983. Angle of Incidence = 70°.

Wavelength (nm)	Angle of Viewing (Deg.)				
	-22	-25	-28	-31	-34
230	0.2298	0.2298	0.2344	0.2354	0.2413
252	.2481	.2505	.2521	.2530	.2574
273.5	.2531	.2548	.2574	.2598	.2625
283	.2653	.2681	.2703	.2721	.2750
292.2	.2676	.2697	.2715	.2744	.2771
301.9	.2581	.2599	.2629	.2657	.2678
312.5	.2635	.2656	.2679	.2701	.2736
331.2	.2693	.2710	.2740	.2760	.2779
339.8	.2652	.2664	.2675	.2700	.2735
350	.2679	.2701	.2714	.2736	.2764
375	.2712	.2730	.2750	.2773	.2809
400	.2703	.2732	.2748	.2768	.2798

NBS Test No.: 534/97D-83

Table 5

Bidirectional Reflectance Distribution Function of BaSO_4 (2"x2" No. 1)
 Measured Sept. 2, 1983. Angle of Incidence = 70° .

Wavelength (nm)	Angle of Viewing (Deg.)				
	-22	-25	-28	-31	-34
230	0.2372	0.2413	0.2455	0.2431	0.2440
252	.2501	.2520	.2550	.2584	.2611
273.5	.2577	.2589	.2606	.2632	.2665
283	.2653	.2674	.2699	.2724	.2753
292.2	.2681	.2688	.2714	.2746	.2771
301.9	.2604	.2628	.2653	.2679	.2704
312.5	.2660	.2676	.2703	.2737	.2775
331.2	.2697	.2728	.2740	.2768	.2796
339.8	.2654	.2668	.2693	.2721	.2750
350	.2663	.2681	.2704	.2725	.2755
375	.2714	.2736	.2778	.2798	.2815
400	.2692	.2715	.2737	.2769	.2800

NBS Test No.: 534/97D-83

Table 6

Bidirectional Reflectance Distribution Function of BaSO_4 (3"x4" No. 2)
 Measured Sept. 7, 1983. Angle of Incidence = 70° .

Wavelength (nm)	Angle of Viewing (Deg.)				
	-22	-25	-28	-31	-34
230	0.2350	0.2372	0.2372	0.2424	0.2430
252	.2528	.2553	.2571	.2591	.2622
273.5	.2563	.2586	.2611	.2640	.2672
283	.2660	.2679	.2706	.2730	.2764
292.2	.2672	.2692	.2718	.2744	.2773
301.9	.2604	.2627	.2649	.2679	.2711
312.5	.2671	.2688	.2711	.2739	.2771
331.2	.2703	.2719	.2744	.2768	.2801
339.8	.2672	.2690	.2715	.2742	.2772
350	.2685	.2703	.2726	.2754	.2790
375	.2726	.2748	.2771	.2797	.2829
400	.2729	.2743	.2765	.2793	.2823

NBS Test No.: 534/97D-83

Table 7

Bidirectional Reflectance Distribution Function of BaSO_4 (3"x4" No. 3)
 Measured Sept. 14, 1983. Angle of Incidence = 70° .

Wavelength (nm)	Angle of Viewing (Deg.)				
	-22	-25	-28	-31	-34
230	0.2352	0.2329	0.2376	0.2405	0.2384
252	.2521	.2535	.2568	.2592	.2620
273.5	.2520	.2538	.2562	.2586	.2613
283	.2632	.2647	.2671	.2699	.2735
292.2	.2632	.2653	.2675	.2694	.2730
301.9	.2566	.2585	.2607	.2632	.2663
312.5	.2656	.2672	.2693	.2718	.2747
331.2	.2683	.2700	.2722	.2750	.2776
339.8	.2657	.2678	.2700	.2729	.2760
350	.2679	.2693	.2717	.2739	.2769
375	.2710	.2729	.2750	.2779	.2811
400	.2724	.2744	.2768	.2796	.2826

NBS Test No.: 534/97D-83

Table 8

Bidirectional Reflectance Distribution Function of Aluminum Diffuser Plate 5083
Measured Sept. 14, 1983. Angle of Incidence = 70°.

Wavelength (nm)	Angle of Viewing (Deg.)				
	-22	-25	-28	-31	-34
230	0.1357	0.1423	0.1527	0.1662	0.1703
252	.1526	.1634	.1746	.1879	.2028
273.5	.1612	.1721	.1836	.1972	.2118
283	.1686	.1794	.1919	.2056	.2213
292.2	.1731	.1840	.1966	.2114	.2274
301.9	.1707	.1817	.1940	.2080	.2233
312.5	.1738	.1850	.1977	.2120	.2276
331.2	.1804	.1923	.2055	.2203	.2366
339.8	.1793	.1911	.2040	.2186	.2350
350	.1796	.1914	.2046	.2196	.2362
375	.1858	.1980	.2116	.2269	.2438
400	.1864	.1988	.2125	.2278	.2448

NBS Test No.: 534/97D-83



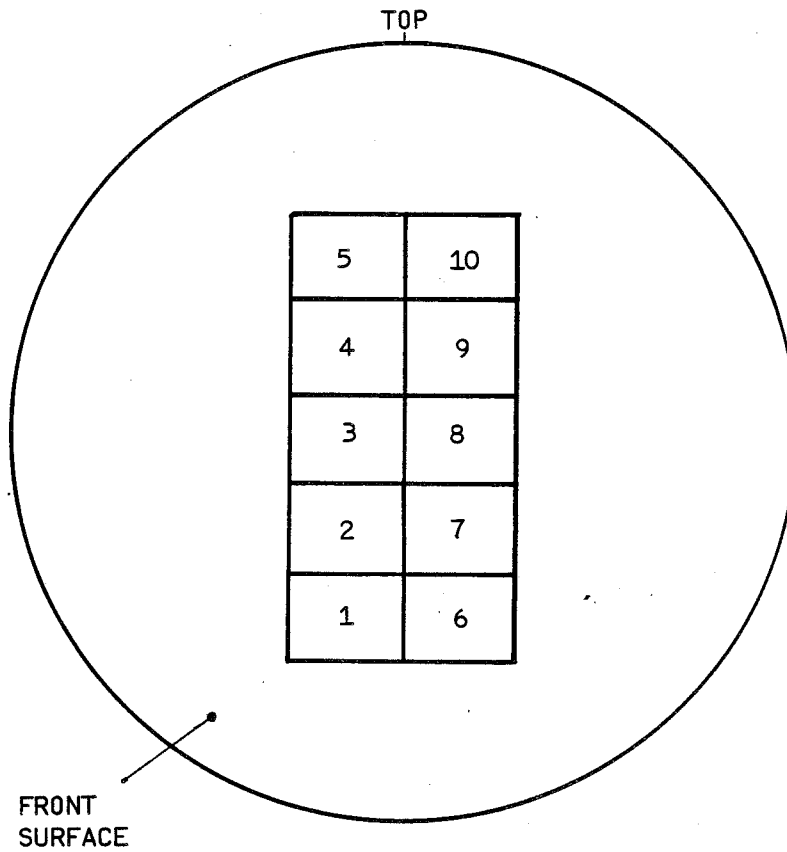
B6802-78

3.5 MEASUREMENTS AT BASD OF REFLECTANCE OF COLLIMATING MIRRORS USED IN
SBUV/2 CALIBRATIONS



B6802-78

POSITIONS AT WHICH MIRROR EFFICIENCIES WERE MEASURED



A/N 3990



B6802-78

MIRROR REFLECTANCE MIRROR A, USED ON PRIMARY FIXTURE

POSITION	WAVELENGTH nm				
	185	230	252	273	283
1	85.6	87.6	87.6	85.9	87.4
2	85.5	87.9	87.6	86.8	86.8
3	85.0	87.5	87.4	85.7	86.1
4	86.0	87.7	87.7	85.6	86.0
5	85.8	88.3	87.1	85.0	86.1
6	86.4	87.8	87.9	85.1	88.4
7	85.9	87.7	87.7	88.2	86.9
8	86.1	87.7	87.5	86.9	87.9
9	85.5	87.7	87.4	86.0	88.1
10	85.7	87.7	87.1	85.8	89.2

COLLIMATOR MIRROR "A"

McP. 225 200 μ SLITS

Cste DIODE #165 95u BIAS 185nm - 252 nm

UDT DIODE #15429 273 nm - 400 nm

BANJO REFLECTOMETER

MINIARC #2 35 A

A/N 3990



B6802-78

MIRROR REFLECTANCE COLLIMATOR MIRROR "A"

POSITION	WAVELENGTH nm				
	292.2	301.9	312.5	331.2	339.8
1	89.1	87.3	88.2	88.0	89.4
2	89.3	86.7	88.5	88.3	89.0
3	89.0	87.4	88.5	88.7	88.4
4	89.8	87.8	88.1	88.6	88.5
5	89.5	87.1	87.9	88.9	88.3
6	89.6	89.6	88.4	87.8	88.4
7	88.5	89.8	88.0	87.3	88.0
8	89.1	90.1	88.9	88.4	88.9
9	89.6	89.9	90.2	88.8	88.9
10	89.2	90.3	89.2	87.8	89.0

A/N 3990



B6802-78

MIRROR REFLECTANCE COLLIMATOR MIRROR "A"

POSITION	WAVELENGTH nm		
	350	375	400
1	89.2	89.2	89.1
2	88.6	89.1	88.6
3	88.3	88.3	88.8
4	88.0	87.7	89.0
5	87.9	88.4	88.9
6	89.2	89.2	89.9
7	89.6	88.6	91.1
8	89.4	88.7	88.8
9	89.4	88.5	89.5
10	89.4	88.7	89.3

A/N 3990



MIRROR REFLECTANCE MIRROR "C" - USED IN VACUUM

POSITION	WAVELENGTH (nm)				
	185	230	252	273	283
1	88.3	89.8	87.1	87.6	88.4
2	89.6	89.3	88.1	87.1	88.2
3	89.1	89.5	87.9	86.1	89.9
4	89.8	89.8	87.7	86.8	88.6
5	90.2	89.6	88.3	86.8	88.1
6	90.2	89.2	87.5	85.3	87.7
7	89.5	89.3	88.0	85.9	87.5
8	89.7	89.3	88.2	86.4	87.3
9	88.3	89.3	88.3	87.5	88.7
10	88.5	89.5	88.5	87.5	88.5

COLLIMATOR MIRROR "C"

MCP 225 200 μ SLITS

Cste DIODE #165 185 nm - 252 nm

UDT DIODE #15429 273 nm - 400nm

BANJO REFELACTOMETER

MINIARC #2 35 A.

A/N 3990



MIRROR REFLECTANCE COLLIMATOR MIRROR "C"

POSITION	WAVELENGTH nm				
	292.2	301.9	312.5	331.2	339.8
1	89.5	89.5	87.1	87.8	88.4
2	89.7	89.6	86.8	88.1	88.4
3	89.6	89.6	86.4	87.6	88.3
4	89.6	89.9	86.6	88.1	88.2
5	89.6	89.7	86.9	88.0	88.5
6	88.7	87.1	87.9	87.4	87.9
7	88.1	87.4	87.0	87.1	87.9
8	88.0	86.9	86.6	87.1	88.4
9	88.6	88.5	87.3	86.9	87.9
10	88.7	88.6	87.0	87.0	88.6

A/N 3990



MIRROR REFLECTANCE COLLIMATOR MIRROR "C"

POSITION	WAVELENGTH nm		
	350	375	400
1	88.4	89.3	88.9
2	88.9	89.2	88.3
3	88.9	89.2	89.7
4	88.7	89.8	89.2
5	88.5	89.8	89.4
6	88.5	89.4	89.2
7	88.8	88.9	89.3
8	88.4	89.8	88.9
9	88.3	89.1	89.2
10	88.4	89.0	88.7

A/N 3990



B6802-78

MIRROR REFLECTANCE COLLIMATOR MIRROR 'C' AT 160.8nm 6/30/83	
POSITION	WAVELENGTH (nm)
1	83.7
2	83.9
3	83.8
4	83.8
5	83.8
6	83.6
7	83.6
8	83.5
9	83.5
10	83.4

A/N 3990



B6802-78

Vacuum Chamber Quartz Window

DATE: 3-29-83

WINDOW S/N W-1

Wavelength n.m.

% Transmission

185.0	85.3
230.0	89.4
253.7	89.6
273.5	90.4
283.0	90.4
292.2	90.5
301.9	90.7
312.5	91.0
331.2	91.0
339.8	91.1
350.0	91.4
375.0	91.5
400.0	91.6



Section 4

RADIOMETRIC CALIBRATION

4.1 METHOD

The instrument is calibrated radiometrically by recording its responses to three types of irradiance standards; a 1000 W tungsten quartz-halogen-type FEL-Lamp, a deuterium arc, and an argon mini-arc. Figure 4-1 shows the approximate spectral irradiance at 50cm of these source types. The calibration fixture is depicted in Figure 4-2. The various sources are mounted on a carousel so that they can be accurately and repeatedly positioned for use. A concave mirror, 50cm from the source, collimates the light. The collimated beam is incident upon the instrument diffuser (for sun viewing mode) at about 70°. The incident angle of sunlight will vary from about 62° to 78°. To provide a source of radiance to calibrate the Earth viewing mode, the instrument diffuser is stowed and a calibrated "test diffuser" takes its place.

A typical calibration sequence runs as follows: A source is selected, positioned, turned on, and allowed to stabilize. The STE computer controlling the instrument is loaded with the macro WLCAL for wavelength and diffuser calibration checks. The internal mercury arc source is turned on and illuminates the entrance slit directly and later via reflection from the diffuser, providing a check on the diffuser's reflectance. The instrument operates in sweep mode to record the position of all the Hg lines, then in position mode to record the instrument profile at 253.7 nm in detail. Next, the macro CALSWEP is used for sweep mode calibration. In this routine, the instrument performs 10 consecutive wavelength sweeps from 400 to 160 nm alternating between sun-viewing (irradiance) and earth-viewing (radiance) modes with each scan. Macro CALSWEP is repeated giving a total of 20 consecutive sweeps of data. Then, the macro DISCAL is loaded for position mode calibration. In this routine, the instrument dwells at 12 selected grating positions, normally at the "discrete wavelengths". Fifty data samples are taken each in sun-viewing and earth-viewing mode at each grating position. Grating position is changed every 100 data samples, going from short to longer wavelengths. Finally, the macro GDISCAL runs the instrument through its discrete mode in which the grating steps to a



new wavelength for each data sample. This more closely resembles orbital operation where signal levels rapidly change. Ten scans through the 12 discrete wavelengths are made from short to long, then the change is made from earth-viewing to sun-viewing mode, then ten more scans are made. This ends a typical sequence with a particular standard lamp.

There are two calibration test fixtures, the primary which is located in a laminar flow clean-room and the vacuum test fixture for which all components except the sources are in a temperature controlled vacuum chamber. Using the vacuum fixture, the temperature dependence of the instrument response is measured and the calibration is extended into the vacuum ultraviolet region. The VUV extension is done only with the mini-arc and its MgF window which can be attached to the vacuum flange on the chamber.

The instrument's radiance response (earth-viewing mode) is also measured by illuminating a BaSO_4 diffuser directly at normal incidence with a FEL lamp. The instrument views the diffuser at an angle of 20° from the normal. CALSWEP, DISCAL, and GDISCAL macros are run, however, no sun-viewing mode (irradiance) data can be taken.

Table 4-1 lists all calibration runs for the EMU/Flight instrument.

4.2 CALCULATIONS INTRODUCTION

The objective of the radiometric calibration is to obtain the instrument's calibration constants at all wavelengths and in all operational modes. The calibration constant is denoted by $(Ldk/C)_\lambda$ or $(Edk/C)_\lambda$ where C is the instrument response in terms of PMT anode current and L and E are radiance and irradiance, respectively. Figure 4-3 shows schematically the variables and calculations involved in arriving at the calibration constants. The calibrated light source and its goniometric mapping determine the average spectral irradiance incidence upon the collimating mirror. The average spectral reflectance of the mirror then yields the spectral irradiance, Edk incident upon the instrument diffuser. In the vacuum chamber the window transmittance is also a factor. For radiance calibration, the diffuser BRDF is combined as a



product integral with the vignetting function of the instrument yielding a weighted average BRDF. This, combined with the incident irradiance and cosine of the angle of incidence, yields the diffuser radiance, L_{dk} . Then the instrument calibration constants for the various wavelengths, modes, temperatures, sources and diffusers are the calculated E_{dk} and L_{dk} divided by the instrument (PMT anode current) responses.

4.2.1 Instrument Response, C_p

The instrument response is received in digital form; ranging from 64 (the zero offset level) to 65535 counts on 3 ranges. These counts are converted to equivalent anode current by the following formulas:

$$C_p \text{ (amps)} = (\text{Counts} - 64) \times .153 \times 10^{-4} \times N_F \times N_M$$

where

$$\begin{aligned} \text{range factor, } N_F &= 10^{-10}, \text{ for range 1} \\ &10^{-8}, \text{ for range 2} \\ &10^{-6}, \text{ for range 3} \end{aligned}$$

$$\begin{aligned} \text{mode factor, } N_M &= 1, \text{ for discrete mode} \\ &12.5 \text{ for sweep mode} \end{aligned}$$

The range factors given above are idealized; in practice they will contain another factor nearly equal to 1 which is determined by comparing the ranges where they overlap.

4.2.2 Average Spectral Irradiance, E_{dk} on the Diffusers

The spectral irradiance, E_λ of the standard sources at 50 cm, is provided by the National Bureau of Standards at 10nm intervals. It is necessary to interpolate between these calibrated points to fill in the SBUV/2 calibration. For the FEL lamp, the NBS also provides a curve fit having the form of the Plank



black body function multiplied by a fourth order polynomial in λ . For the arc lamps there is no such analytic expression for their spectral output, therefore, cubic spline interpolation was used for them.

The angular field of illumination of the sources which we use is quite large, about $\pm 5^\circ$ in elevation and $\pm 3^\circ$ in azimuth. The NBS measures the angular dependence $\mathcal{E}_s(\theta, \phi)$ of the output from the FEL lamps and mini-arcs, normalized at $\theta, \phi = 0$. We take the average, $\overline{\mathcal{E}_s(\theta, \phi)}$ of this and multiply it by the on-axis irradiance to obtain a field-average irradiance, $\overline{E}_\lambda = E_\lambda \overline{\mathcal{E}_s(\theta, \phi)}$

The spectral reflectance, $\mathcal{E}_m(x, y, \lambda)$ of the collimating mirror is measured at 12 wavelengths and at 10 locations on the mirror. We average this over the mirror's surface to obtain $\overline{\mathcal{E}_m(\lambda)}$.

When we are using the FEL or D₂ lamps at the vacuum chamber, we have a quartz window whose spectral transmittance, $\mathcal{E}_w(\lambda)$ must be included.

The average irradiance incident at the diffusers is then given by:

$$\overline{E}_{dk} = E_\lambda \overline{\mathcal{E}_s(\theta, \phi)} \mathcal{E}_w(\lambda) \overline{\mathcal{E}_m(\lambda)}.$$

The mini-arcs are not located at 50cm from the collimating mirrors. On the primary test fixture the distance is 51.75cm and on the vacuum test fixture the distance is 54.43 cm. The inverse square relation was used to correct for these distance differences, which should be sufficiently accurate for deviations of this size. The corrections applied were:

Mini-arc I, primary test fixture,

$$E_\lambda = E_\lambda(50\text{cm}) \left(\frac{50}{51.75} \right)^2 = 0.934 E_\lambda(50\text{cm})$$

Mini-arc II, vacuum test fixture,

$$E_\lambda = E_\lambda(50\text{cm}) \left(\frac{50}{54.43} \right)^2 = 0.844 E_\lambda(50\text{cm})$$



The mini-arc irradiances were also corrected for the change in window transmittance as measured in September 1983. See Section 3.2. This is justified because much of the mini-arcs' operating time was spent prior to the final calibration.

4.2.3 Spectral Radiance of the Diffuser into SBUV/2

Calculating the radiance of the target for earth-viewing mode calibration is a complex process. A brief verbal description is given here followed by a more involved mathematical justification. The method used here is not irrevocable; the raw data exist and can be reanalyzed in any way the user wishes.

Knowing the spectral irradiance and its angle of incidence upon the test diffuser, we calculate the radiance of the diffuser in the direction of the entrance slit by applying the appropriate value of BRDF of the diffuser. With the diffuser so close to the instrument, the vignetting along the entrance slit is extreme, causing the instrument to be not uniformly sensitive to all parts of the diffuser. We use this vignetting function to assign weights to the BRDF at locations over the diffuser. Then we take the weighted average BRDF to calculate a radiance. Although this calculated radiance does not agree point by point with what is there, it represents the uniform distant radiance that would elicit the same instrument response.

4.2.4 Details of Calculation

The diffusers used to provide a radiance target for SBUV/2 calibration are measured at the NBS to provide the BRDF at 70° angle of incidence and at $\gamma = -22^\circ, -25^\circ, -28^\circ, -31^\circ, \text{ and } -34^\circ$ angles of scatter. See the NBS report in Section 3.4 for details. At any point (x, y) on the diffuser, there is a corresponding diffuse reflectance described by the BRDF in the direction (θ, ϕ) of the entrance slit. The radiance in the direction of the entrance slit is:

$$I(\theta, \phi) = E_{dk} (BRDF(\theta, \phi)) \cos i \quad (1)$$



where $i = 70.58^\circ$ is the angle of incidence of E_{dk} on the diffuser. The instrument's solid angle of acceptance of light scattered from the point (x, y) on the diffuser depends on the direction (θ, ϕ) from the slit to that point because of vignetting over the slit length (3cm) of an object so close (20cm). The field of view vignetting geometry and resulting angular response profile are shown in Figures 4-4 and 4-5.

Since the instrument is not uniformly viewing a uniform scene, we must relate this situation to that of viewing a uniform, distant scene. The instrument response is proportional to the flux that enters the slit. For a uniform scene that is simply

$$\Phi_\infty = \mathcal{L} A_s \Omega \quad (2)$$

where \mathcal{L} is the radiance, A_s is the slit area and Ω is the solid angle of view. For the nearby nonuniform scene, the flux is

$$\Phi = \iint \mathcal{L}(x, y) \cdot \omega(x, y) dx dy \quad (3)$$

where $\mathcal{L}(x, y)$ is the radiance distribution on the diffuser in the direction of the slit, and $\omega(x, y)$ is the solid angle subtended at x, y by the collecting area of the instrument (which varies because of vignetting). Transforming (1) to x, y coordinates and substituting in (3),

$$\Phi = E_{dk} \cos i \iint \text{BRDF}(x, y) \cdot \omega(x, y) dx dy \quad (4)$$

Figure 4.6 shows the functions BRDF and ω overlaid in the plane of the diffuser. Constant value contours are straight lines crossing at 34° , the angle at which the diffuser is tuned relative to the slit. We estimate the value of the double integral of (4) graphically. First we rotate the coordinate system to x', y' , where y' is parallel to lines of constant BRDF, so that BRDF is now dependent on one variable only, x' . This allows us to rewrite (4) as:



$$\Phi = E_{dk} \cos i \int BRDF(x') \int \omega(x', \gamma') d\gamma' dx' \quad (5)$$

We evaluate $W(x') = \int \omega(x', \gamma') d\gamma'$ at five values of x' by taking slices through the vignetting function along lines of constant BRDF at $x' = -22^\circ$, -25° , -28° , -31° , and -35° . This results in the profiles of Figure 4.7 whose areas are the values of the integrals.

We complete the integration with the approximation,

$$\int BRDF(x') \cdot W(x') dx \cong \sum_{x'=-22^\circ}^{x'=34^\circ} BRDF(x') \cdot W(x') \quad (6)$$

In the summation $W(x')$ acts as a weighting factor at each value of BRDF. So, in the test situation, the flux entering the instrument is

$$\Phi = E_{dk} \cos i \sum_{x'} BRDF(x') \cdot W(x') \quad (7)$$

whereas in the uniform distant scene,

$$\Phi_\infty = \mathcal{L} A_s \Omega \quad (2)$$

For the same instrument response in each case, $\Phi = \Phi_\infty$, so equating (2) and (7) and solving for \mathcal{L} ,

$$\mathcal{L} = \frac{E_{dk} \cos i}{A_s \Omega} \sum_{x'} BRDF(x') \cdot W(x') \quad (8)$$



In our evaluation of $W(x')$, the areas of the profiles, we normalize so that the sum of the areas is equal to 1.

$$\sum W_n(x') = 1 \quad (9)$$

This implicitly includes the factor $\frac{1}{A_s \Omega}$, that is,

$$W_n(x') = \frac{W(x')}{A_s \Omega} \quad (10)$$

Note that we used the Helmholtz invariant (constancy of the product $A_s \Omega$) since this treatment requires that

$$\int \omega(x, y) dx dy = A_s \Omega \quad (11)$$

So we arrive at the equation

$$L_{dk} = E_{dk} \cos i \sum_{x'} BRDF(x') \cdot W_n(x') \quad (12)$$

which is how we calculate L_{dk} for the radiance calibrations.

Many approximations are made in this treatment; for instance, the instrument field of view projected on the diffuser is not quite rectangular as in Figure 4-6, because of the compound angle of tilt of the diffuser. Including this, however, would make only a very small second order correction. When the first order correction is evaluated by comparing it with taking a straight average of the BRDF which neglects the vignetting, the difference is only 0.2% on the average over the wavelengths. So, second order corrections are certainly unnecessary.



4.2.5 Estimation of Normal Incidence Diffuser Radiance into SBUV/2

As a check on the formal calibration of SBUV/2, which is done with collimated light incident upon the test diffuser, a 30x30cm Kodak White diffuser is placed 50cm from an FEL lamp and viewed by SBUV/2 from a distance of 60cm and at an angle of 20° (See Figure 4-8). The diffuser plate is too large for the NBS to measure its BRDF, so they measured its 6° (angle of incidence) hemispherical reflectance at many wavelengths.

Assuming Lambertian behavior, the spectral radiance of the diffuser at its center is

$$I_{\lambda} = \frac{R_{\lambda} E_{\lambda}}{\pi}$$

where R_{λ} = spectral 6° hemispherical reflectance of the diffuser
 E_{λ} = spectral irradiance of the FEL lamp at 50cm

At other points on the diffuser, the radiance is different for several reasons, and furthermore, the response of SBUV/2 is not uniform in all directions. The reasons why the radiance is not uniform are:

1. The non-uniform angular distribution from the lamp, due mostly to self occlusion of the coiled filament, is most pronounced in changes of elevation.
2. The $\cos^3 \theta$ effect, where θ is the angle of incidence at the diffuser.

The main cause of non-uniform angular SBUV/2 response is vignetting by the 3cm slit when viewing a nearby scene. The radiance distribution on the diffuser is expressed by

$$I_{\lambda}(x, y) = \frac{E_{\lambda} R_{\lambda}}{\pi} \cdot f(x, y) \cdot g(x, y),$$

where $f(x, y)$ is the $\cos^3 \theta$ function transformed to x, y coordinates, and $g(x, y)$ is the angular distribution of irradiance of the lamp



Using the same method as in the previous section, the flux into the instrument is

$$\Phi = \frac{E_{\lambda} R_{\lambda}}{\pi} \iint f(x, y) \cdot g(x, y) \cdot \omega(x, y) dx dy$$

where $\omega(x, y)$ is the solid angle subtended at point x, y on the diffuser by the instrument's collecting area.

The lamp's angular distribution, $g(x, y)$, is not expressed analytically, nor is it known over the total field of view. To estimate Φ , we take $g(x, y)$ outside the integral and extrapolate its probable values over the field of view. Then we estimate the remaining integral by summing over fairly large areas. There is probably more error due to the partly unknown $g(x, y)$ than to the approximations used for this estimate. The result is a correction factor of 0.981. The calculated spectral radiance are listed in Table 4-3m.

Details of the estimation follow.

Figure 4-9 shows the field of view of SBUV/2 projected on the 30x30cm diffuser plate assuming 60cm slit to plate-center distance and a 20° tilt of the plate (plate-normal to SBUV/2 optic axis). Superimposed are iso-irradiance contours $f(x, y)$ normalized to 1 at the center and based on a $\cos^3 \theta$ dependence with the source 50cm from the plate. Calculation shows that rings of equal irradiance-increment are of very nearly equal area. This means the area-weighted average is very nearly the same as the simple average over a circular area of the plate. For the part of the plate included in the 0.98 circle, the average is then 0.99. The 0.98 circle occupies about 3/4 of the area viewed by SBUV/2. The weighted average of the corners must be greater than 0.970, say 0.973. This results in an overall average of

$$(0.75 \times 0.99) + (0.25 \times 0.973) = 0.986$$

(An error of ± 0.004 in estimating the corners contributes an error of ± 0.001 in the final result.) So we set $f(x, y) = 0.986$, a constant multiplicative factor.



The circular contour pattern is correct only for an ideal point source. The 2cm x 0.7cm filament of the FEL lamp has the effect of applying a "boxcar" smoothing function to the pattern. Because of the symmetry of the pattern, the effect on the average will be negligible.

Another correction to make is for the vignetting effect $\omega(x, y)$, of the 3 cm long slit when viewing a nearby source. In the cross-slit direction, the field of view has a sharp cutoff, but parallel to the slit the field of view response is a trapezoid, the sloping sides of which are between the long dashed lines in Figure 4-9. Over the sloped region, the radiance changes about 2%. The difference between integrating the product of the radiance and response over this sloped interval;

$$\iint f(x, y) \cdot \omega(x, y) dx dy$$

and of assuming a sharp cut-off at its midpoint, $A\Omega$, is -0.005 out of 1. The area affected is 1/5 of the total, so the correction is about -0.001, and we set

$$\iint f(x, y) \cdot \omega(x, y) dx dy = 0.999 A\Omega$$

The goniometric output of the FEL lamp was measured over a 6° by 10° field, shown in short dashed lines in Figure 4-9. An iso-irradiance contour map is shown in Figure 4-10, imposed on the percent differences actually measured over the ±3° by ±5° grid. Note that there is little change of irradiance with azimuth, but a fairly constant decrease with elevation. Inspection of the lamp reveals that filament shadowing continues to increase as the lamp is tilted to about 8 to 10°, then the far side of the coils begin to re-emerge from behind the near side. So, we can assume that the irradiance continues to drop off, as extrapolated in the graph of Figure 4-11, to the edges of the field of view. To estimate the effect of this, the irradiance at a given angle is multiplied by the fractional area in the field of view at that angle and these products are summed,

$$\int g(x, y) dx dy \cong \sum g(y) \cdot x \Delta y$$

This process is shown in Table 4-2 and the result is a weighted average of 0.9862.



This results in

$$\Phi = \frac{E_{\lambda} R_{\lambda}}{\pi} (0.986)(0.999)(0.986) A \Omega$$

Again, viewing a distant uniform radiance,

$$\Phi_{\infty} = \mathcal{I} A_s \Omega$$

and equating these and solving for \mathcal{I} ,

$$\mathcal{I}_{dk} = \frac{0.971 E_{\lambda} R_{\lambda}}{\pi}$$

4.2.6 Radiance and Irradiance Tables

Using these methods and formulas, the radiances (\mathcal{I}_{dk}) and irradiances (E_{dk}) for all of the calibration runs were calculated. The resulting values are tabulated in Tables 4-3a through 4-3m. These are the values that are input to the computer utility as described in the next section.

Units are as follows for tables and graphs:

radiance, \mathcal{I}_{dk}	$\text{mW} \cdot \text{m}^{-2} \cdot \text{sr}^{-1} \cdot \text{nm}^{-1}$
irradiance, E_{dk}	$\text{mW} \cdot \text{m}^{-2} \cdot \text{nm}^{-1}$
wavelength, λ	nm
anode current, C_p	amps
BRDF	sr^{-1}

4.3 RESULTS

After a calibration run, the instrument responses are matched with the E_{dk} or \mathcal{I}_{dk} appropriate to the particular calibration situation; that is, the particular combination of source, mirror, diffuser, window, and fixture used. This is done using an off-line utility on the STE computer which fills in the E_{dk} and \mathcal{I}_{dk} values over the spectrum using cubic spline interpolation, matches them with instrument responses, and tabulates the results.



4.3.1 Position and Discrete Modes

Table 4-1 is a listing of all the position mode (DISCAL) and discrete mode (GDISCAL) runs. Before day 223, an aluminum test diffuser that was not directly calibrated by the NBS was used. This data is mostly from thermal-vacuum testing and serves to measure relative changes in calibration constants as a function of temperature. From day 223 onwards, a BaSO_4 test diffuser was used on the primary calibration fixture and a ground aluminum test diffuser was used in vacuum. Both of these latter diffusers were measured directly by the NBS for BRDF. Similarly, the ball-bearing type instrument was replaced by a ground aluminum diffuser after day 224, placing the irradiance calibration on a new scale.

We have chosen the data sets LC 26 (Figure 4-12), and EC 26 (Figure 4-13) as the baseline calibration against which to compare the other runs. What follows are comparisons of other runs to these with some remarks concerning the differences. Due to the surplus of data and scarcity of time, many useful comparisons have not been made, and much analysis remains undone.

4.3.1.1 Source Differences

Figures 4-14 and 4-15 show the calibration constants obtained using the three standard source types, all other conditions being the same. The percentage differences of the calibration constants obtained using the D_2 939 lamp and the mini-arc I relative to the FEL 127 lamp are plotted in Figures 4-16 thru 4-19. The constants obtained using the D_2 939 lamp are generally 12% to 14% higher than when using FEL 127, and mini-arc I produces constants that are 20% to 23% higher. A larger constant indicates a higher estimate of the target radiance or a lower than calibrated lamp output. Figures 4-20 to 4-23 show comparisons of results from lamps of the same types; Figures 4-20 and 4-21 show FEL 124 relative to FEL 127 and Figures 4-22 and 4-23 show D_2 964 relative to D_2 939. The two mini-arcs are compared in terms of irradiance only in Figure 4-24; radiance comparisons of the mini-arcs are too remote because of test diffuser changes. The two FEL lamps agree to within about 3% except for one point of 5% at 273 nm. No error in calculation has been found to account



for this point, but we suspect bad data of some sort is responsible. The D₂ lamps agree to within 2.5%. The mini-arcs show a strongly wavelength-dependent disagreement, perhaps due to more advanced window contamination of mini-arc 1.

4.3.1.2 Temperature Effects

During thermal-vacuum testing, calibration runs were made at 0, 10, 20, 25, and 30 degrees centigrade. The relative values of the calibration constants that resulted from these runs are a measure of the temperature dependency of the calibration. The absolute values of the constants have little meaning because of changes of diffusers and the differences in the vacuum chamber set-up. Figures 4-24 to 4-28 show radiance calibration constants as a function of temperature for all twelve discrete wavelengths. Data was taken using the FEL 127 source and the DISCAL procedure. The slope of a least squares straight line fit to the data of 301 nm is 4.6×10^6 or about 0.38% per degree centigrade. The increasing calibration constant with temperature means a decrease in the instrument sensitivity with higher temperature.

4.3.1.3 Radiance/Irradiance Calibration Ratio

The ratio of radiance to irradiance calibration constant determines the results of the SBUV/2 albedo measurements. The ratio is plotted for the baseline calibration (LC26/EC26) in Figure 4-29, and for comparison, the last such DISCAL run on day 244 (LC38/EC38) is also plotted. The plots agree to within 1.1% even though different sources, FEL 127 and FEL 124, were used on different days, 240 and 244. A more remote comparison is with a vacuum run as plotted in Figure 4-30. In this case the test diffusers are different; BaSO₄ #3 being used in air and Al 5083 being used in vacuum. These ratios, LC26/EC36 and LC33/EC33 differ by 6 to 7%.

The difference between radiance and irradiance calibrations is the diffusers being used. By comparing the instrument output signals as the diffusers are alternated, we can compare the quantities $\cos i$ (BRDF) for the various diffusers.



At 301.86 nm wavelength, the ratios come out approximately

$$\text{in air: } \frac{\text{BaSO}_4 \text{ diffuser}}{\text{instrument diffuser}} = 1.23$$

$$\text{in vacuum: } \frac{\text{Al 5083 diffuser}}{\text{instrument diffuser}} = 0.864$$

Combining these,

$$\frac{\text{BaSO}_4 \text{ diffuser}}{\text{Al 5083 diffuser}} = 1.42$$

(The $\cos i$ factors are not shown, but they drop out in the last ratio.) Now the BRDF's of both the BaSO_4 and Al 5083 were measured at the NBS and the ratio of those was 1.33. So, considering the procedures at Ball and at the NBS as two ways of comparing two diffusers, the results are in disagreement by about 7%.

A suspicious characteristic of the results is the double maximum in all the radiance calibrations (except for normal incidence diffuser "A") while all irradiance calibrations show a single maximum. This causes the kinks in the Radiance/Irradiance curves of Figures 4-29 and 4-30, which do not seem reasonable, particularly in the case of the two very similar aluminum diffusers being used in the vacuum runs of day 243. This leads us to suspect that the double maximum may be an artifact of the measurement of the test diffuser, or the calculation of the test diffuser radiance, rather than a real instrument characteristic.

4.3.1.4 Normal Incidence Diffusers

Calibration constants obtained using the normal incidence diffusers without a collimator are compared with constants obtained with the collimator in Figures 4-31 to 4-36. Source FEL 127 was used in all these runs.

Figure 4-31 shows the baseline calibration LC26, together with results from the normal incidence diffusers "A" and "B"; LC23 and 32 respectively. Figures 4-32, 4-33 and 4-34 are plots of the differences of the constants.



Figure 4-35 shows the constants obtained in two GDISCAL runs, one from the normal incidence diffuser "A" (LC24), and the other collimated (LC25), and Figure 4-36 is a plot of their difference.

The differences are all large, even between the two normal incidence diffusers which are +6% to -1.5%. Remember that the large, 12x12 inches, normal incidence diffusers could not be measured in BRDF at the NBS. The 6° (angle of incidence) hemispherical reflectance was measured instead, and the diffuser was assumed to be Lambertian to calculate its radiance.

4.3.2 Sweep Mode Calibration

The results of Sweep Mode runs (CALSWEP) are tabulated and plotted in computer print-out form. First there is a table of raw counts at each grating position for ten scans. In the next table the counts at each grating position are averaged over the ten scans and converted to equivalent anode current. These are associated with the corresponding calculated radiances and irradiances and the resulting calibration constants Edk/Cn and Ldk/Cn are listed.

For selected runs, the calibration constants versus wavelength are plotted by computer, each full scan occupying seven pages. It is important to remember the ranges of validity for various types of scans which are imposed by the ranges of calibration of the sources and diffusers:

FEL lamps	250 to 400 nm
D ₂ lamps	200 to 350 nm
Mini-arcs (vacuum)	160 to 335 nm
Radiance mode test diffusers	230 to 400 nm

Because a single CALSWEP involves 3360 values of calibration constant, the amount of analysis done here is very small compared to the body of data.

To make some comparisons similar to those done for position and discrete modes, we used the same IDL program to plot values of calibration constants at 4 nm intervals. This serves to show general trends in the results.



Figure 4-37 shows the irradiance calibration constants results of the CALSWEP runs SEC 26, made on day 240 using FEL 127 lamp and BaSO₄ #3 diffuser. Also, on the graph are the position mode (DISCAL) results from the same run EC 26. The CALSWEP calibration constants are an average of 4.07% lower than DISCAL. When compared to GDISCAL, EC 25, the CALSWEP constants average 2.64% lower. Figure 4-38 shows the corresponding radiance calibration constants, LC 26 and SIC 26.

To extend the sweep mode irradiance calibration to the vacuum ultraviolet, run SEC 36 is used; day 243, mini-arc 2, mirror C, Al 5083 diffuser. The calibration constants from this run are plotted in Figure 4-39 together with SEC 26, our baseline calibration in air with FEL 127. If the vacuum/mini-arc constants are multiplied by 0.89, the results are as shown in Figure 4-40, matching the values better where they overlap in wavelength.

Figure 4-41 is a plot of the ratio of radiance to irradiance calibration constants; both sweep and DISCAL data from the baseline were run on day 240 (LC26/EC26 and SLC26/SEC26). The sweep and DISCAL ratios agree to within about 1.5%.

4.3.3 Cloud Cover Radiometer

Whenever any calibration runs are made with the monochromator, the output of the CCR is also recorded. Since only the FEL lamp is calibrated out to 379 nm, only that data is useable to determine a calibration constant for the CCR. Using our baseline calibration runs LC26 and EC26, the CCR responses, recorded as the monochromator goes through the DISCAL procedure; are listed in Table 4-5. There is a slight reproducible dependency of the CCR output on the grating position. We believe this to be due to a cross-talk between the range 1 counts of the monochromator and the CCR output that causes lower CCR readings with higher range 1 counts. With the FEL lamp, range 1 saturates at 300 nm and then registers lower apparent counts. This effect has not been thoroughly studied. Assuming the effect to be least at low range 1 counts, the CCR calibration constants are



$$E/C_E = 1.94 \text{ E12}$$

$$\text{mW-m}^{-2}\text{-nm}^{-1} \text{ per amp}$$

$$L/C_L = 2.06 \text{ E11}$$

$$\text{mW -m}^{-2}\text{-sr}^{-1} \text{ nm}^{-1} \text{ per amp}$$

Looking at the normal incidence diffuser data of day 241, the CCR current is 24.2 E-12 amps and the calculated radiance of the diffuser is 4.23 $\text{mW-m}^{-2}\text{-sr}^{-1}\text{-nm}^{-1}$. This results in a CCR calibration constant of

$$L/C_L = 1.75 \text{ E11}$$

which is a -15% difference relative to the collimated calibration run. (Compare to Figure 4-33.)

The ratio of radiance to irradiance calibration constants for the CCR is 0.106 sr^{-1} . This compares to a value of 0.078 sr^{-1} for the monochromator at 379 nm. Again, this is the relative efficiency of two diffusers as compared by two different radiometers. In analyzing CCR data, we have made no correction for the spectral response function of the CCR, believing it to be negligible when viewing continuum sources.



B6802-78

Table 4.1
CALIBRATION LOG

DATE	PROCEDURE MACRO	LAMP	MIRROR	TEST DIFFUSER	SPECIAL CONDITIONS COMMENTS
7/16/83 197	CALSWEP	FEL #124	C	ALUMINUM	0° TEMPERATURE PLATEAU
	DISCAL	FEL #124	C	ALUMINUM	0° TEMPERATURE PLATEAU
	CALSWEP	D ₂ #939	C	ALUMINUM	0° TEMPERATURE PLATEAU
	DISCAL	D ₂ #939	C	ALUMINUM	0° TEMPERATURE PLATEAU
	CALSWEP	FEL #124	C	ALUMINUM	+10° TEMPERATURE PLATEAU
	DISCAL	FEL #124	C	ALUMINUM	+10° TEMPERATURE PLATEAU
	CALSWEP	D ₂ #939	C	ALUMINUM	+10° TEMPERATURE PLATEAU
	DISCAL	D ₂ #939	C	ALUMINUM	+10° TEMPERATURE PLATEAU
	CALSWEP	MINI ARC #2	C	ALUMINUM	+10° TEMPERATURE PLATEAU
	DISCAL	MINI ARC #2	C	ALUMINUM	+10° TEMPERATURE PLATEAU
7/17/83 198	CALSWEP	FEL #124	C	ALUMINUM	+20° TEMPERATURE PLATEAU
	DISCAL	FEL #124	C	ALUMINUM	+20° TEMPERATURE PLATEAU
	GDISCAL	FEL #124	C	ALUMINUM	+20° TEMPERATURE PLATEAU
	CALSWEP	D ₂ #939	C	ALUMINUM	+20° TEMPERATURE PLATEAU
	DISCAL	D ₂ #939	C	ALUMINUM	+20° TEMPERATURE PLATEAU
8/29/83 241	CALSWEP	MINI ARC #1	A	BaSO ₄ #3	FIRST DATA SET BAD
	DISCAL	MINI ARC #1	A	BaSO ₄ #3	MINI ARC ERRATIC
	DISCAL	FEL #127	-	12 x 12 BaSO ₄ B	NORMAL INCIDENCE
8/30/83					PUMP-DOWN
8/31/83 243	CALSWEP	FEL #127	C	AL FLIGHT SPARE	VACUUM
	DISCAL	FEL #127	C	AL FLIGHT SPARE	VACUUM
	GDISCAL	FEL #127	C	AL FLIGHT SPARE	VACUUM
	CALSWEP	D ₂ #939	C	AL FLIGHT SPARE	VACUUM
	DISCAL	D ₂ #939	C	AL FLIGHT SPARE	VACUUM
	CALSWEP	MINI ARC #2	C	AL FLIGHT SPARE	VACUUM
	DISCAL	MINI ARC #2	C	AL FLIGHT SPARE	VACUUM
9/1/83 244	GDISCAL	FEL #124	A	BaSO ₄ #3	
	DISCAL	FEL #124	A	BaSO ₄ #3	
	GDISCAL	FEL #124	A	BaSO ₄ #3	
	CALSWEP	D ₂ #939	A	BaSO ₄ #3	

A/N 3990



Table 4-2
CALCULATION OF WEIGHTED AVERAGE

ELEVATION	NORMALIZED IRRADIANCE	AREA	$\left[\frac{\text{IRRADIANCE X AREA}}{\text{TOTAL AREA}} \right]$
-10	.930	0	0
-9	.940	.8	0.43×10^{-2}
-8	.948	2.87	1.56
-7	.957	4.94	2.71
-6	.967	7.01	3.88
-5	.975	9.09	5.07
-4	.983	11.16	6.28
-3	.986	13.23	7.40
-2	.993	15.30	8.70
-1	.998	15.30	8.74
0	1.001	15.30	8.77
1	1.002	15.30	8.78
2	.999	15.30	8.75
3	.994	13.23	7.53
4	.988	11.16	6.31
5	.980	9.09	5.10
6	.971	7.01	3.90
7	.961	4.94	2.72
8	.951	2.87	1.56
9	.940	.8	0.43
10	.930	0	0
TOTAL AREA		174.7	TOTAL 98.62×10^{-2}

* EXTRAPOLATED VALUES

A/N 3990



B6802-78

Table 4-3a
RADIANCES & IRRADIANCES
(70.58 ANGLE OF
INCIDENCE)

<u>TEST THERMAL VACUUM</u>			<u>DAY 197-201</u>		<u>TEST DIFFUSER AI-AI</u>	
<u>MIRROR C</u>						
<u>REV B</u>						
<u>WINDOW #1</u>						
λ	# 124		# II		# 939	
	\bar{E}_{d_k}	\bar{L}_{d_k}	\bar{E}_{d_k}	\bar{L}_{d_k}	\bar{E}_{d_k}	\bar{L}_{d_k}
185			.121 E+1	.857 E-1	.349 E0	.247 E-1
230	.290 E-1	.227 E-2	.305 E+1	.240 E0	.332 E0	.262 E-1
252.03	.136 E0	.113 E-1	.372 E+1	.311 E0	.252 E0	.212 E-1
273.07	.422 E0	.382 E-1	.432 E+1	.386 E0	.178 E0	.160 E-1
283.00	.663 E0	.602 E-1	.481 E+1	.435 E0	.157 E0	.124 E-1
292.20	.973 E0	.807 E-1	.537 E+1	.444 E0	.137 E0	.113 E-1
301.86	.139 E1	.118 E0	.576 E+1	.486 E0	.118 E0	.100 E-1
312.50	.195 E1	.185 E0	.592 E+1	.563 E0	.987 E-1	.935 E-2
331.21	.346 E1	.340 E0	.657 E+1	.647 E0	.769 E-1	.758 F-2
339.81	.442 E1	.442 E0			.693 E-1	.694 E-2
350	.577 E1	.584 E0			.624 E-1	.630 E-2
375	.1018 E2	.107 E+1				
379	.1100 E2	.113 E+1				
400	.1582 E2	.174 E+1				

A/N 3990



B6802-78

Table 4-3b
RADIANCES & IRRADIANCES

TEST POST T/V DAY 216, 217, 220
MIRROR A TEST DIFFUSER AI OLD
REV. B & D

λ	# 127		MINI-ARC # I		D2 LAMP # 964	
	\bar{E}_{dk}	\bar{L}_{dk}	\bar{E}_{dk}	\bar{L}_{dk}	\bar{E}_{dk}	\bar{L}_{dk}
185			.133 E1	.939 E-1	.458 E0	.324 E-1
230			.317 E1	.249 E0	.379 E0	.299 E-1
252.03	.156 E0	.130 E-1	.399 E1	.332 E0	.282 E0	.235 E-1
273.07	.486 E0	.436 E-1	.469 E1	.420 E0	.196 E0	.176 E-1
283.00	.755 E0	.682 E-1	.514 E1	.464 E0	.169 E0	.153 E-1
292.20	.113 E1	.935 E-1	.579 E1	.479 E0	.150 E0	.124 E-1
301.86	.160 E1	.135 E0	.614 E1	.517 E0	.128 E0	.108 E-1
312.50	.231 E1	.219 E0	.650 E1	.617 E0	.110 E0	.105 E-1
331.21	.405 E1	.399 E0	.713 E1	.701 E0	.853 E-1	.84 E-2
339.81	.514 E1	.513 E0			.774 E-1	.775 E-2
350	.666 E1	.675 E0			.683 E-1	.693 E-2
375	.116 E2	.123 E1				
379	.126 E2	.129 E1				
400	.183 E2	.201 E1				

A/N 3990



B6802-78

Table 4-3c

RADIANCES AND IRRADIANCES FOR AMBIENT RADIOMETRIC CALIBRATION

λ	DAY 217	SOURCE D ₂ 964	MIRROR A	TEST DIFFUSER	AL OLD			
	WINDOW EFFICIENCY	MIRROR REFLECTANCE	GONIO-METRIC FACTOR	SOURCE IRRADIANCE	EdK	DIFF BRDF	COS 70.58°	LdK
160	1		1				.33249	
185	1	.857	1	.535	.458 E0	?	.33249	.324E-1
230	1	.877	1	.432	.379 E0	.237	.33249	.299E-1
252.03	1	.872	1	.323	.282 E0	.251	.33249	.235E-1
273.07	1	.8615	1	.228	.196 E0	.270	.33249	.176E-1
283.00	1	.8711	1	.194	.169 E0	.272	.33249	.153E-1
292.20	1	.8939	1	.168	.150 E0	.249	.33249	.124E-1
301.86	1	.8830	1	.145	.128 E0	.254	.33249	.108E-1
312.50	1	.8875	1	.124	.110 E0	.286	.33249	.105E-1
331.21	1	.8844	1	.0965	.853 E-1	.297	.33249	.84 E-2
339.81	1	.8875	1	.0872	.774 E-1	.301	.33249	.775 E-2
350	1	.8871	1	.0770	.683 E-1	.305	.33249	.693E-2
375								
379								
400								

A/N 3990



B6802-78

Table 4-3d

RADIANCES AND IRRADIANCES FOR AMBIENT RADIOMETRIC CALIBRATION

DAY 240 SOURCE FEL 127 MIRROR A TEST DIFFUSER BaSO₄ #3

λ	WINDOW EFFI- CIENCY	MIRROR REFLEC- TANCE	GONIO- METRIC FACTOR	SOURCE IRRA- DIANCE	EdK	DIFF BRDF	COS 70.58°	LdK
160	1						.33249	
185	1						.33249	
230	1						.33249	
252.03	1	.8750	.9981	.1784	.156 E0	.256	.33249	.133 E-1
273.07	1	.8615	.9981	.5657	.486 E0	.256	.33249	.414 E-1
283.00	1	.8711	.9981	.8685	.755 E0	.267	.33249	.670 E-1
292.20	1	.8939	.9981	1.265	.113 E1	.267	.33249	.100 E0
301.86	1	.8830	.9981	1.813	.160 E1	.260	.33249	.138 E0
312.50	1	.8875	.9981	2.604	.231 E1	.270	.33249	.208 E0
331.21	1	.8844	.9981	4.586	.405 E1	.273	.33249	.367 E0
339.81	1	.8875	.9981	5.799	.514 E1	.270	.33249	.461 E0
350	1	.8871	.9981	7.521	.666 E1	.271	.33249	.601 E0
375	1	.8848	.9981	13.187	.116 E2	.276	.33249	.106 E1
379	1	.8890	.9981	14.282	.126 E2	.276	.33249	.115 E1
400	1	.8895	.9981	20.646	.183 E2	.277	.33249	.169 E1

A/N 3990



B6802-78

Table 4-3e

RADIANCES AND IRRADIANCES FOR AMBIENT RADIOMETRIC CALIBRATION
 DAY 224 SOURCE MINI-ARC II MIRROR A TEST DIFFUSER BaSO₄ #3

λ	WINDOW EFFI- CIENCY	MIRROR REFLEC- TANCE	GONIO- METRIC FACTOR	SOURCE IRRA- DIANCE	EdK	DIFF BRDF	COS 70.58°	LdK
160	1		1				.33249	.97 E-1*
185	1	.857	1	1.70	.146 E1		.33249	.243 E0
230	1	.877	1	3.52	.309 E1	.237	.33249	.331 E0
252.03	1	.875	1	4.45	.389 E1	.256	.33249	.401 E0
273.07	1	.8615	1	5.47	.471 E1	.256	.33249	.459 E0
283.00	1	.8711	1	5.93	.517 E1	.267	.33249	.522 E0
292.20	1	.8939	1	6.58	.588 E1	.267	.33249	.541 E0
301.86	1	.8830	1	7.09	.626 E1	.260	.33249	.549 E0
312.50	1	.8875	1	7.45	.661	.270	.33249	.661 E0
331.21	1	.8844	1	8.23	.728 E1	.273	.33249	
339.81	1	.8875						
350	1							
375	1							
379	1							
400	1							

*DUMMY VALUE

A/N 3990



B6802-78

Table 4-3f

RADIANCES AND IRRADIANCES FOR AMBIENT RADIOMETRIC CALIBRATION

DAY 240 & 224 SOURCE D₂ #939 MIRROR A TEST DIFFUSER BaSO₄ #3

λ	WINDOW EFFI- CIENCY	MIRROR REFLEC- TANCE	GONIO- METRIC FACTOR	SOURCE IRRA- DIANCE	EdK	DIFF BRDF	COS 70.58°	LdK
160	1		1				.33249	
185	1	.857	1	.478	.410 E0		.33249	.284 E-1*
230	1	.877	1	.415	.364 E0	.237	.33249	.287 E-1
252.03	1	.872	1	.319	.279 E0	.256	.33249	.238 E-1
273.07	1	.8615	1	.229	.197 E0	.256	.33249	.168 E-1
283.00	1	.8711	1	.196	.171 E0	.267	.33249	.152 E-1
292.20	1	.8939	1	.170	.152 E0	.267	.33249	.135 E-1
301.86	1	.8830	1	.146	.129 E0	.260	.33249	.112 E-1
312.50	1	.8875	1	.125	.111 E0	.270	.33249	.100 E-1
331.21	1	.8844	1	.0965	.853 E-1	.273	.33249	.774 E-2
339.81	1	.8875	1	.0862	.765 E-1	.270	.33249	.687 E-2
350	1	.8871	1	.0770	.683 E-1	.271	.33249	.616 E-2
375	1						.33249	
379	1						.33249	
400	1						.33249	

*DUMMY VALUES FOR COMPUTER

A/N 3990



B6802-78

Table 4-3g

RADIANCES AND IRRADIANCES FOR AMBIENT RADIOMETRIC CALIBRATION

DAY 240 SOURCE D₂ #964 MIRROR A TEST DIFFUSER BaSO₄ #3

λ	WINDOW EFFI- CIENCY	MIRROR REFLEC- TANCE	GONIO- METRIC FACTOR	SOURCE IRRA- DIANCE	EdK	DIFF BRDF	COS 70.58°	LdK
160	1		1				.33249	
185	1	.857	1	.535	.458 E0		.33249	.344 E-1
230	1	.877	1	.432	.379 E0	.237	.33249	.240 E-1
252.03	1	.872	1	.323	.282 E0	.256	.33249	.167 E-1
273.07	1	.8615	1	.228	.196 E0	.256	.33249	.150 E-1
283.00	1	.8711	1	.194	.150 E0	.267	.33249	.133 E-1
292.20	1	.8939	1	.168	.128 E0	.260	.33249	.111 E-1
301.86	1	.8830	1	.145	.110 E0	.270	.33249	.987 E-2
312.50	1	.8875	1	.124	.853 E-1	.273	.33249	.774 E-2
331.21	1	.8844	1	.0965	.774 E-1	.270	.33249	.695 E-2
339.81	1	.8875	1	.0872	.683 E-1	.271	.33249	.615 E-2
350	1	.8871	1	.0770				
375								
379								
400								

A/N 3990



B6802-78

Table 4-3h

RADIANCES AND IRRADIANCES FOR AMBIENT RADIOMETRIC CALIBRATION

DAY 241 SOURCE MINI-ARC I MIRROR A TEST DIFFUSER BaSO₄ #3

λ	WINDOW EFFI- CIENCY	MIRROR REFLEC- TANCE	GONIO- METRIC FACTOR	SOURCE IRRA- DIANCE	EdK	DIFF BRDF	COS 70.58°	LdK
160	1		1				.33249	.858 E-1*
185	1	.857	1	1.45	.124 E1		.33249	.241 E0
230	1	.877	1	3.48	.305 E1	.237	.33249	.332 E0
252.03	1	.8750	1	4.45	.389 E1	.256	.33249	.399 E0
273.07	1	.8615	1	5.44	.469 E1	.256	.33249	.456 E0
283.00	1	.8711	1	5.89	.513 E1	.267	.33249	.515 E0
292.20	1	.8939	1	6.48	.579 E1	.267	.33249	.532 E0
301.86	1	.8830	1	6.95	.614 E1	.260	.33249	.583 E0
312.50	1	.8875	1	7.32	.650 E1	.270	.33249	.647 E0
331.21	1	.8844	1	8.06	.713 E1	.273	.33249	
339.81	1	.8875	1					
350	1		1					
375	1		1					
379	1		1					
400	1		1					

*DUMMY VALUE FOR UTILITY

A/N 3990



B6802-78

Table 4-3i

RADIANCES AND IRRADIANCES FOR RADIOMETRIC CALIBRATION IN VACUUM

DAY 243 SOURCE MINI-ARC II MIRROR C TEST DIFFUSER AL 5083
REV 6

λ	WINDOW EFFI- CIENCY	MIRROR REFLEC- TANCE	GONIO- METRIC FACTOR	SOURCE IRRA- DIANCE	EdK	DIFF BRDF	COS 70.58°	LdK
160	1	.837	1	.518	.278 E0		.33249	.346 E-1*
185	1	.850	1	1.54	.131 E1		.33249	.602 E-1*
230	1	.895	1	3.18	.285 E1	.1585	.33249	.150 E0
252.03	1	.881	1	4.02	.354 E1	.1758	.33249	.208 E0
273.07	1	.861	1	4.94	.425 E1	.1847	.33249	.262 E0
283.00	1	.885	1	5.36	.474 E1	.1929	.33249	.305 E0
292.20	1	.892	1	5.95	.531 E1	.1980	.33249	.349 E0
301.86	1	.891	1	6.41	.571 E1	.1951	.33249	.371 E0
312.50	1	.868	1	6.73	.584 E1	.1988	.33249	.386 E0
331.21	1	.876	1	7.44	.652 E1	.2066	.33249	.447 E0
339.81	1	.883	1					
350	1	.887	1					
375	1	.894	1					
379	1		1					
400	1	.889	1					

*DUMMY VALUES FOR UTILITY

A/N 3990



B6802-78

Table 4-3j

RADIANCES AND IRRADIANCES FOR RADIO-METRIC CALIBRATION IN VACUUM

DAY 243 SOURCE D₂ #939 MIRROR C TEST DIFFUSER AL5083
REV 6

λ	WINDOW EFFI- CIENCY	MIRROR REFLEC- TANCE	GONIO- METRIC FACTOR	SOURCE IRRA- DIANCE	EdK	DIFF BRDF	COS 70.58°	LdK
160			1				.33249	
185	.853	.850	1	.478	.347 E0		.33249	.159 E-1*
230	.894	.895	1	.415	.332 E0	.1585	.33249	.174 E-1
252.03	.896	.881	1	.319	.252 E0	.1758	.33249	.147 E-1
273.07	.904	.861	1	.229	.178 E0	.1847	.33249	.109 E-1
283.00	.904	.885	1	.196	.157 E0	.1929	.33249	.100 E-1
292.20	.905	.892	1	.170	.137 E0	.1980	.33249	.903 E-2
301.86	.907	.891	1	.146	.118 E0	.1951	.33249	.766 E-2
312.50	.910	.868	1	.125	.987 E-1	.1988	.33249	.652 E-2
331.21	.910	.876	1	.096	.765 E-1	.2066	.33249	.526 E-2
339.81	.911	.883	1	.086	.692 E-1	.2051	.33249	.472 E-2
350	.914	.887	1	.077	.624 E-1	.2058	.33249	.426 E-2
375	.915	.894	1					
379			1					
400	.916	.889	1					

*DUMMY VALUE FOR UTILITY

A/N 3990



B6802-78

Table 4-3k

RADIANCES AND IRRADIANCES FOR RADIOMETRIC CALIBRATION IN VACUUM

DAY 242-243 SOURCE FEL #127 MIRROR C TEST DIFFUSER AL 5083
REV 6

λ	WINDOW EFFI- CIENCY	MIRROR REFLEC- TANCE	GONIO- METRIC FACTOR	SOURCE IRRA- DIANCE	EdK	DIFF BRDF	COS 70.58°	LdK
160			.998				.33249	
185	.853	.850	.998				.33249	
230	.894	.895	.998				.33249	
252.03	.896	.881	.998	.1784	.141 E0	.1758	.33249	.821 E-2
273.07	.904	.861	.998	.5657	.439 E0	.1847	.33249	.270 E-1
283.00	.904	.885	.998	.8685	.693 E0	.1929	.33249	.444 E-1
292.20	.905	.892	.998	1.265	.102 E1	.1980	.33249	.672 E-1
301.86	.907	.891	.998	1.813	.146 E1	.1951	.33249	.948 E-1
312.50	.910	.868	.998	2.604	.205 E1	.1988	.33249	.136 E0
331.21	.910	.876	.998	4.586	.363 E1	.2066	.33249	.249 E0
339.81	.911	.883	.998	5.799	.466 E1	.2051	.33249	.317 E0
350	.914	.887	.998	7.521	.609 E1	.2058	.33249	.417 E0
375	.915	.894	.998	13.187	.108 E2	.2125	.33249	.760 E0
379			.998	14.282			.33249	
400	.916	.889	.998	20.646	.168 E2	.2136	.33249	.119 E1

A/N 3990



B6802-78

Table 4-31

RADIANCES AND IRRADIANCES FOR AMBIENT RADIOMETRIC CALIBRATION

DAY 244 SOURCE FEL #124 MIRROR A TEST DIFFUSER BaSO₄ #3

λ	WINDOW EFFI- CIENCY	MIRROR REFLEC- TANCE	GONIO- METRIC FACTOR	SOURCE IRRA- DIANCE	EdK	DIFF BRDF	COS 70.58°	LdK
160	1		.9965				.33249	
185	1		.9965				.33249	
230	1		.9965				.33249	
252.03	1	.8750	.9965	.180	.157 E0	.256	.33249	.134 E-1
273.07	1	.8615	.9965	.553	.475 E0	.256	.33249	.404 E-1
283.00	1	.8711	.9965	.863	.749 E0	.267	.33249	.665 E-1
292.20	1	.8939	.9965	1.253	.112 E1	.267	.33249	.991 E-1
301.86	1	.8830	.9965	1.793	.158 E1	.260	.33249	.136 E0
312.50	1	.8875	.9965	2.570	.227 E1	.270	.33249	.204 E0
331.21	1	.8844	.9965	4.51	.397 E1	.273	.33249	.361 E0
339.81	1	.8875	.9965	5.69	.503 E1	.270	.33249	.452 E0
350	1	.8871	.9965	7.36	.651 E1	.271	.33249	.586 E0
375	1	.8848	.9965	12.83	.113 E2	.276	.33249	.104 E1
379	1	.8890	.9965	13.89	.123 E2	.276	.33249	.113 E1
400	1	.8895	.9965	20.1	.178 E2	.277	.33249	.164 E1

A/N 3990



RADIANCE FOR CALIBRATION RUNS WITH NORMAL INCIDENCE DIFFUSERS AND FEL #127

WAVELENGTH	DIFFUSER A USED DAY 224	DIFFUSER B USED DAY 241
	Ldk	Ldk
252.03	.507 E-1	.513 E-1
273.47	.163 E0	.161 E0
283.00	.252 E0	.252 E0
292.20	.368 E0	.363 E0
301.86	.534 E0	.518 E0
312.50	.763 E0	.767 E0
331.21	.135 E1	.136 E1
339.81	.171 E1	.170 E1
350.00	.222 E1	.222 E1
375.00	.391 E1	.394 E1
400.00	.612 E1	.611 E1

Table 4-3m

A/N 3990



Table 4-4

RADIOMETRIC CALIBRATION CATALOG FOR DISCRETE AND POSITION MODES

Radiometric calibration catalog for discrete (GDISCAL) and position (DISCAL) mode data. The first column is the file name of the data in the [SBUV2.PLOT.-RADIOMTRC] directory. The other columns identify the data run. Each file contains just twelve numbers, either L/C or E/C for earth or sun viewing modes respectively, in order of increasing wavelength. Only the L/C files are listed here. For each L/C file there is a corresponding E/C file except for the runs using the 12x12 diffusers.

By using the IDL procedures "RADPLOT" or "IRADPLOT", semilog plots can be produced in standard format. Assign the data values to the 12 element vector Y.



B5802-78

<u>Filename</u>	<u>Date</u>	<u>Source</u>	<u>Mirror</u>	<u>Diffuser</u>	<u>Temp</u>	<u>Macro</u>
LC01	197	FEL124	C	AL old	0	DISCAL
LC02	"	D2 939	"	"	"	"
LC03	198	FEL124	"	"	10	"
LC04	"	D2 939	"	"	"	"
LC05	"	MINAR2	"	"	"	"
LC06	"	FEL124	"	"	20	"
LC07	"	"	"	"	"	GDISCAL
LC08	"	D2 939	"	"	"	DISCAL
LC09	"	MINAR2	"	"	"	"
LC10	199	FEL124	"	"	30	"
LC11	"	"	"	"	"	GDISCAL
LC12	"	D2 939	"	"	"	DISCAL
LC13	"	MINAR2	"	"	"	"
LC14	201	FEL124	"	"	25	"
LC15	"	"	"	"	"	GDISCAL
LC15B	"	MINAR2	"	"	0	DISCAL
LC16	217	FEL127	A	AL old	AMB	DISCAL
LC17	"	"	"	"	"	GDISCAL
LC18	"	D2 964	"	"	"	DISCAL
LC19	220	MINAR1	"	"	"	"
LC20	223	FEL127	"	BS 3	"	"
LC21	224	MINAR2	"	"	"	"
LC22	"	D2 939	"	"	"	"
LC23	"	FEL127	NONE	BS A 12 x 12	"	DISCAL
LC24	"	"	"	"	"	GDISCAL
LC25	240	"	A	BS 3	"	"
LC26	"	"	"	"	"	DISCAL
LC27	"	"	"	"	"	GDISCAL
LC28	"	D2 939	"	"	"	DISCAL
LC29	"	"	"	"	"	GDISCAL
LC30	"	D2 964	"	"	"	"
LC31	241	MINAR1	"	"	"	DISCAL
LC32	"	FEL127	NONE	BS B 12 x 12	"	"
LC33	243	"	C	Al flt spr	20 VAC	"

Table 4-4 Cont'd



B6802-78

<u>Filename</u>	<u>Date</u>	<u>Source</u>	<u>Mirror</u>	<u>Diffuser</u>	<u>Temp</u>	<u>Macro</u>
LC34	243	FEL 127	C	Al flt spr	20 VAC	GDISCAL
LC35	"	D2 939	"	"	"	DISCAL
LC36	"	MINAR2	"	"	"	"
LC37	244	FEL124	A	BS 3	AMB	GDISCAL
LC38	"	"	"	"	"	DISCAL
LC39	"	"	"	"	"	GDISCAL

Table 4-4 (Cont'd)



B6802-78

Table 4-5
CLOUD COVER RADIOMETER CALIBRATION CONSTANTS FROM RUNS EC26 AND LC26, LAMP FEL 127, DIFFUSER
BaSO₄ #3, DAY 240, DISCAL Ldk = 1.15, Edk = 12.6 AT 379 nm

MONOCHROMOTOR λ	CCR CURRENT		CALIBRATION L/C_L	CONSTANTS E/C_L	$\frac{L}{C_L} / \frac{E}{C_E}$
	EARTH MODE	SUN MODE			
252.03	.6488 E-11	.5583 E-11	2.06 E11	1.94 E12	0.106
273.47	.6441 E-11	.5547 E-11	2.07 E11	1.96 E12	0.106
283.00	.6409 E-11	.5524 E-11	2.08 E11	1.97 E12	0.106
287.57	.6401 E-11	.5506 E-11	2.09 E11	1.97 E12	0.106
292.20	.6386 E-11	.5491 E-11	2.09 E11	1.97 E12	0.106
297.47	.6358 E-11	.5483 E-11	2.10 E11	1.98 E12	0.106
301.86	.6348 E-11	.5463 E-11	2.11 E11	1.98 E12	0.107
305.80	.6341 E-11	.5444 E-11	2.11 E11	1.99 E12	0.106
312.50	.6343 E-11	.5439 E-11	2.11 E11	1.99 E12	0.106
317.50	.6350 E-11	.5432 E-11	2.12 E11	1.98 E12	0.107
331.21	.6373 E-11	.5461 E-11	2.11 E11	1.98 E12	0.107
339.81	.6387 E-11	.5475 E-11	2.10 E11	1.97 E12	0.107

A/N 3990

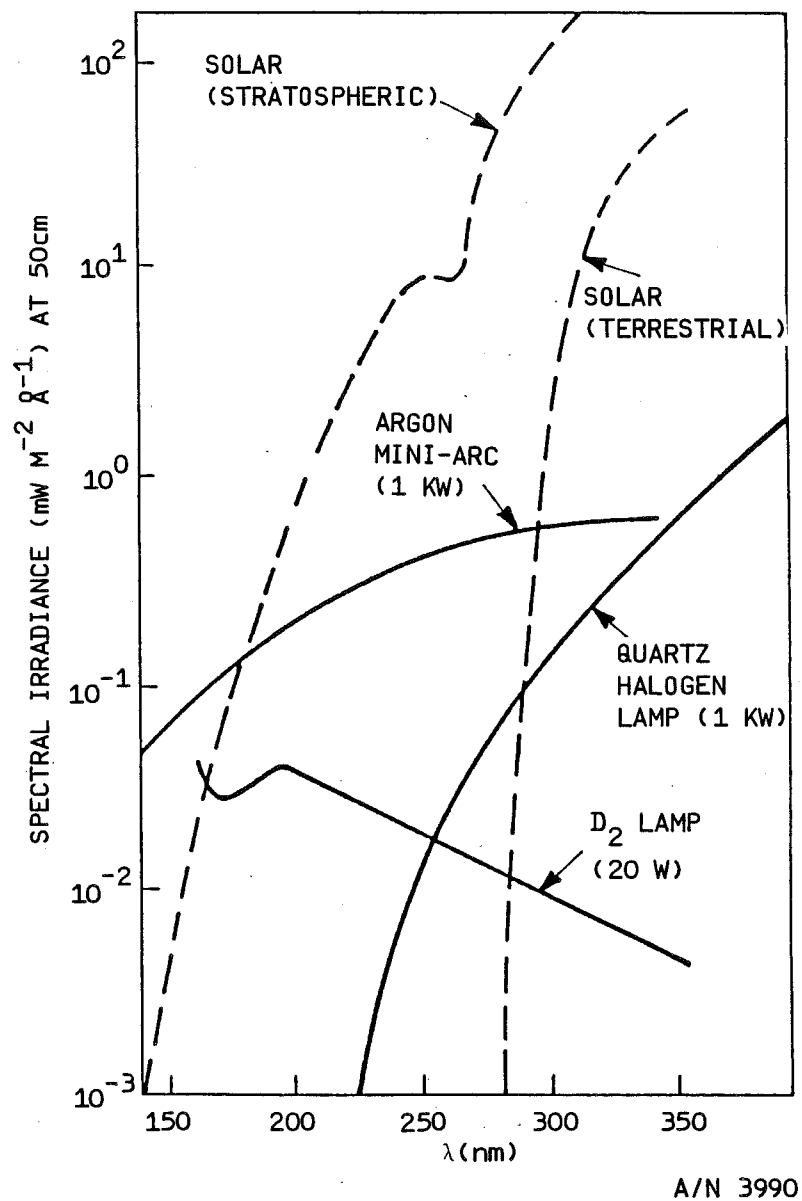


Figure 4-1 Comparison of Spectral Irradiance from Sun & from NBS Transfer Standard Sources



B6802-78

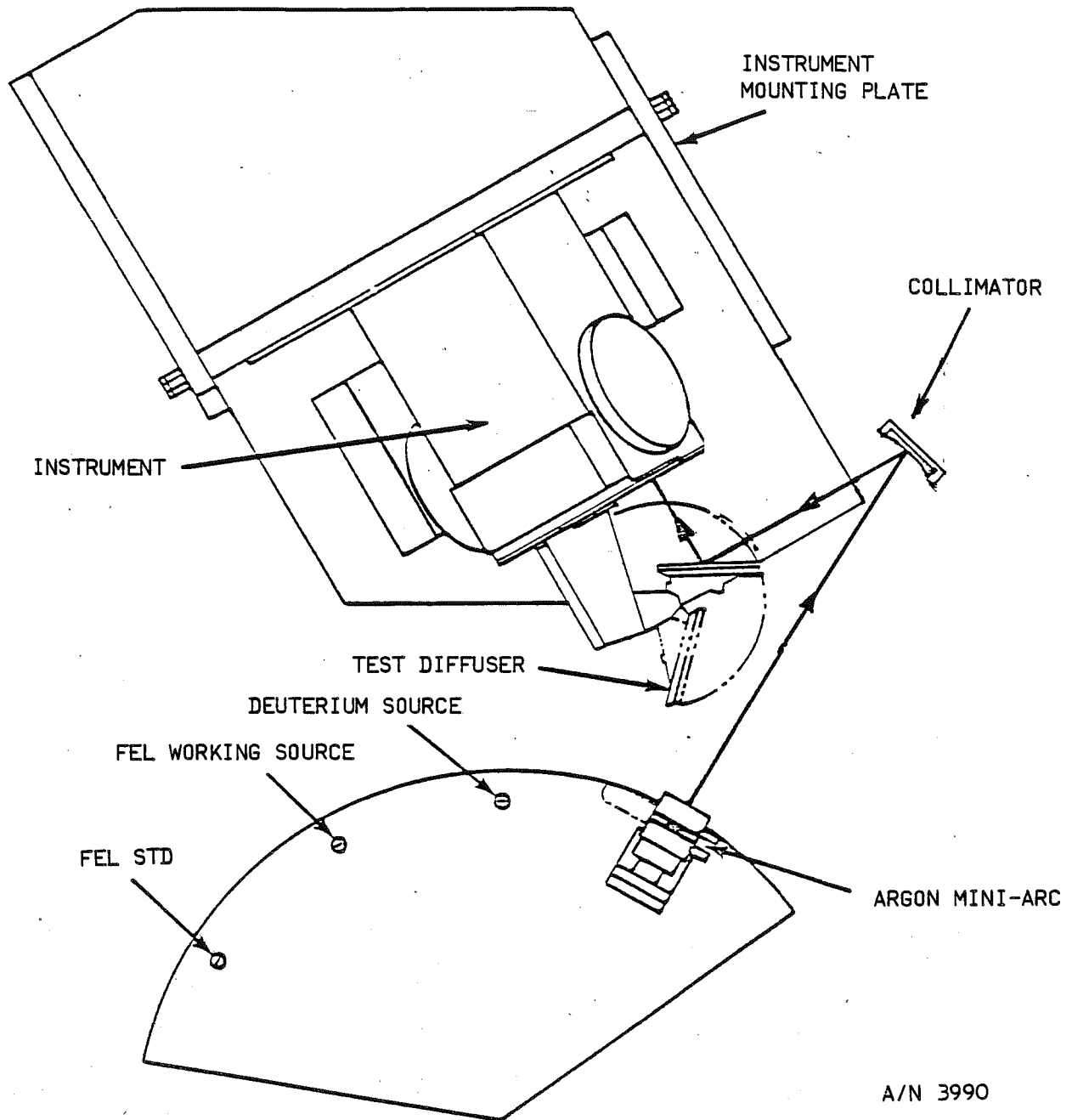
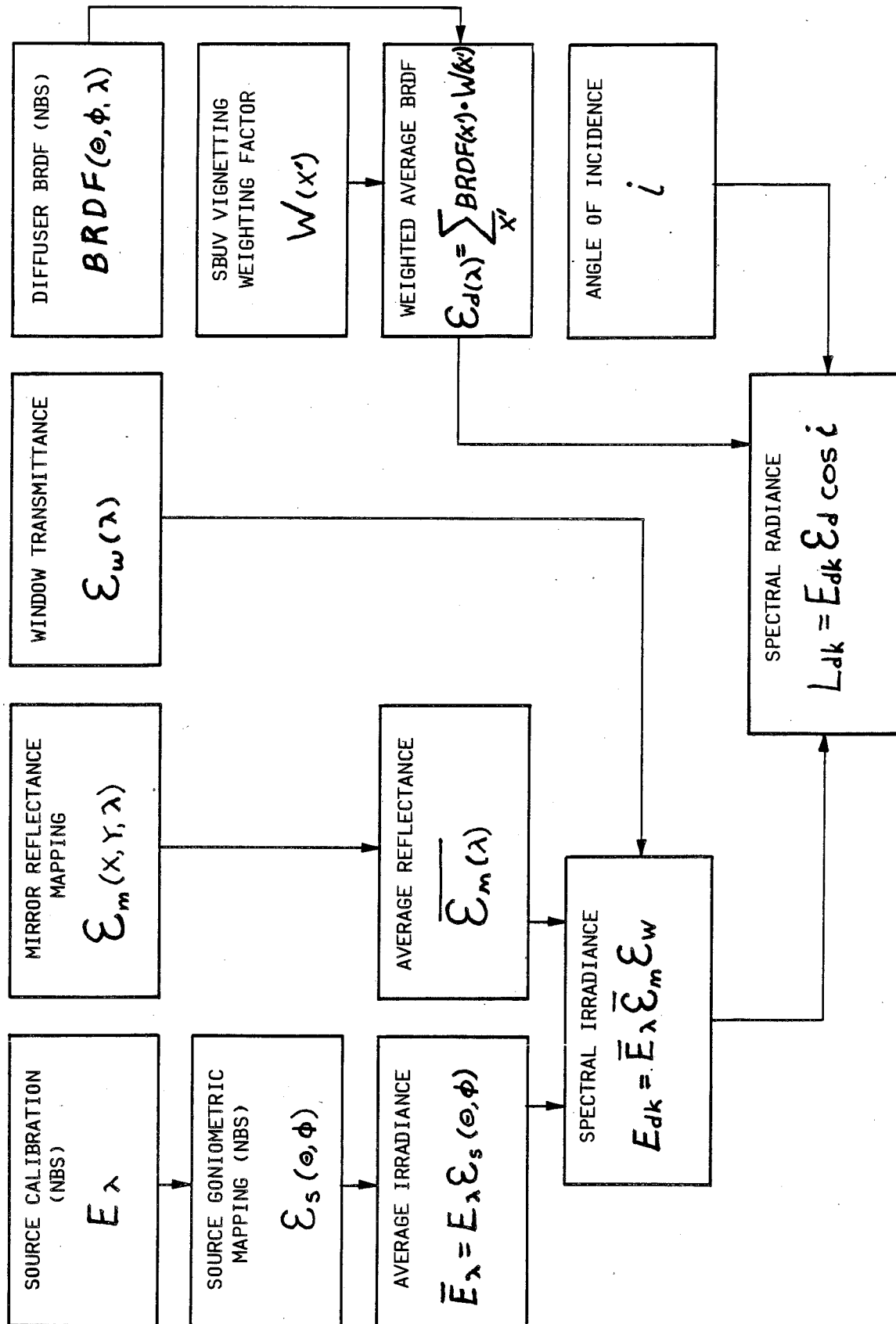


Figure 4-2 Calibration Setup



A/N 3990

Figure 4-3 Determination of Radiance and Irradiance for SBUV2 Calibration

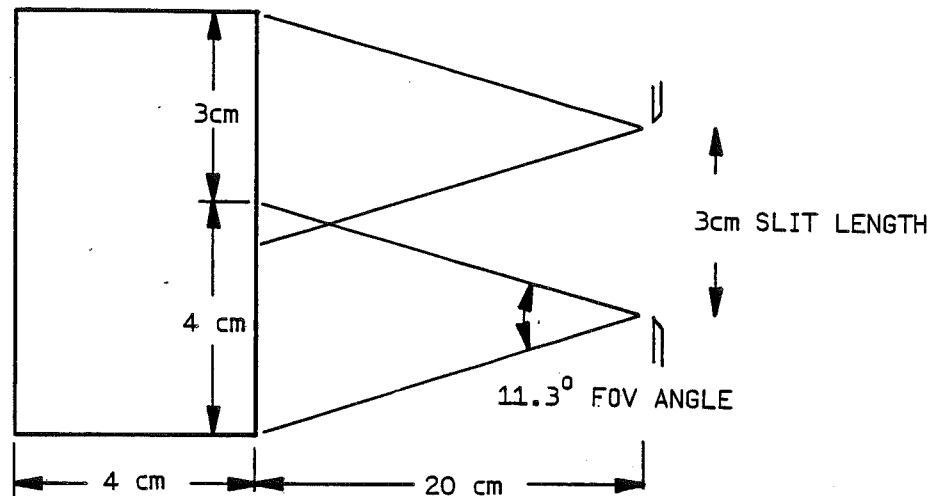
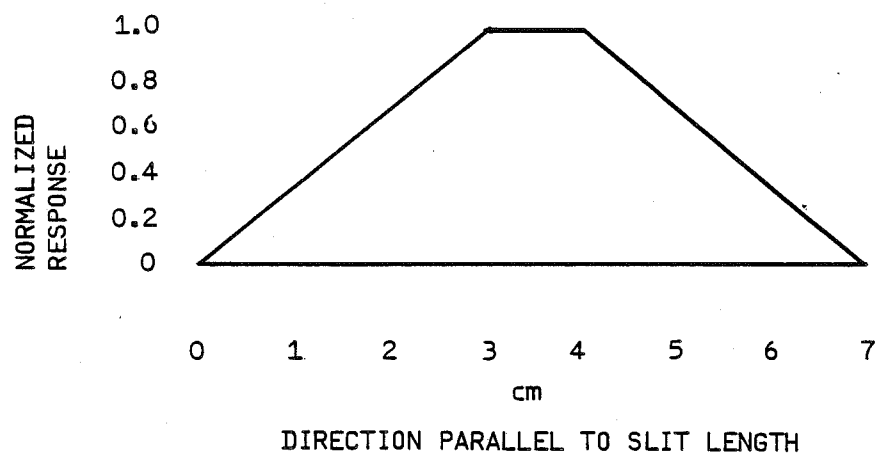


Figure 4-4 Optical Geometry of Viewing Nearby Diffuser

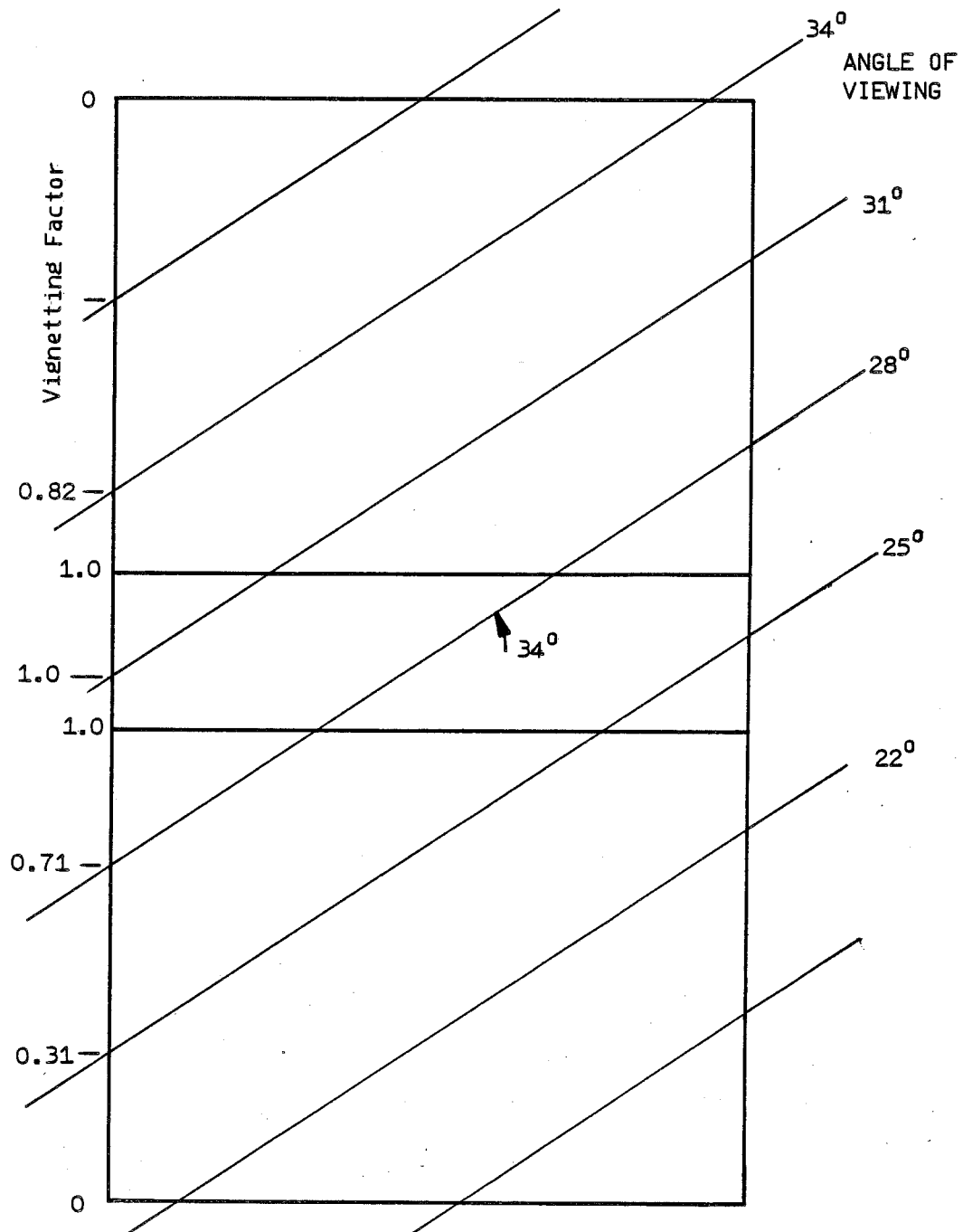


A/N 3990

Figure 4-5 Vignetting Profile



B6802-78

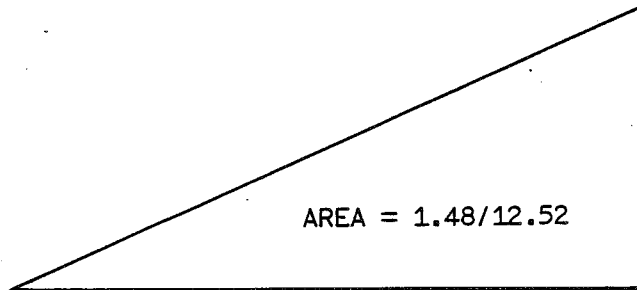


A/N 3990

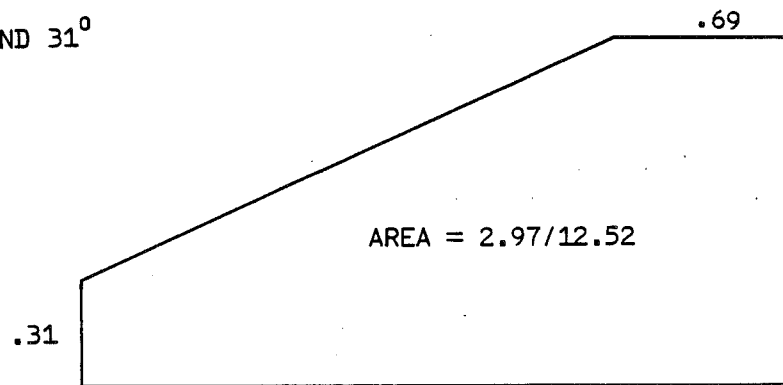
Figure 4-6 BRDF Angles and Vignetting Function Overlayed in Plane of Diffuser



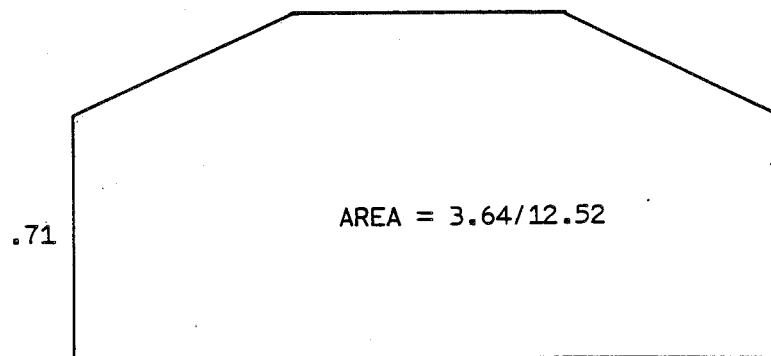
22° AND 34°



25° AND 31°



28°

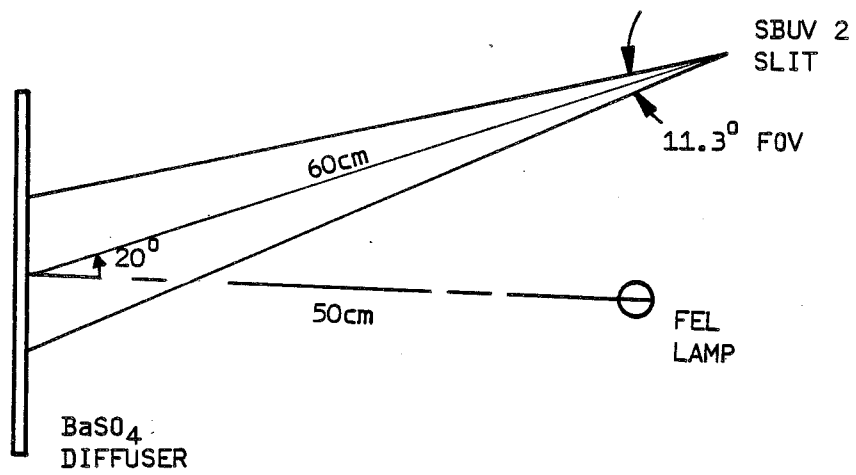


A/N 3990

Figure 4-7 Constant Angle Profiles



B6802-78



A/N 3990

Figure 4-8 Setup Geometry for Normal Incidence Diffuser



B6802-78

A/N 3990

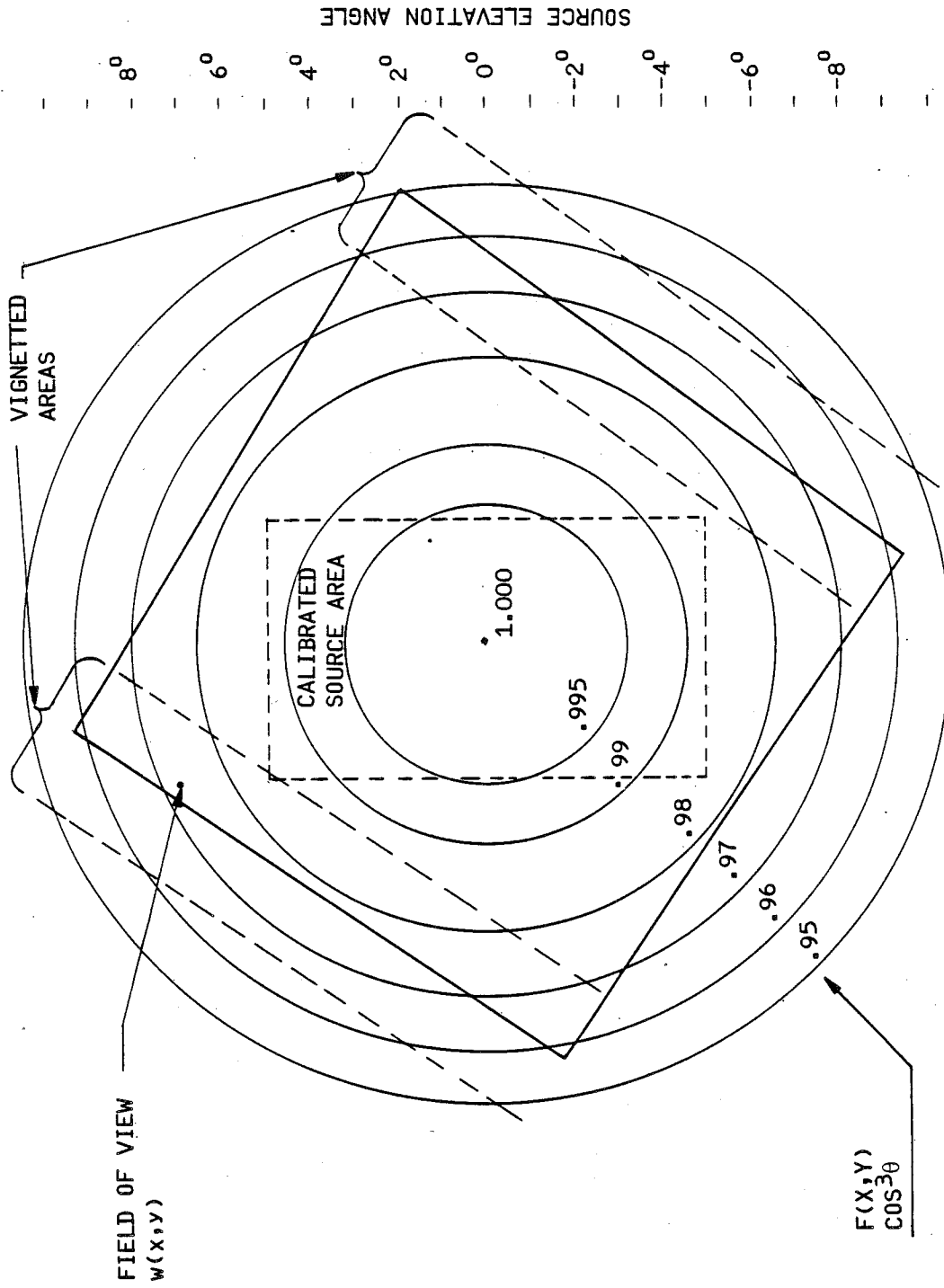
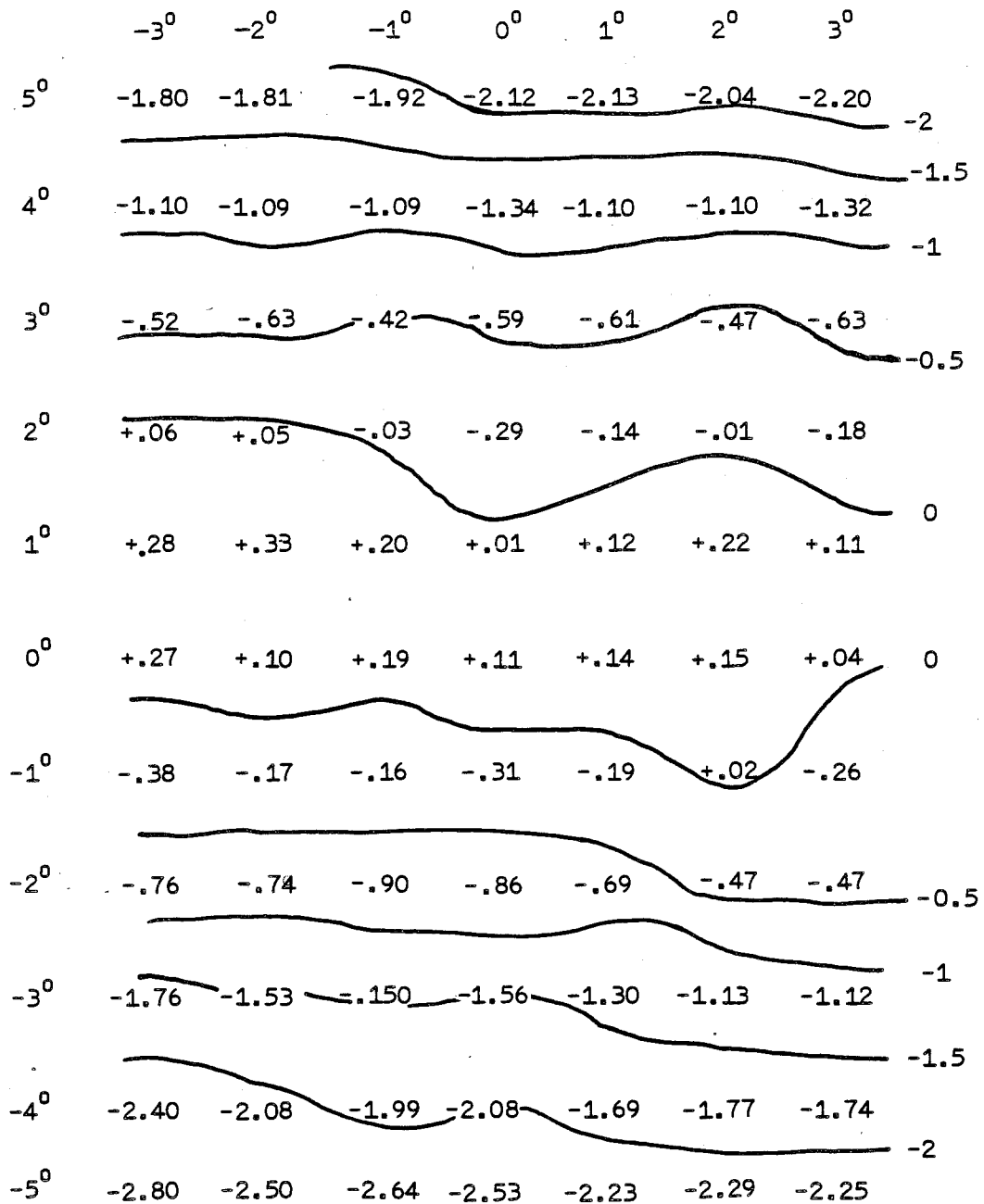


Figure 4-9 Overlay of $w(x, y)$ and $f(x, y)$ in Plane of Diffuser



B6802-78



A/N 3990

Figure 4-10 Isoirradiance Contours of FEL #127



B6802-78

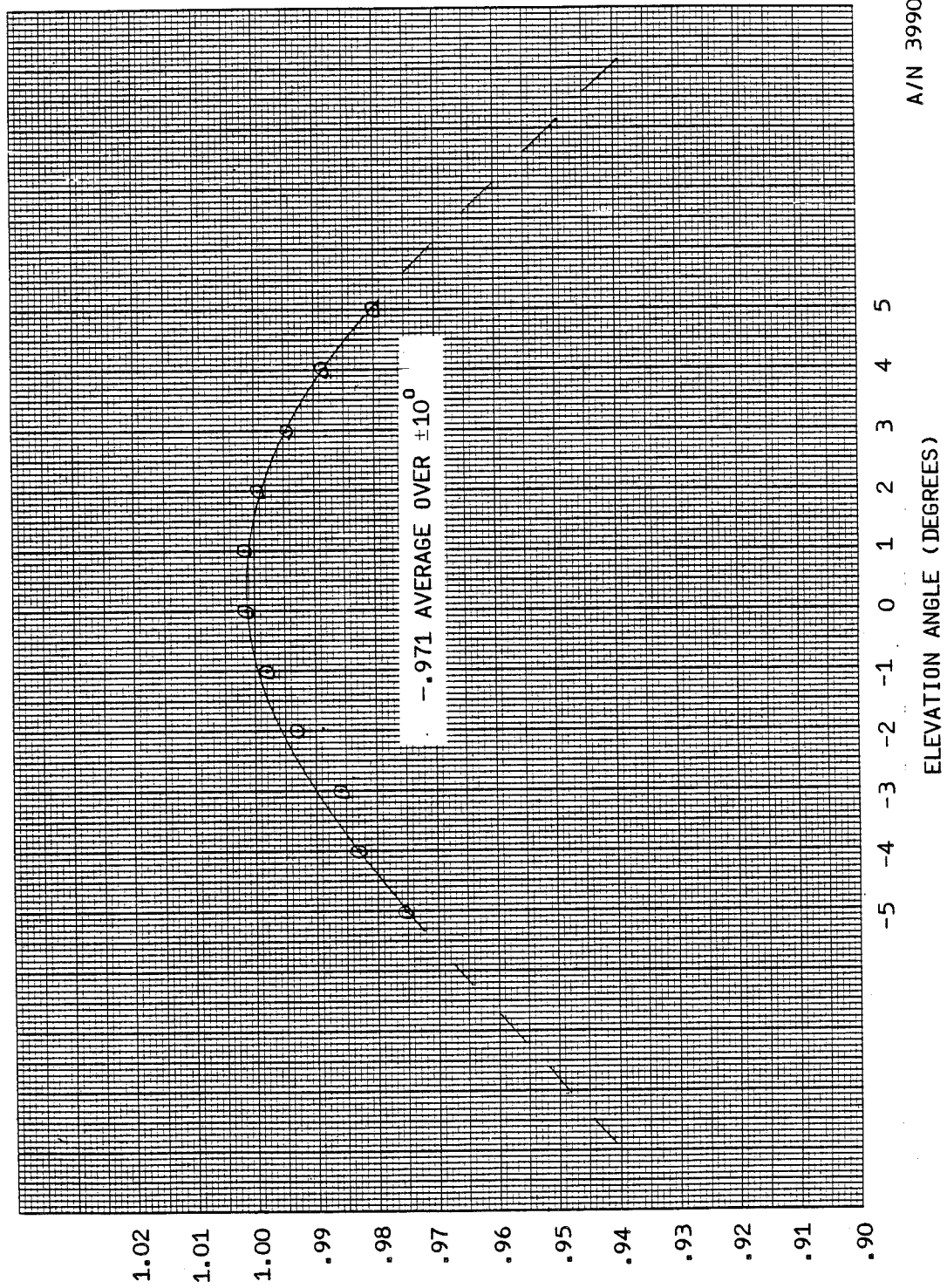


Figure 4-11 Average Normalized Irradiance Across Field vs. Elevation Angle, FEL #127



B6802-78

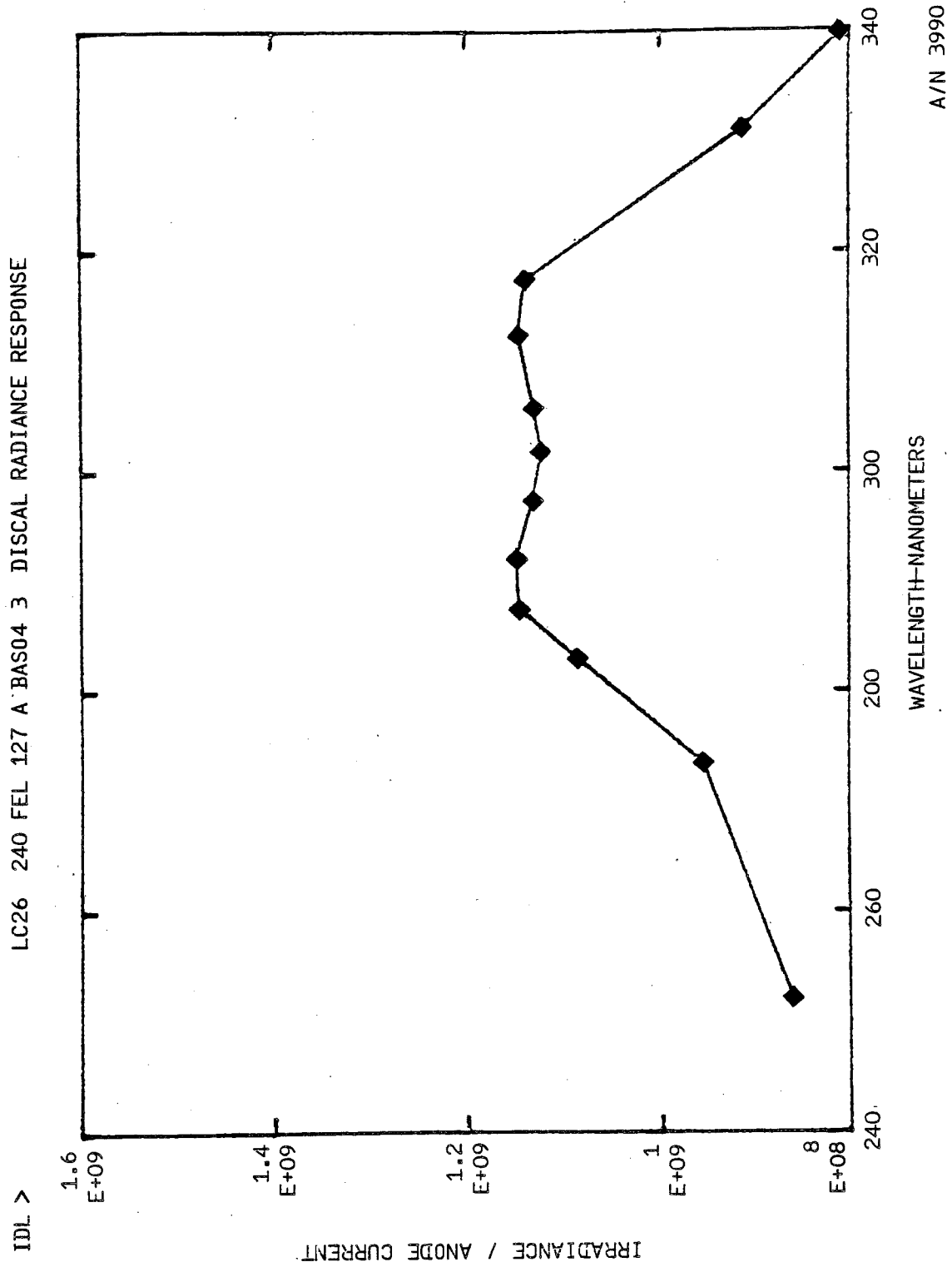


Figure 4-12



B6802-78

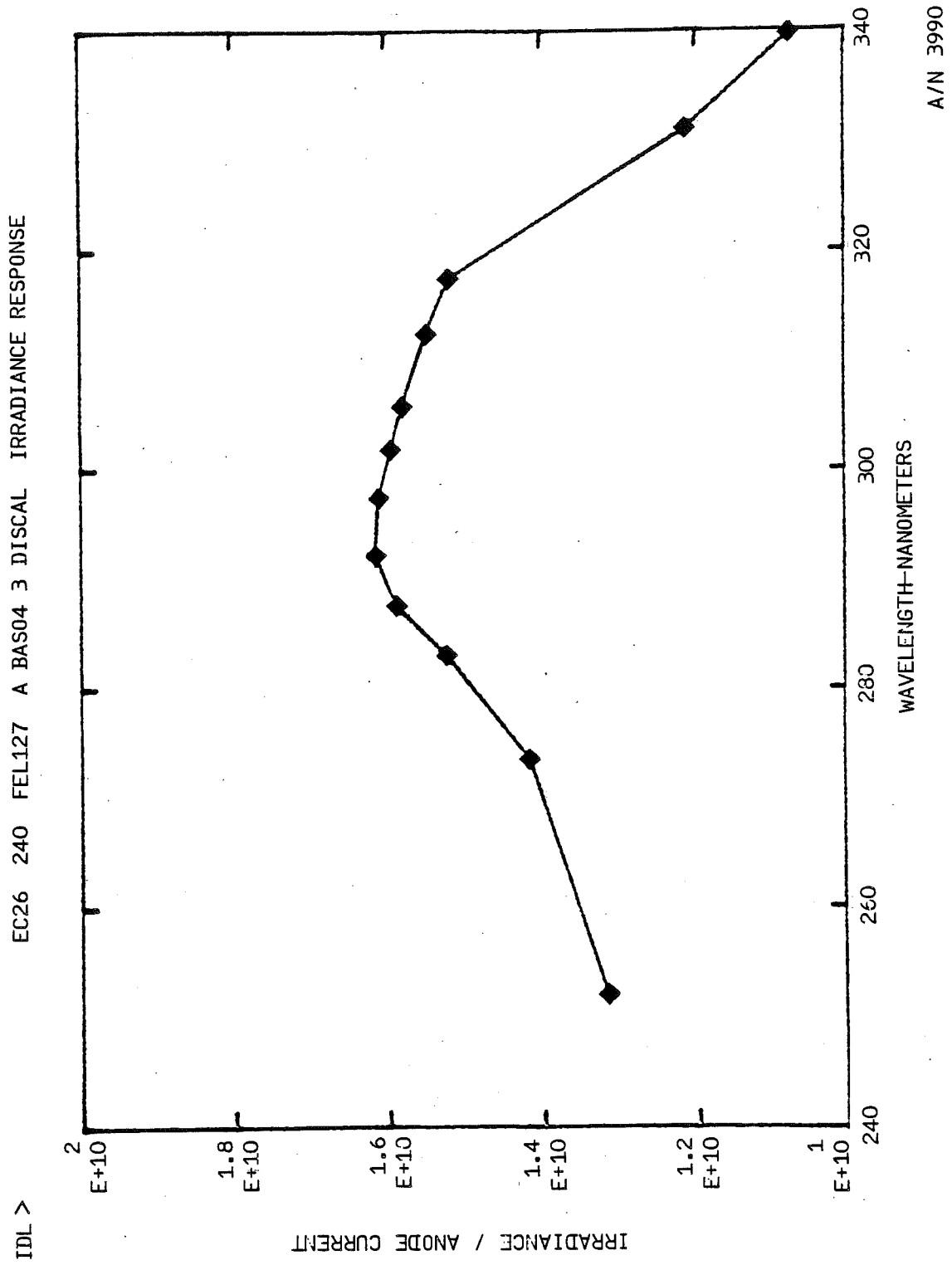


Figure 4-13



B6802-78

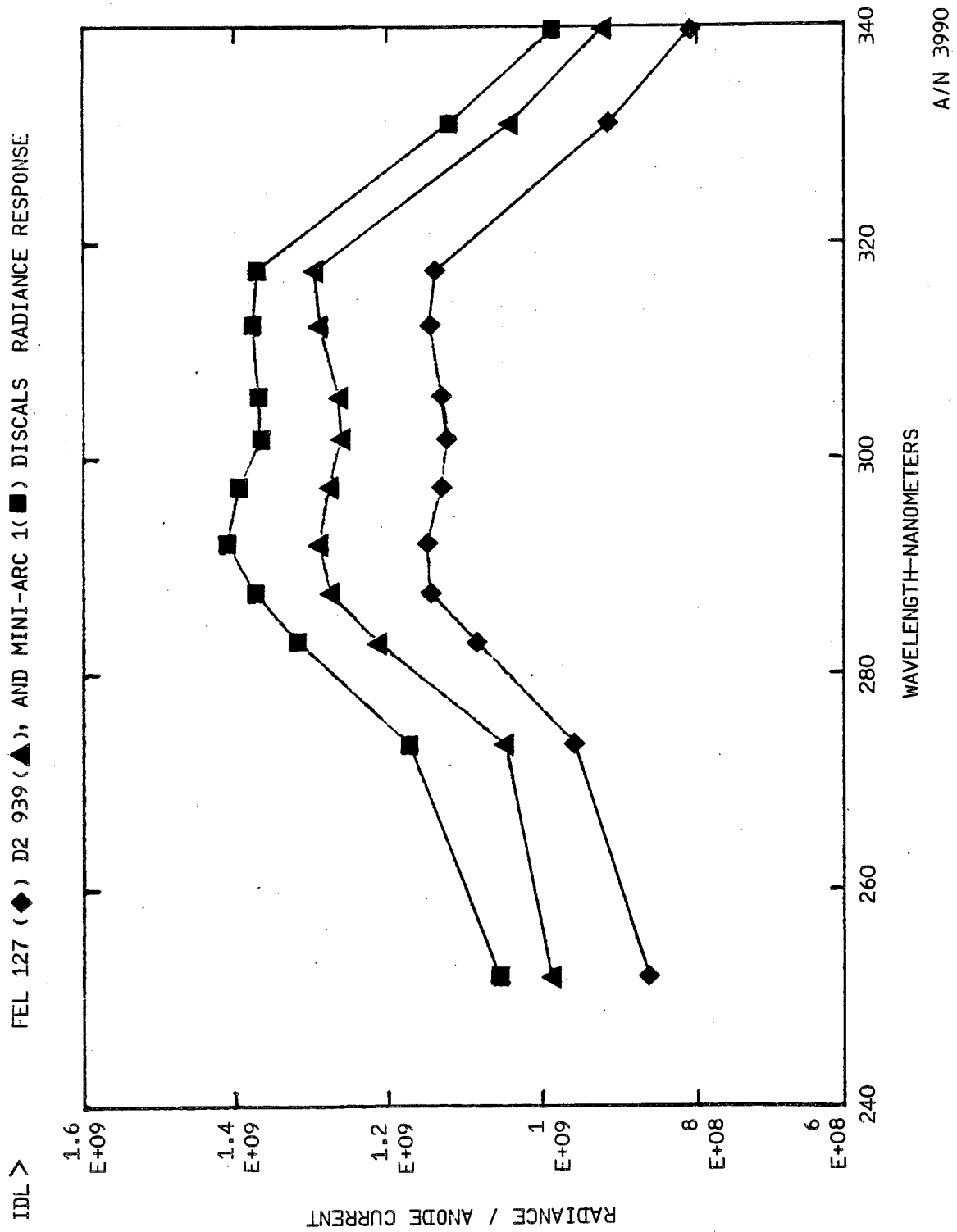


Figure 4-14



B6802-78

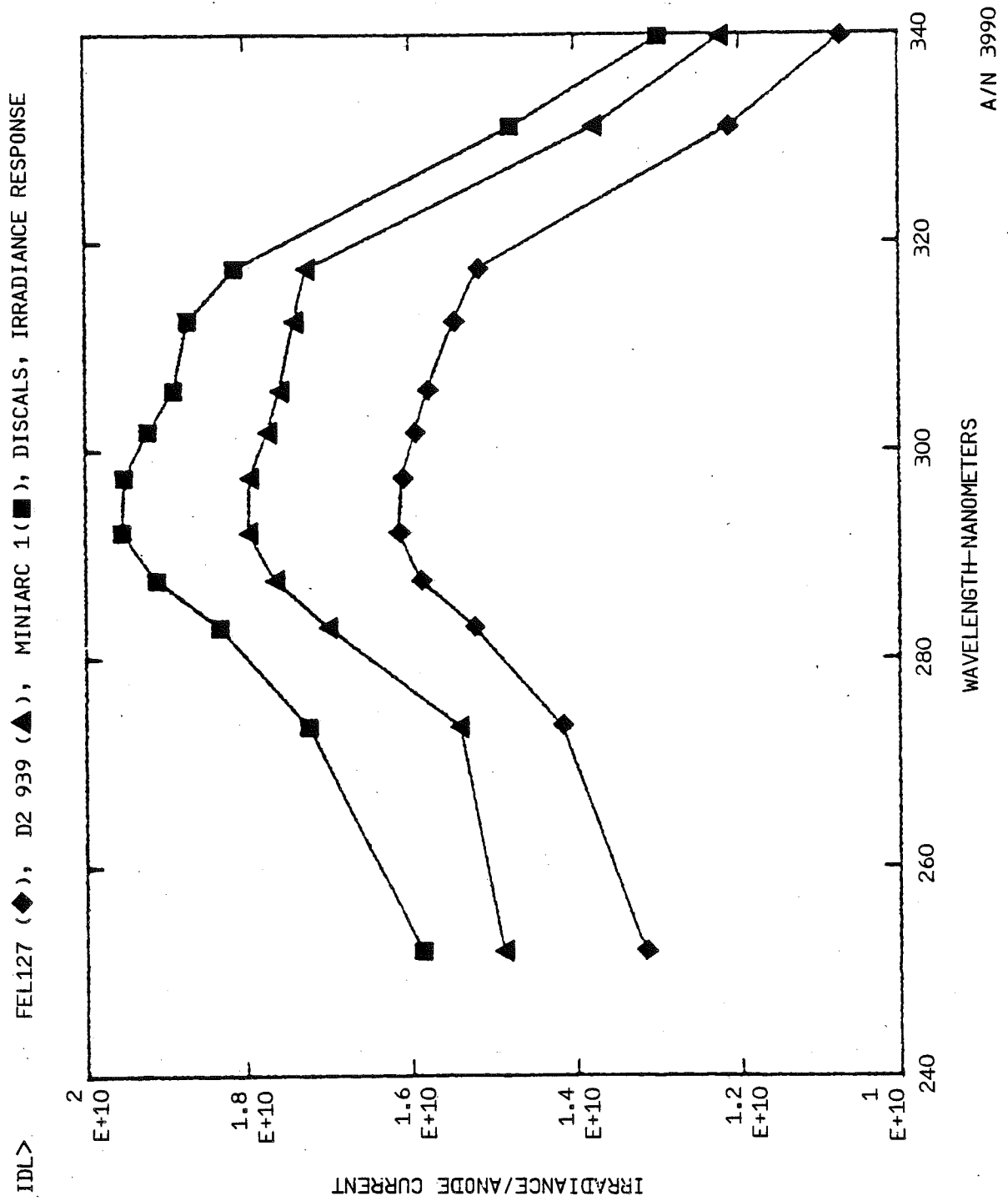


Figure 4-15



B6802-78

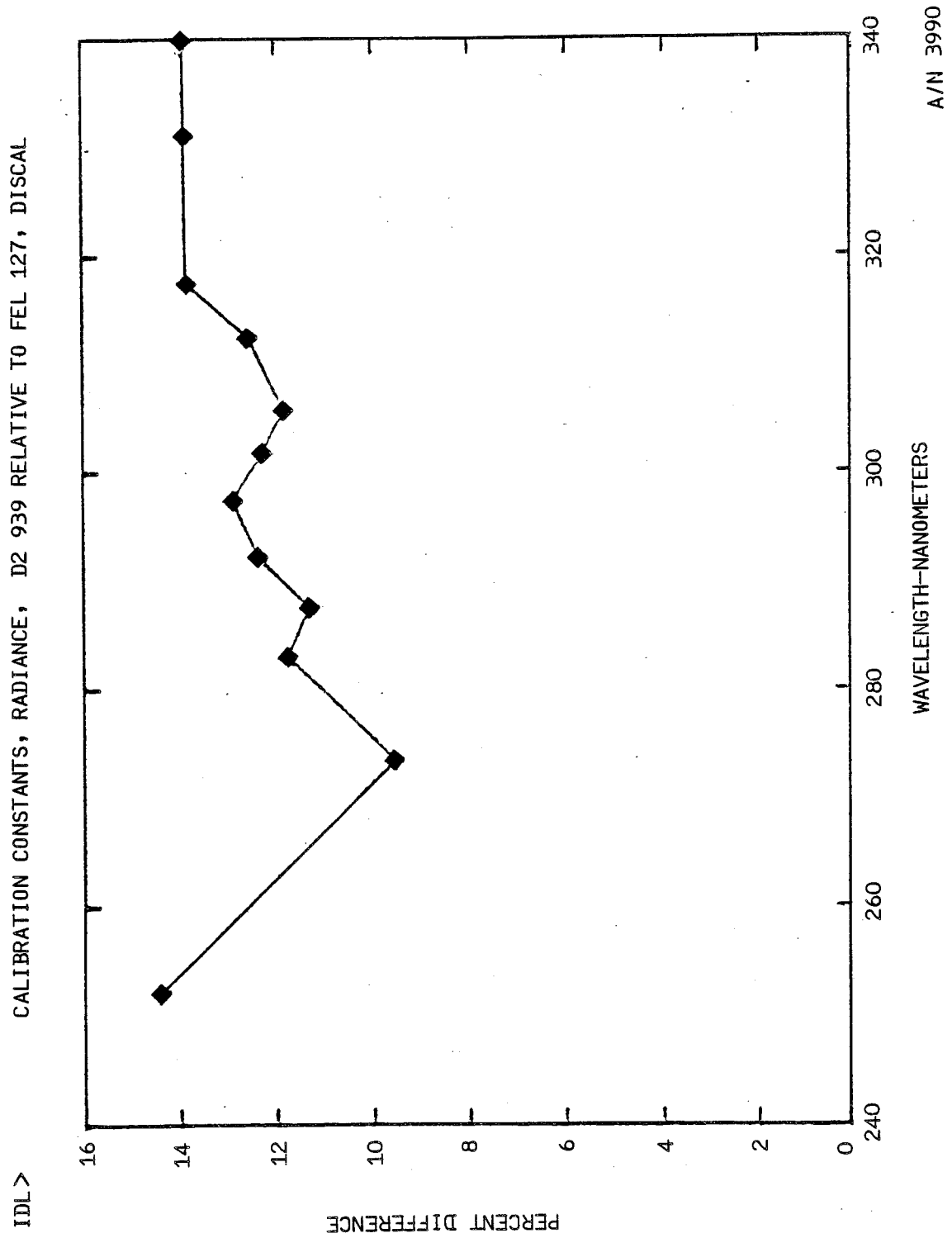


Figure 4-16



B6802-78

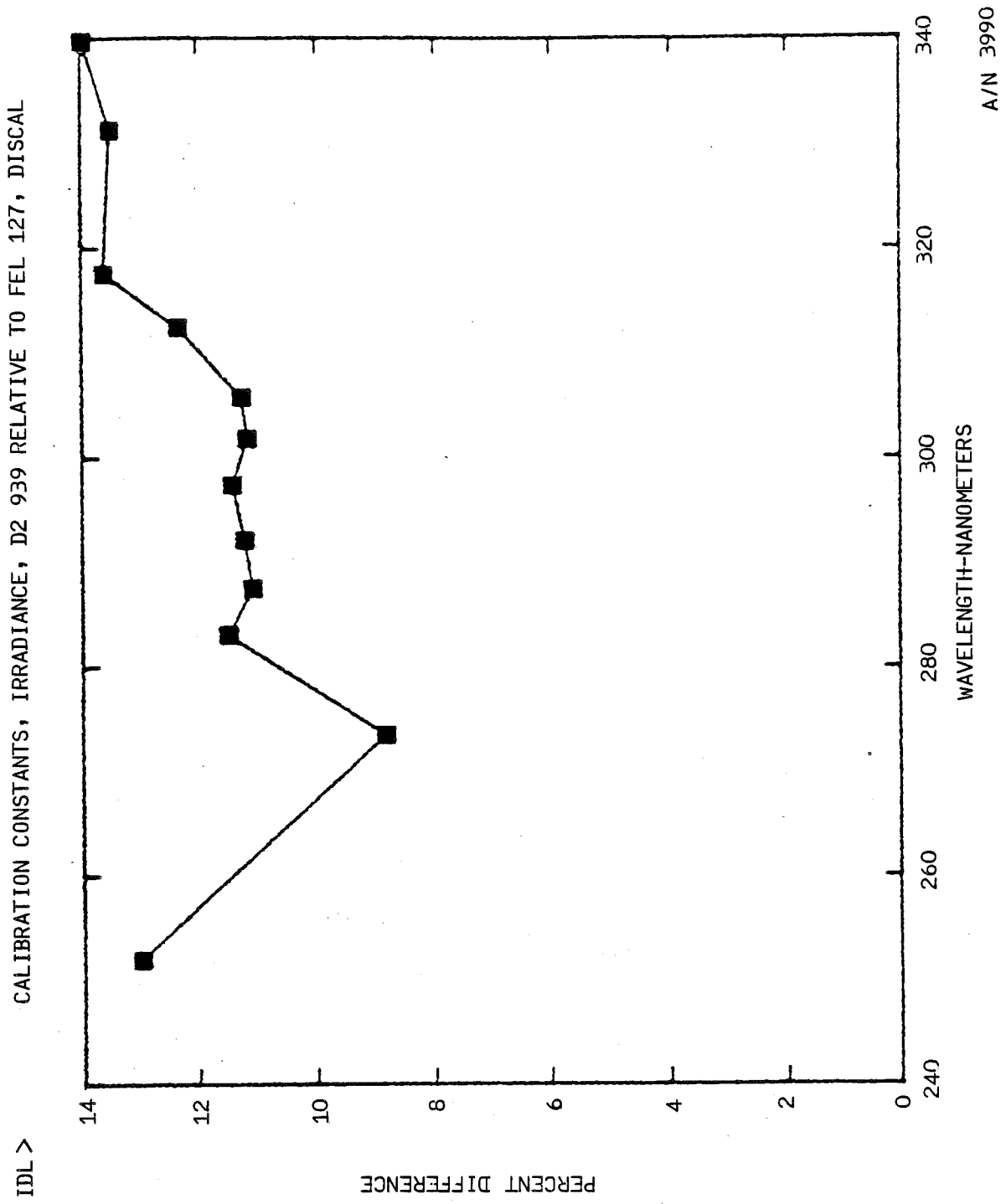


Figure 4-17



B6802-78

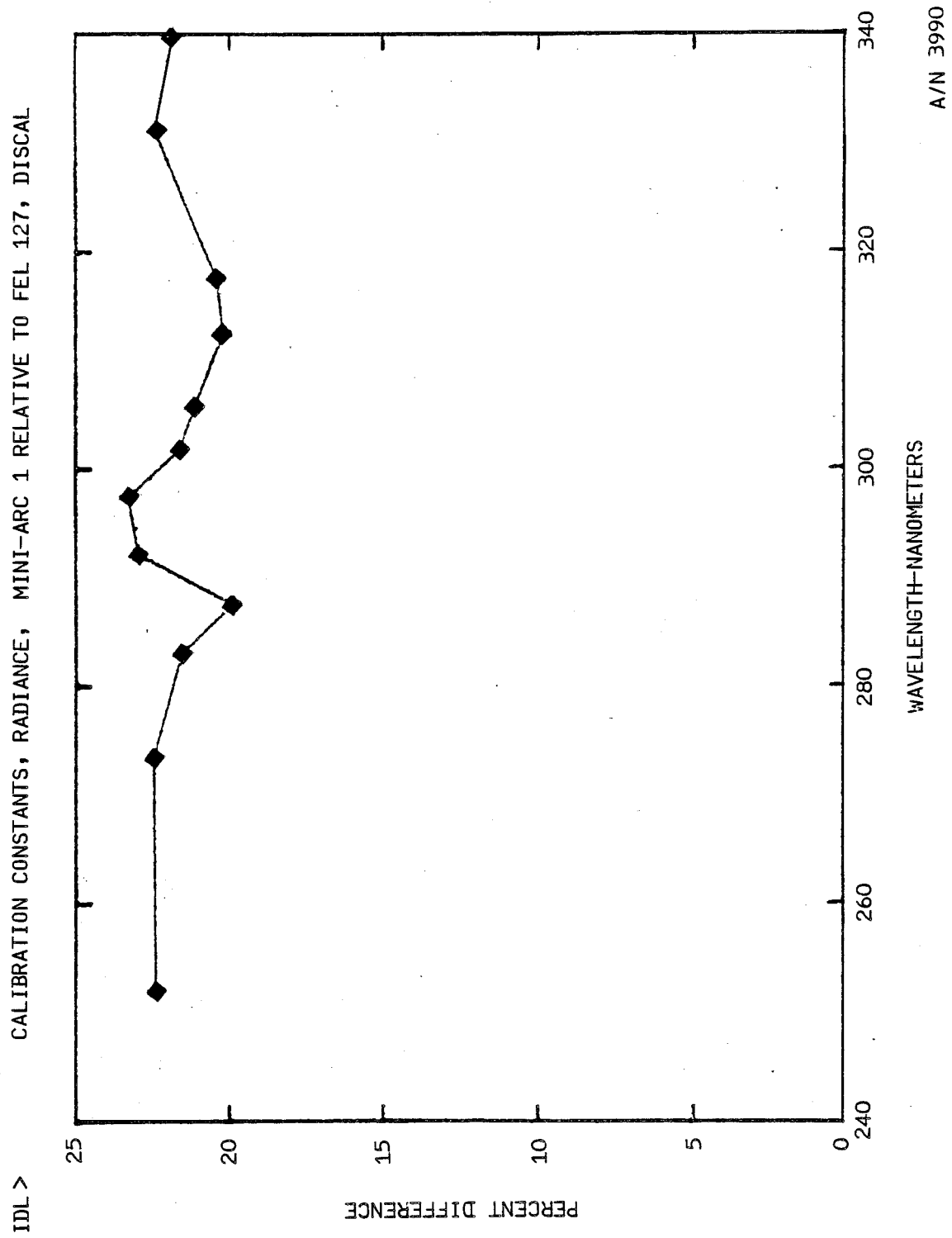


Figure 4-18



B6802-78

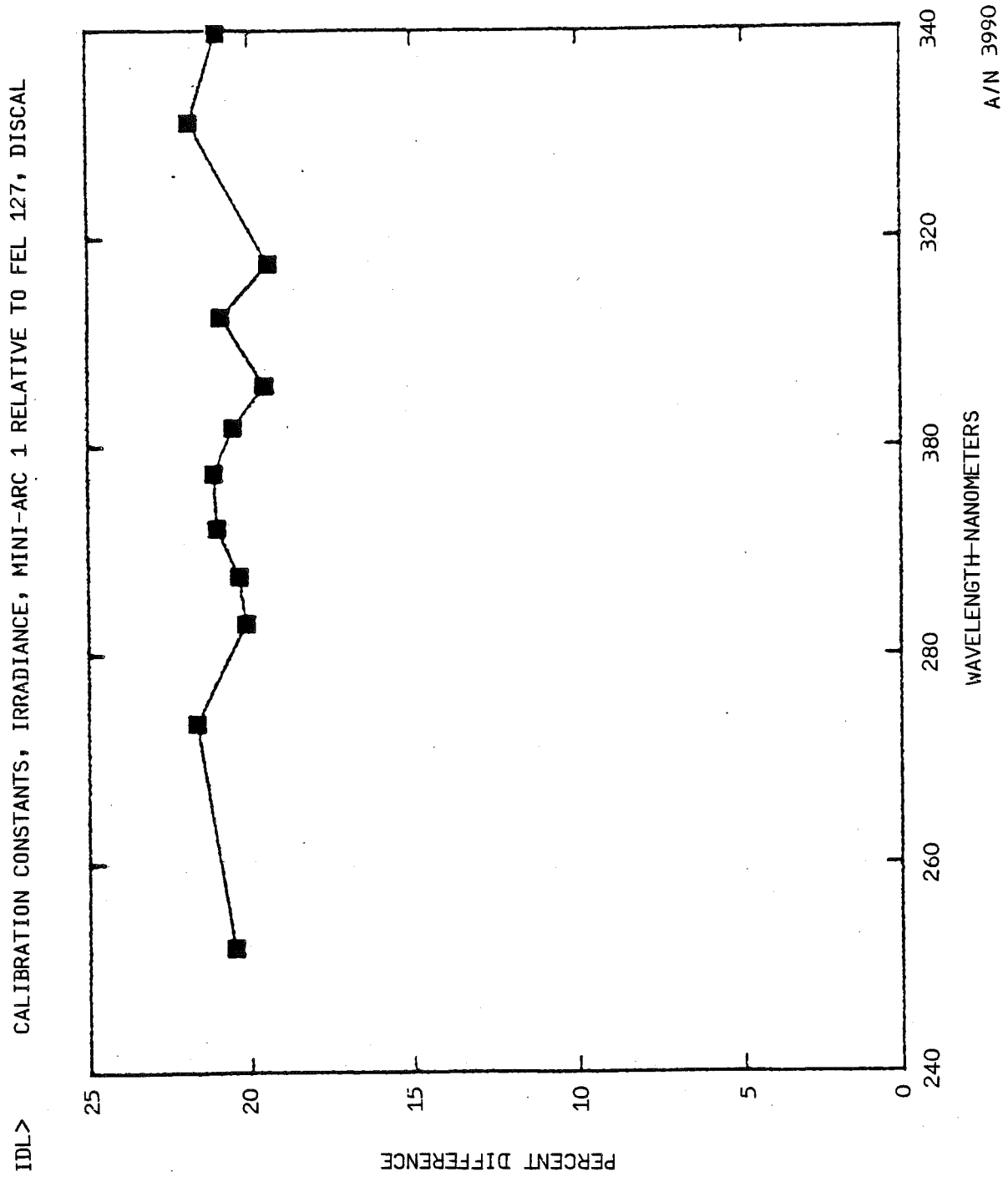


Figure 4-19



B6802-78

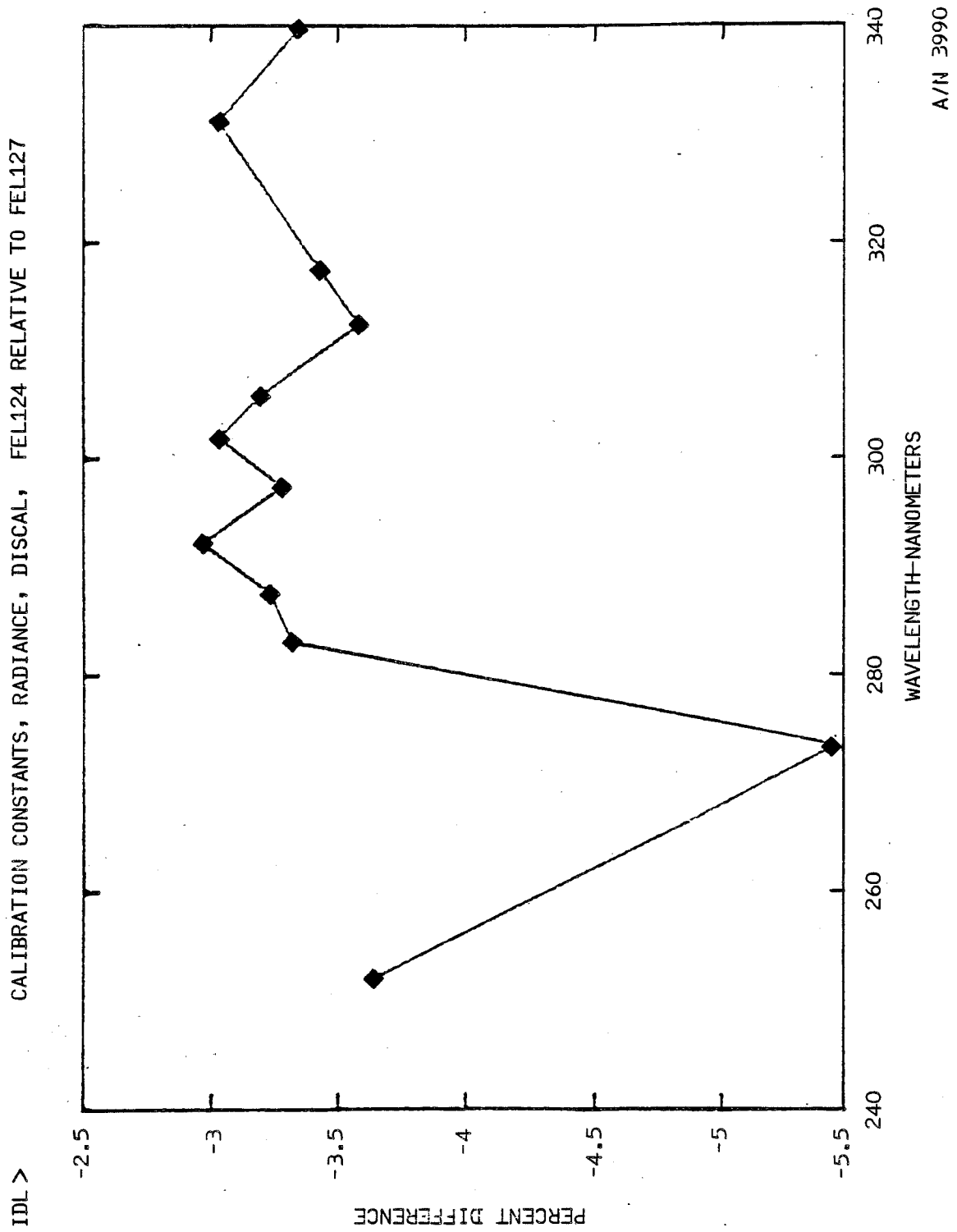


Figure 4-20



B6802-78

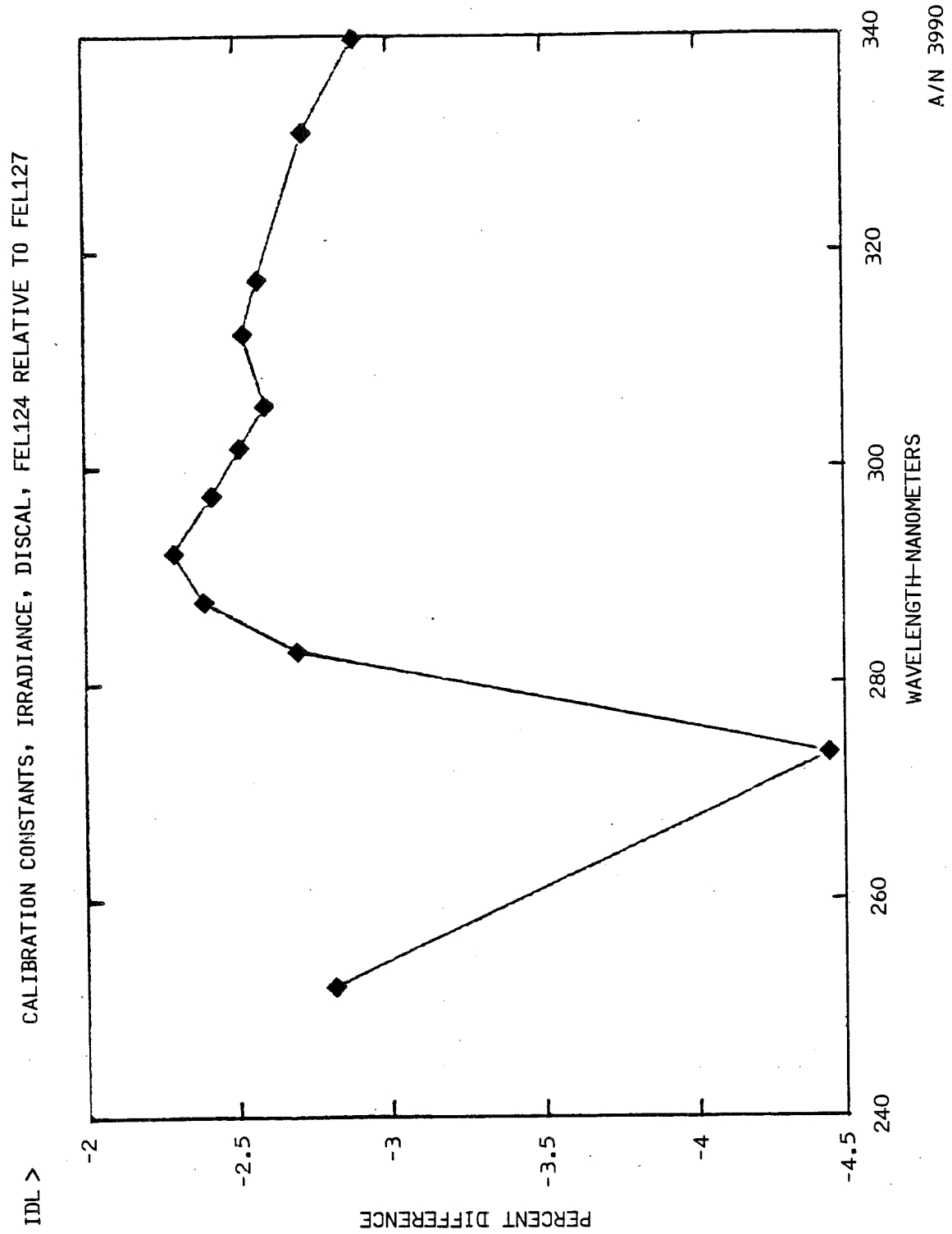


Figure 4-21



B6802-78

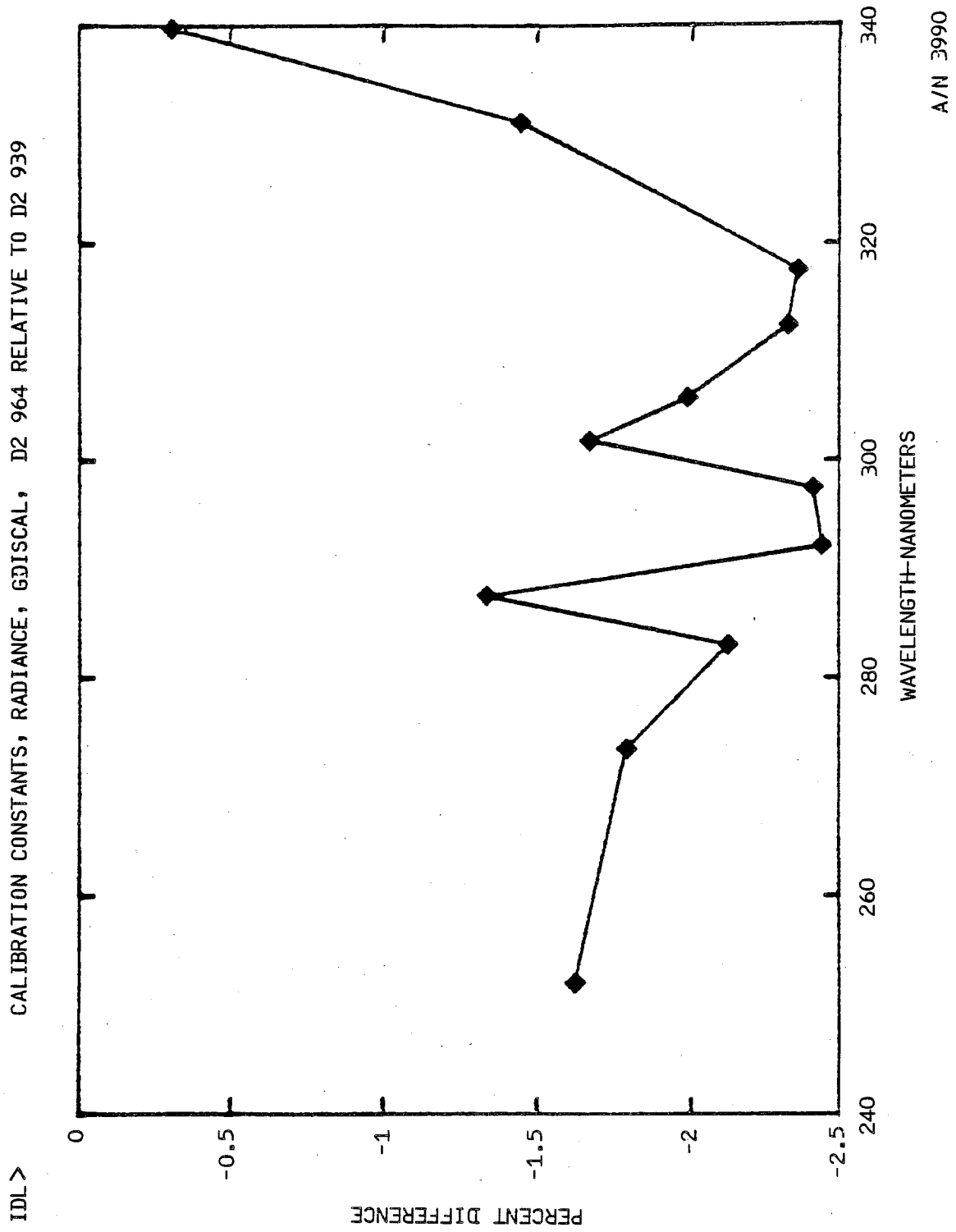


Figure 4-22



B6802-78

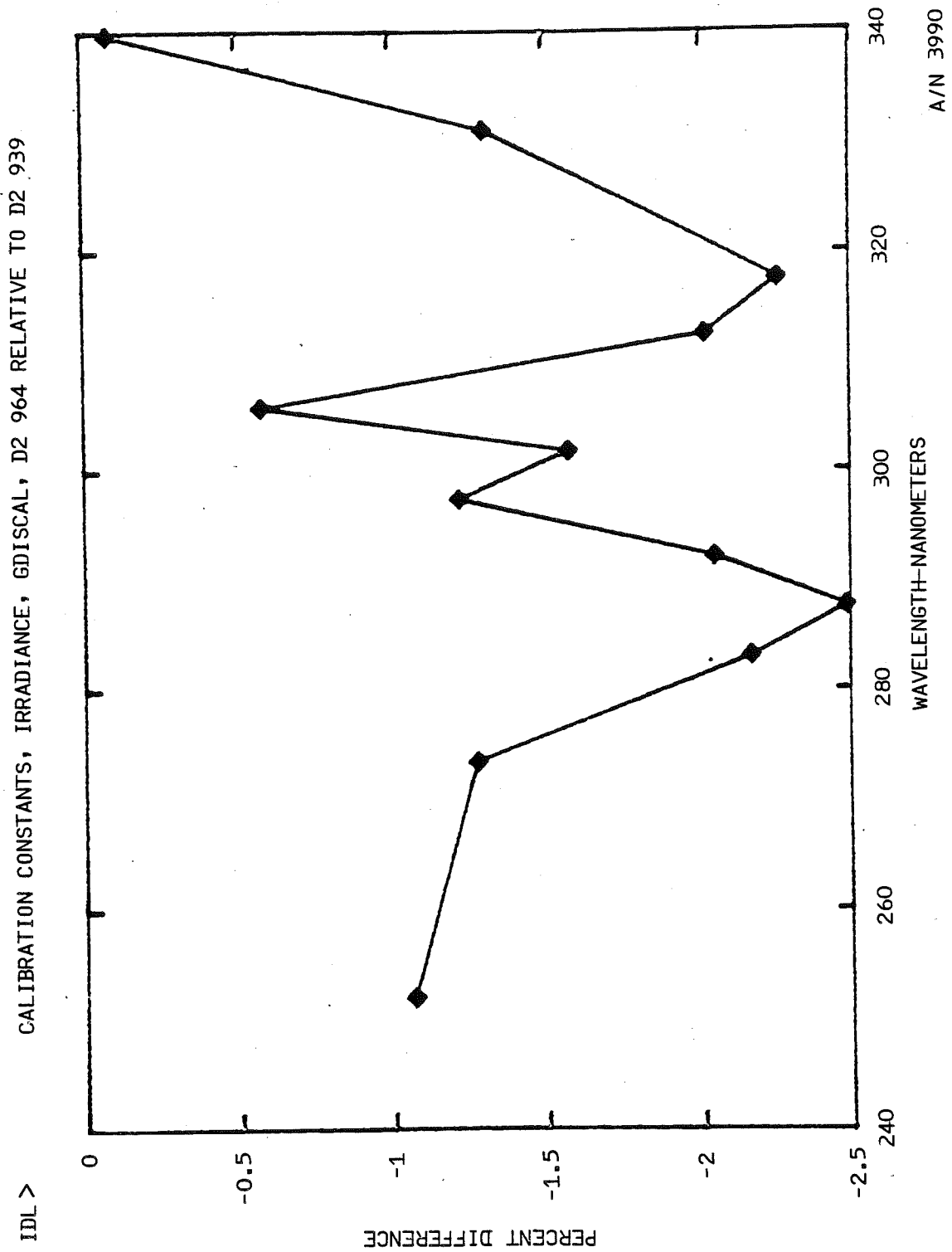


Figure 4-23



B6802-78

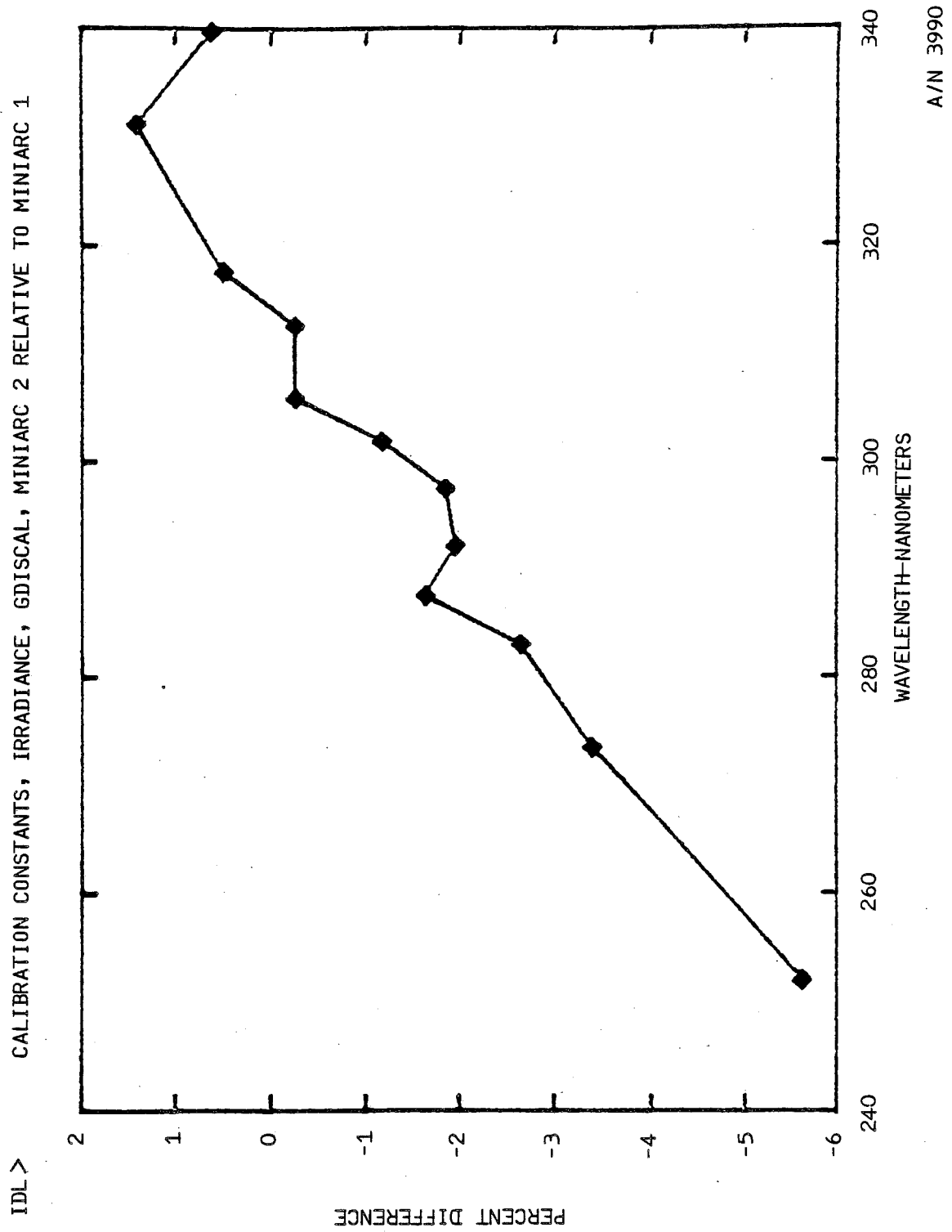


Figure 4-24



B6802-78

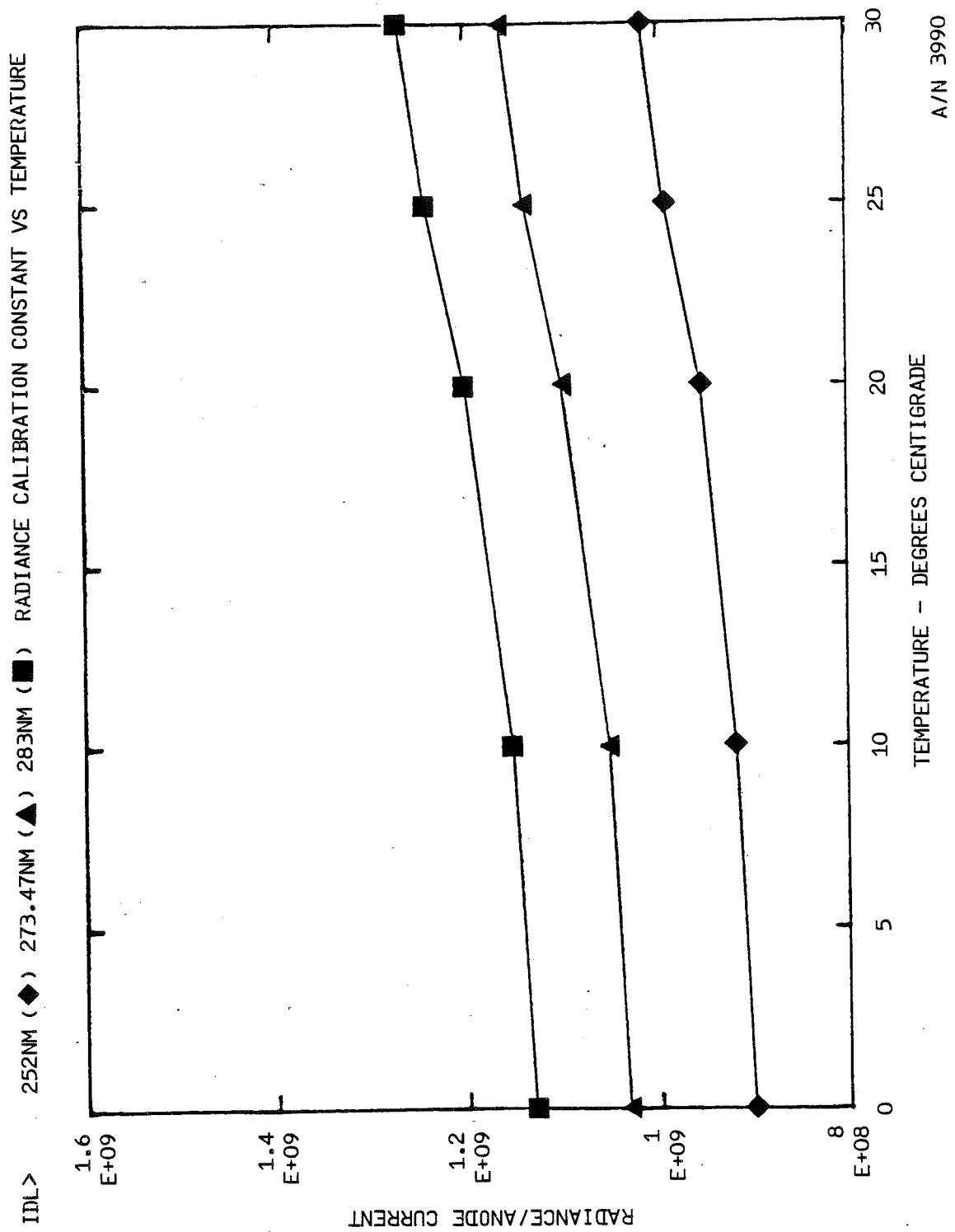


Figure 4-25



B6802-78

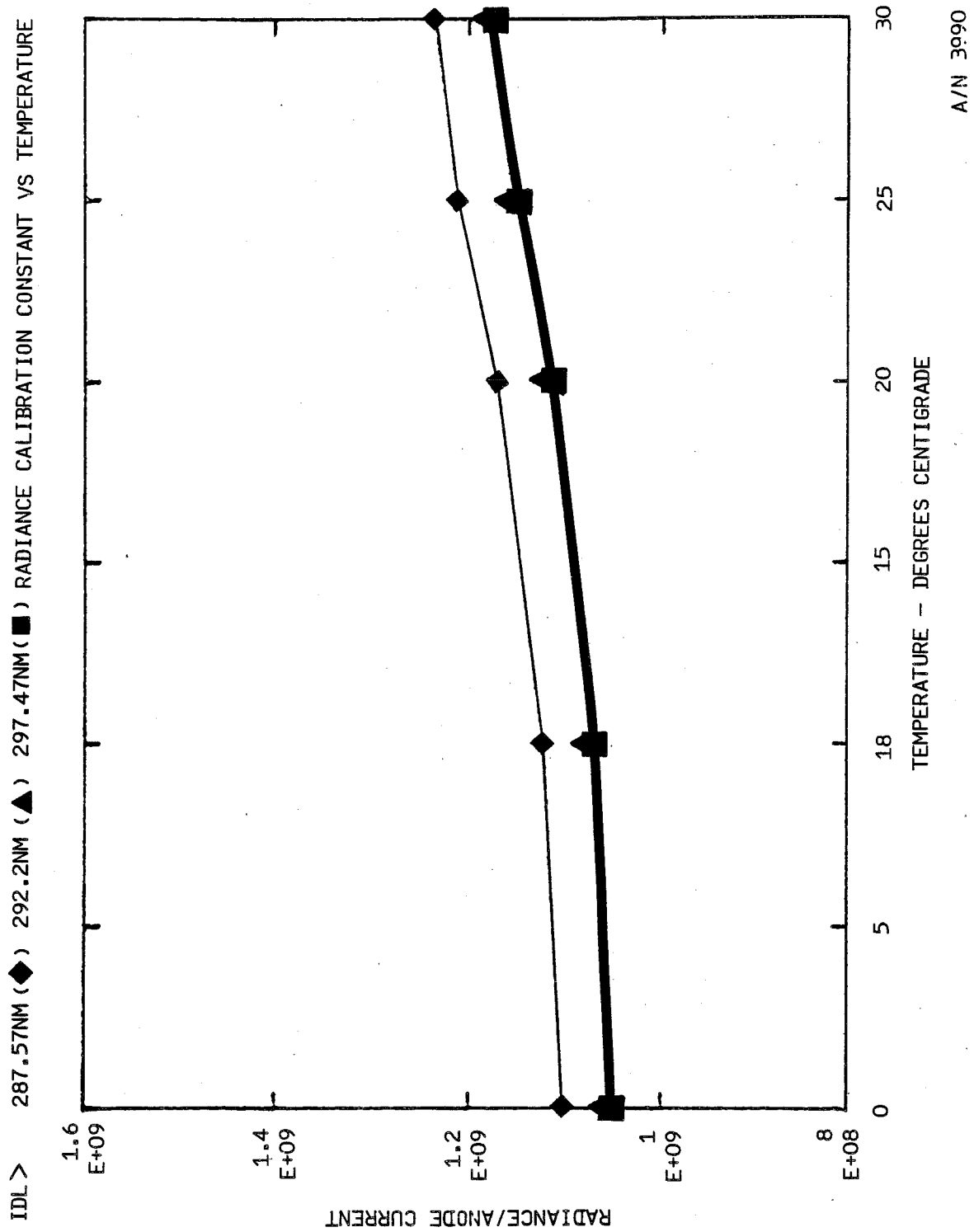


Figure 4-26



B6802-78

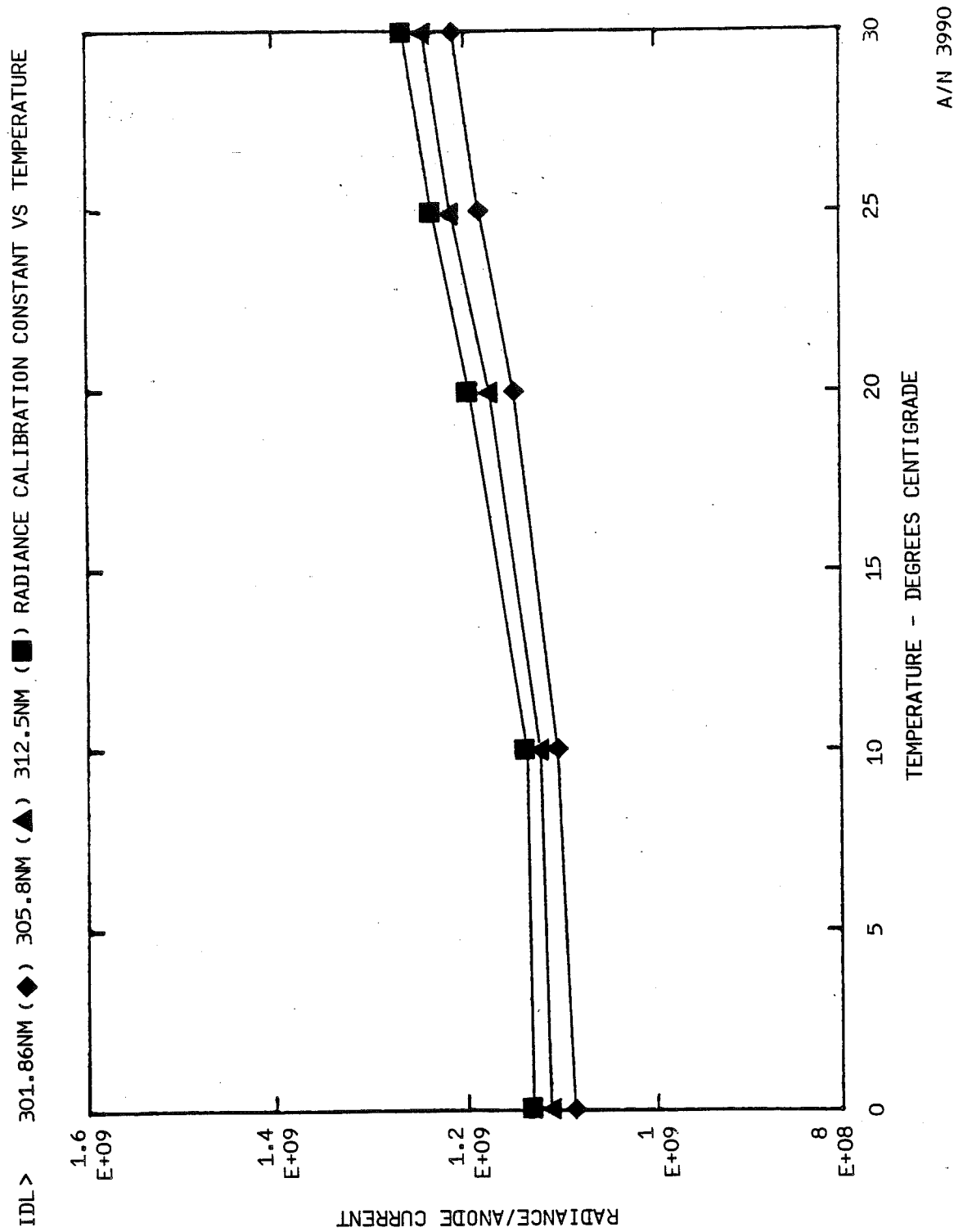


Figure 4-27



B6802-78

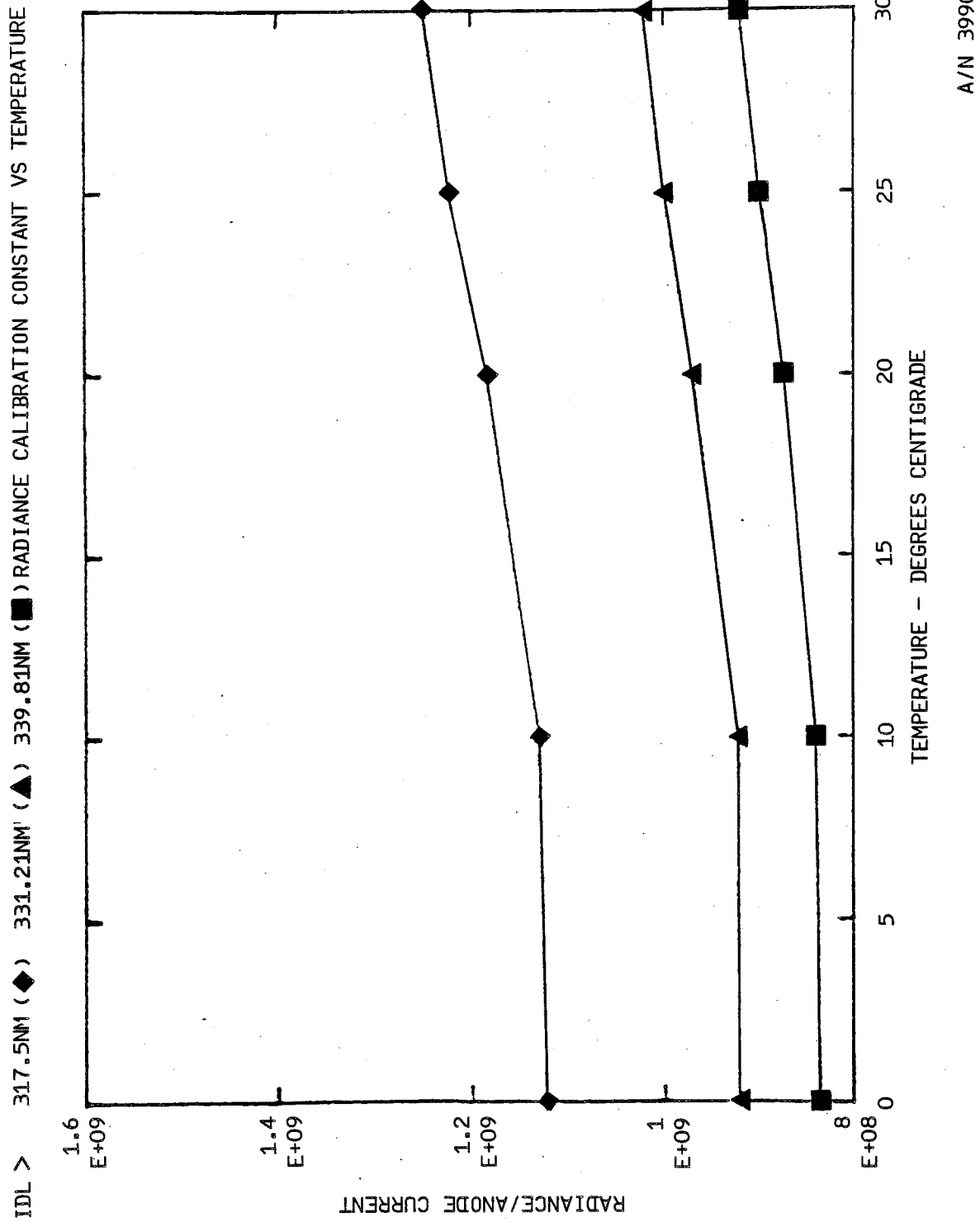


Figure 4-28



B6802-78

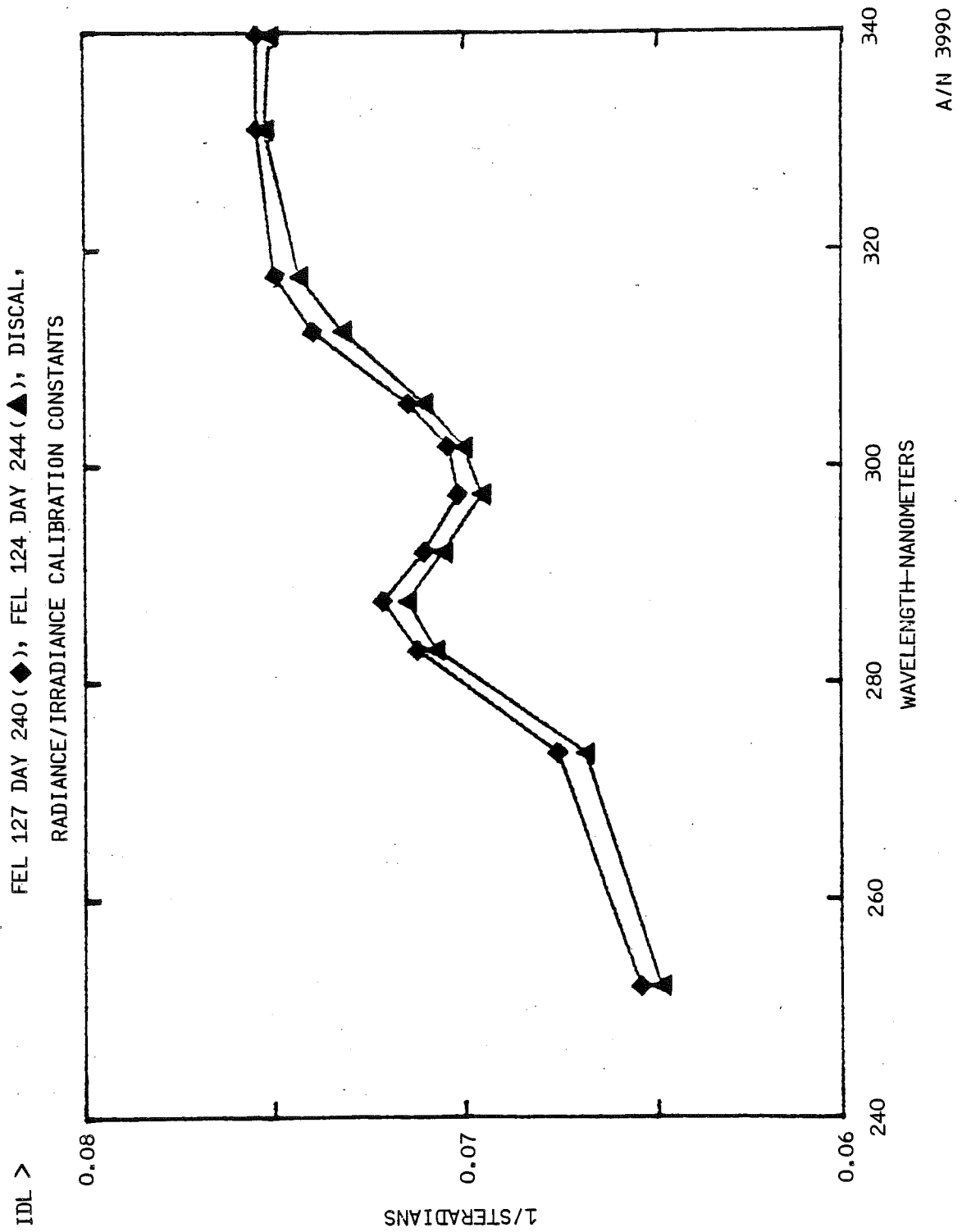


Figure 4-29



B6802-78

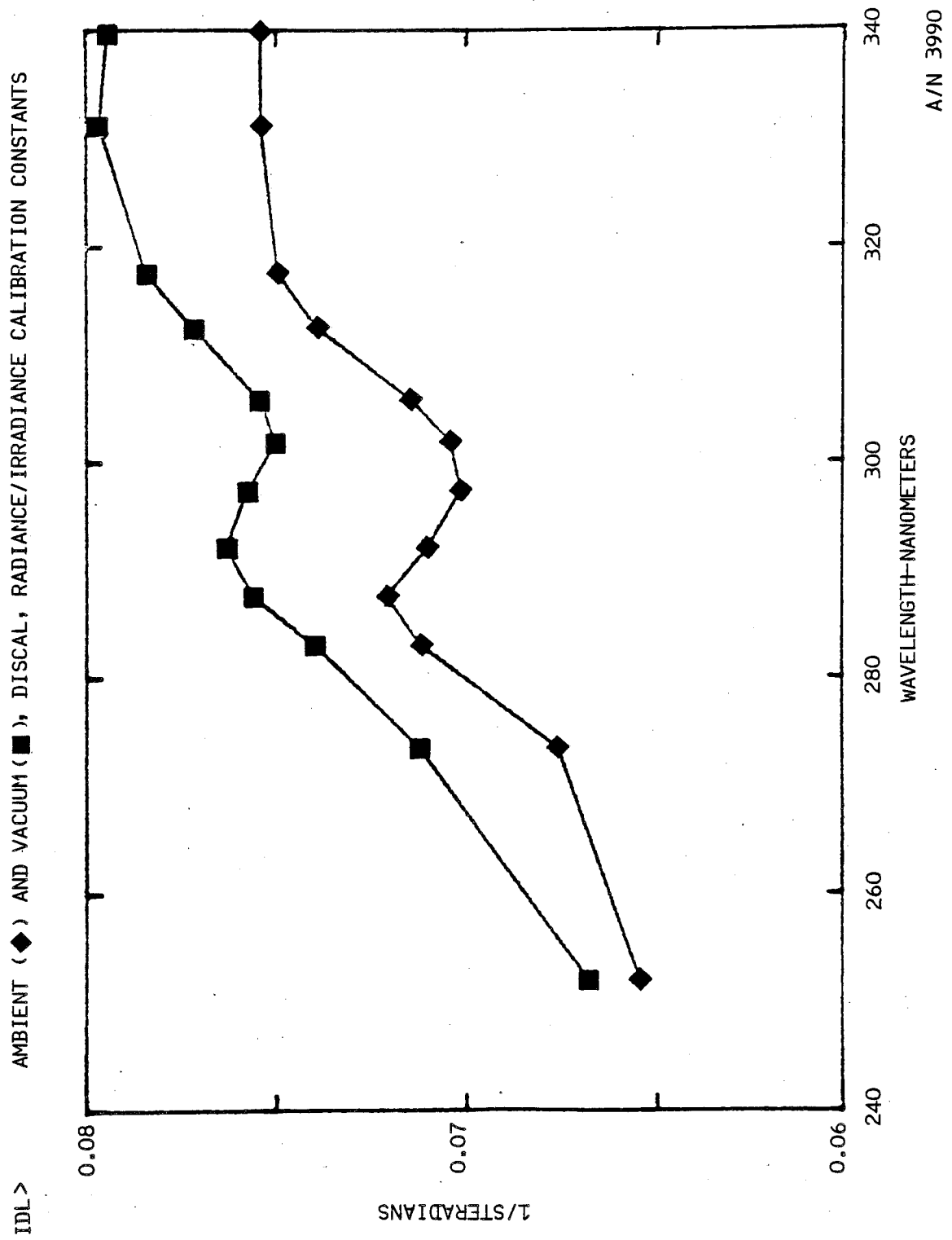


Figure 4-30



B6802-78

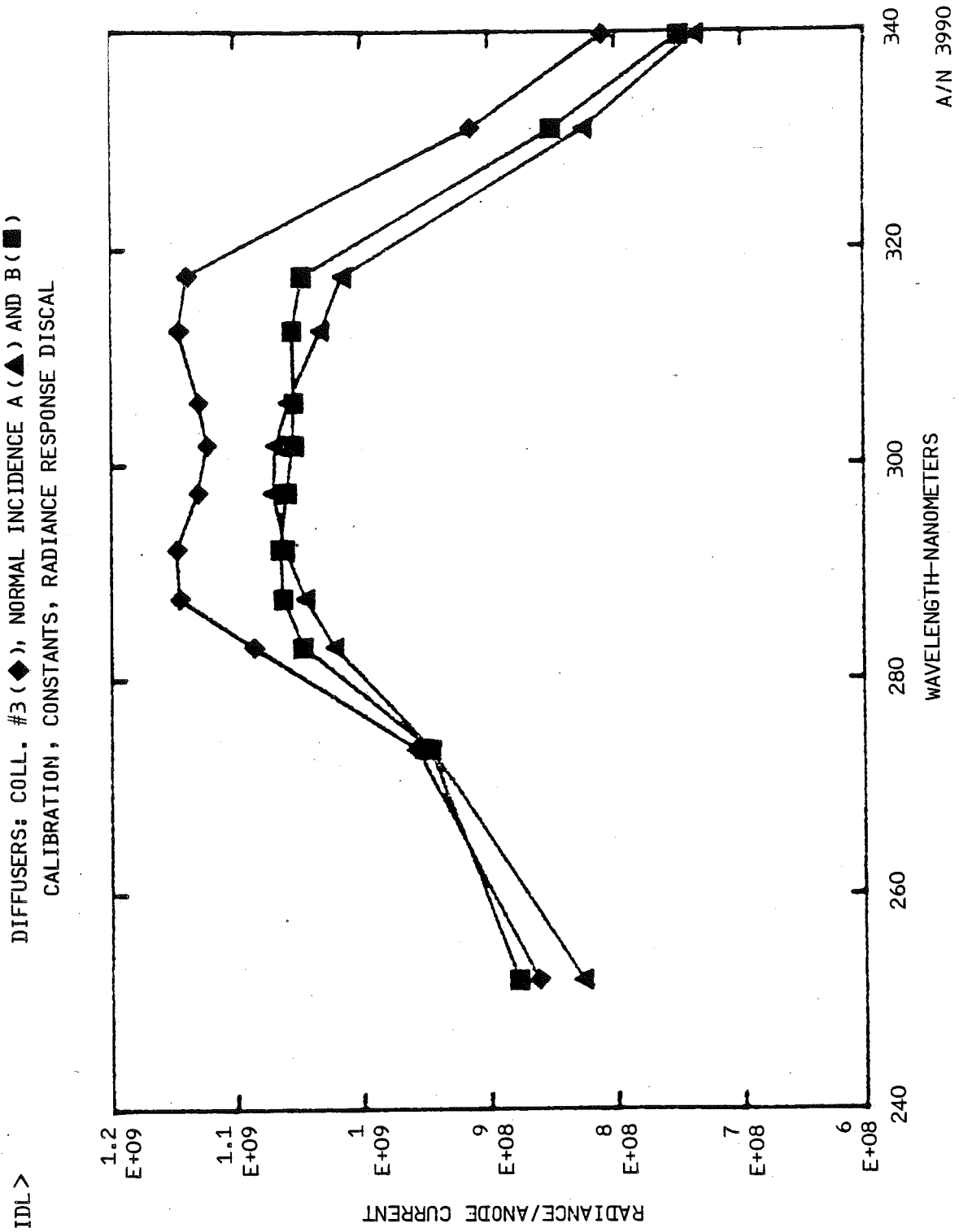


Figure 4-31



B6802-78

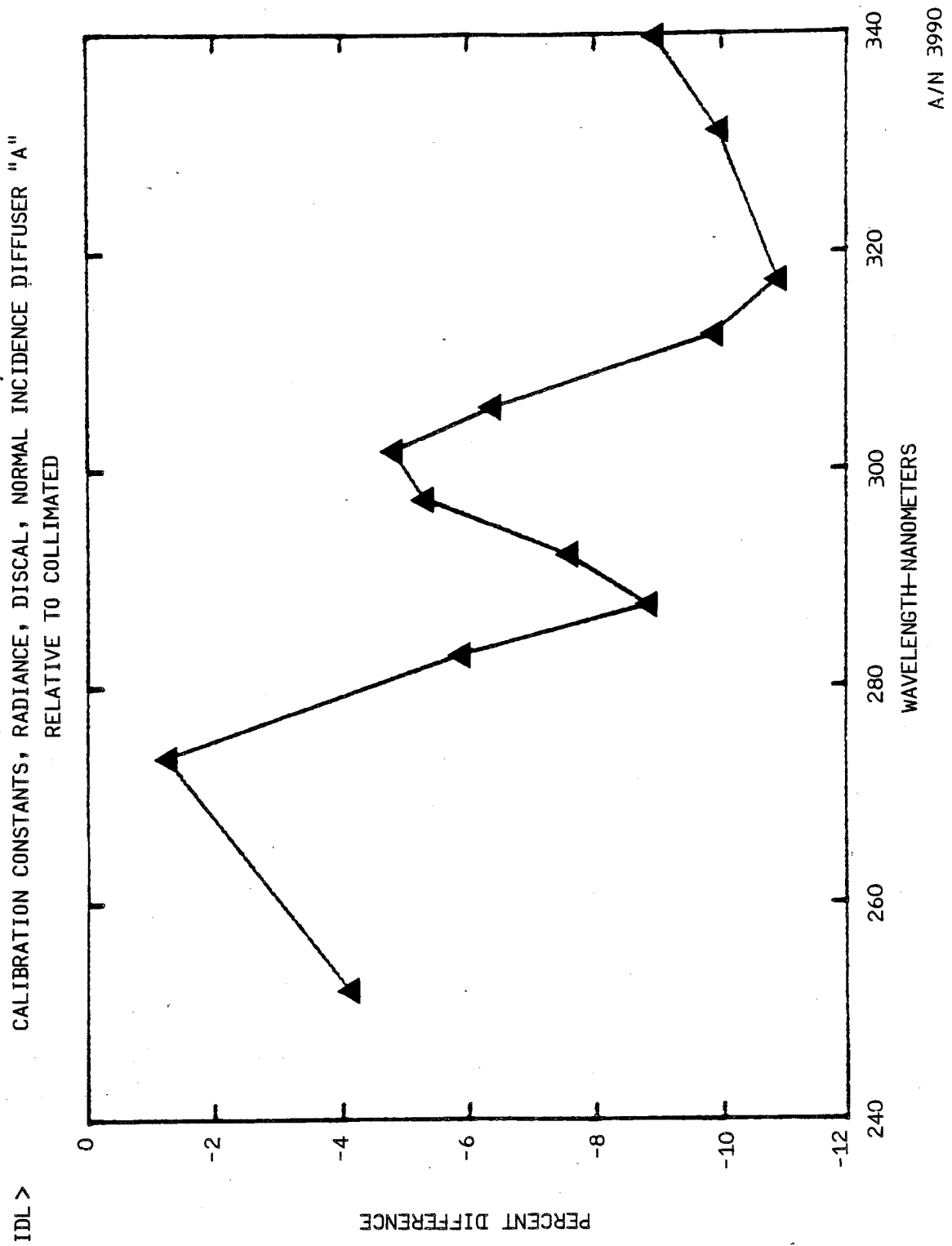


Figure 4-32



B6802-78

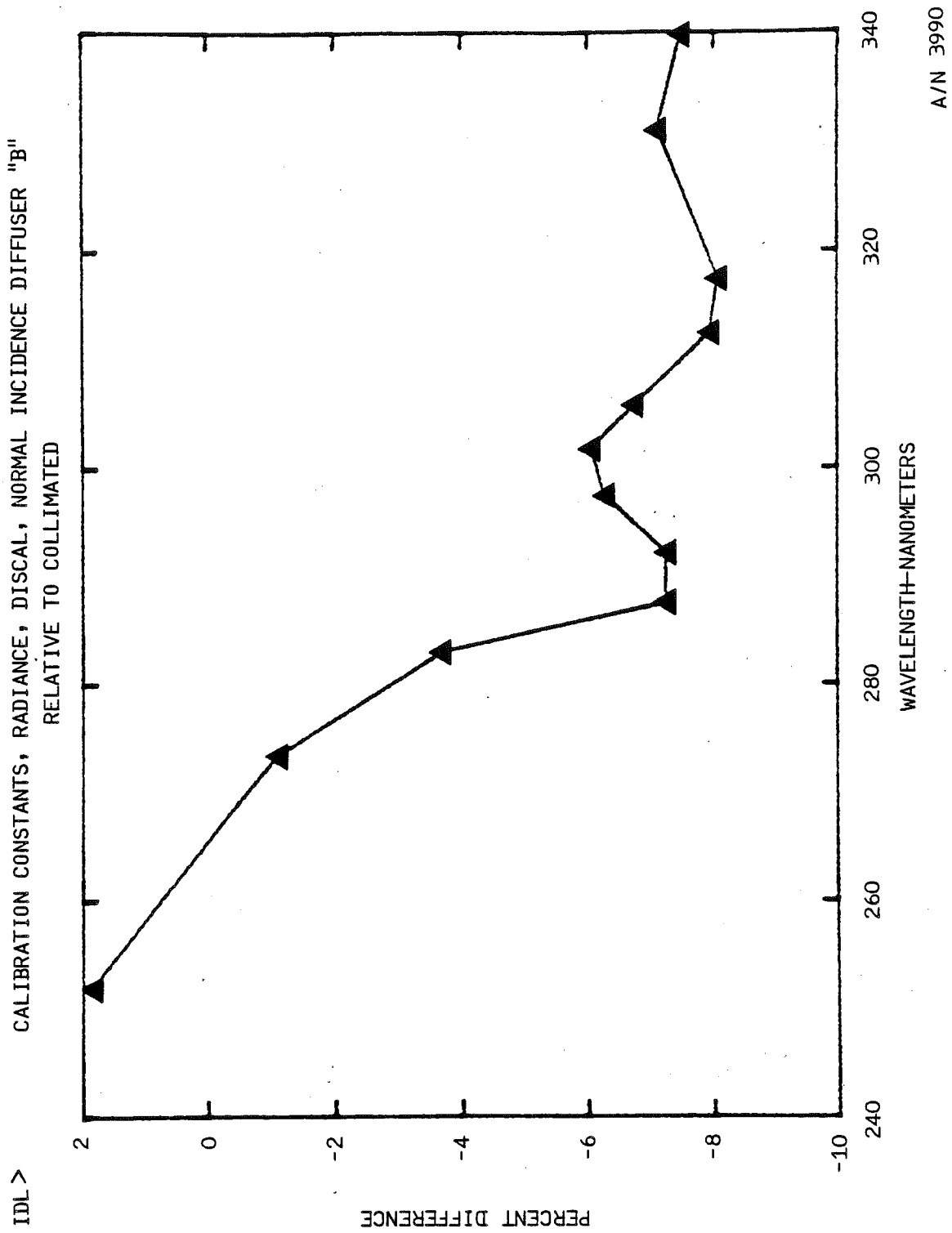


Figure 4-33



B6802-78

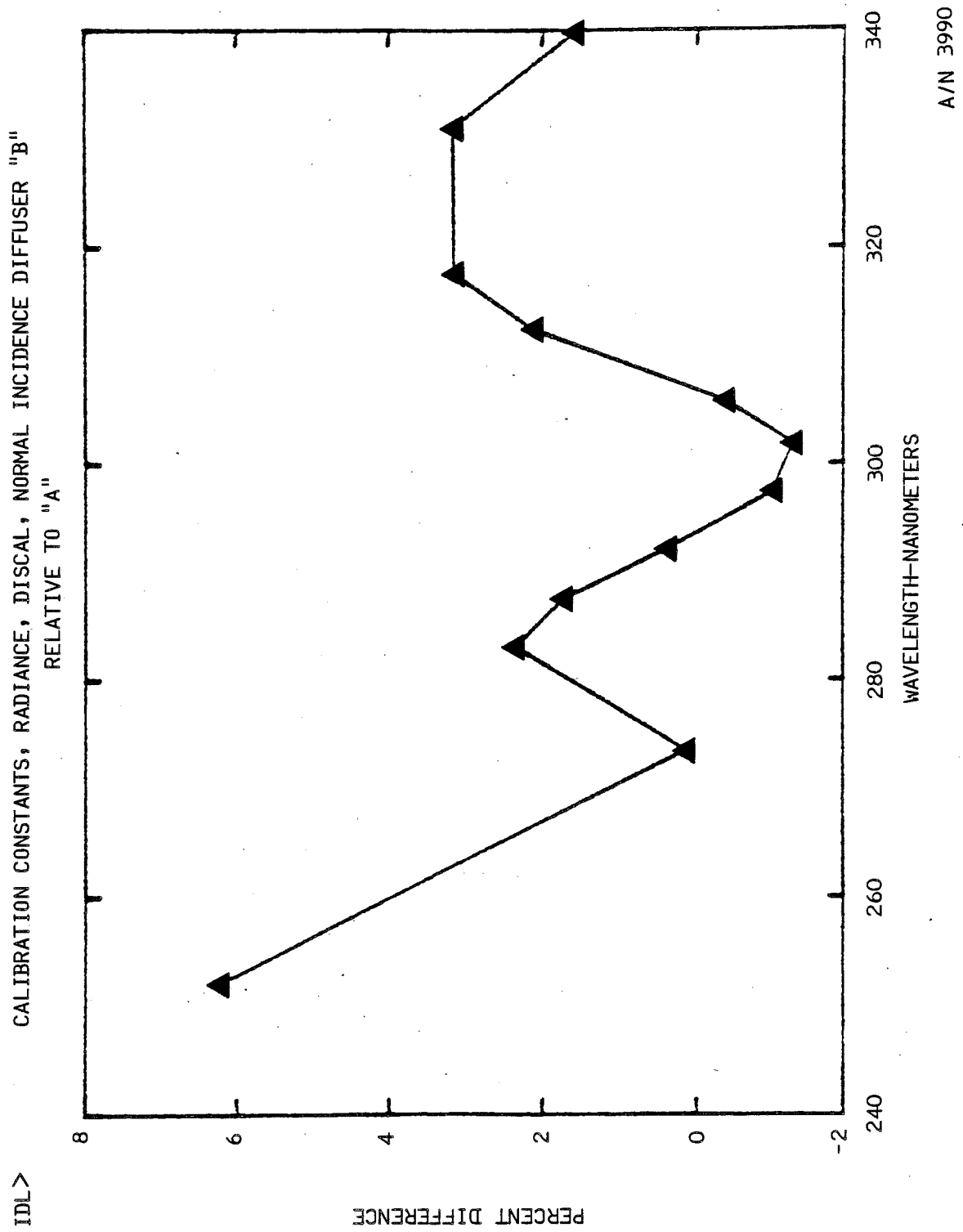


Figure 4-34



B6802-78

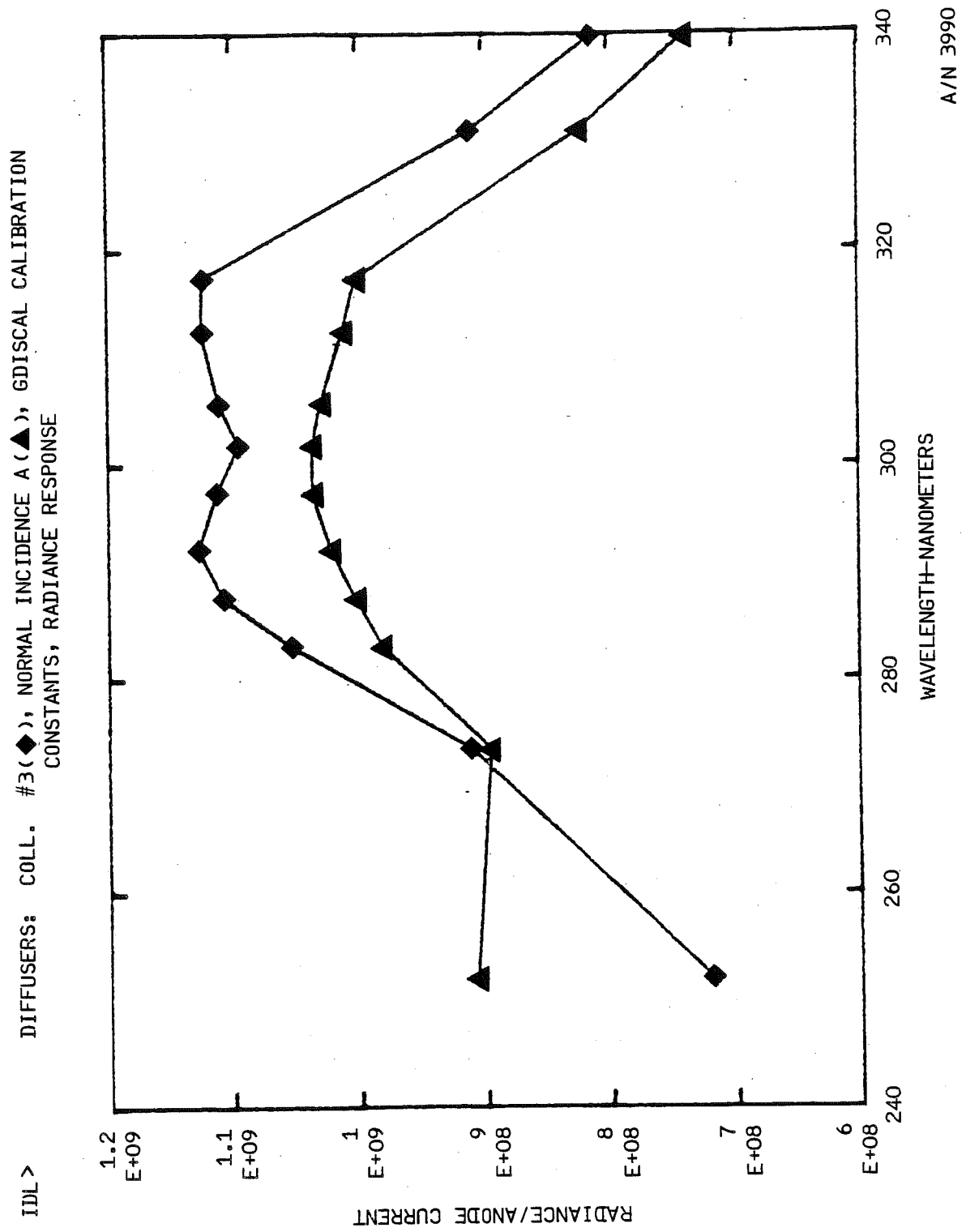


Figure 4-35



B6802-78

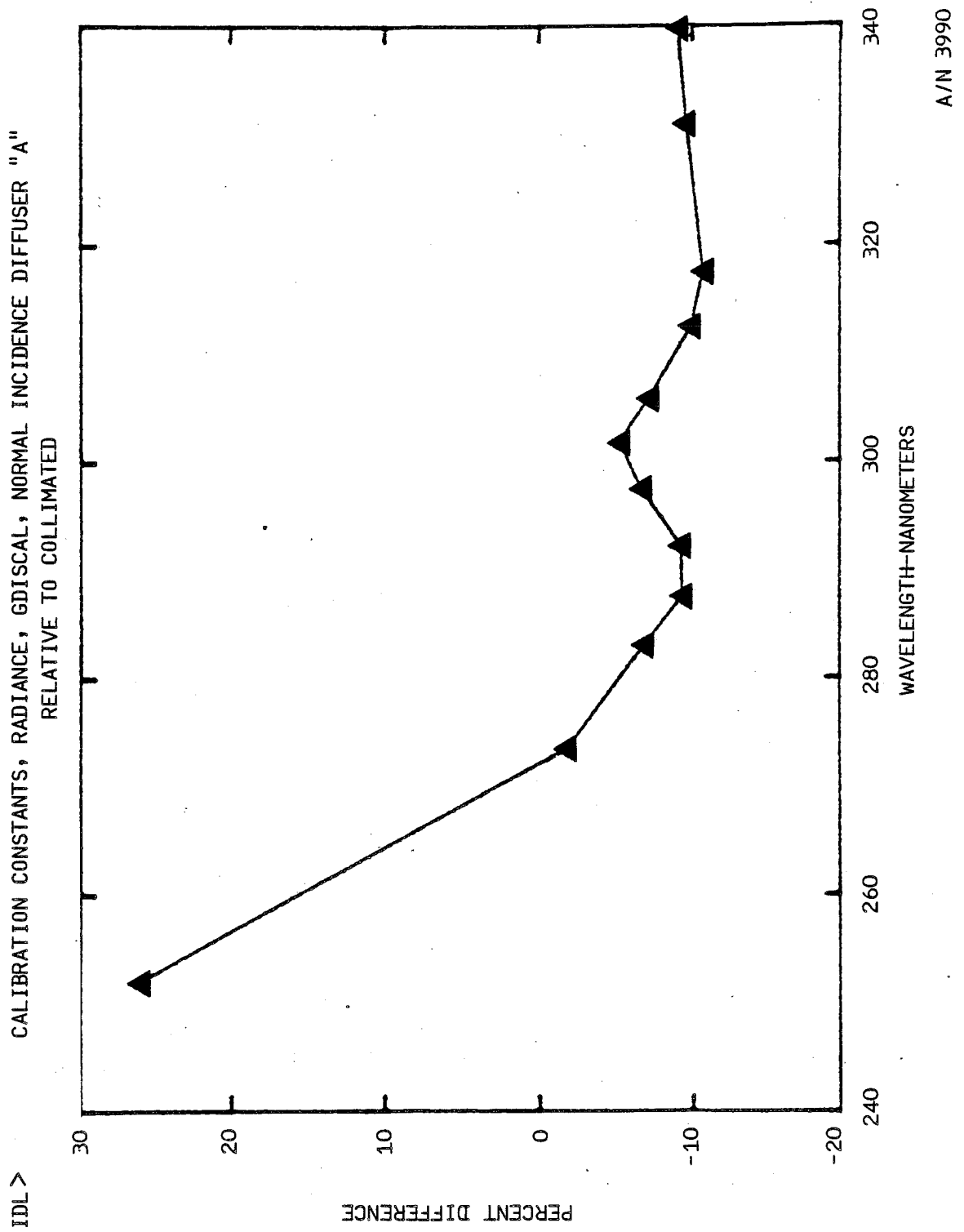


Figure 4-36



B6802-78

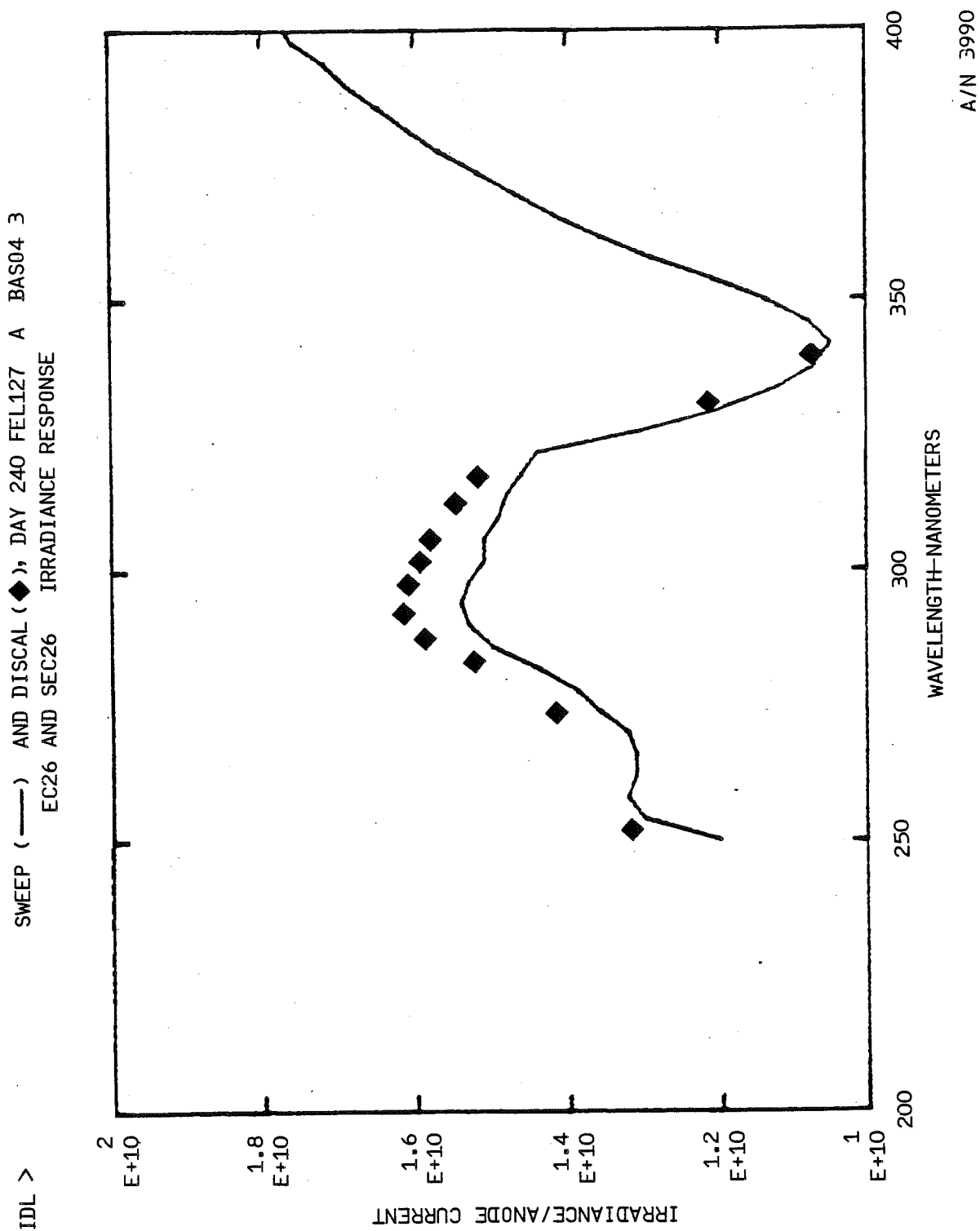


Figure 4-37



B6802-78

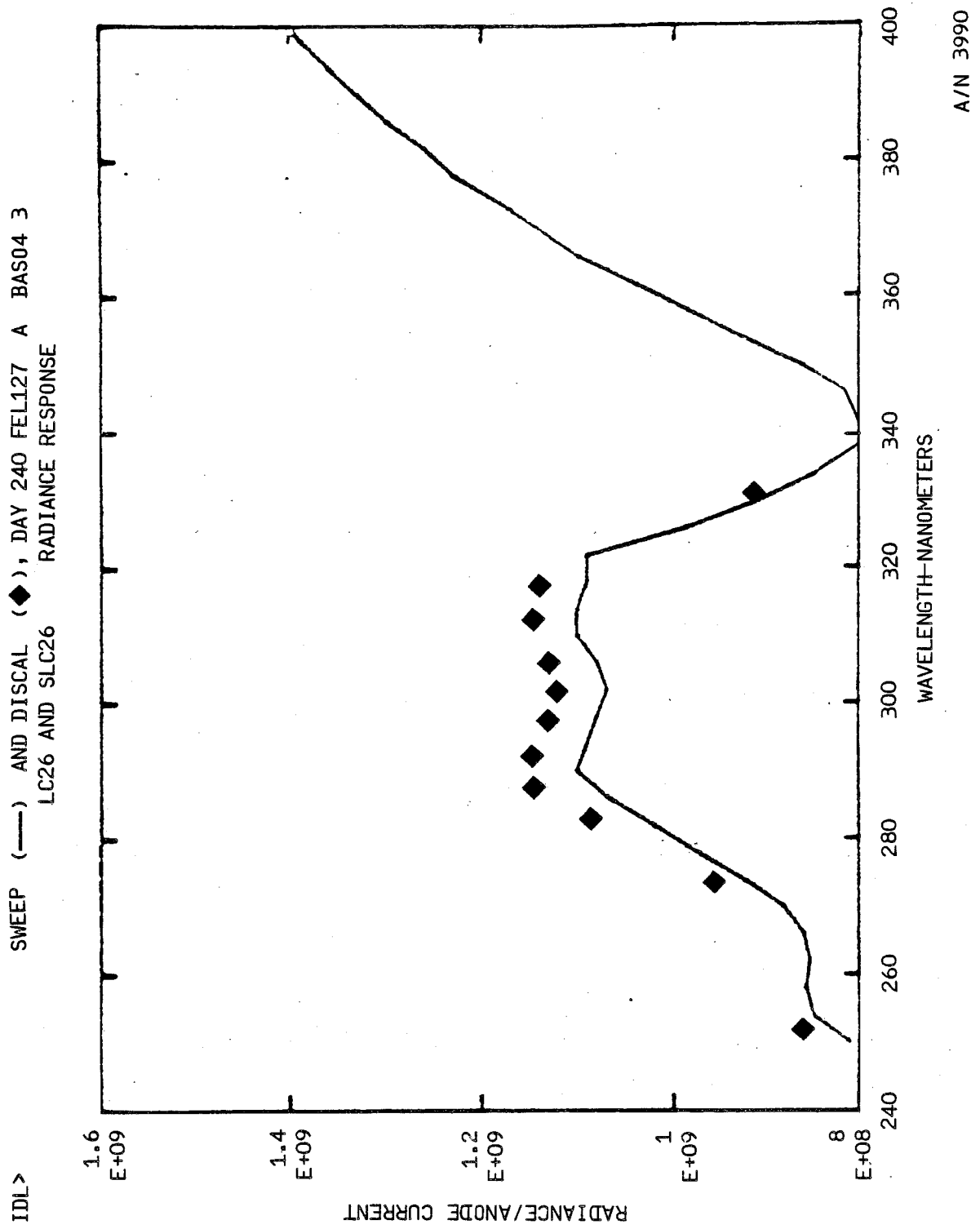


Figure 4-38



B6802-78

IDL > SWEEPS: SEC26 AND SEC36 IRRADIANCE RESPONSE

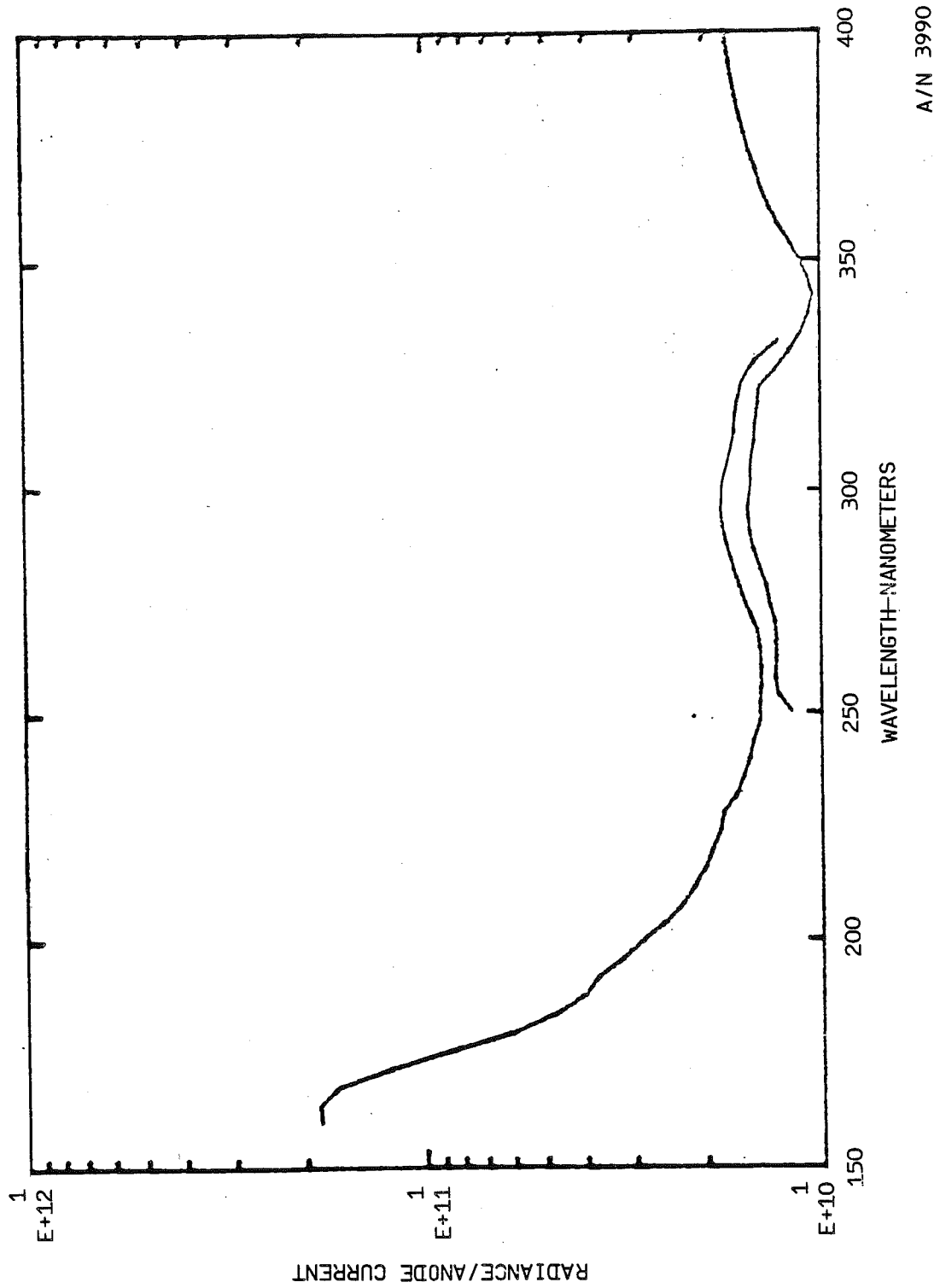


Figure 4-39



B6802-78

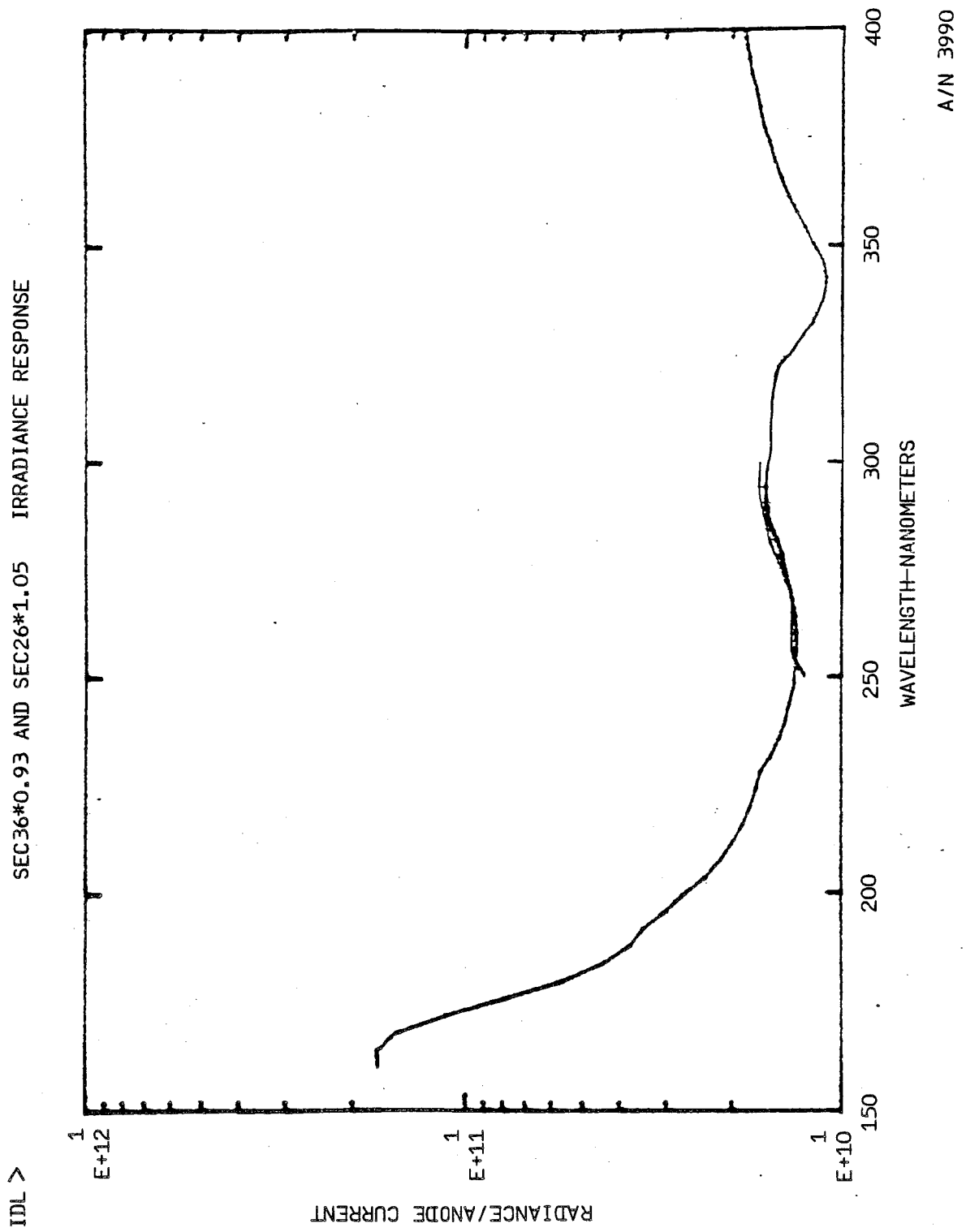


Figure 4-40



B6802-78

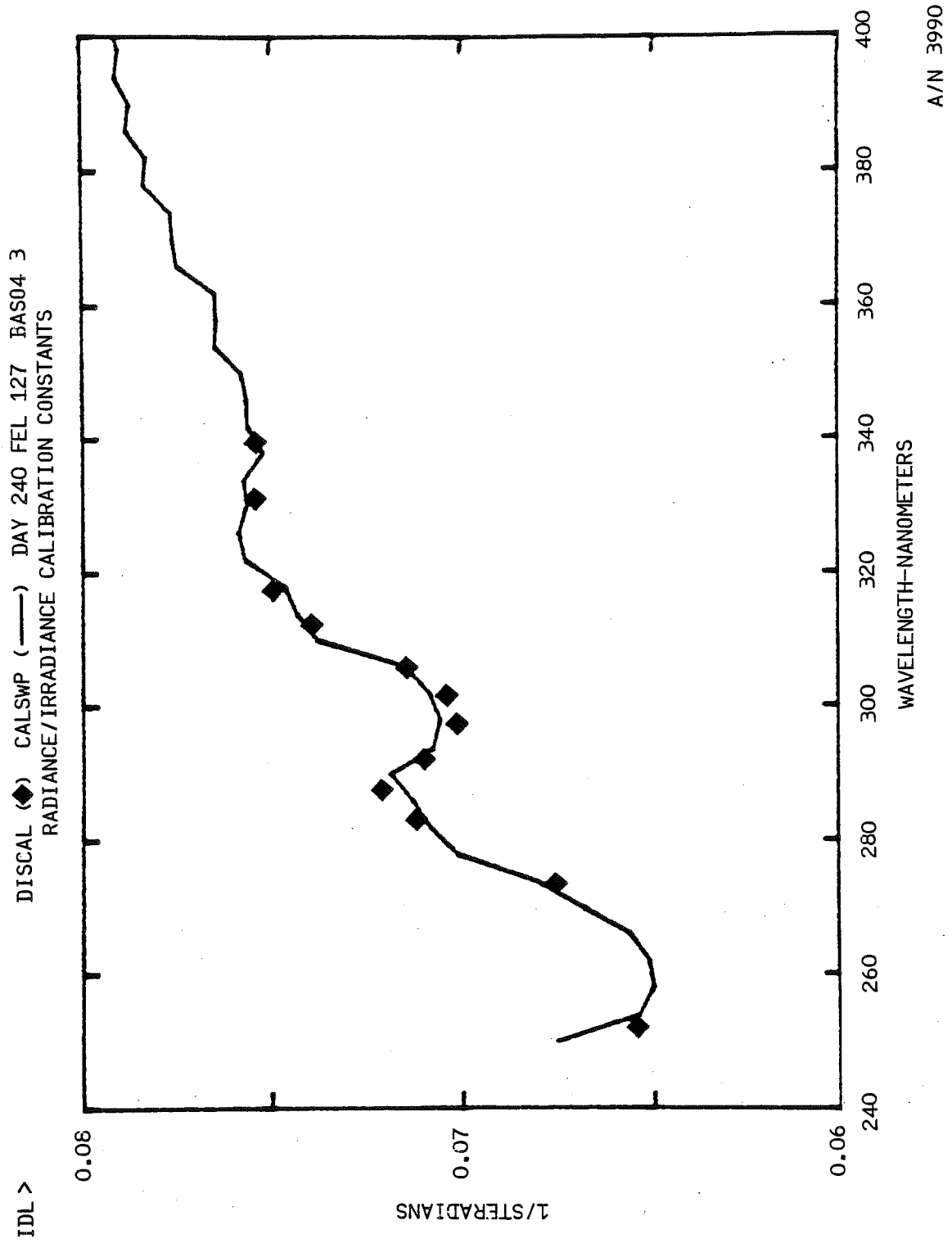


Figure 4-41



B6802-78

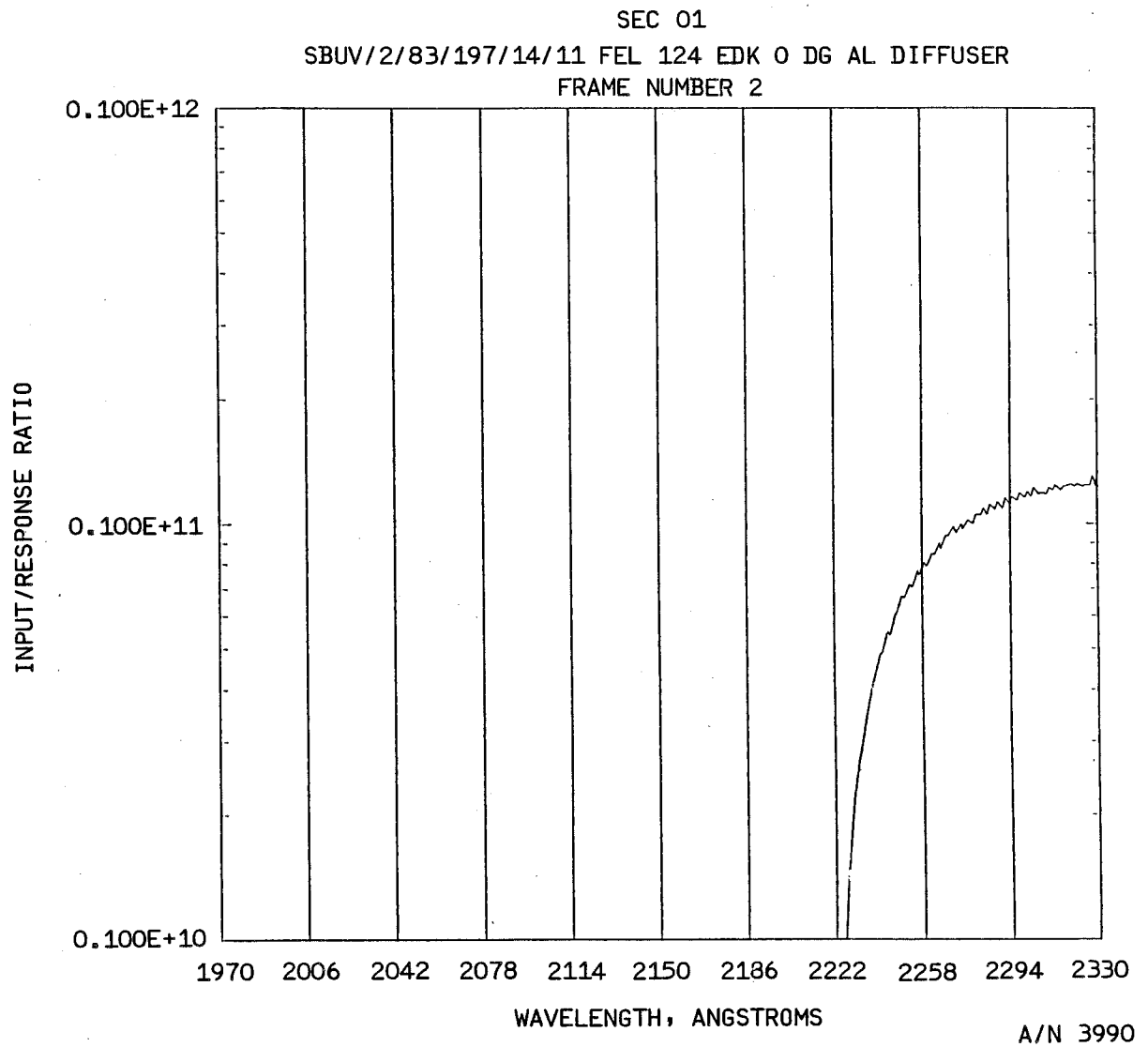


Figure 4-42



B6802-78

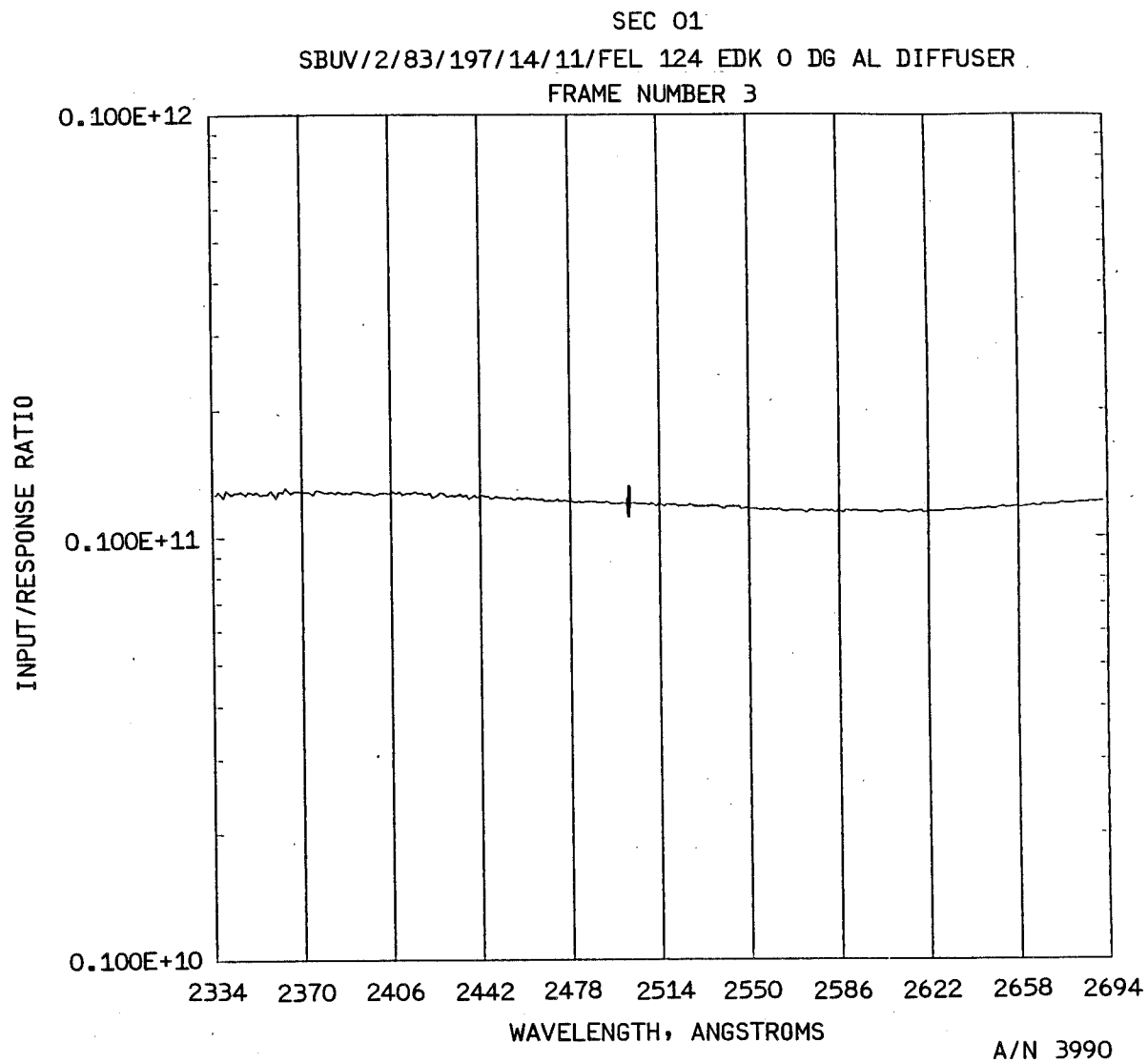


Figure 4-42(cont.)



B6802-78

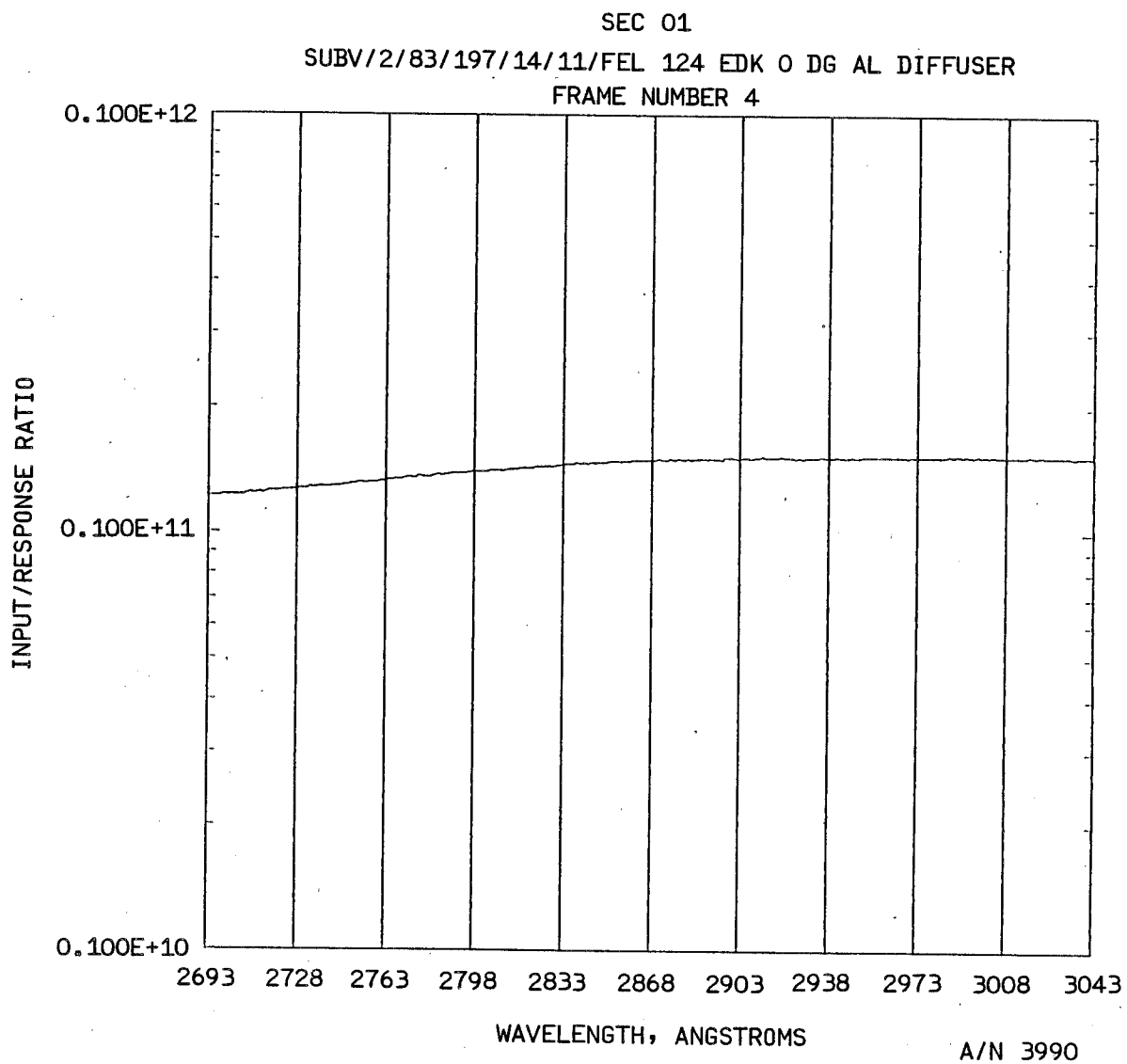


Figure 4-42 (cont.)



B6802-78

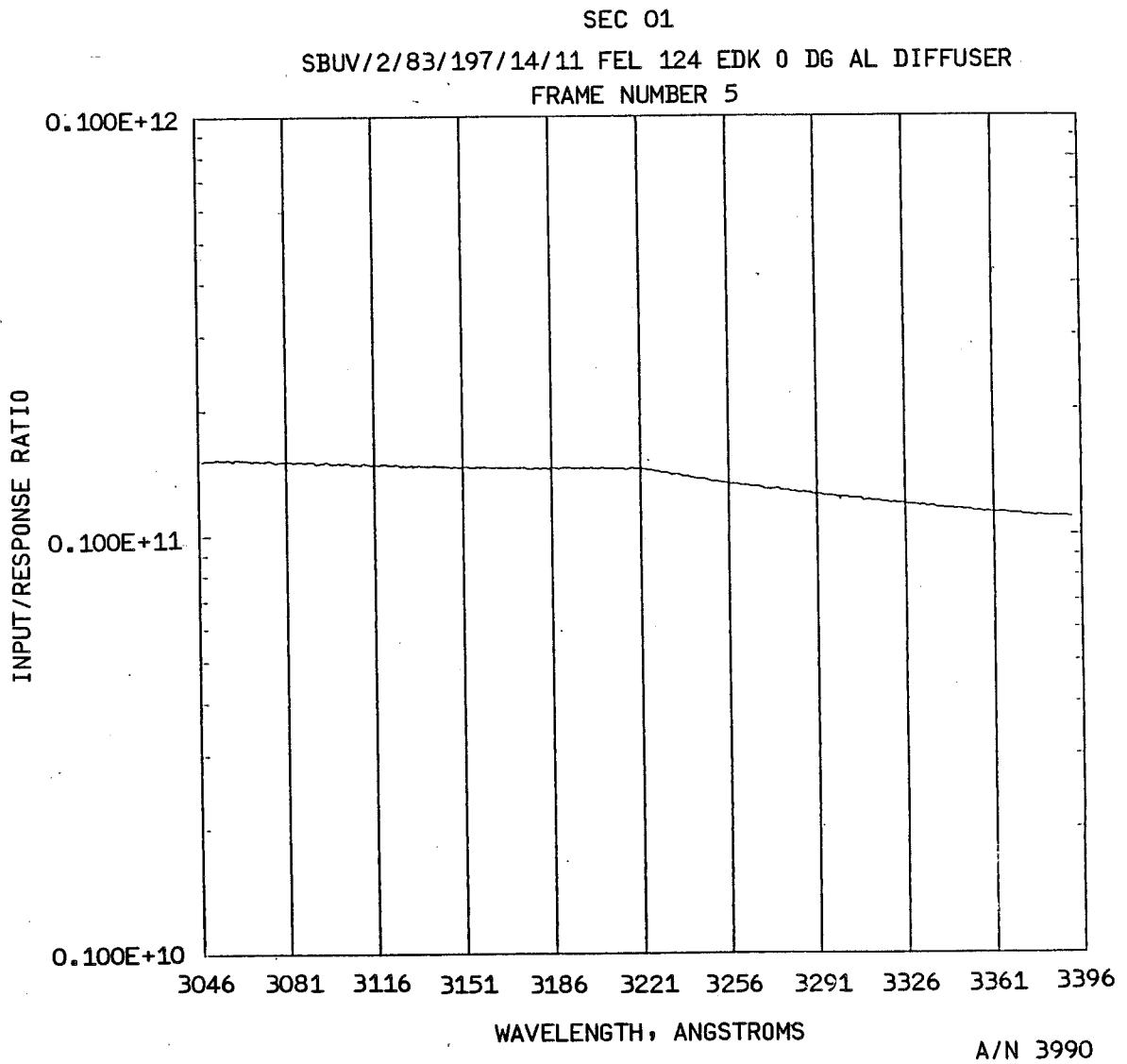


Figure 4-42 (cont.)



B6802-78

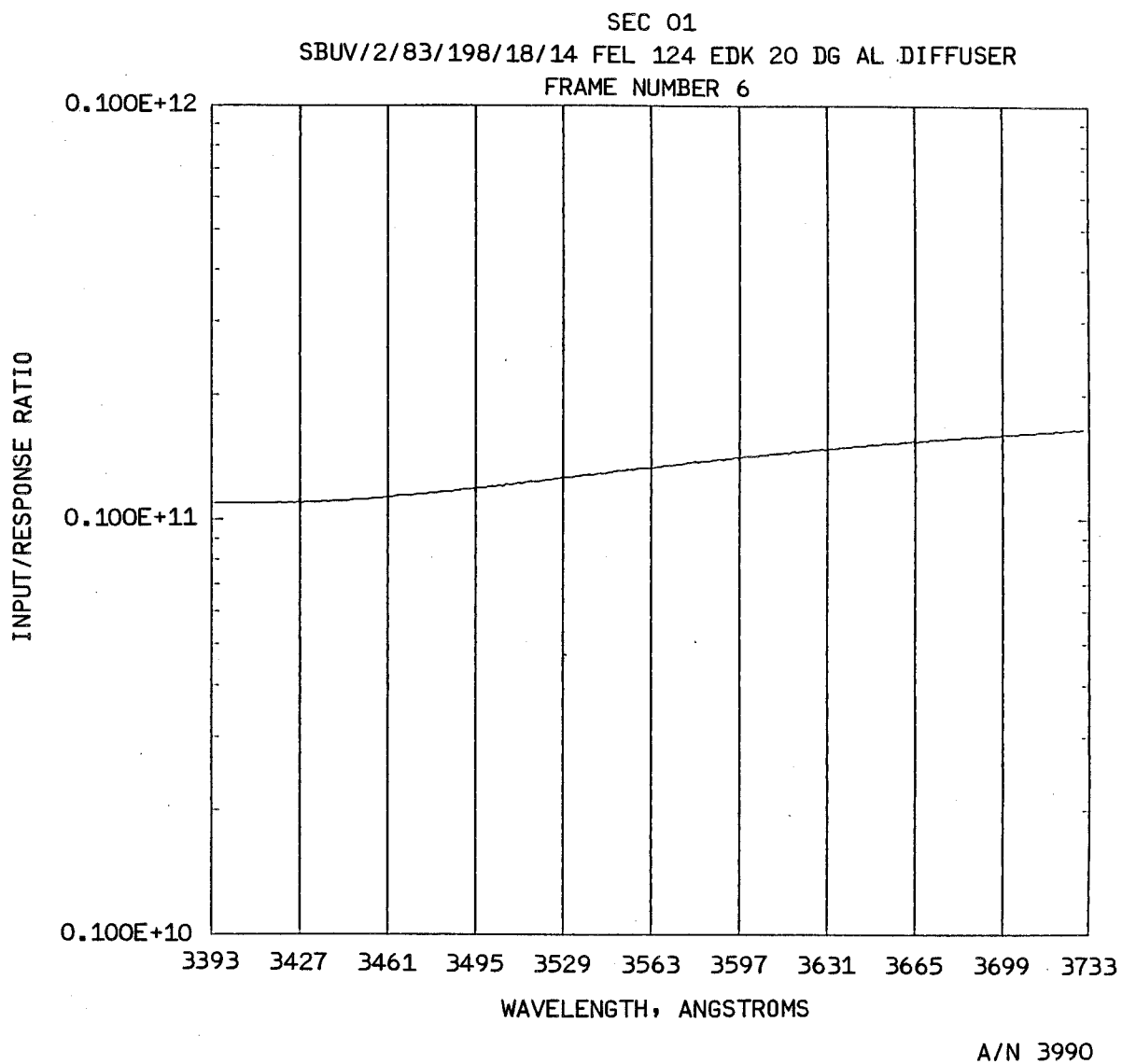
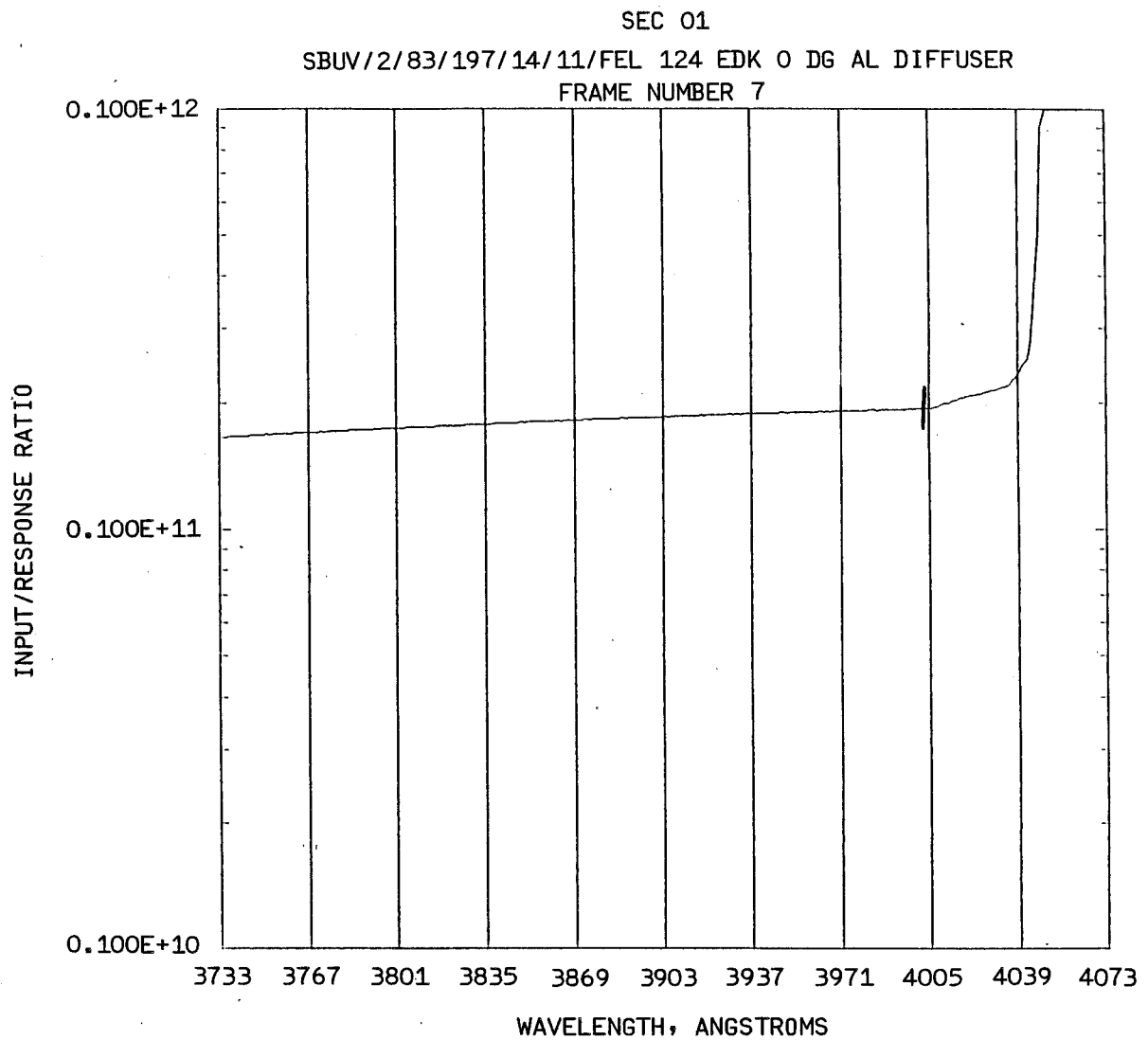


Figure 4-42 (cont.)



B6802-78

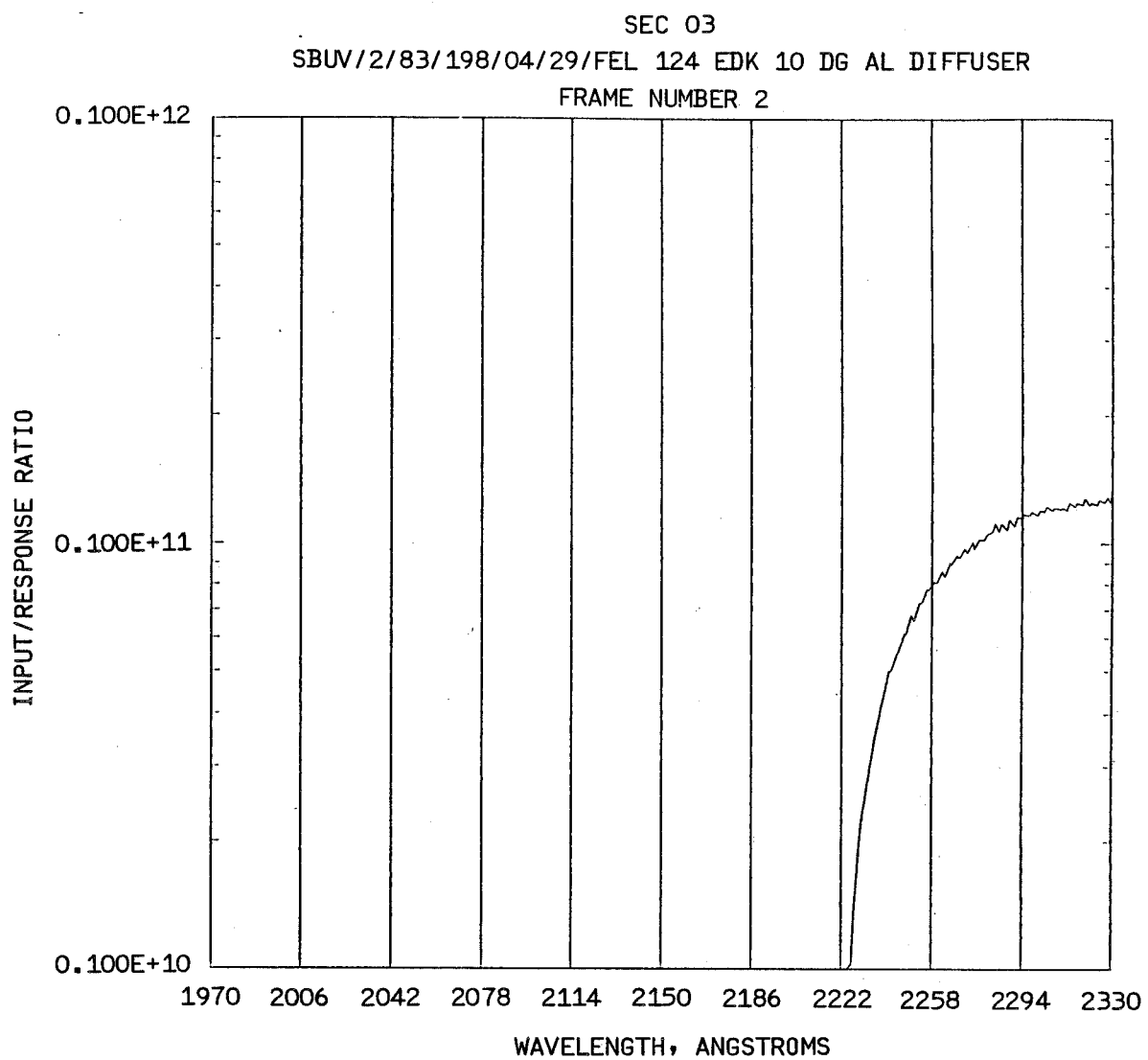


A/N 3990

Figure 4-42 (cont.)



B6802-78

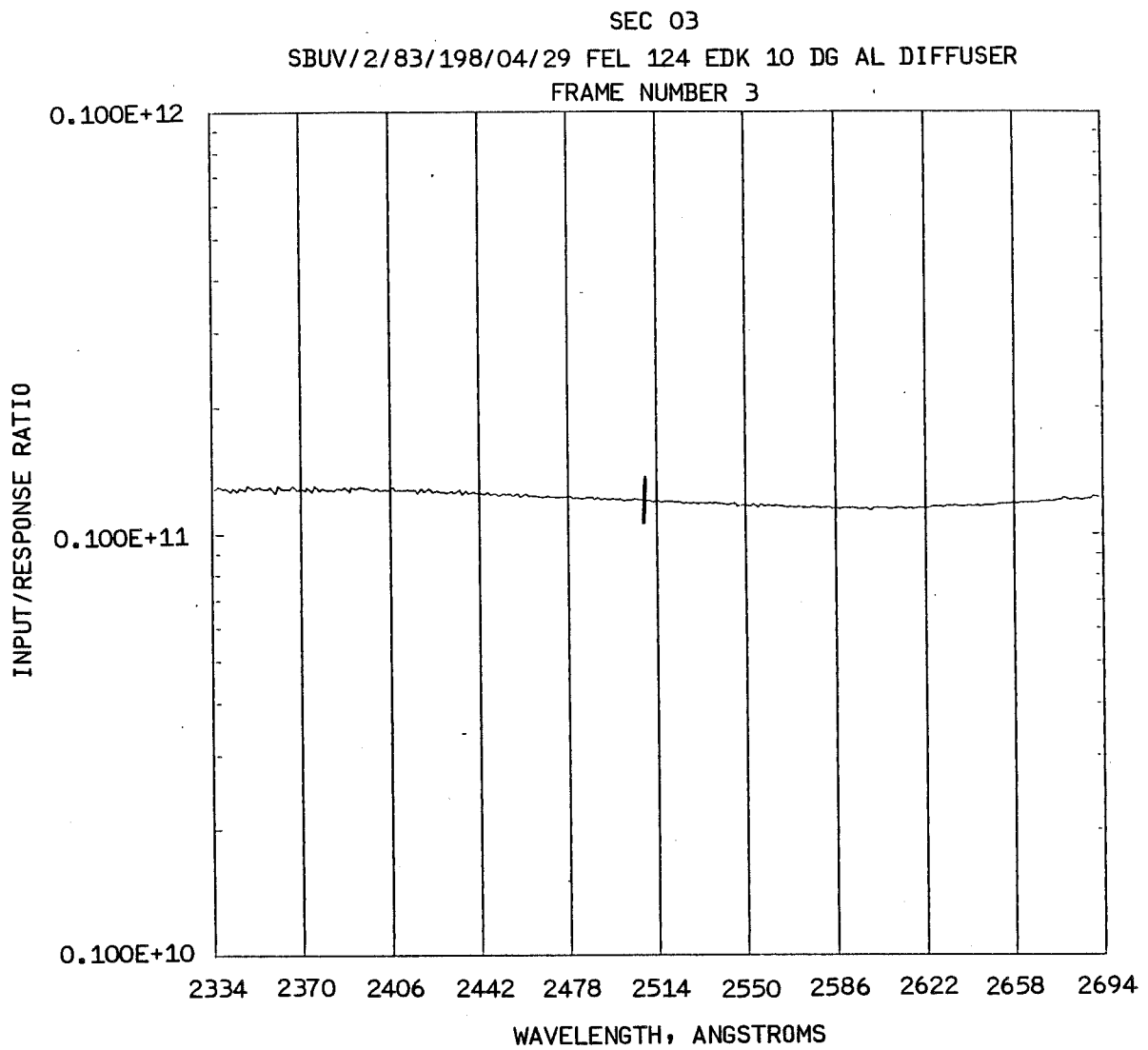


A/N 3990

Figure 4-43



B6802-78



A/N 3990

Figure 4-43 (cont.)



B6802-78

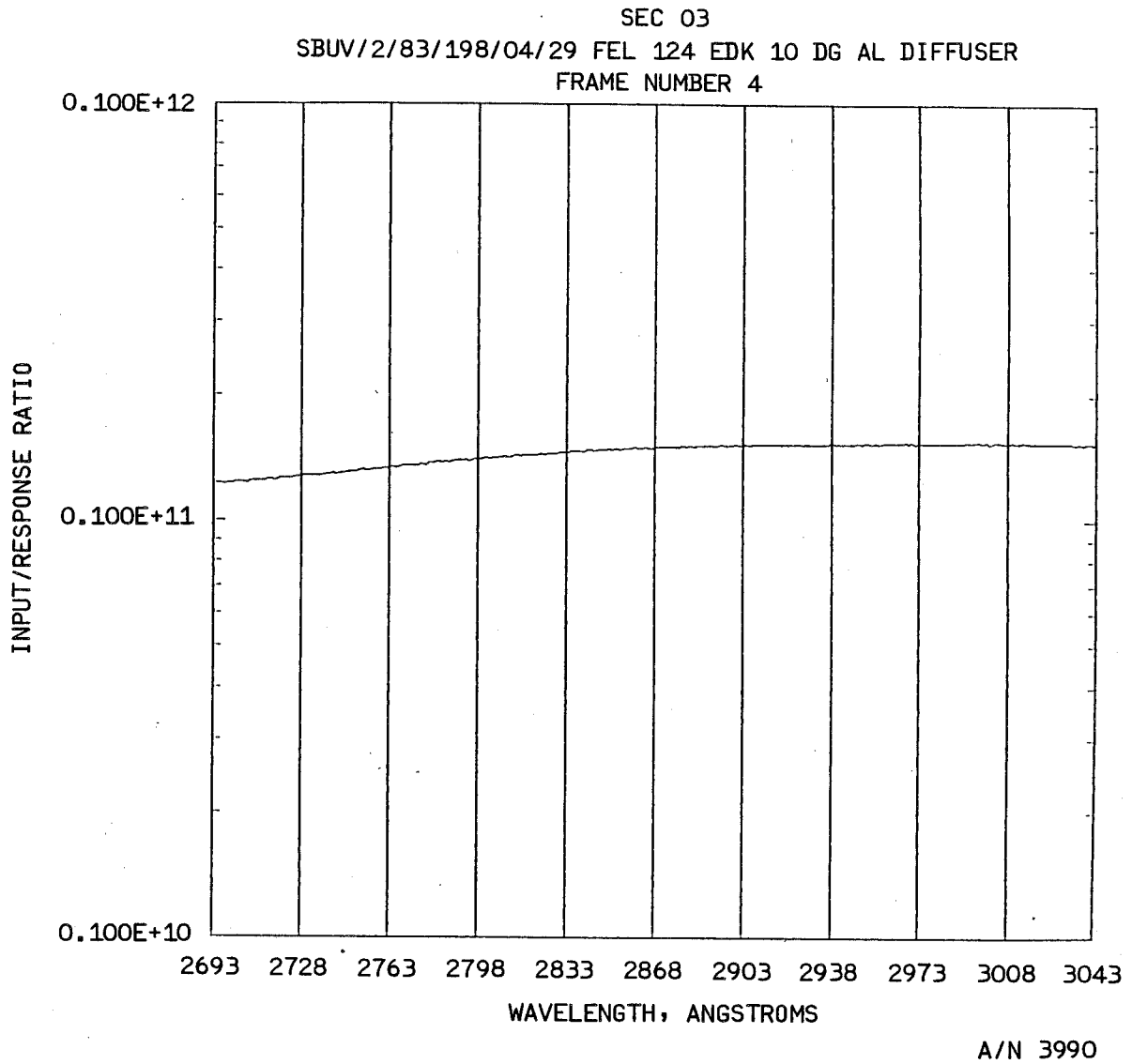


Figure 4-43 (cont.)



B6802-78

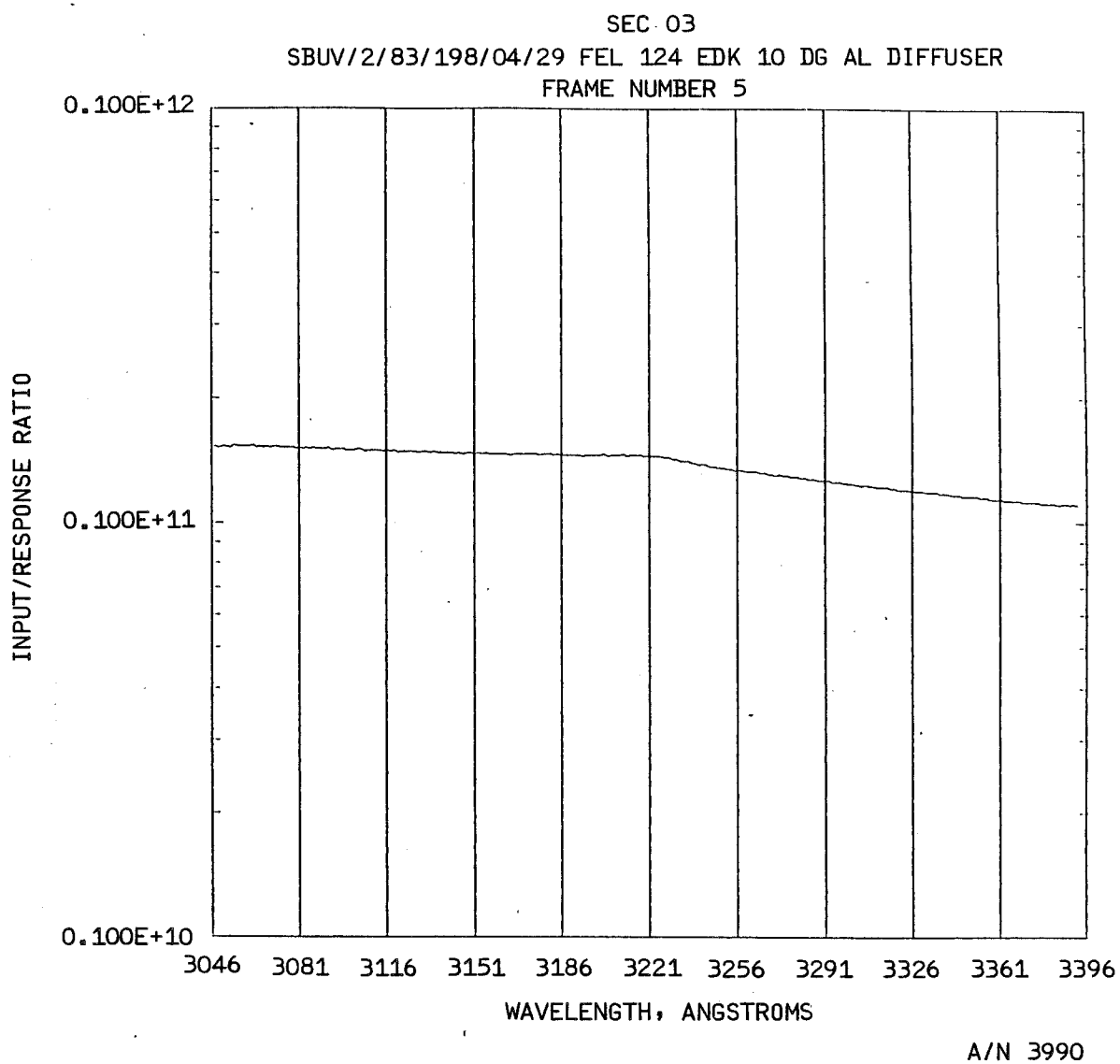


Figure 4-43 (cont.)



B6802-78

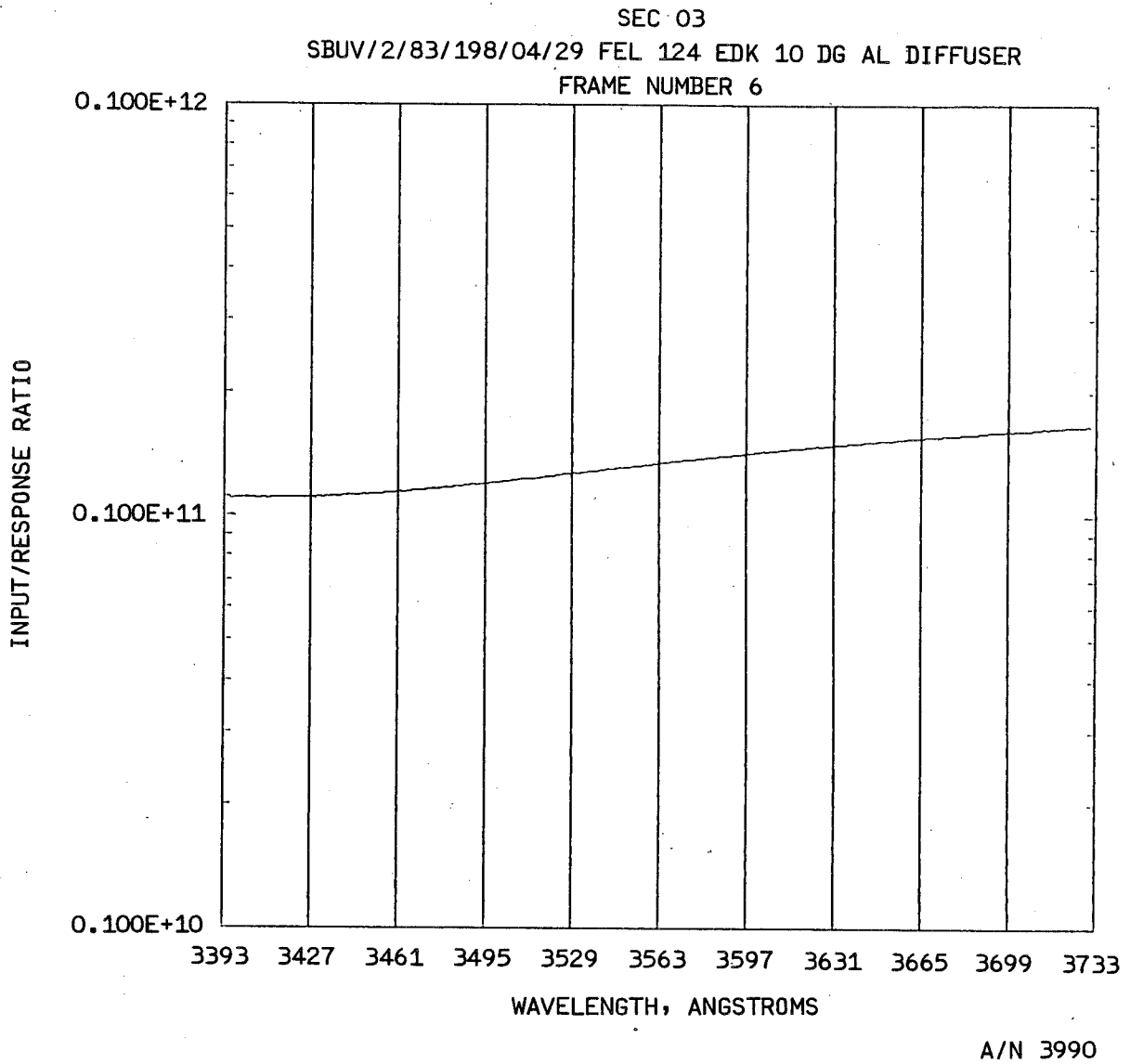


Figure 4-43 (cont.)



B6802-78

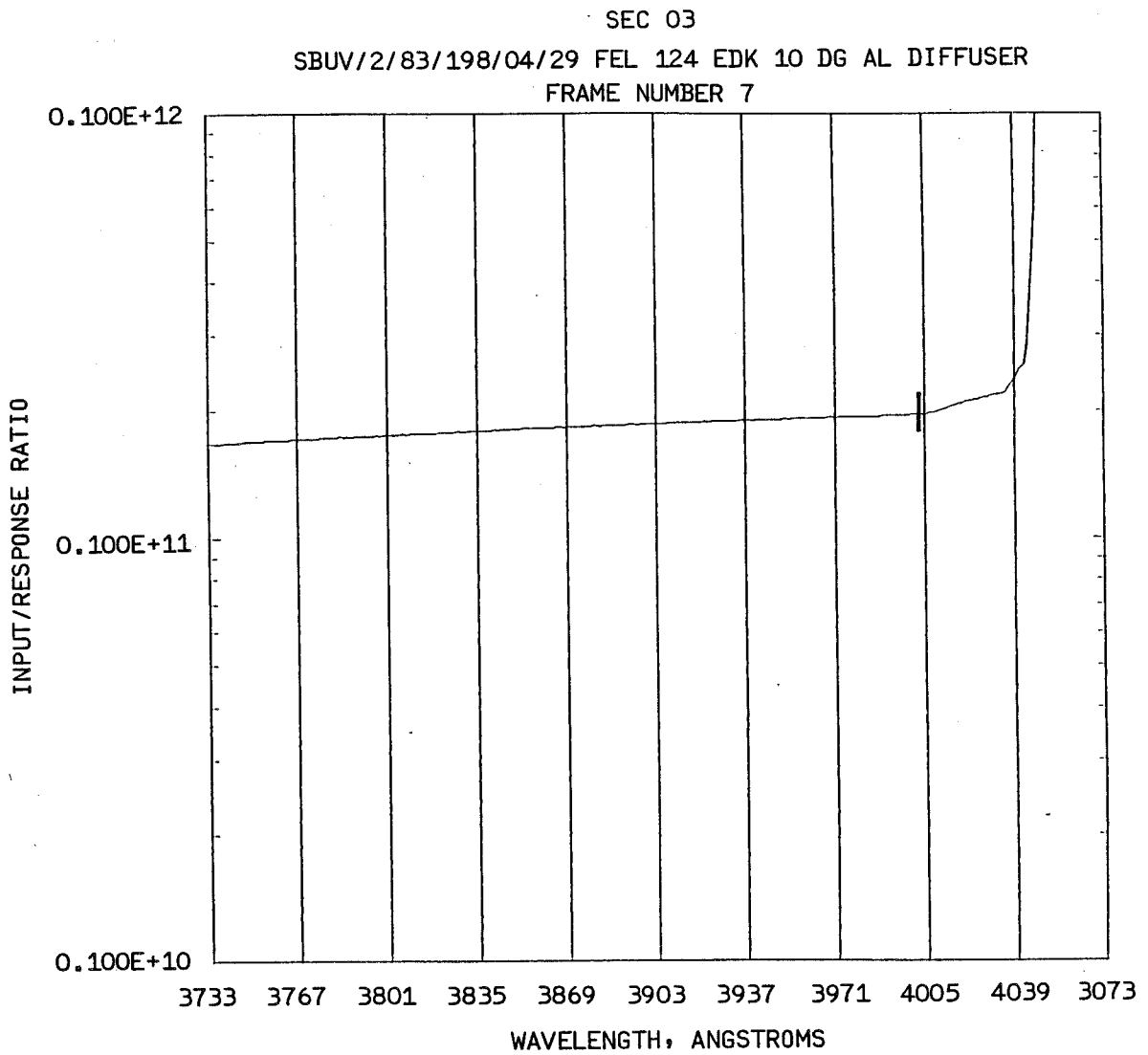


Figure 4-43 (cont.)



B6802-78

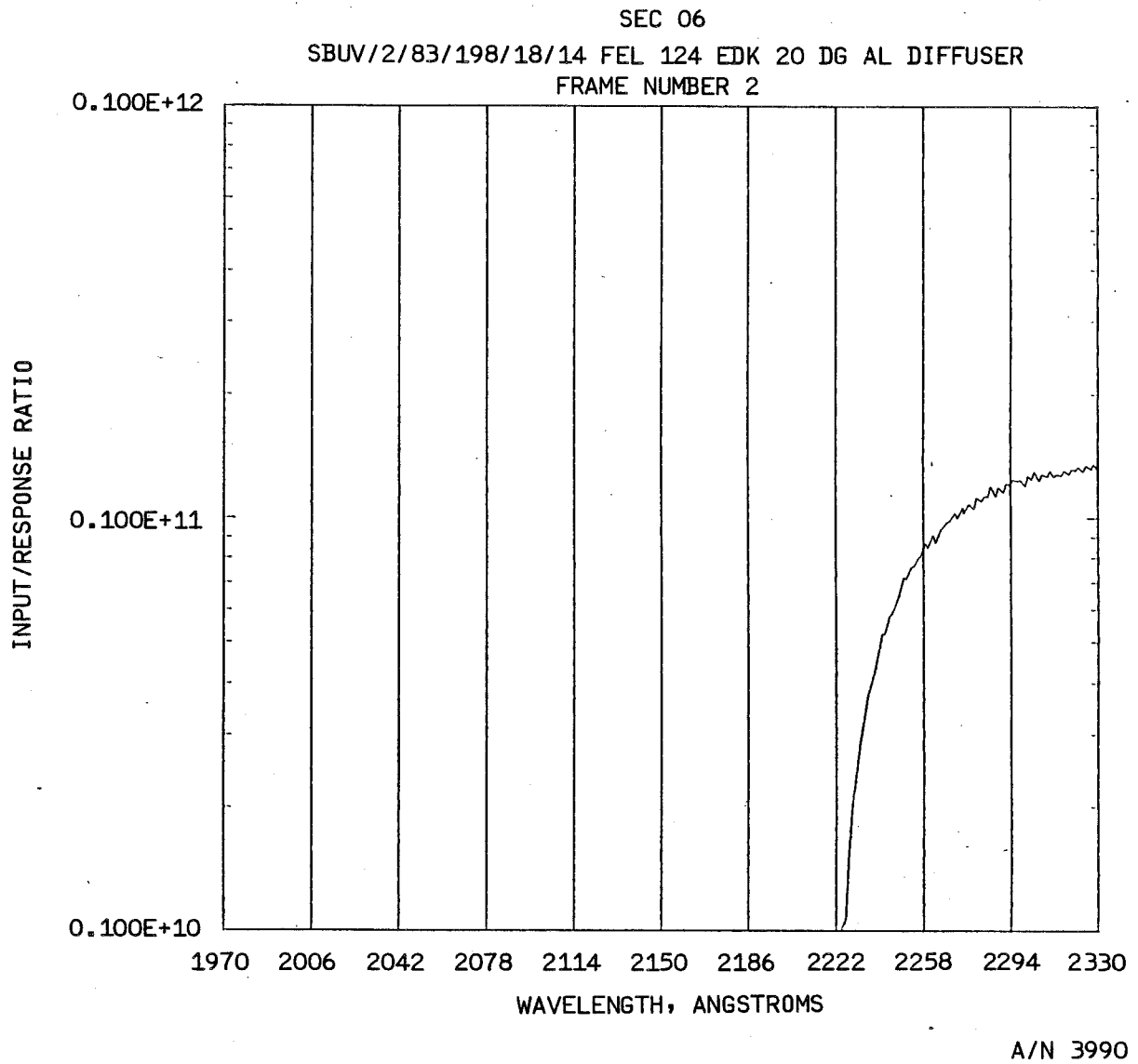
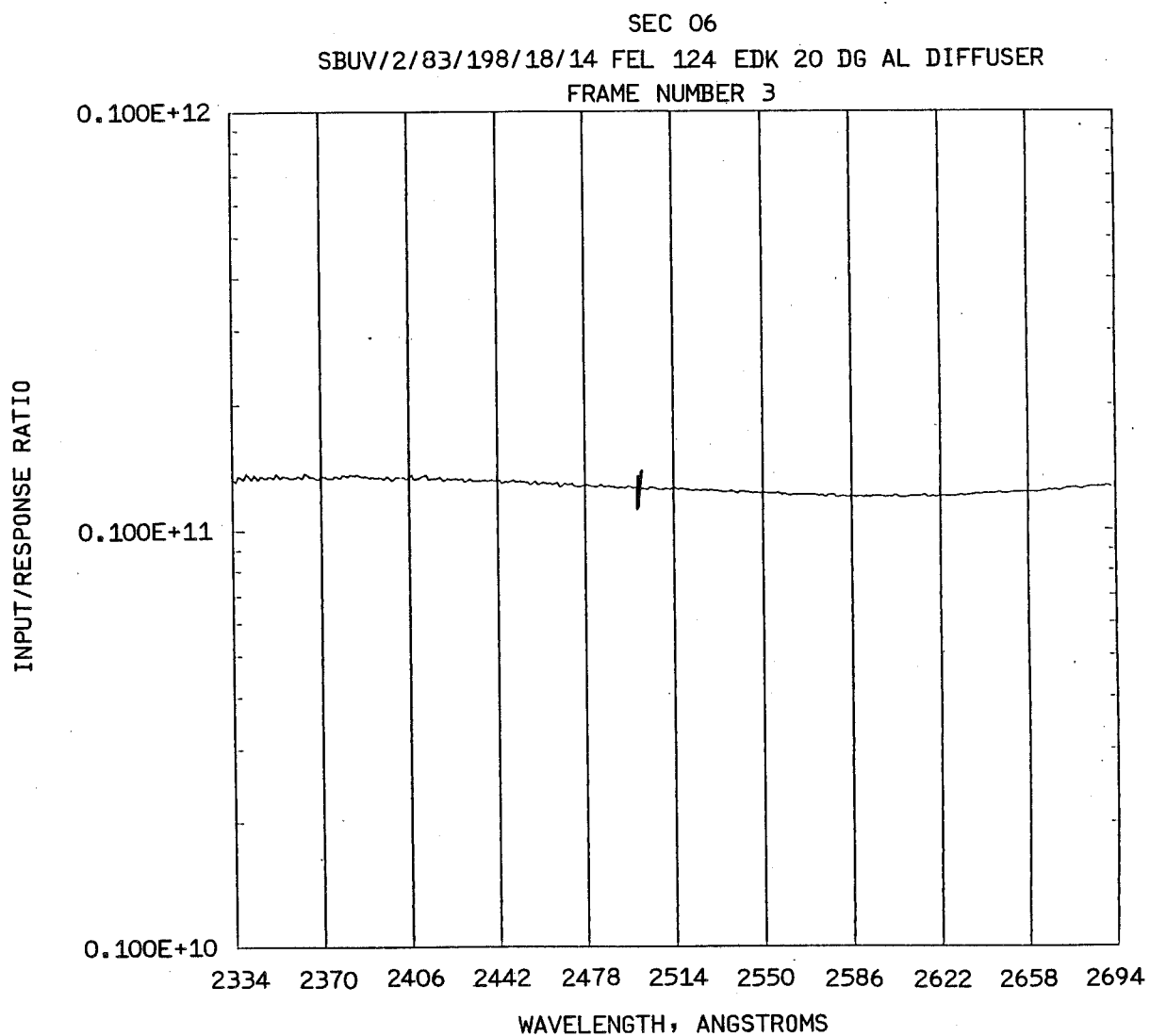


Figure 4-44



B6802-78

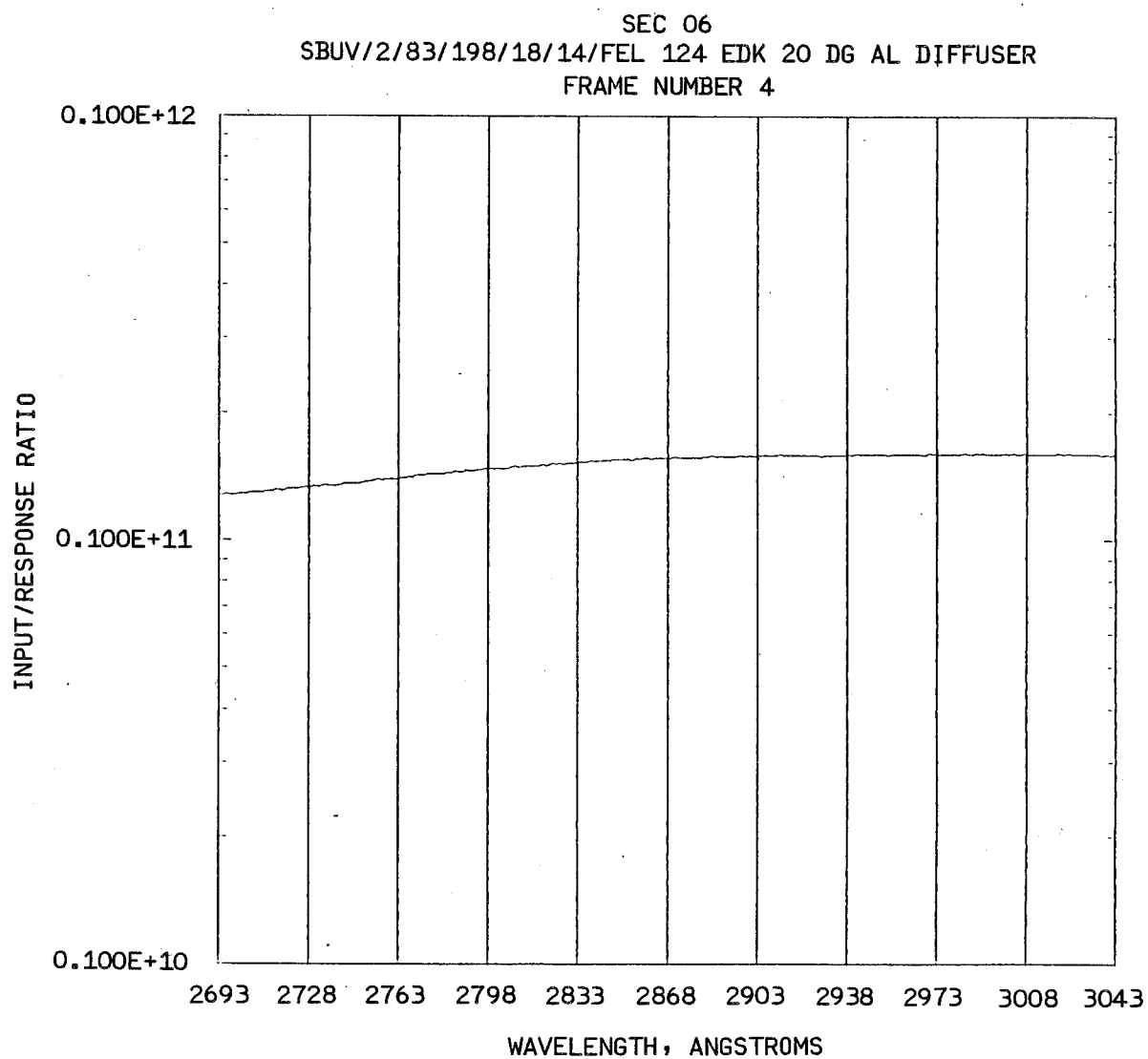


A/N 3990

Figure 4-44 (cont.)



B6802-78



A/N 3990

Figure 4-44 (cont.)



B6802-78

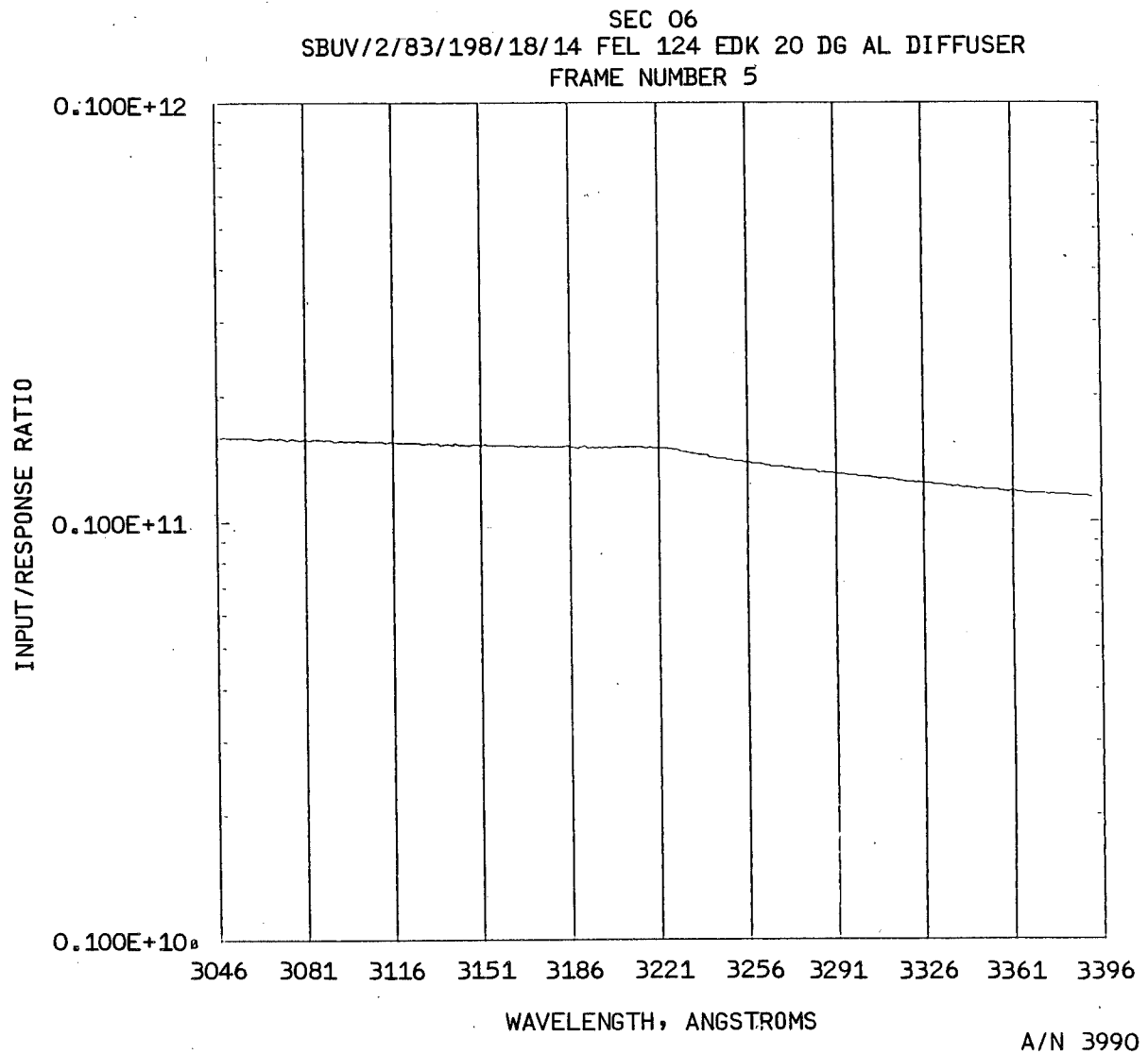


Figure 4-44 (cont.)

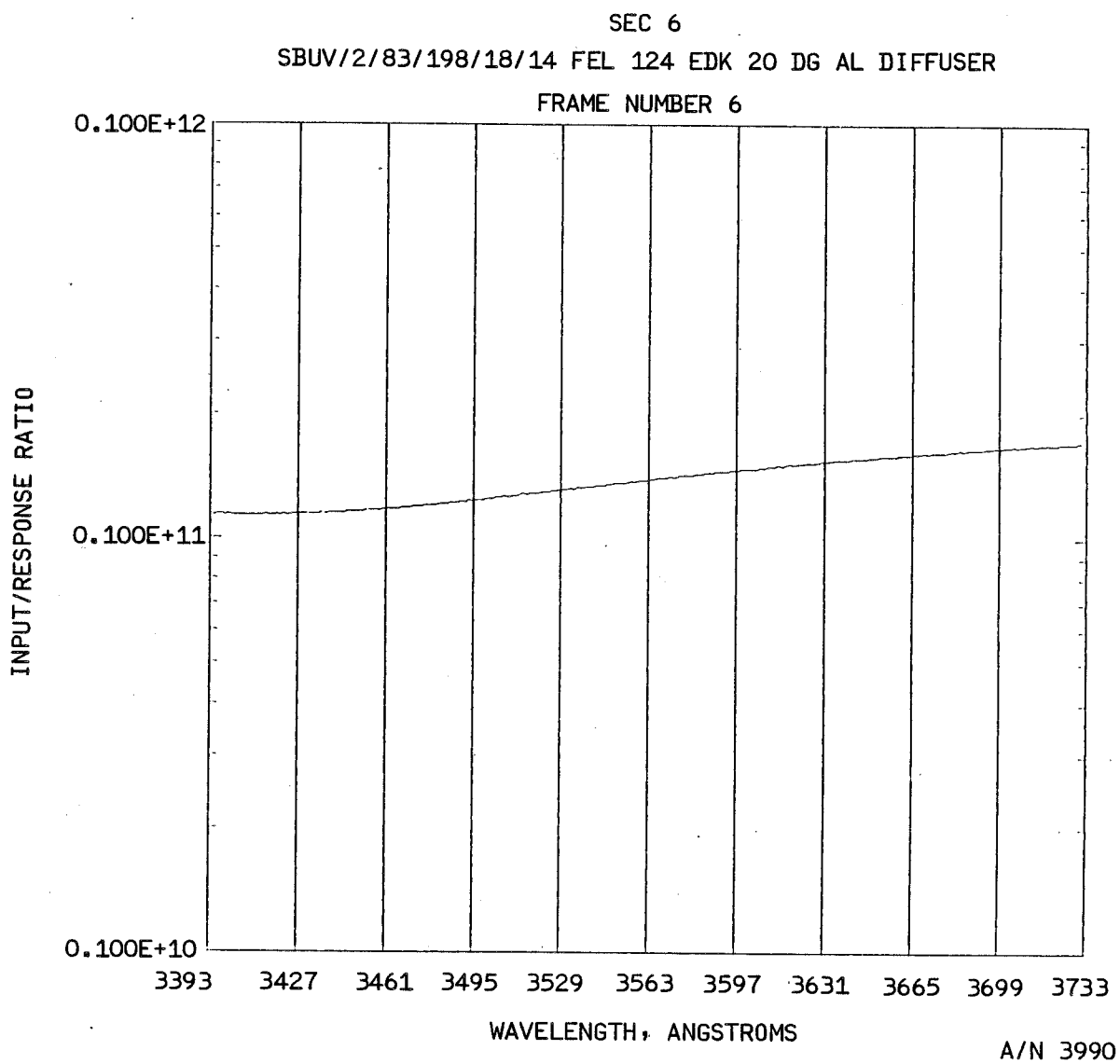


Figure 4-44 (cont.)



B6802-78

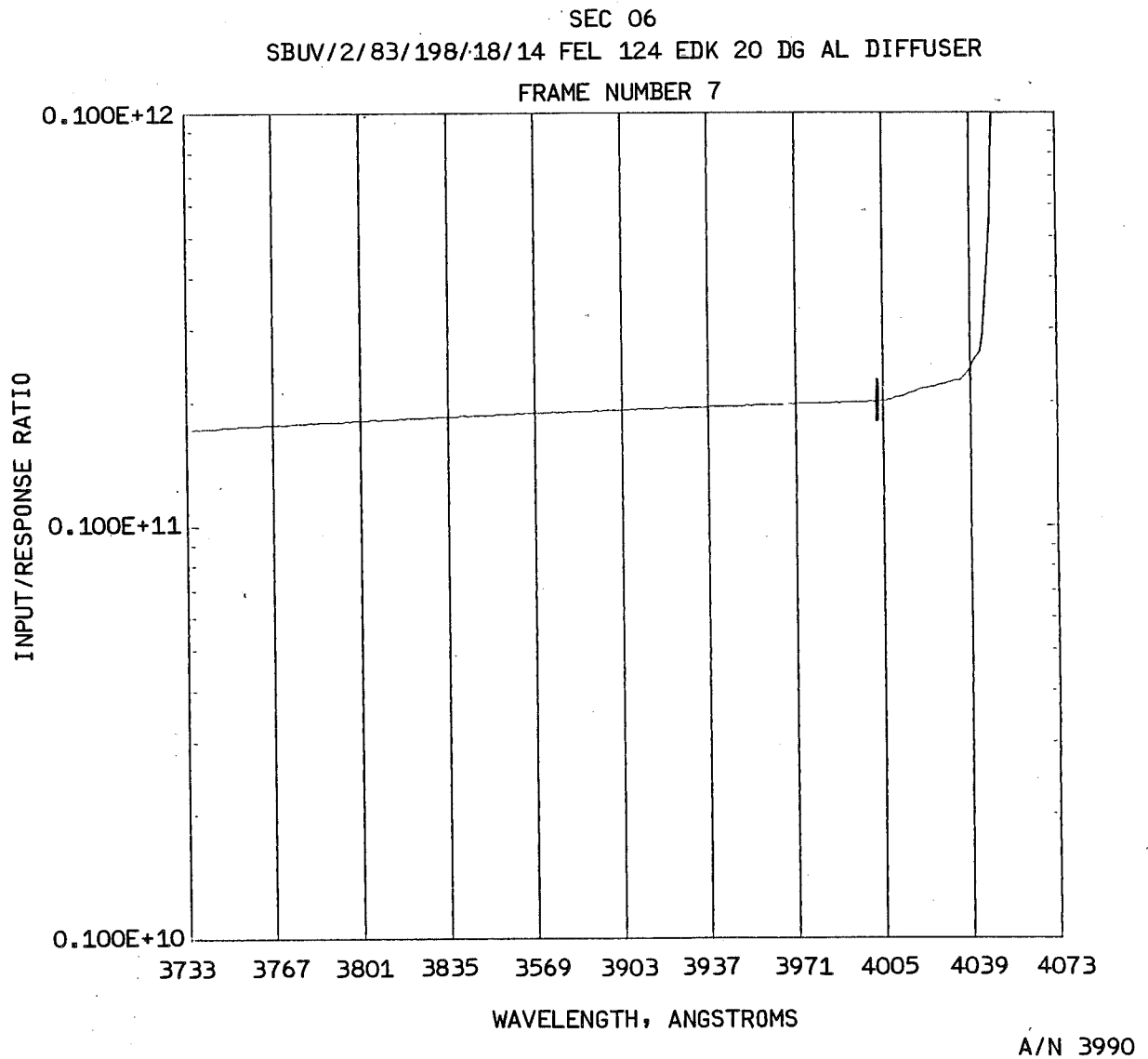


Figure 4-44 (cont.)



B6802-78

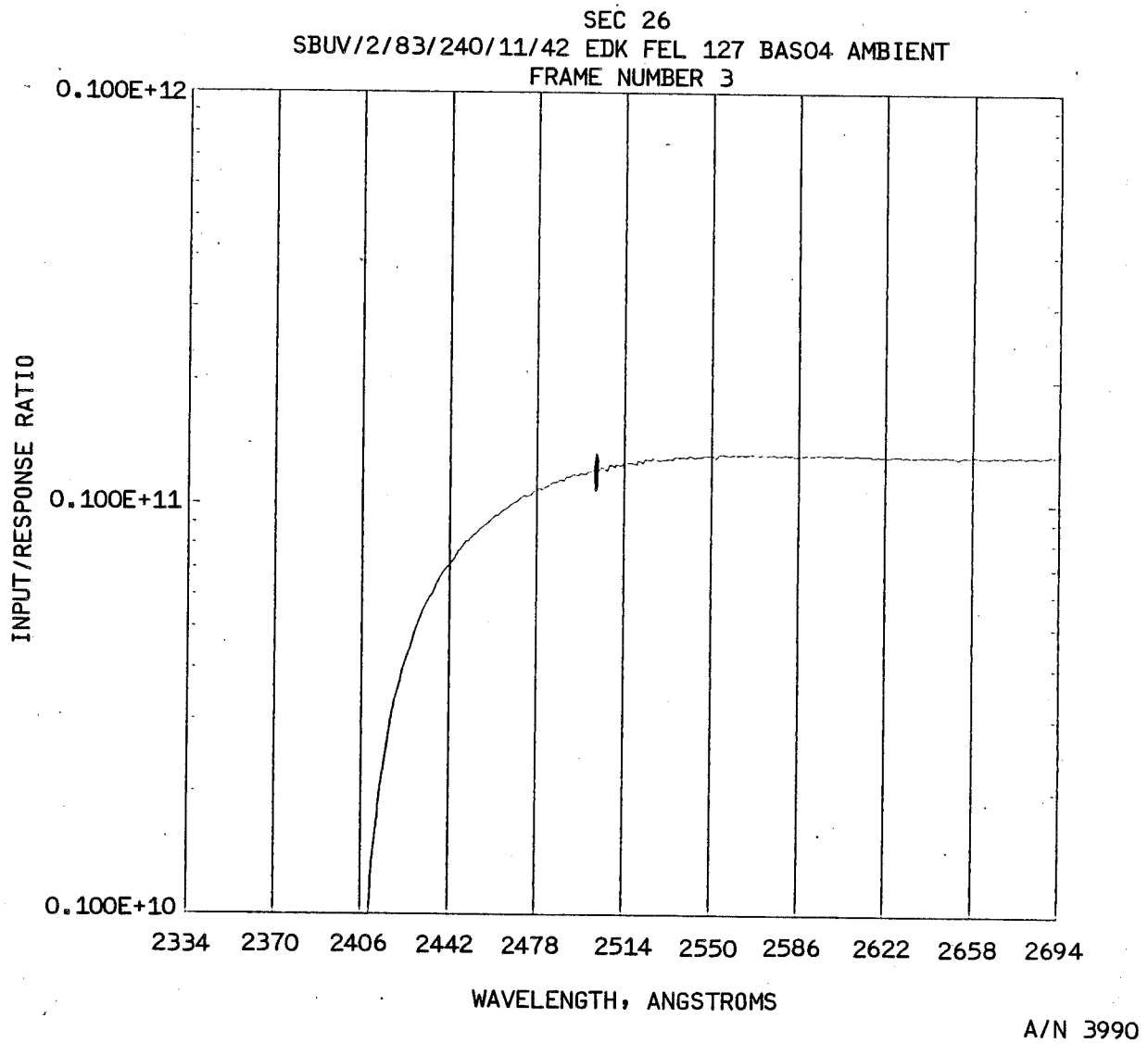


Figure 4-45



B6802-78

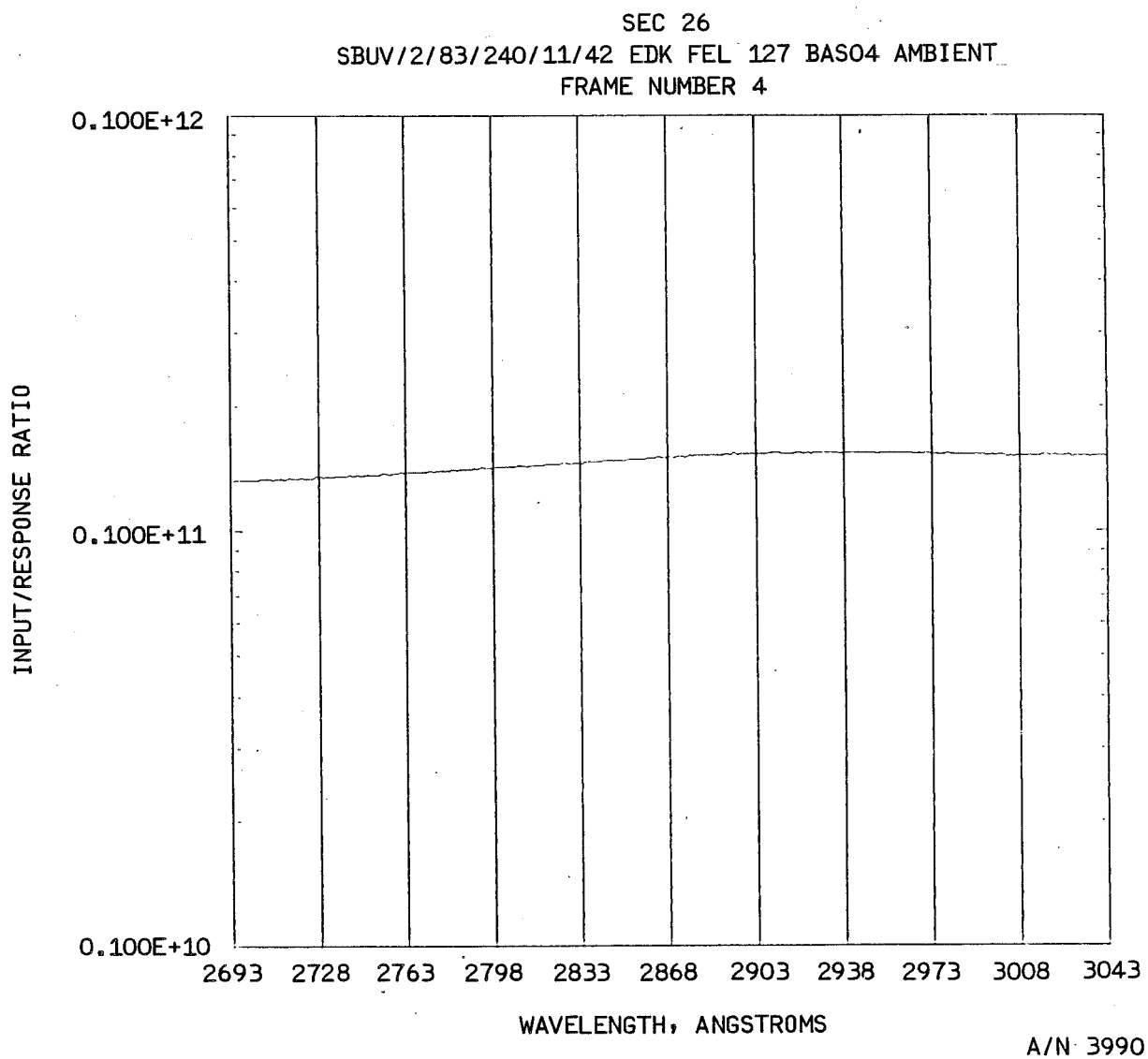
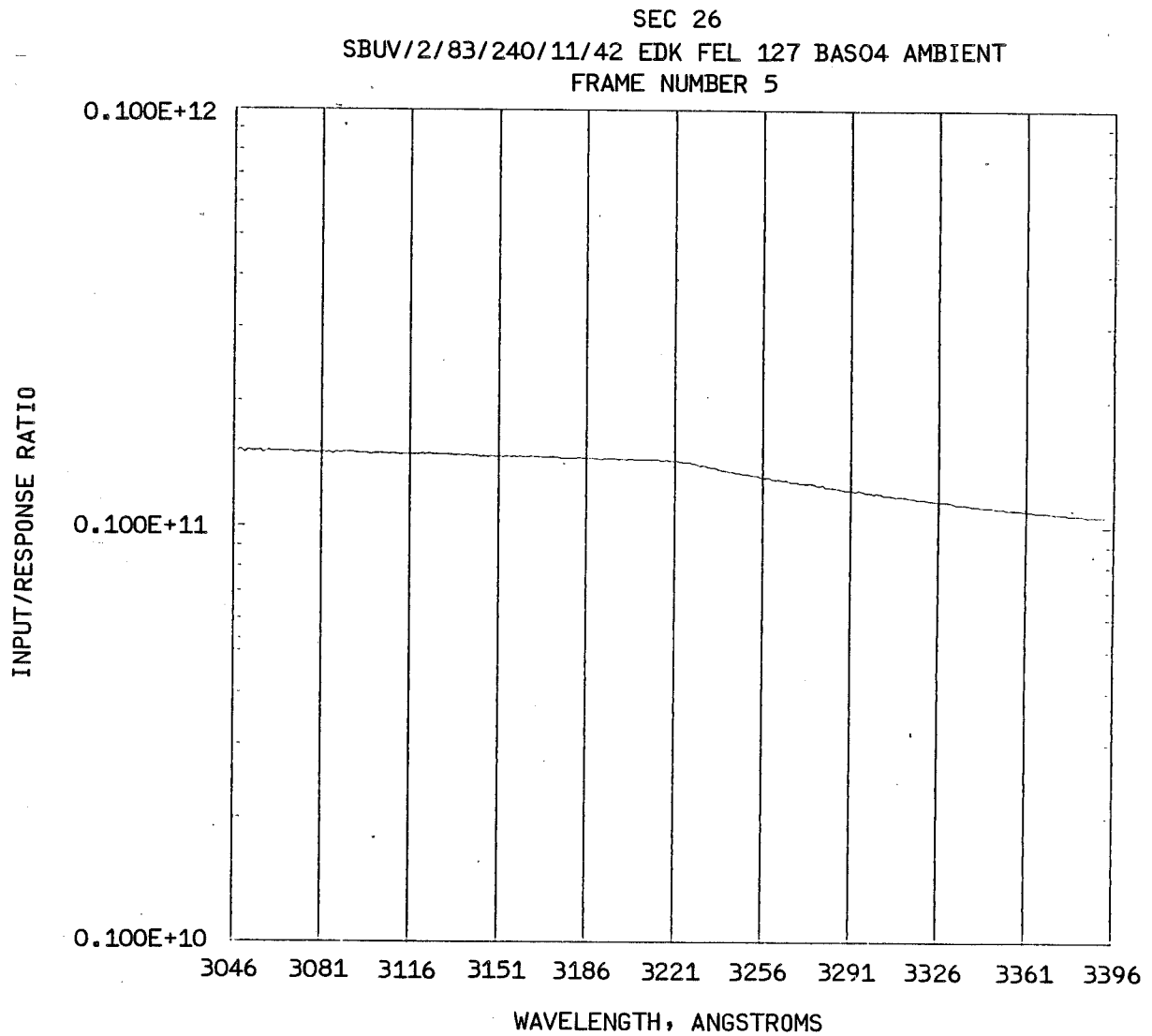


Figure 4-45 (cont.)



B6802-78



A/N 3990

Figure 4-45 (cont.)



B6802-78

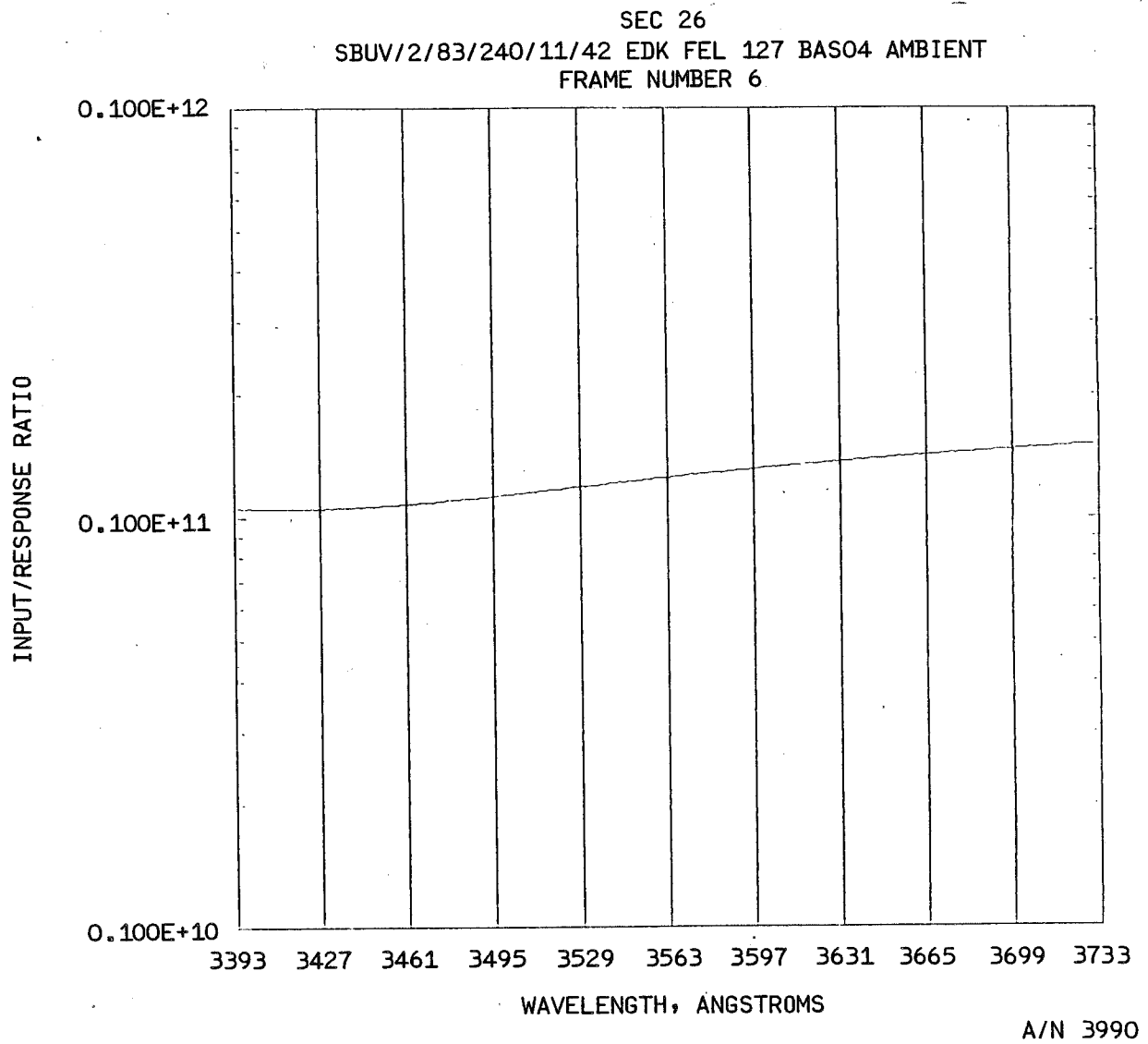


Figure 4-45 (cont.)



B6802-78

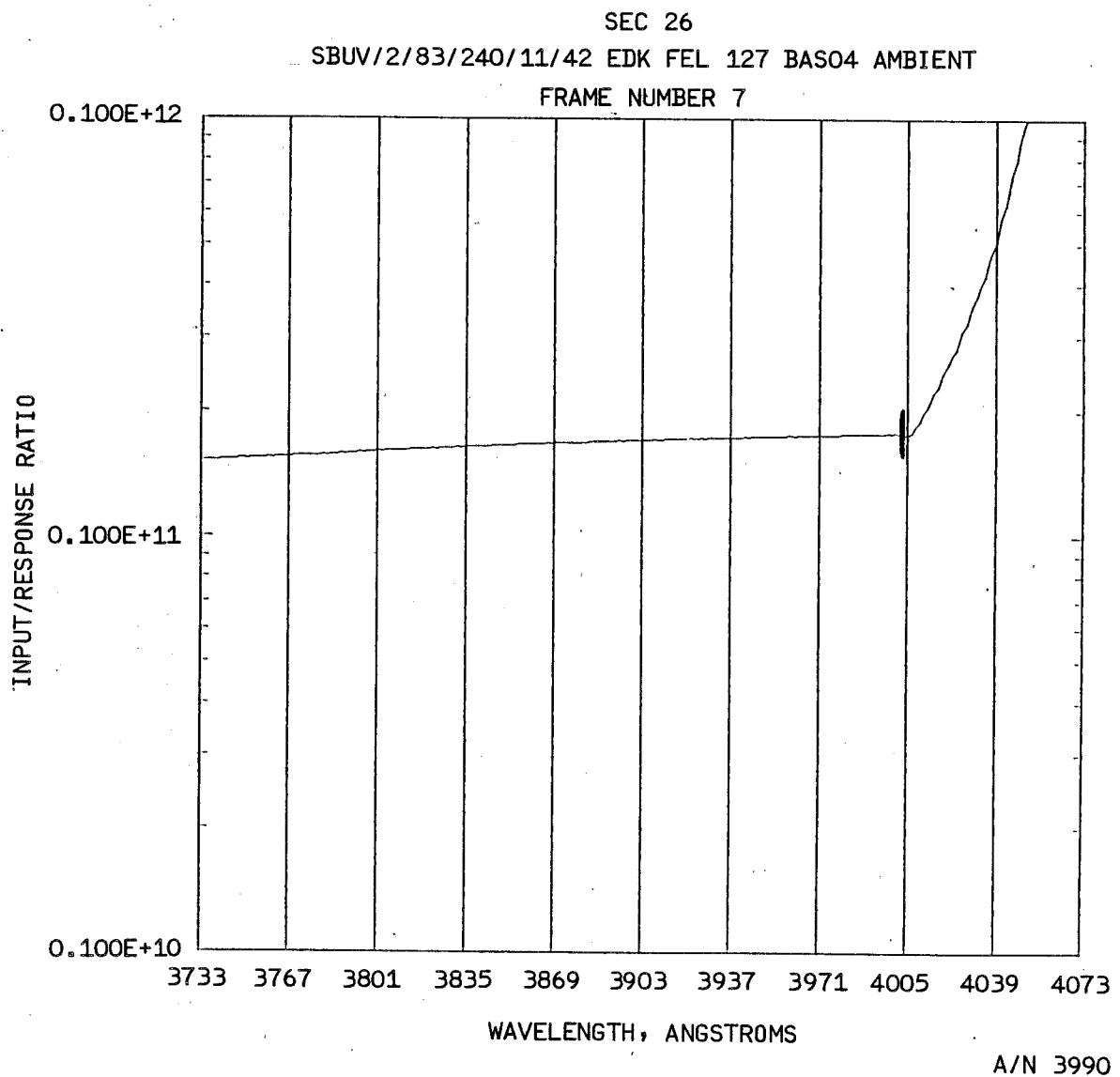


Figure 4-45 (cont.)



B6802-78

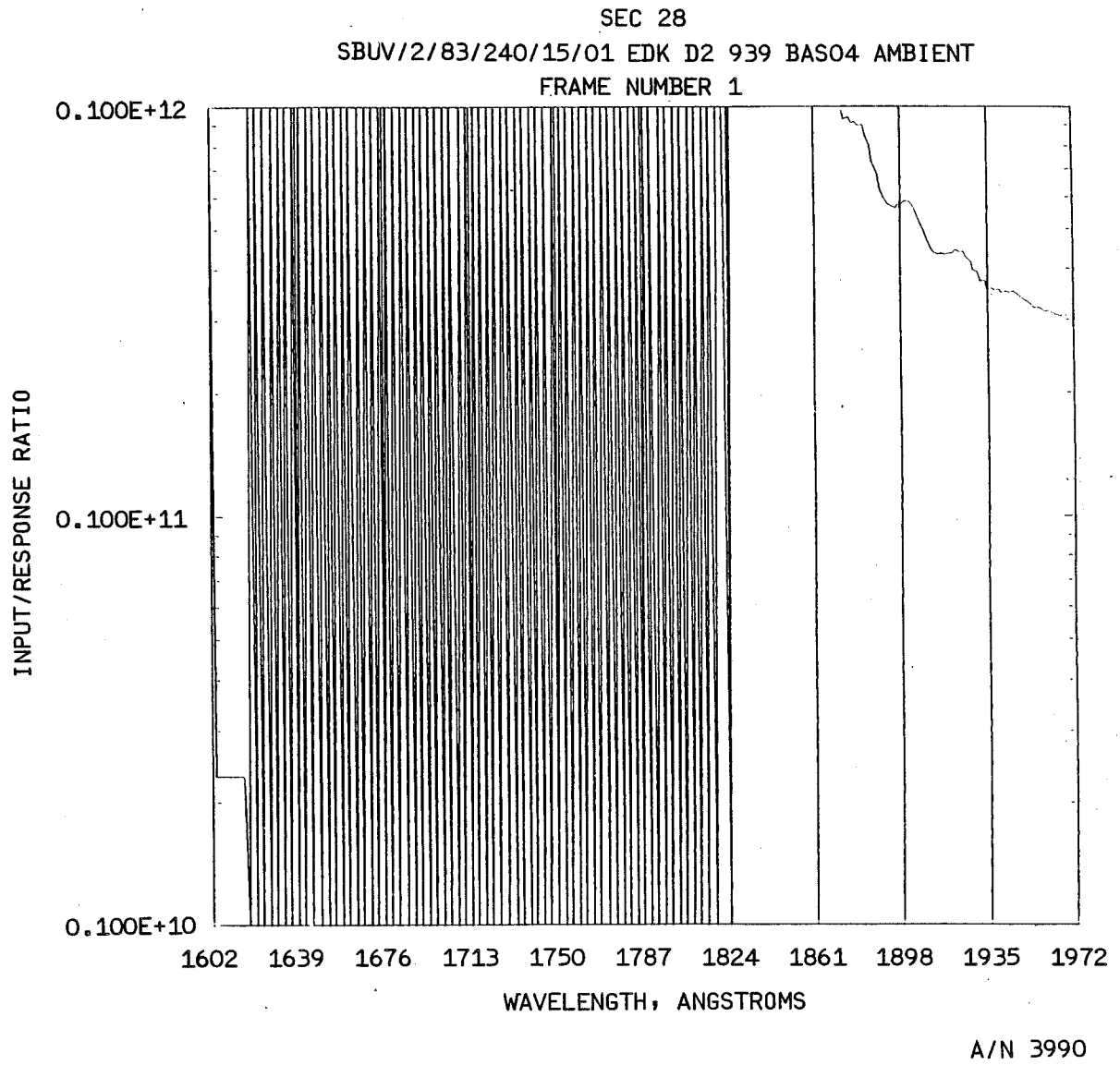
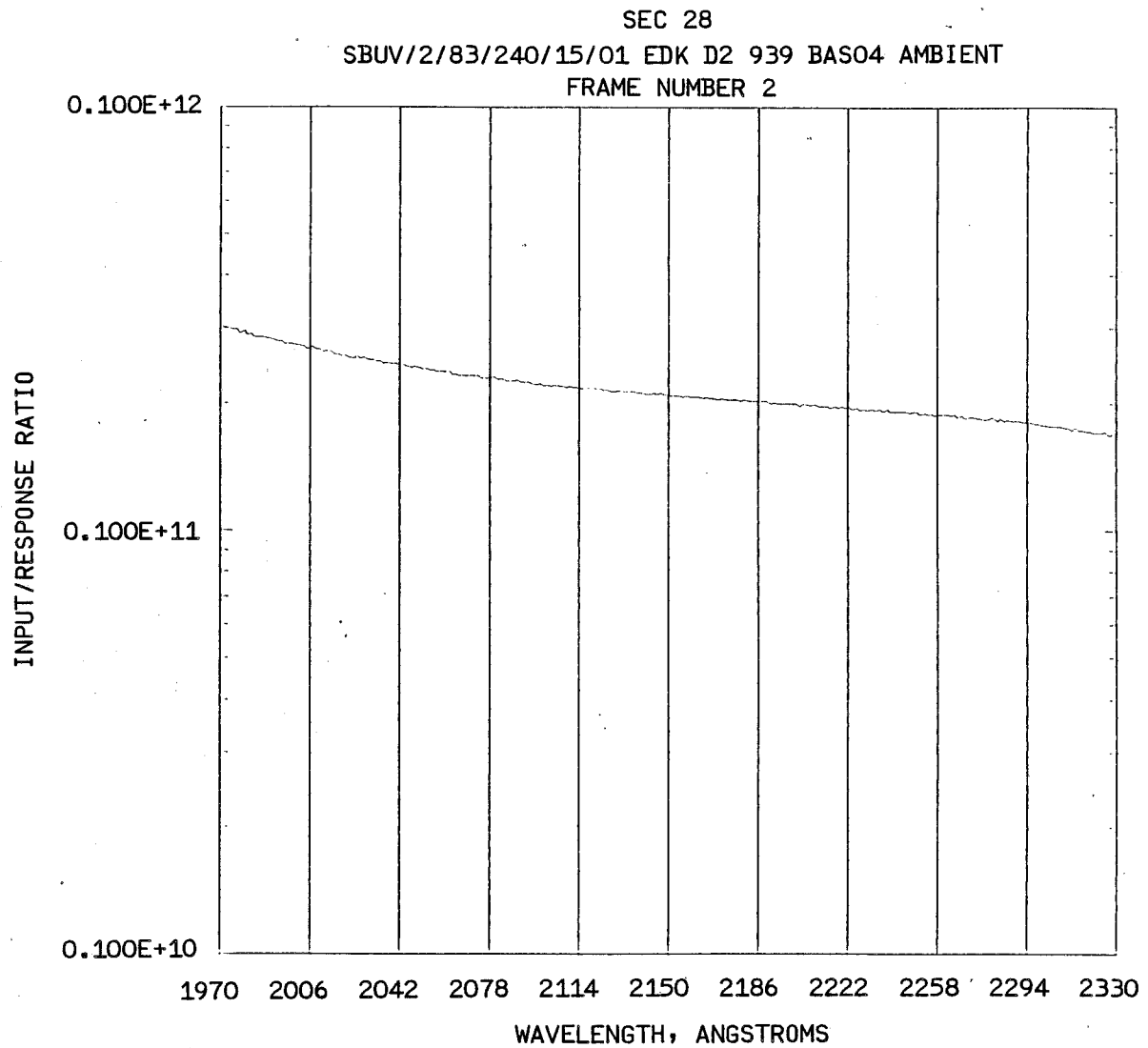


Figure 4-46



B6802-78



A/N 3990

Figure 4-46 (cont.)



B6802-78

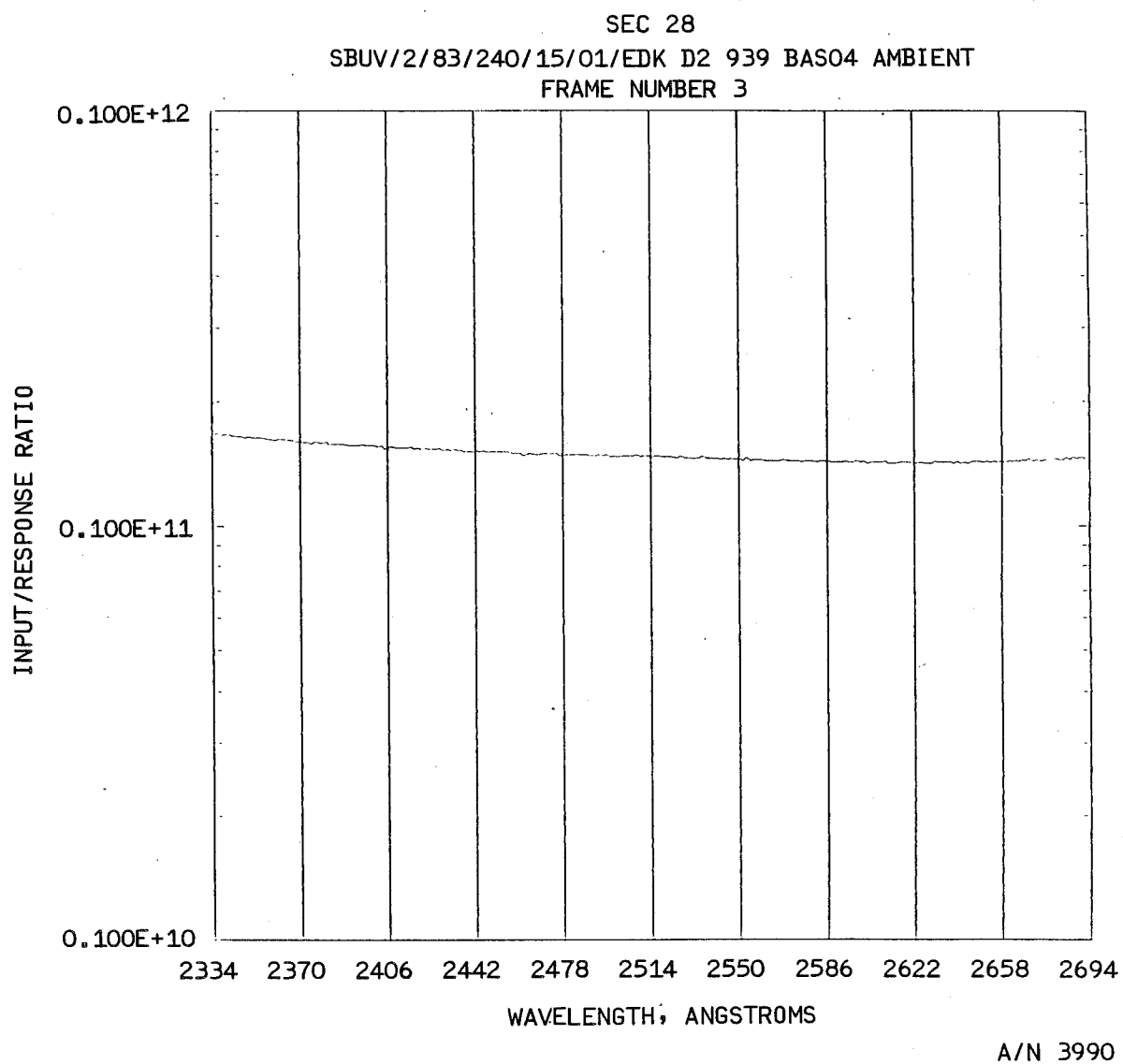


Figure 4-46 (cont.)



B6802-78

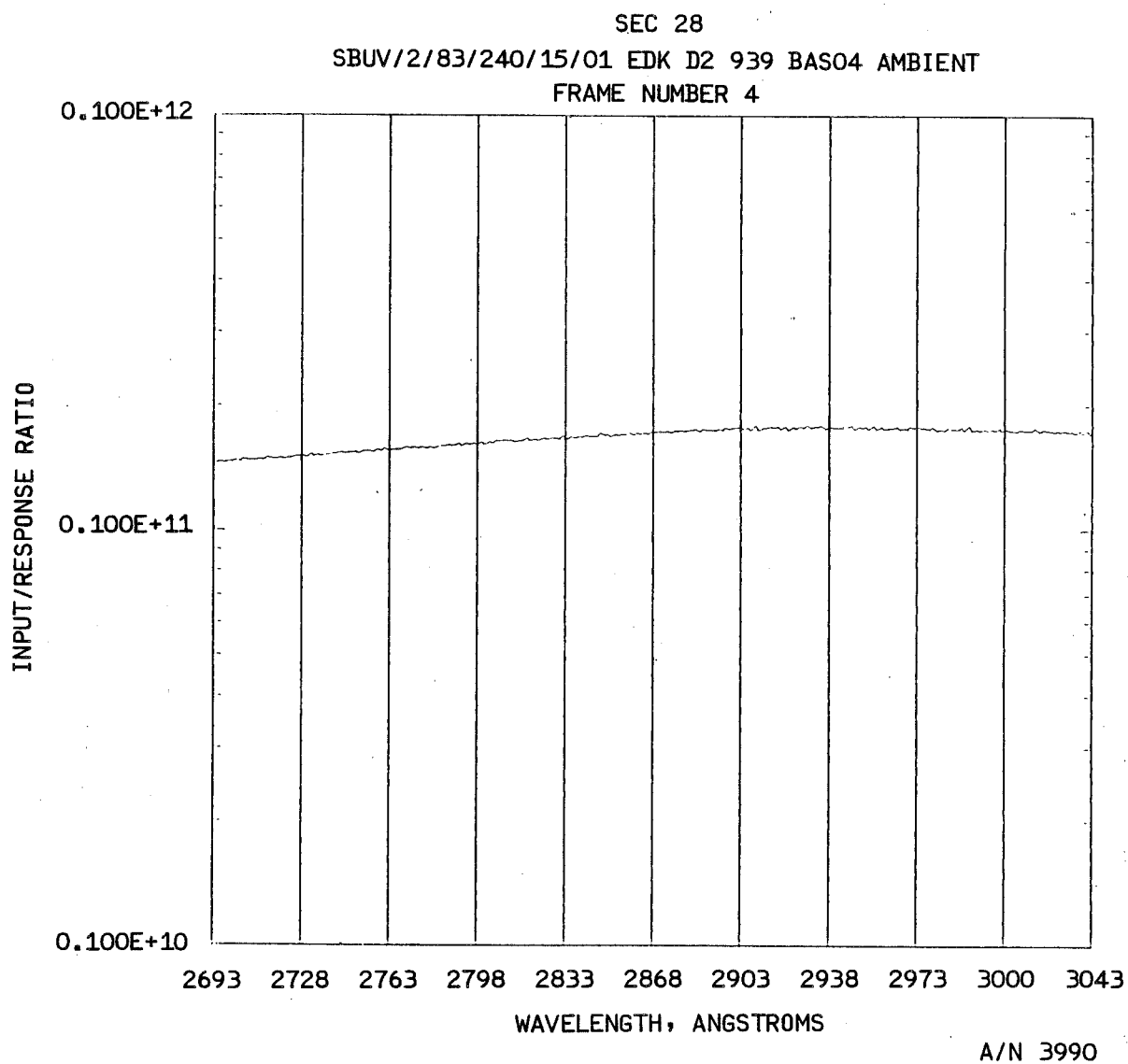


Figure 4-46 (cont.)



B6802-78

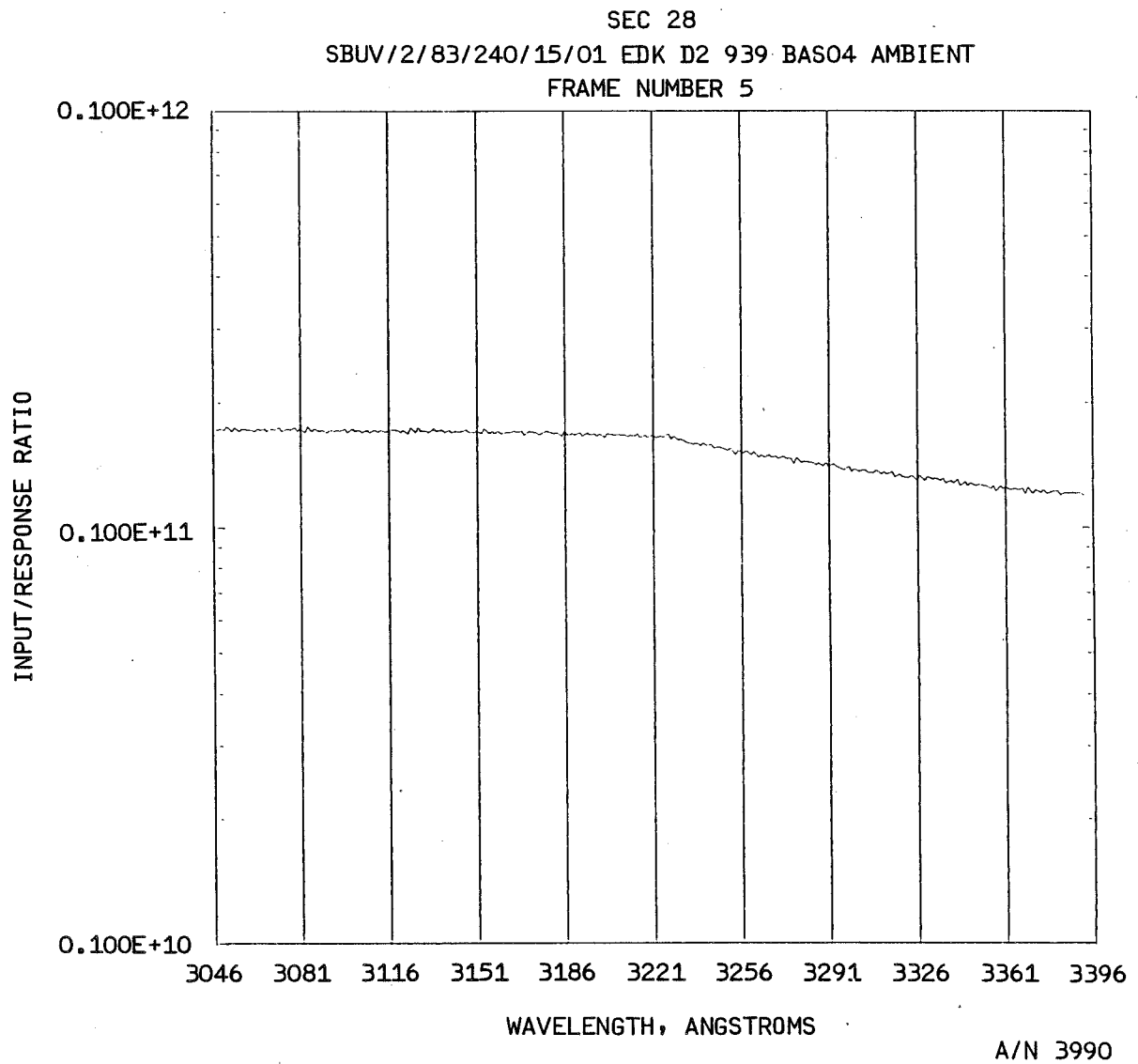


Figure 4-46 (cont.)



B6802-78

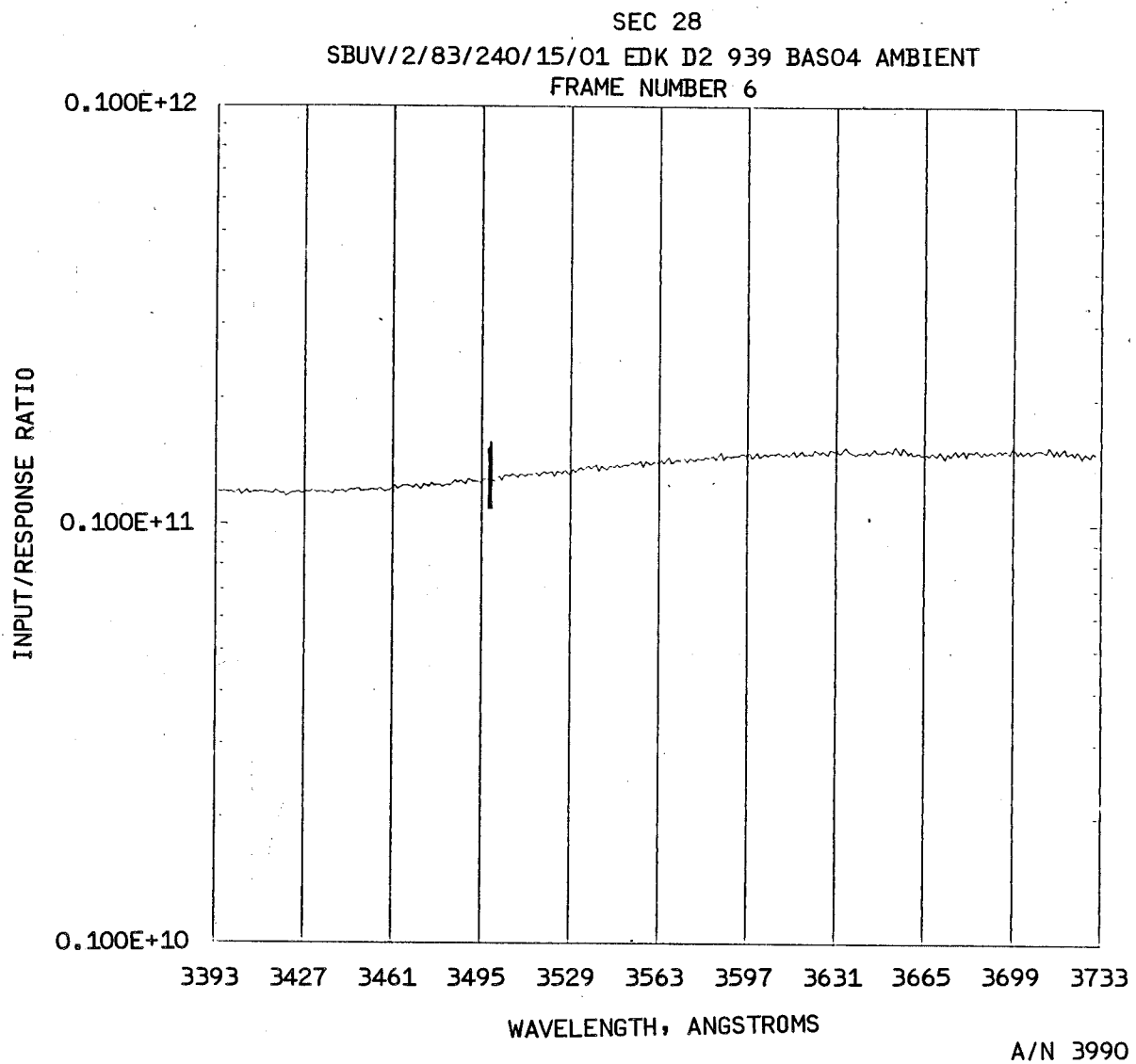


Figure 4-46 (cont.)



B6802-78

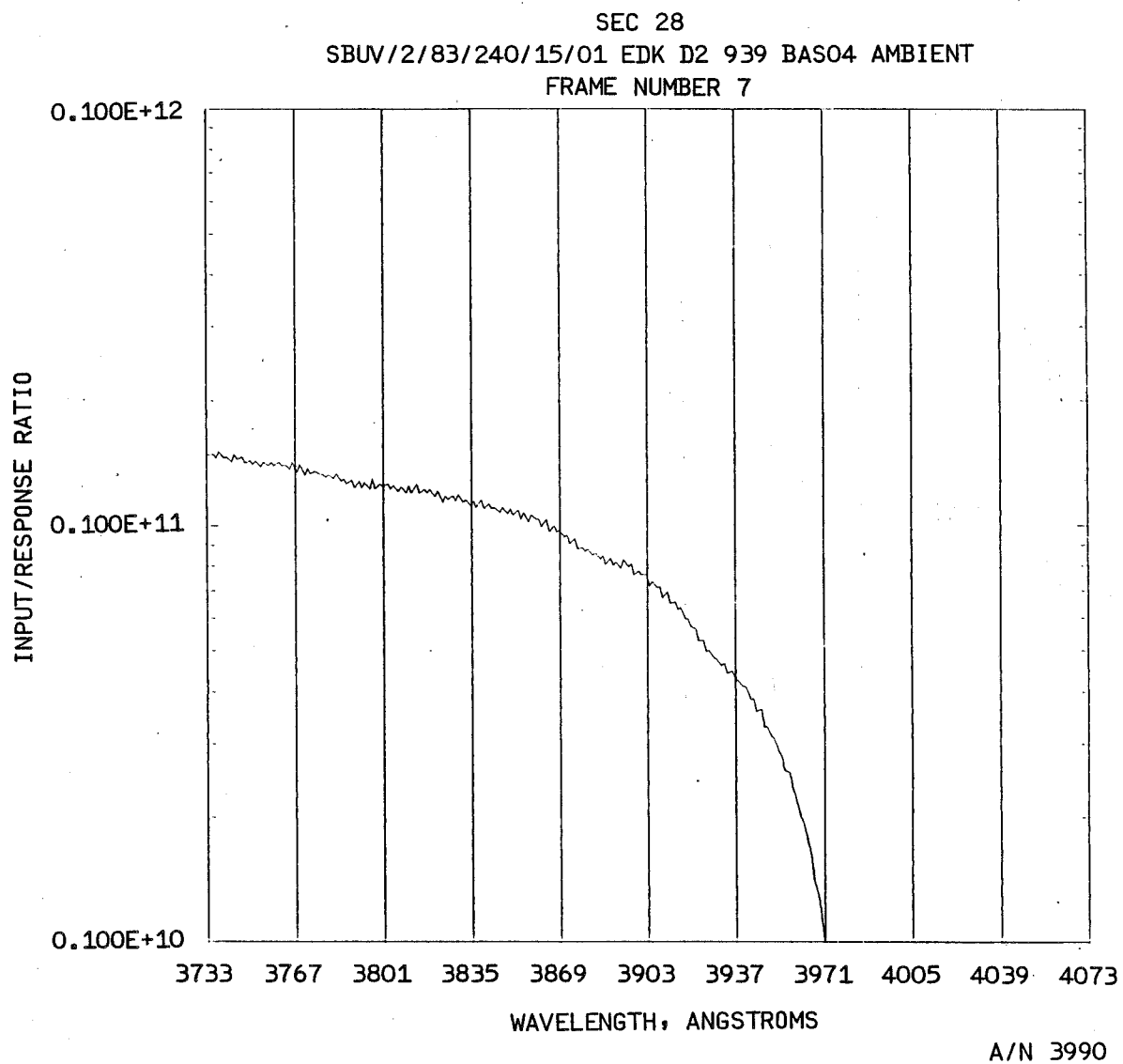


Figure 4-46 (cont.)



B6802-78

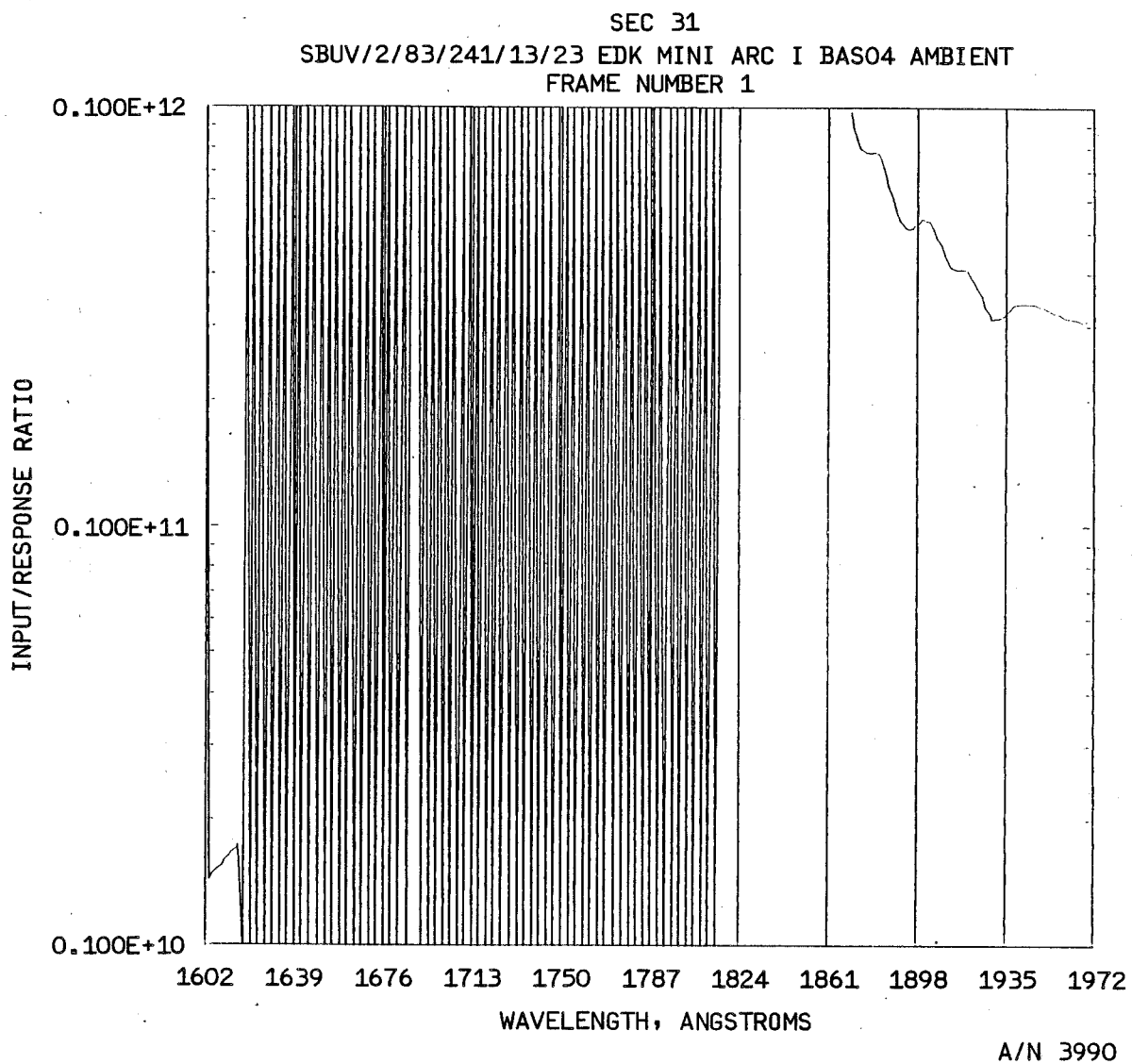


Figure 4-47



B6802-78

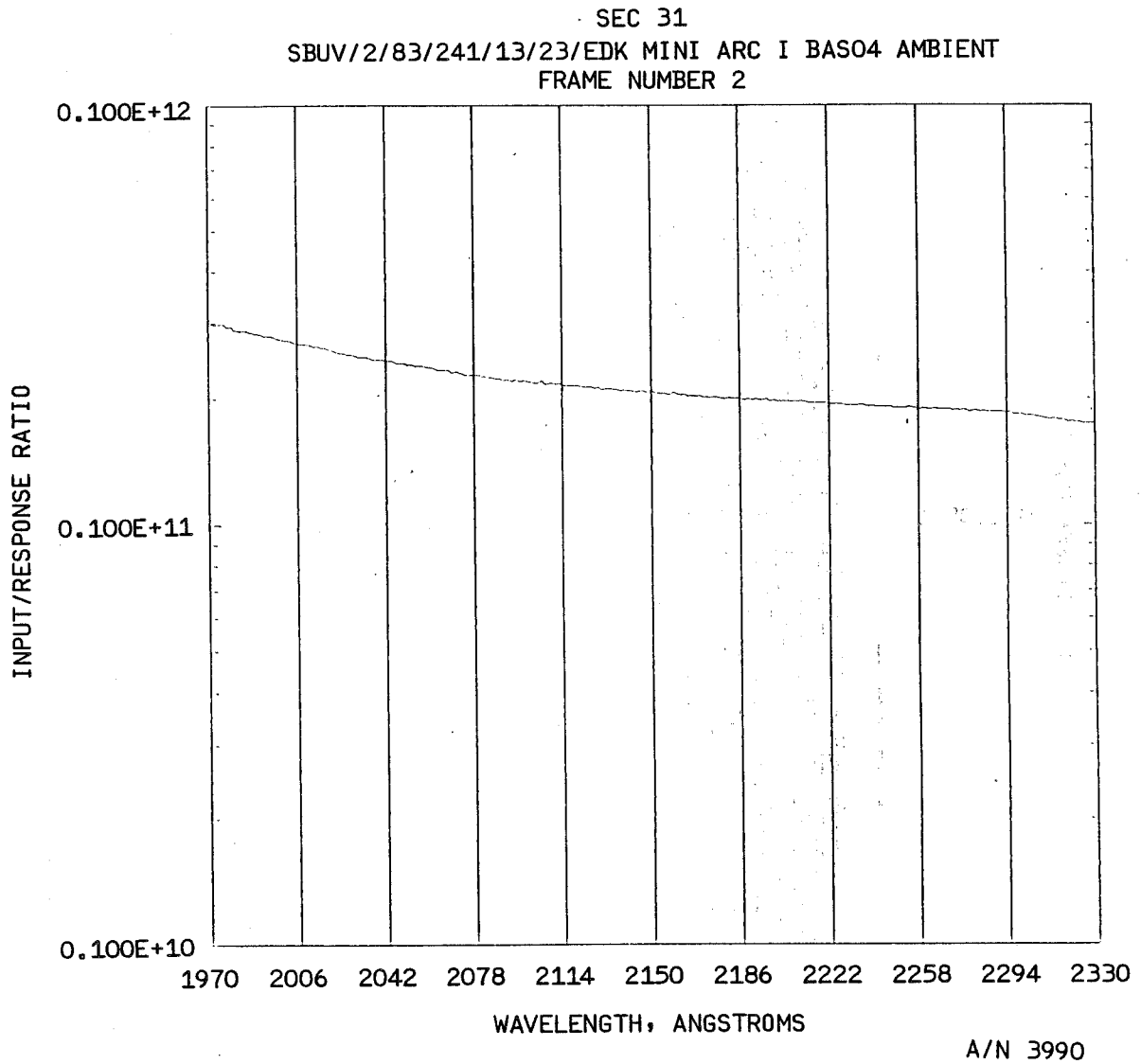
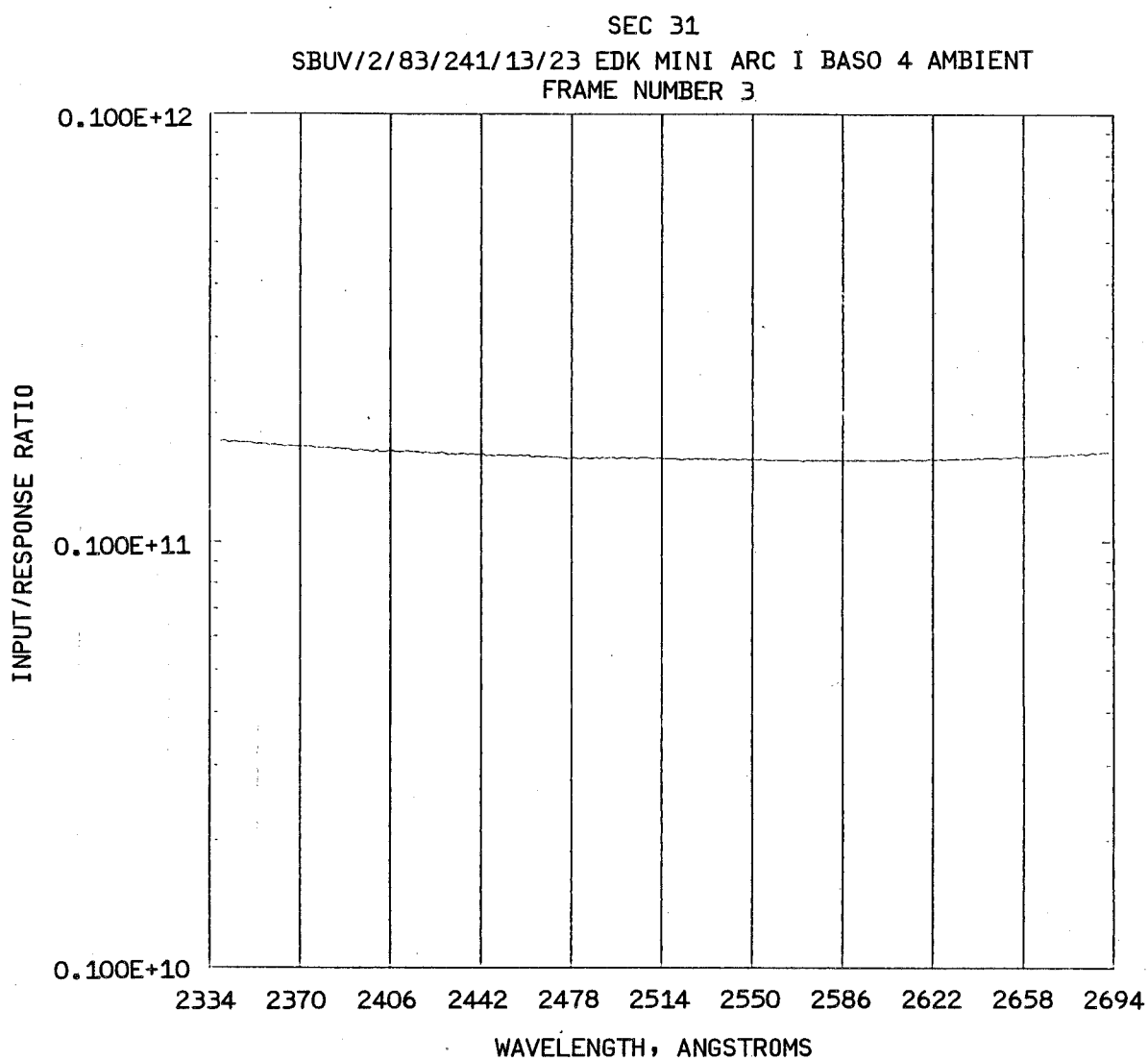


Figure 4-47 (cont.)



B6802-78



A/N 3990

Figure 4-47 (cont.)



B6802-78

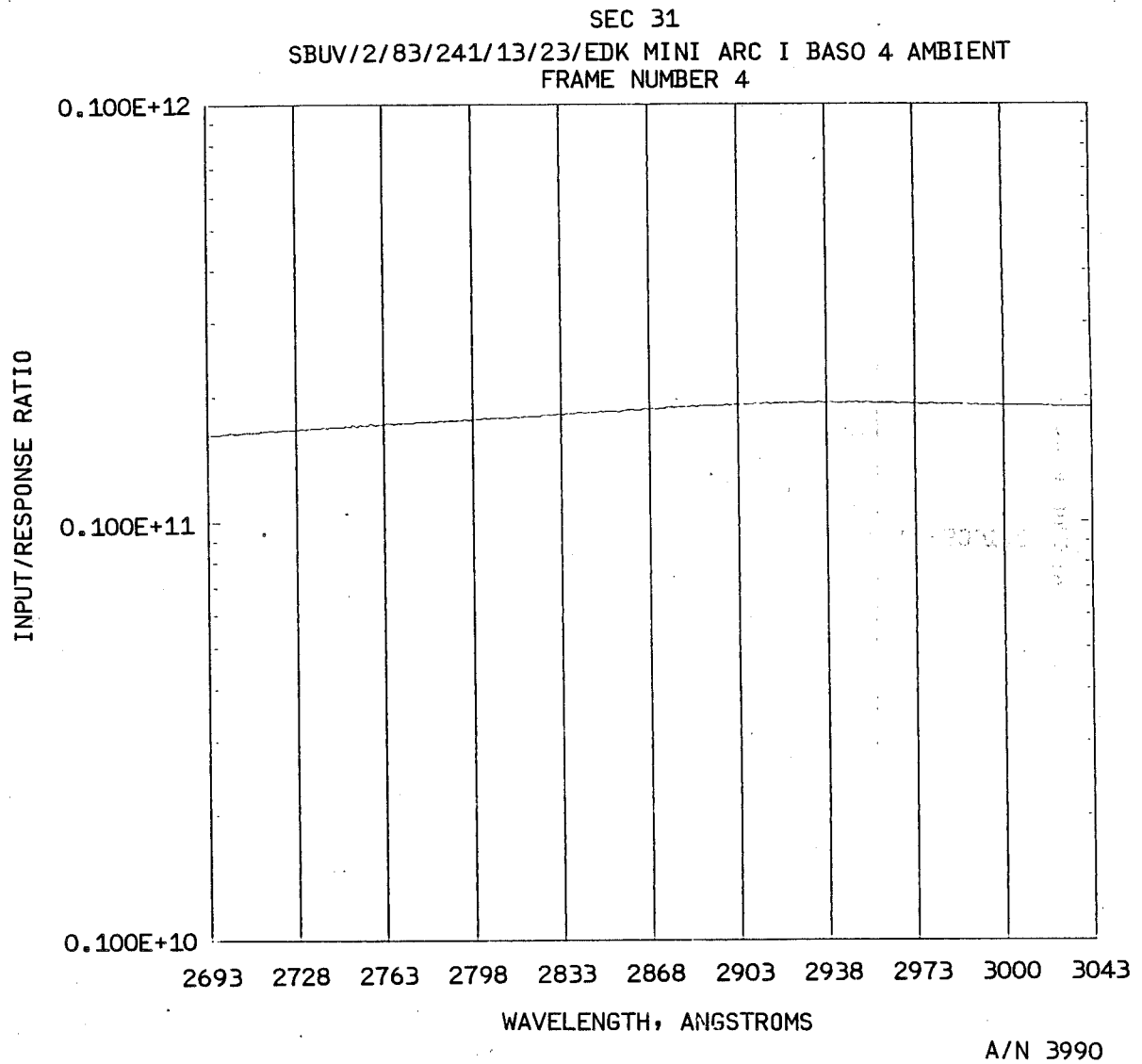


Figure 4-47 (cont.)



B6802-78

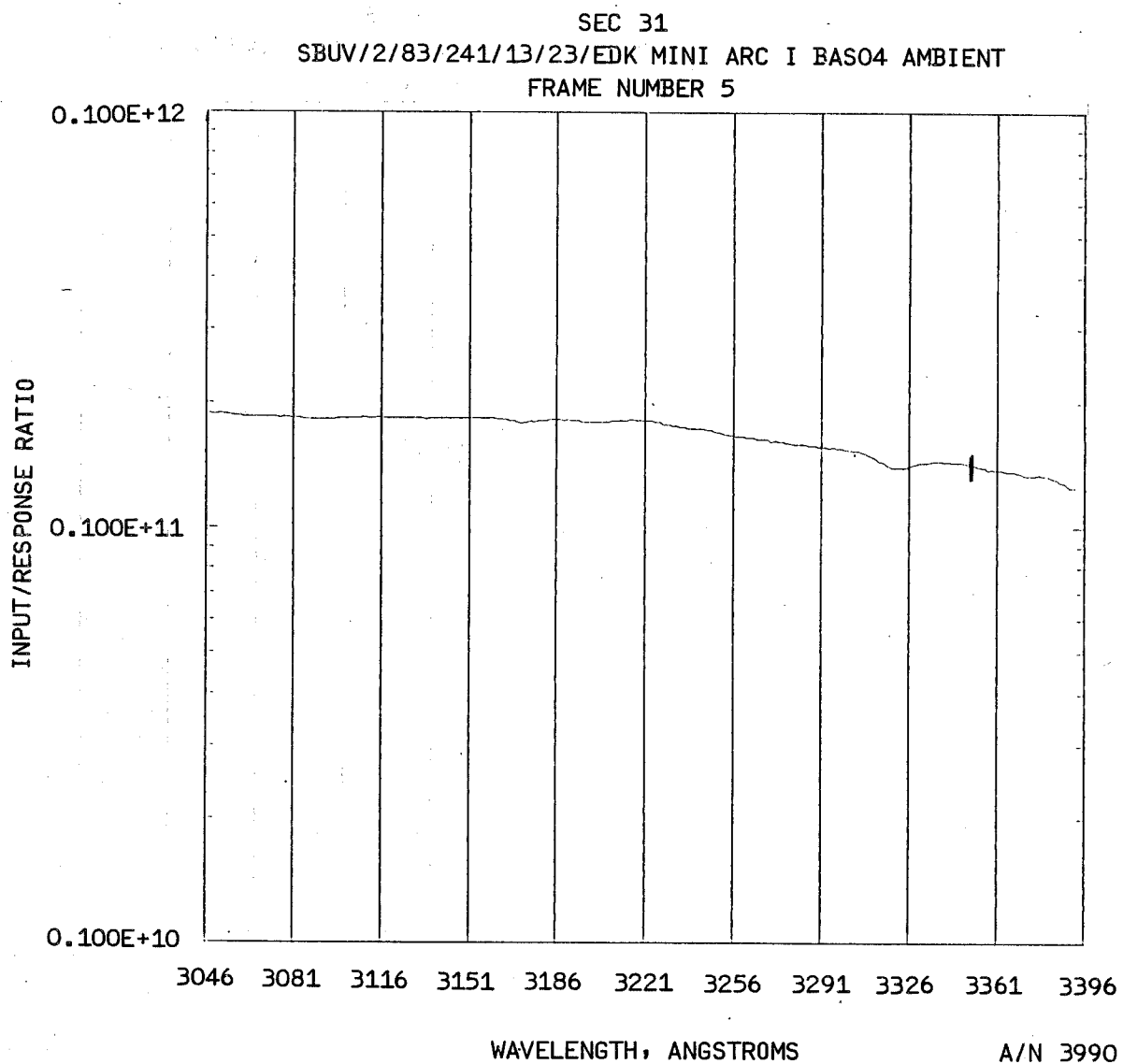


Figure 4-47 (cont.)



B6802-78

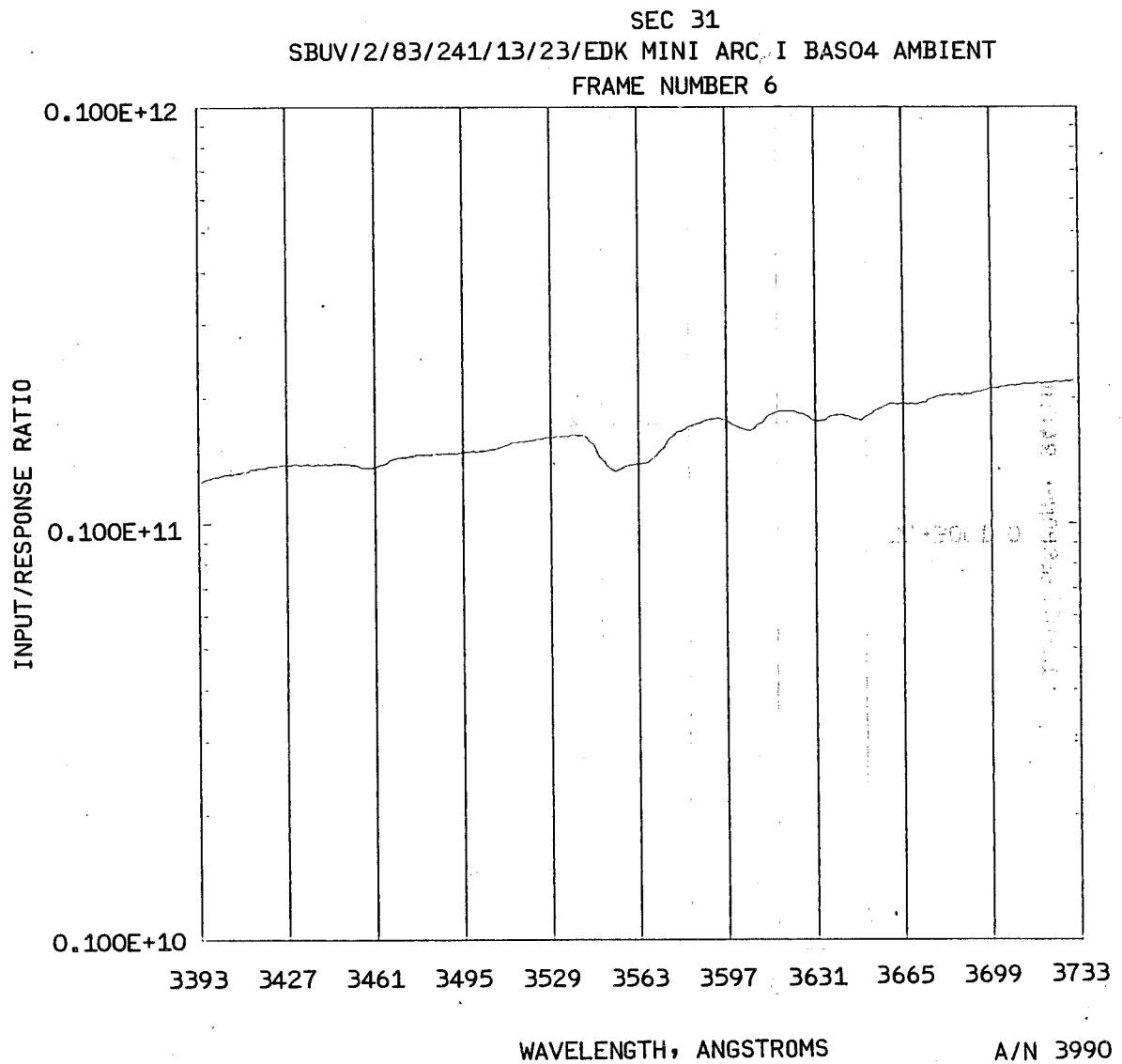


Figure 4-47 (cont.)



B6802-78

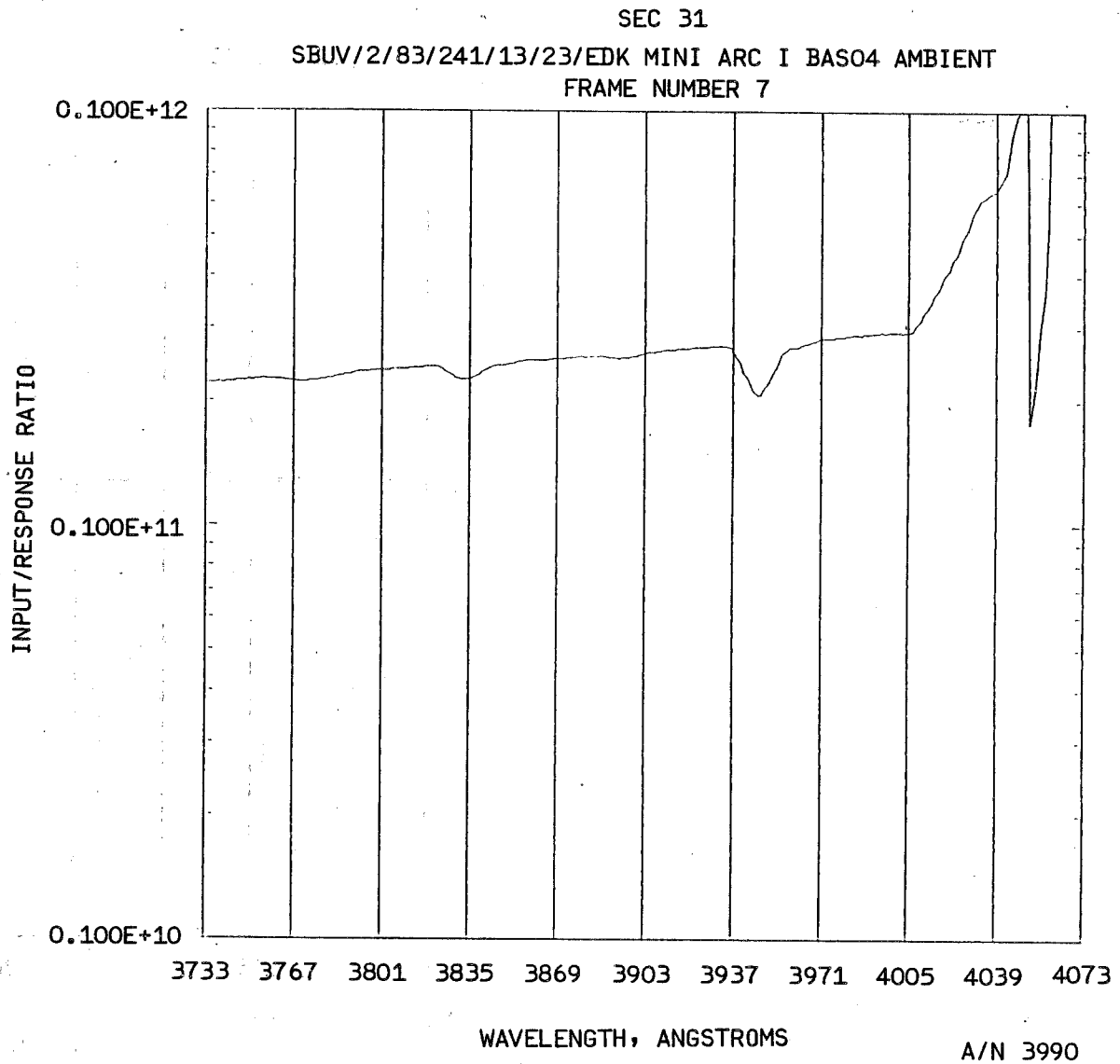


Figure 4-47 (cont.)



B6802-78

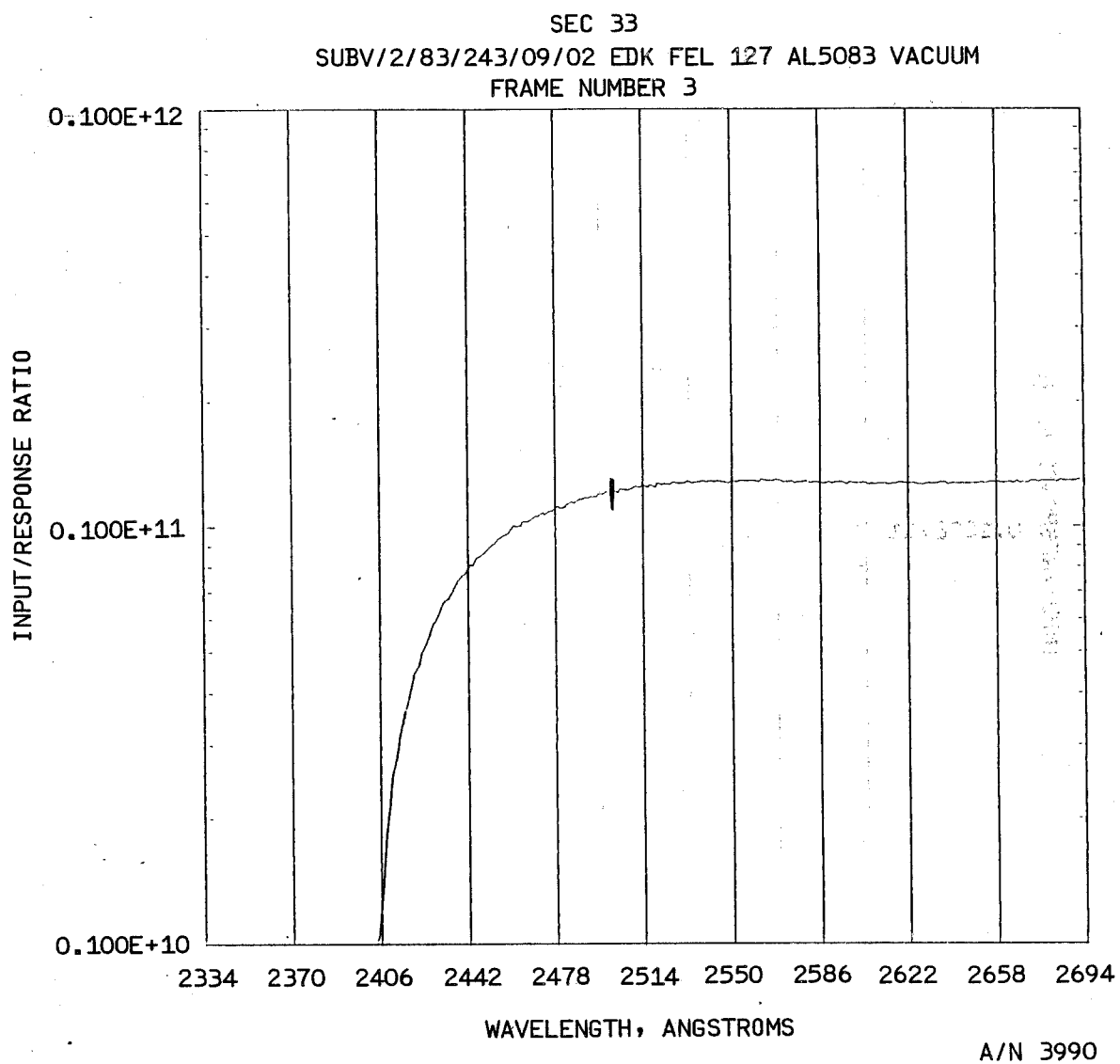


Figure 4-48



B6802-78

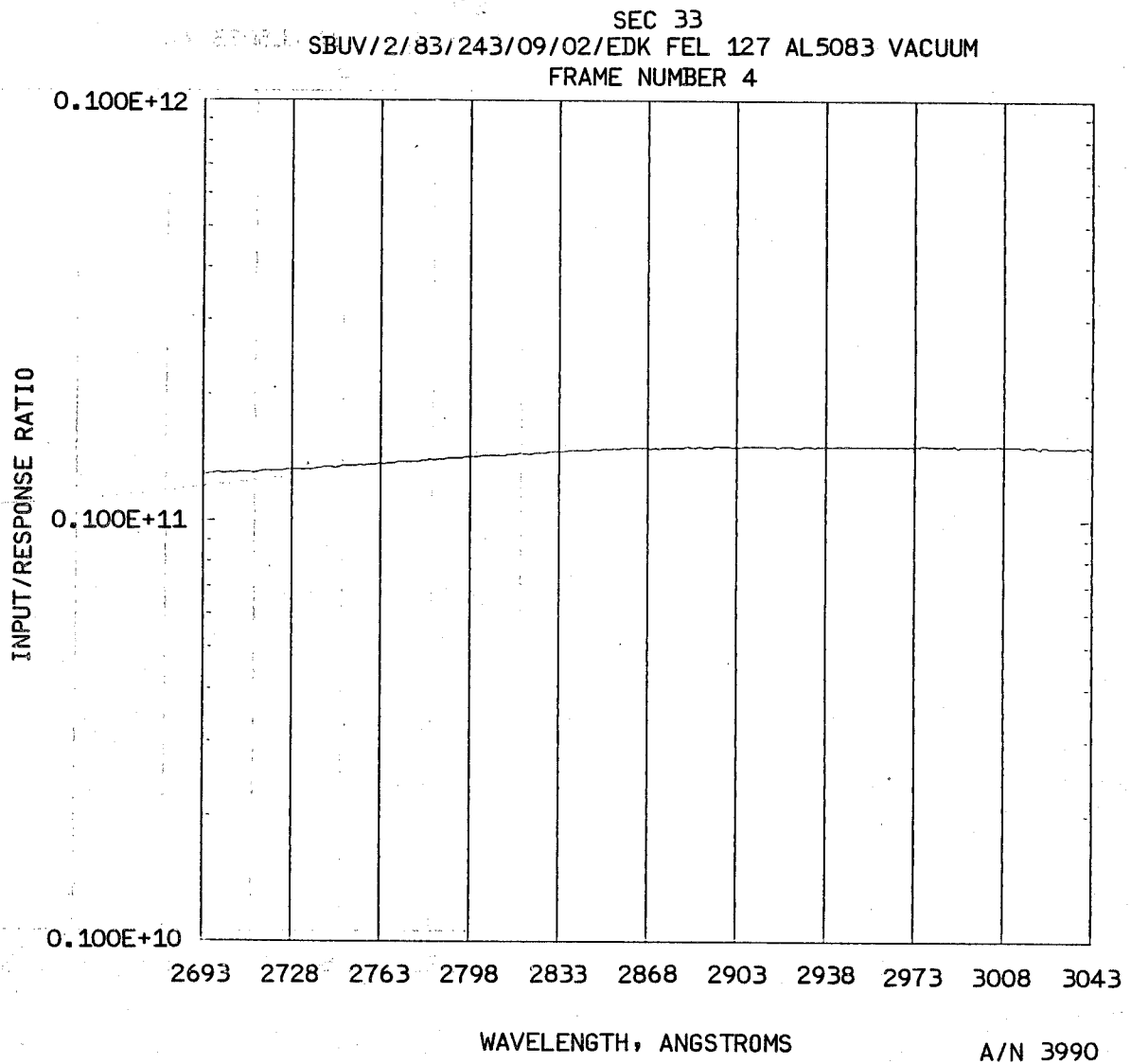


Figure 4-48 (cont.)



B6802-78

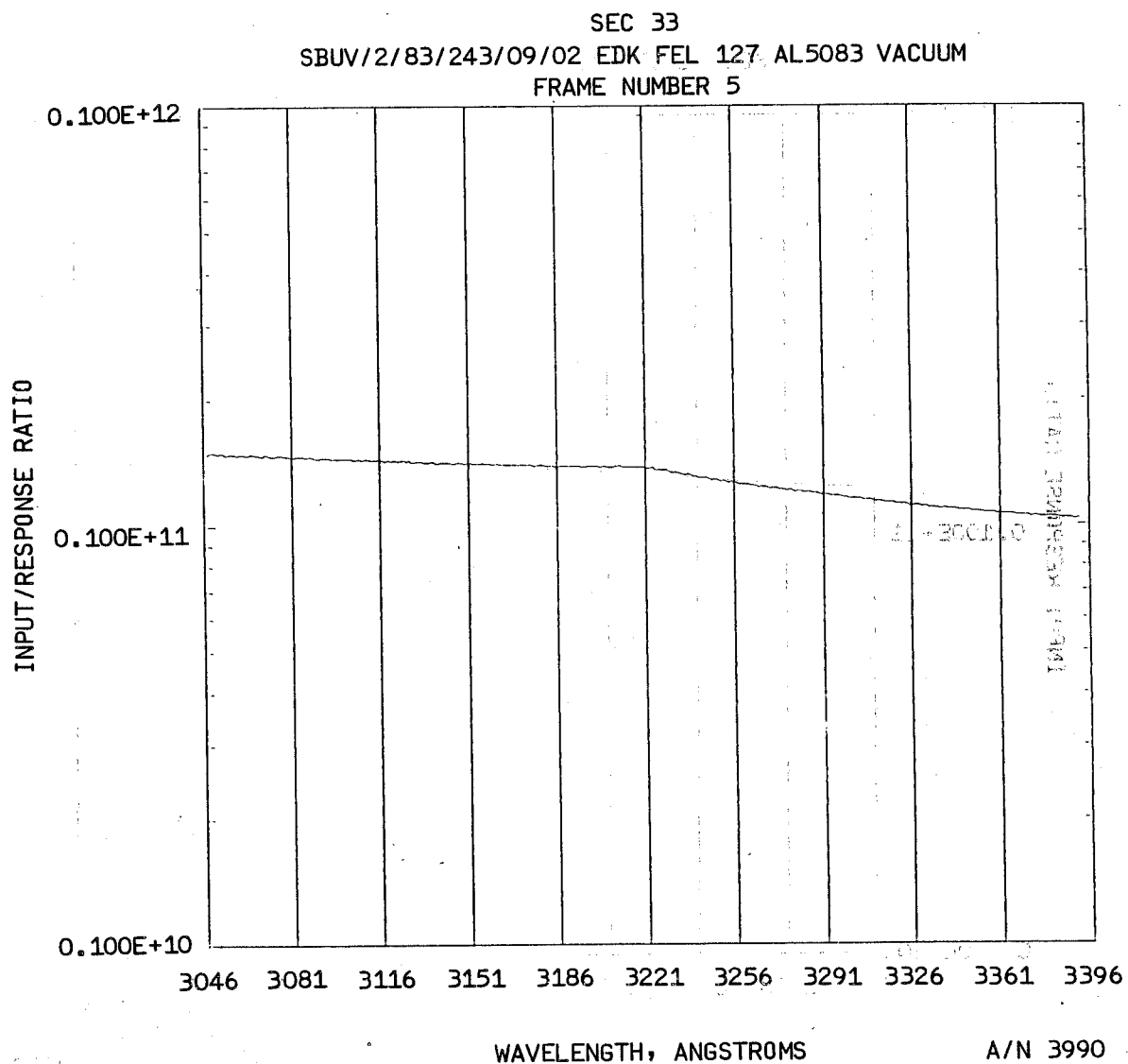


Figure 4-48 (cont.)

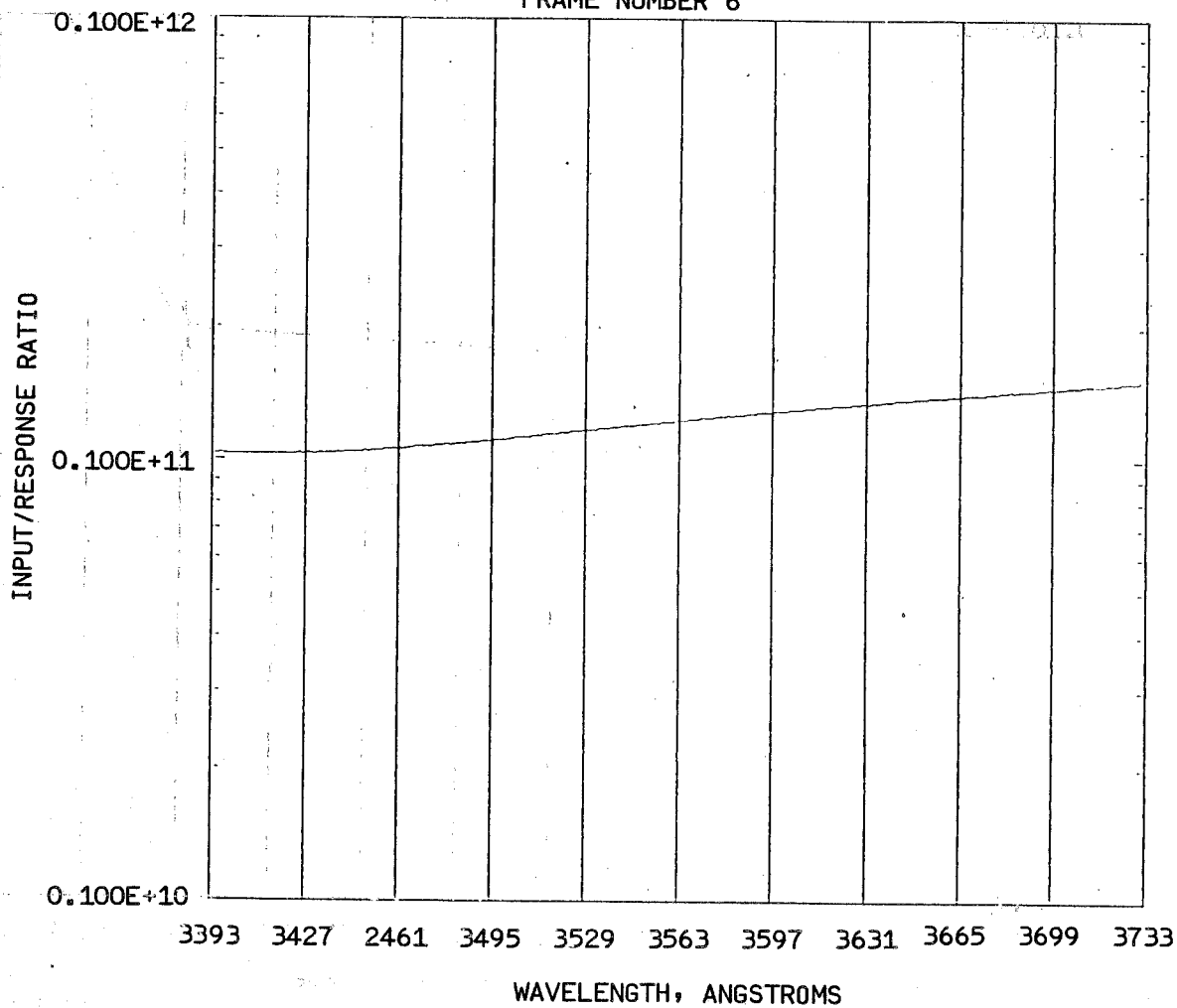


B6802-78

SEC 33

NO. 1045 89011A SBUV/2/83/243/09/02/EDK FEL 127 AL5083 VACUUM

FRAME NUMBER 6



A/N 3990

Figure 4-48 (cont.)



B6802-78

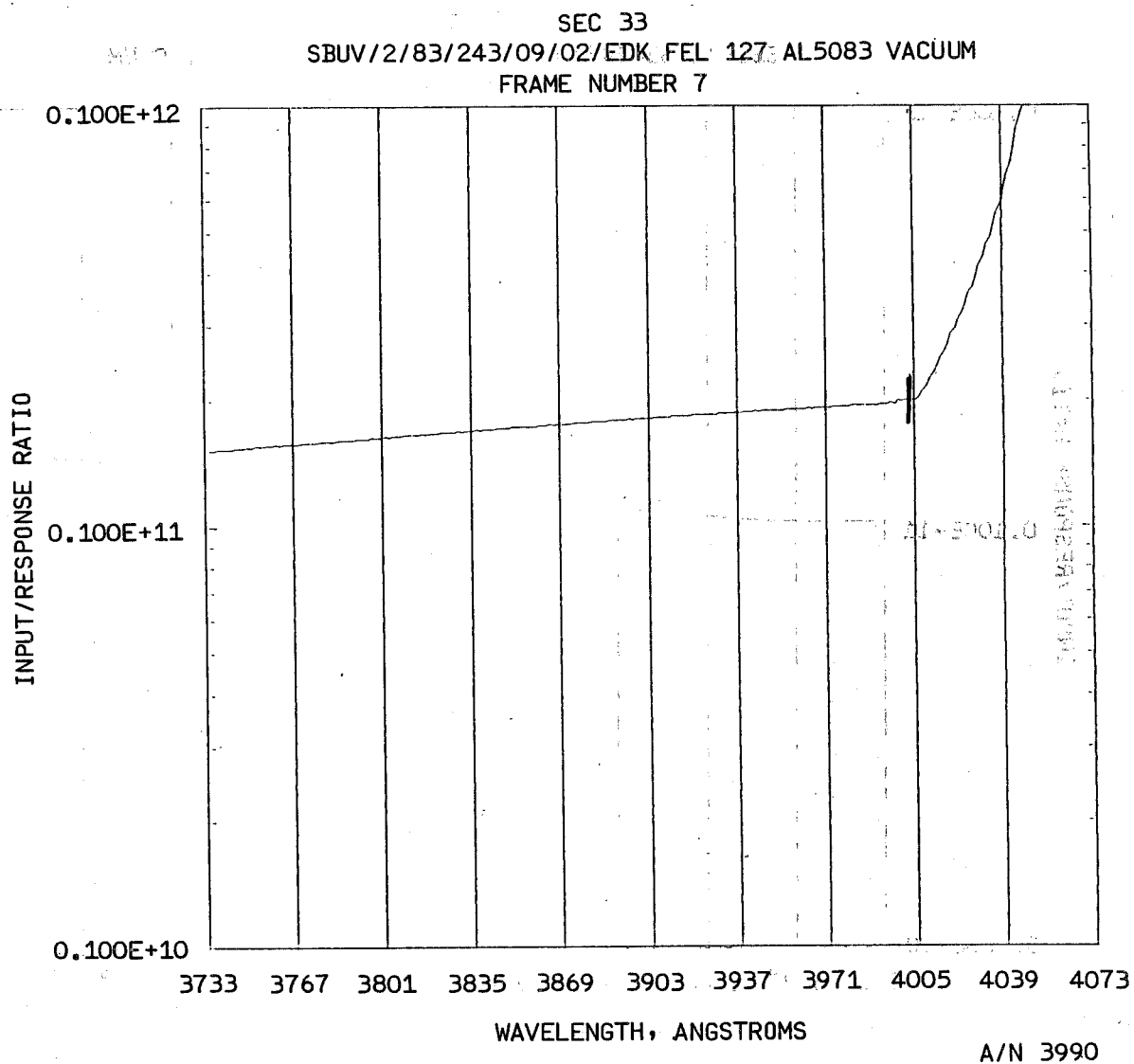


Figure 4-48 (cont.)



B6802-78

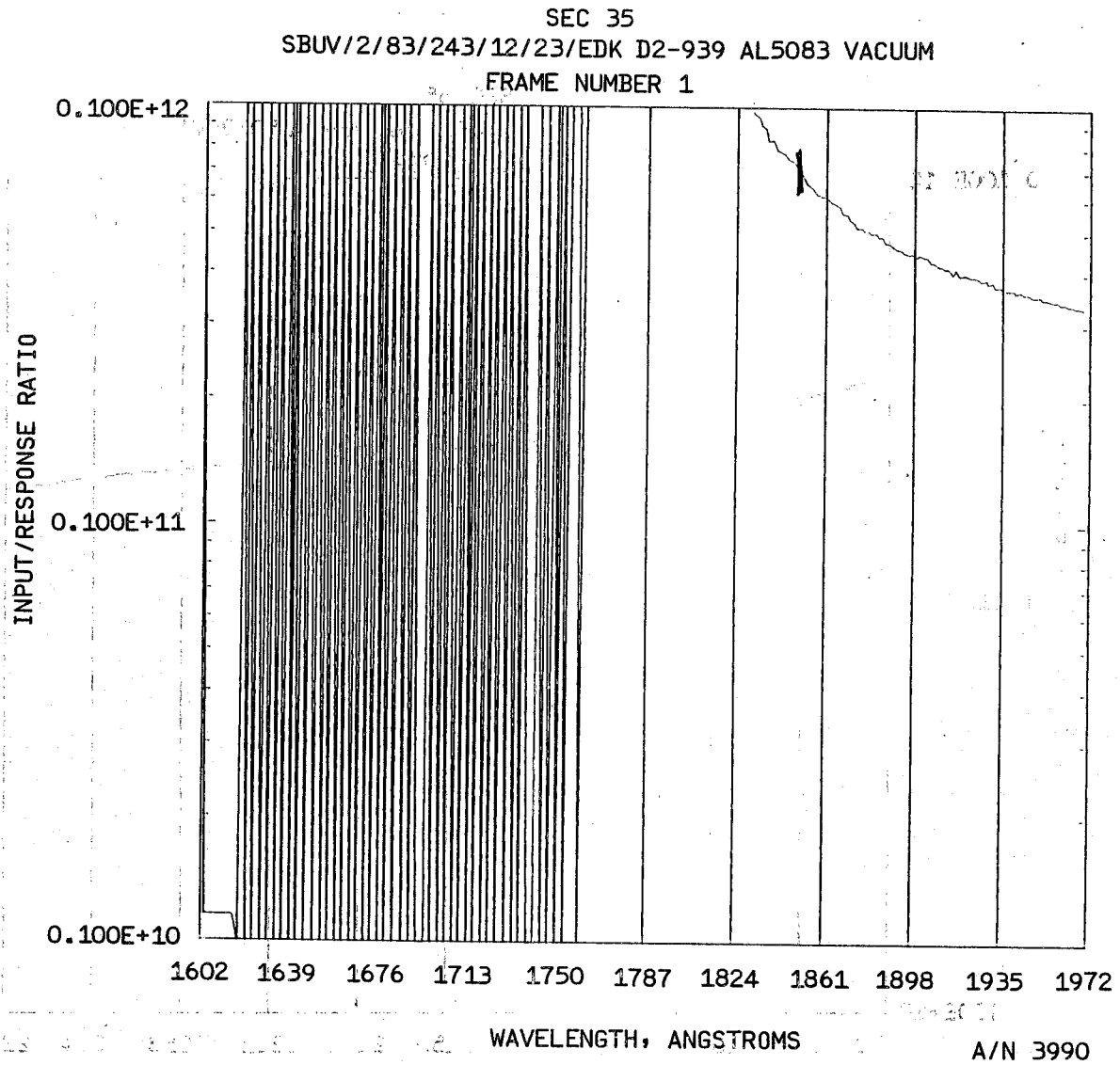


Figure 4-49



B6802-78

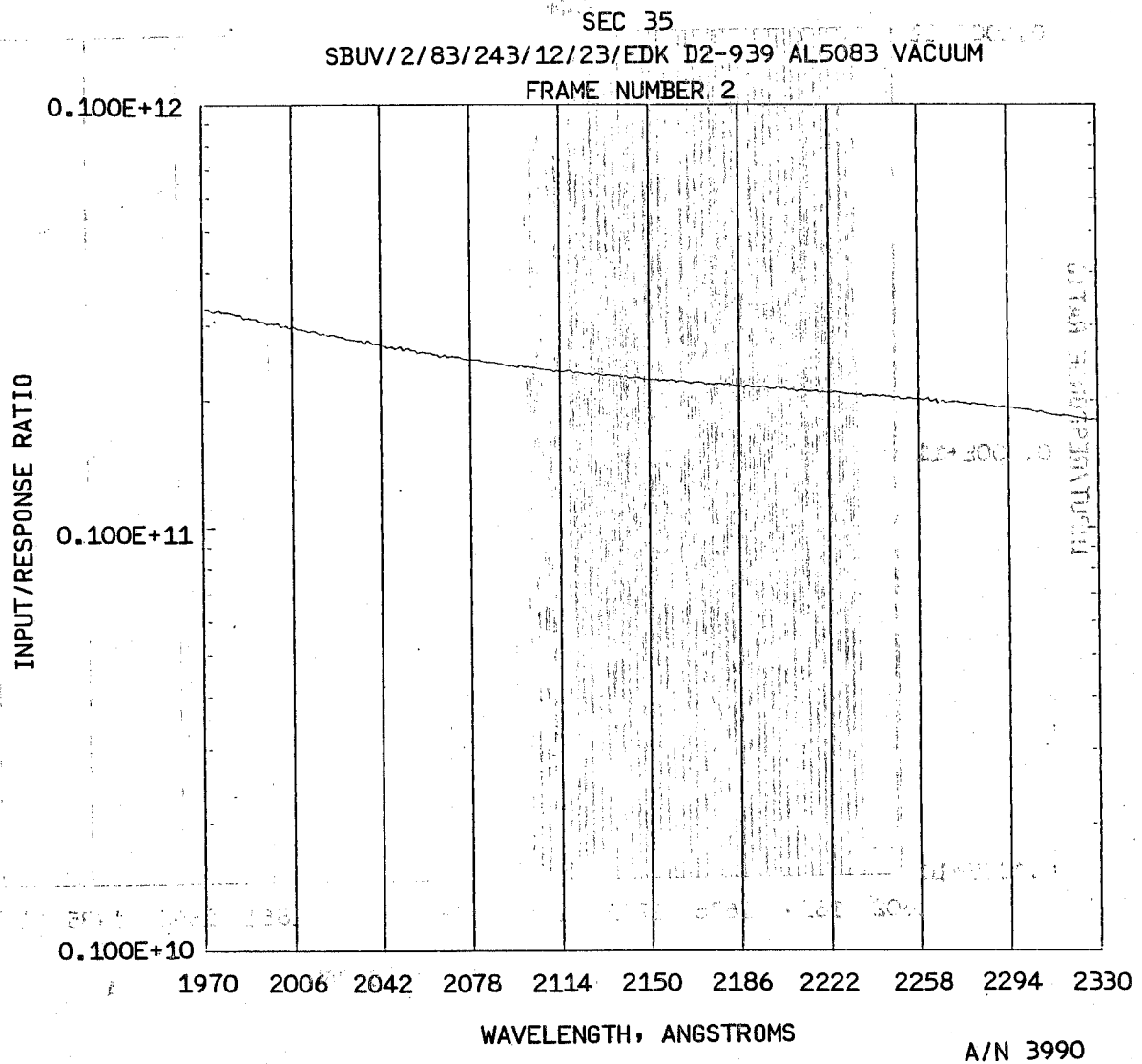


Figure 4-49 (cont.)



B6802-78

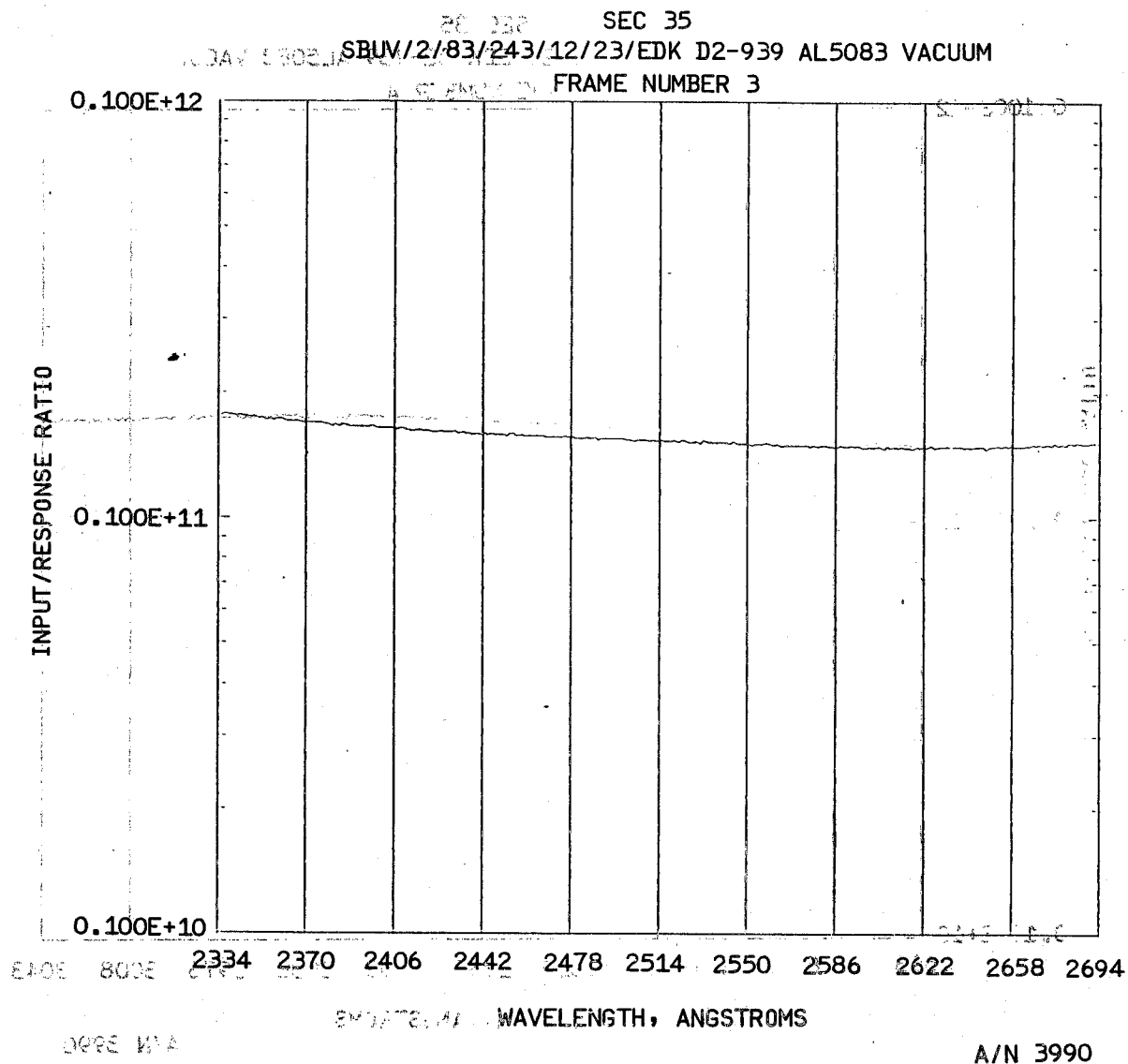


Figure 4-49 (cont.)



B6802-78

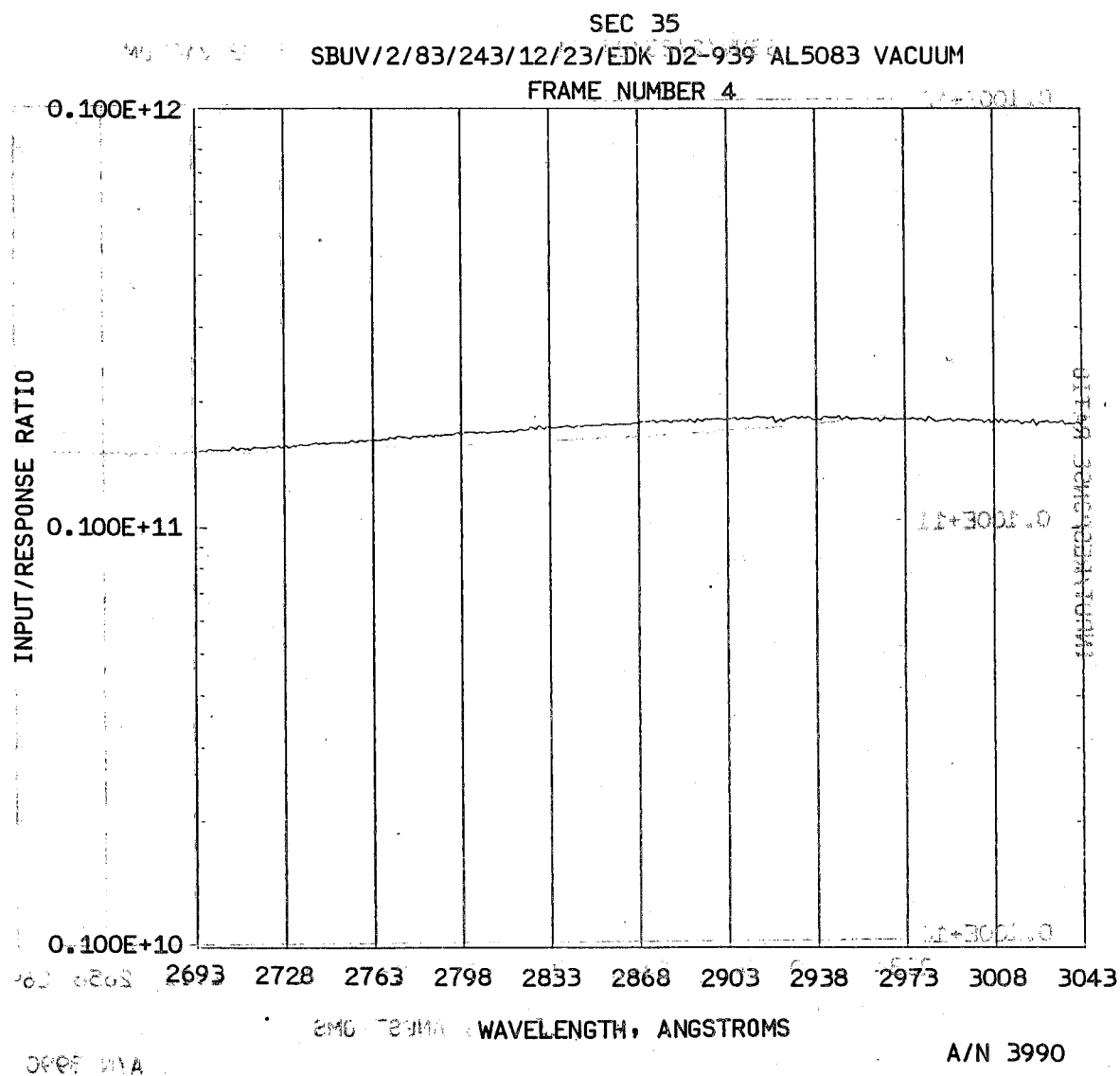


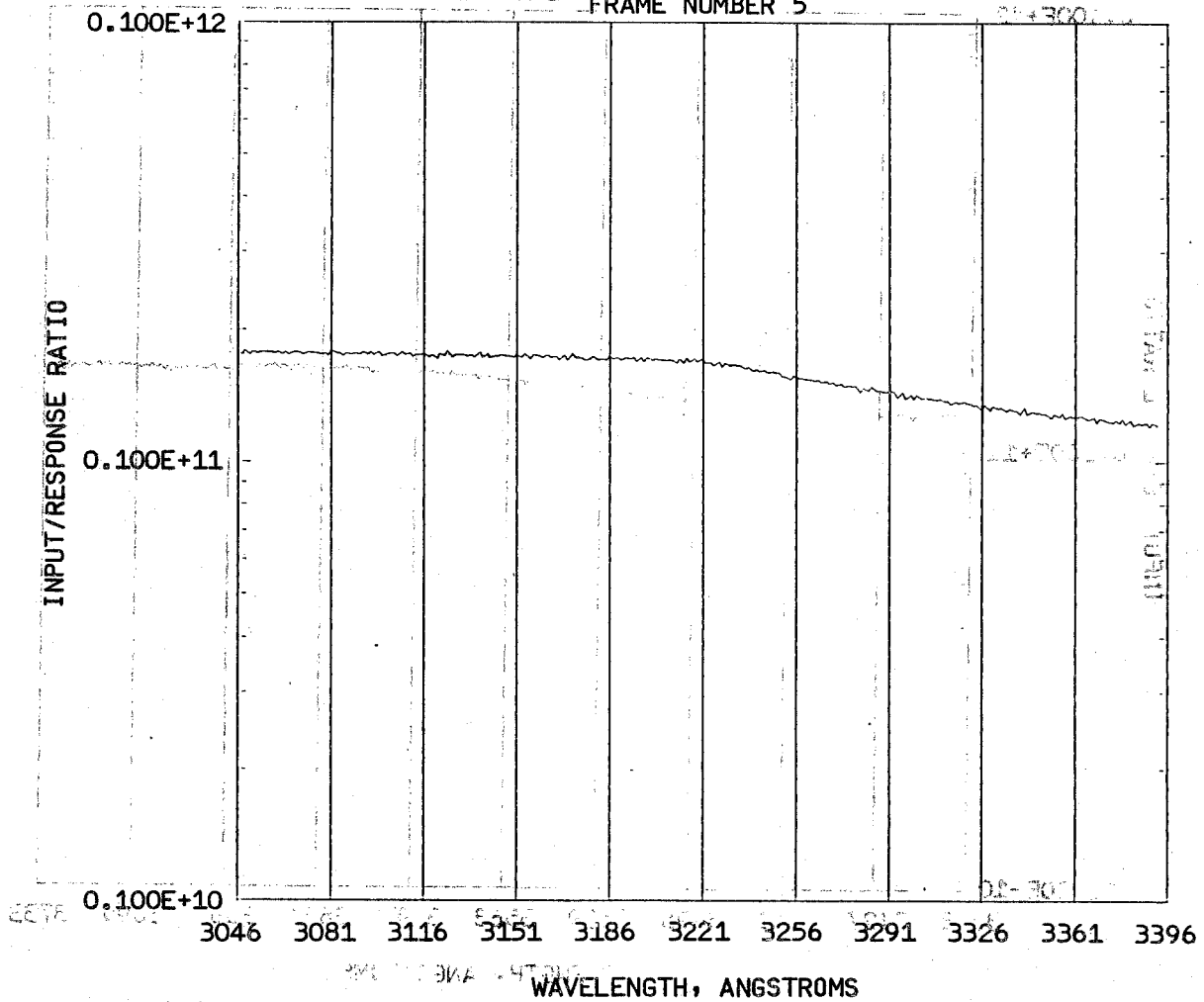
Figure 4-49 (cont.)



SEC 35

SBUV/2783/243/12/23 EDK D2-939 AL5083 VACUUM

FRAME NUMBER 5



A/N 3990

Figure 4-49 (cont.)



B6802-78

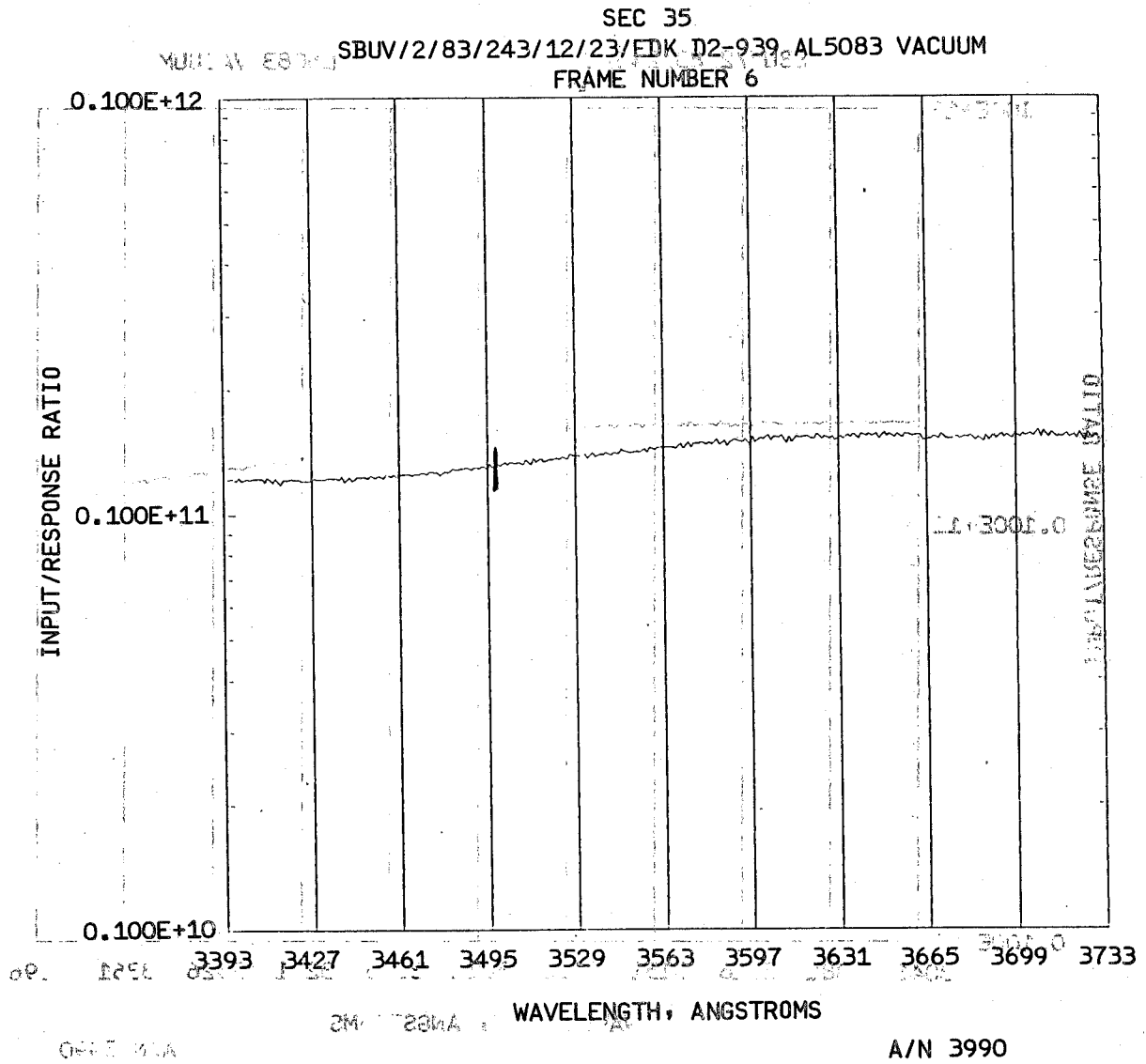


Figure 4-49 (cont.)



B6802-78

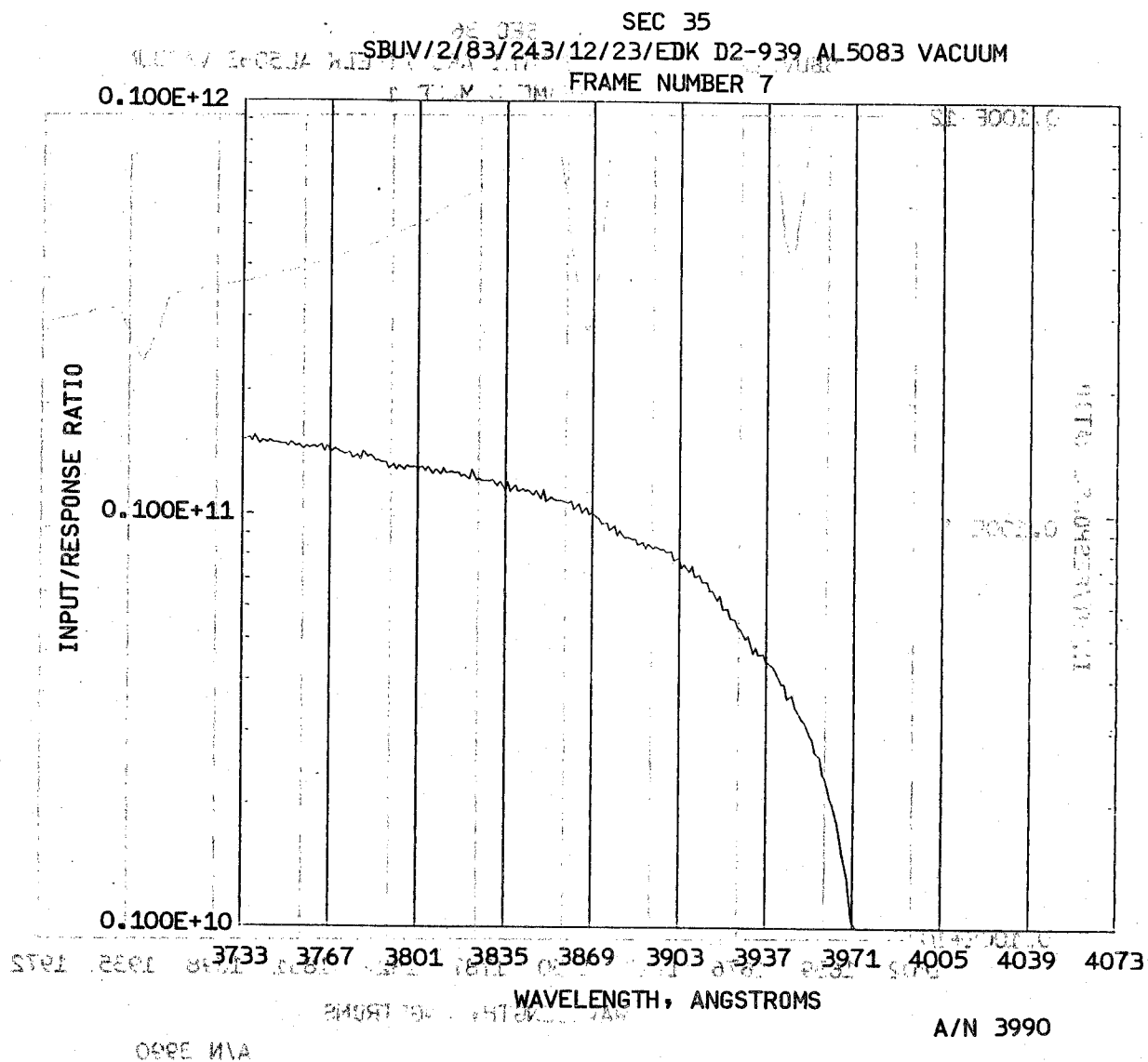


Figure 4-49 (cont.)



B6802-73

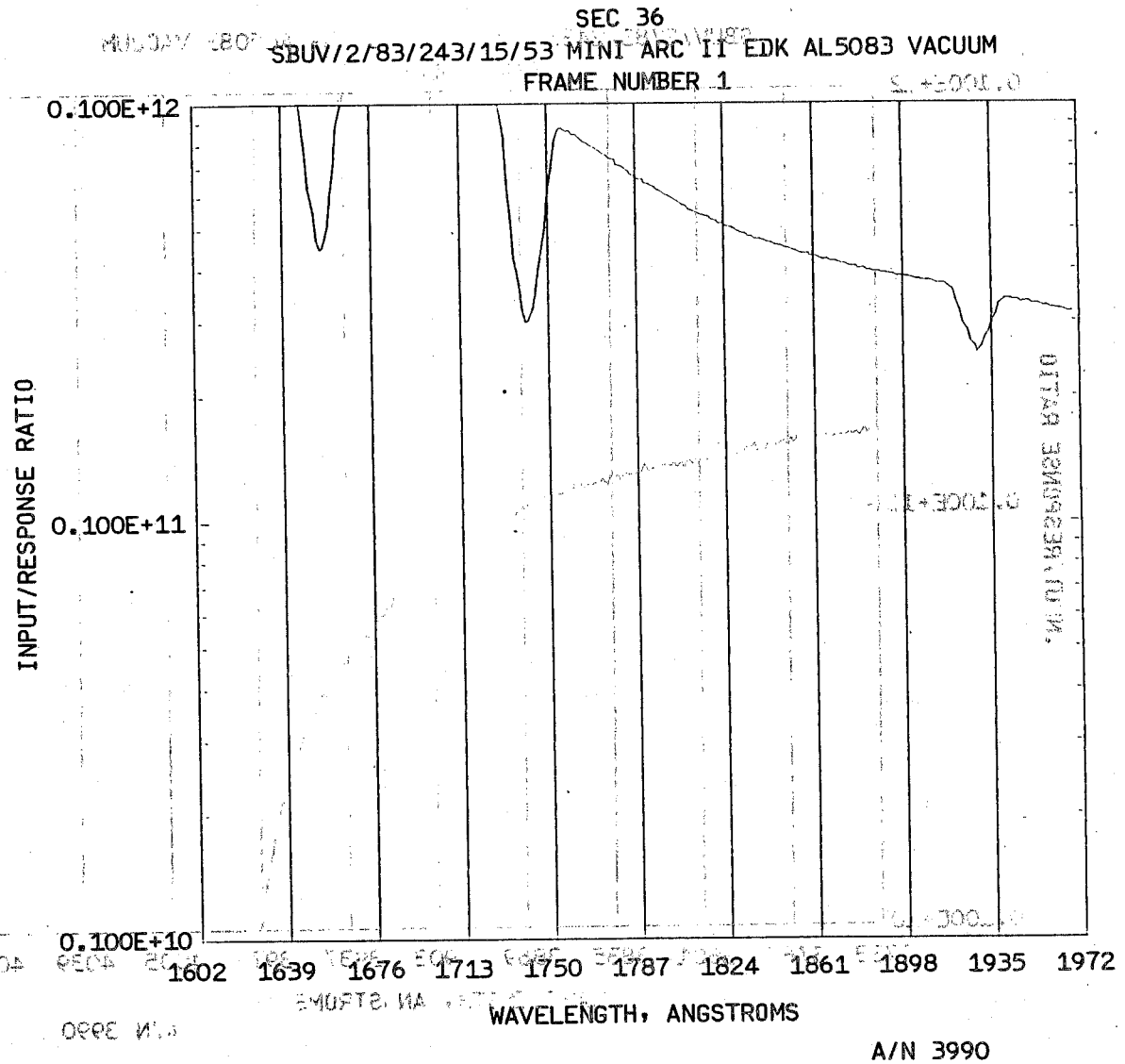


Figure 4-50



B6802-78

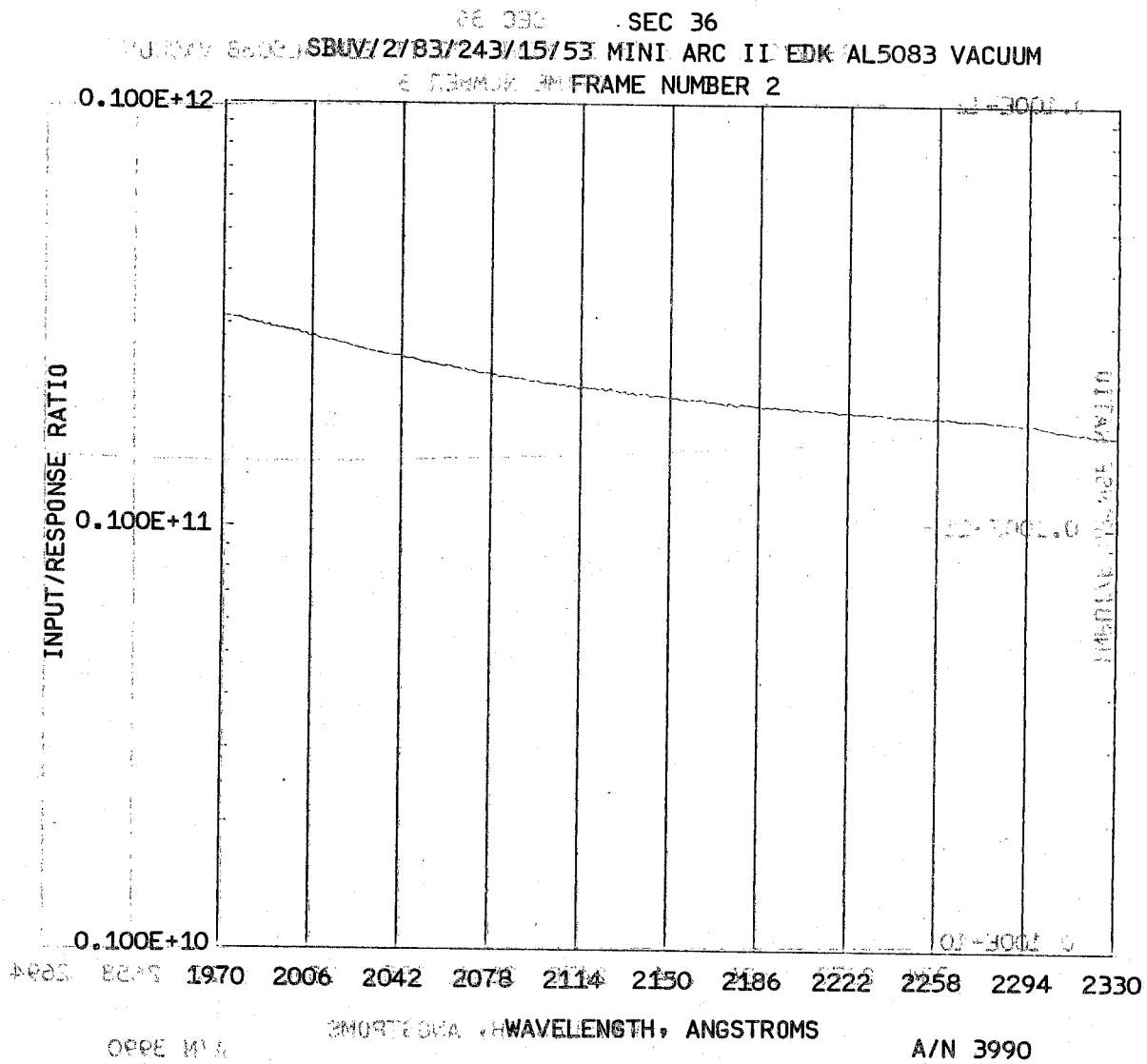


Figure 4-50 (cont.)

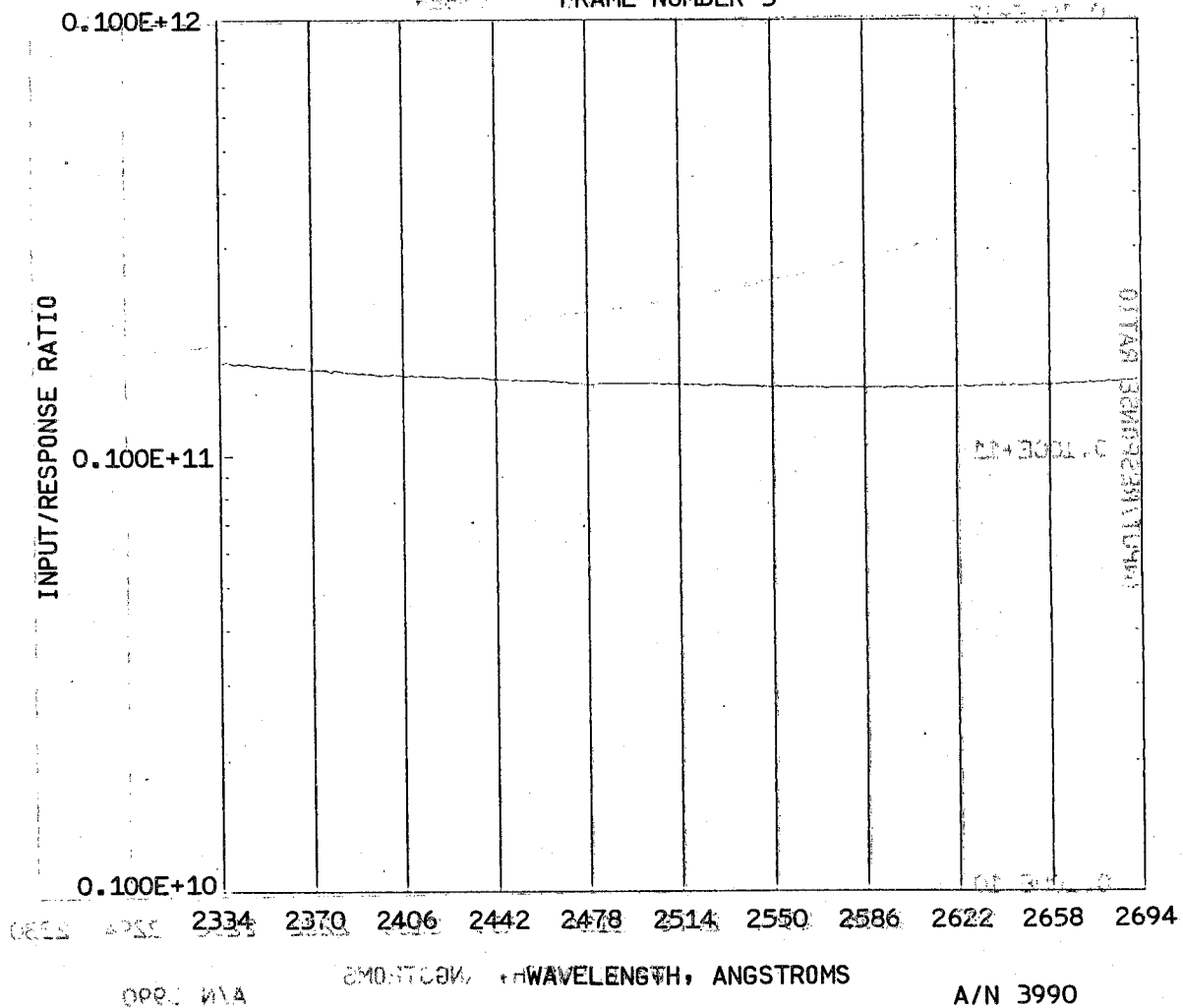


B6802-78

SEC 36

MULCA 1802 SBUY/2/83/243/15/53 MINI-ARC 11 EDK AL5083 VACUUM

FRAME NUMBER 3



(. Figure 4-50 (cont.)

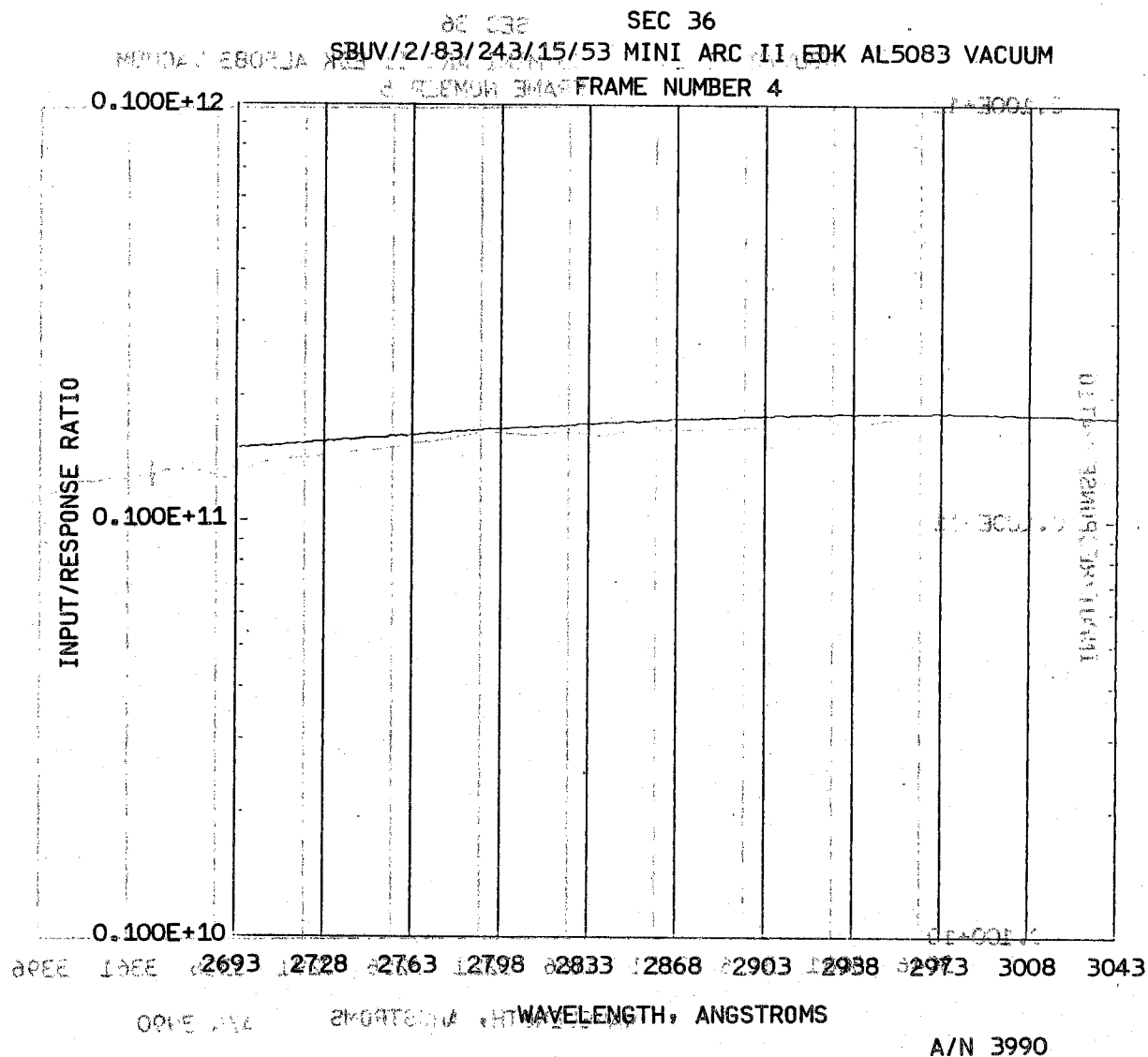


Figure 4-50 (cont.)



382

B6802-78

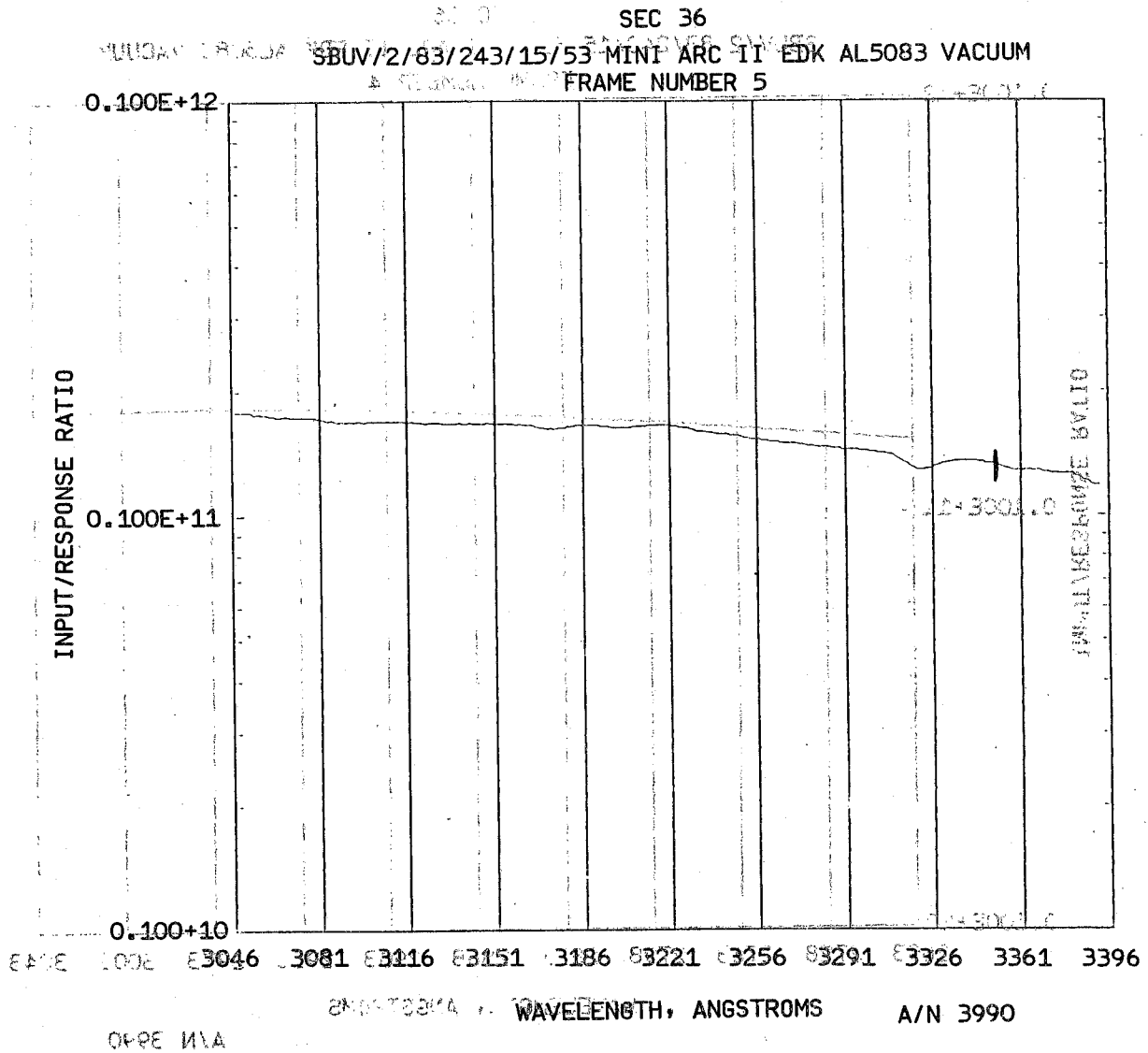


Figure 4-50 (cont.)



05 036

SEC 36

SBUV/2483/243/15/53 MINI ARC II EDK AL5083 VACUUM

0.100E+12

FRAME NUMBER 6

INPUT/RESPONSE RATIO

0.100E+11

0.100E+10

3393 3427 3461 3495 3529 3563 3597 3631 3665 3699 3733

WAVELENGTH, ANGSTROMS

A/N 3990

0000 1111

Figure 4-50 (cont.)

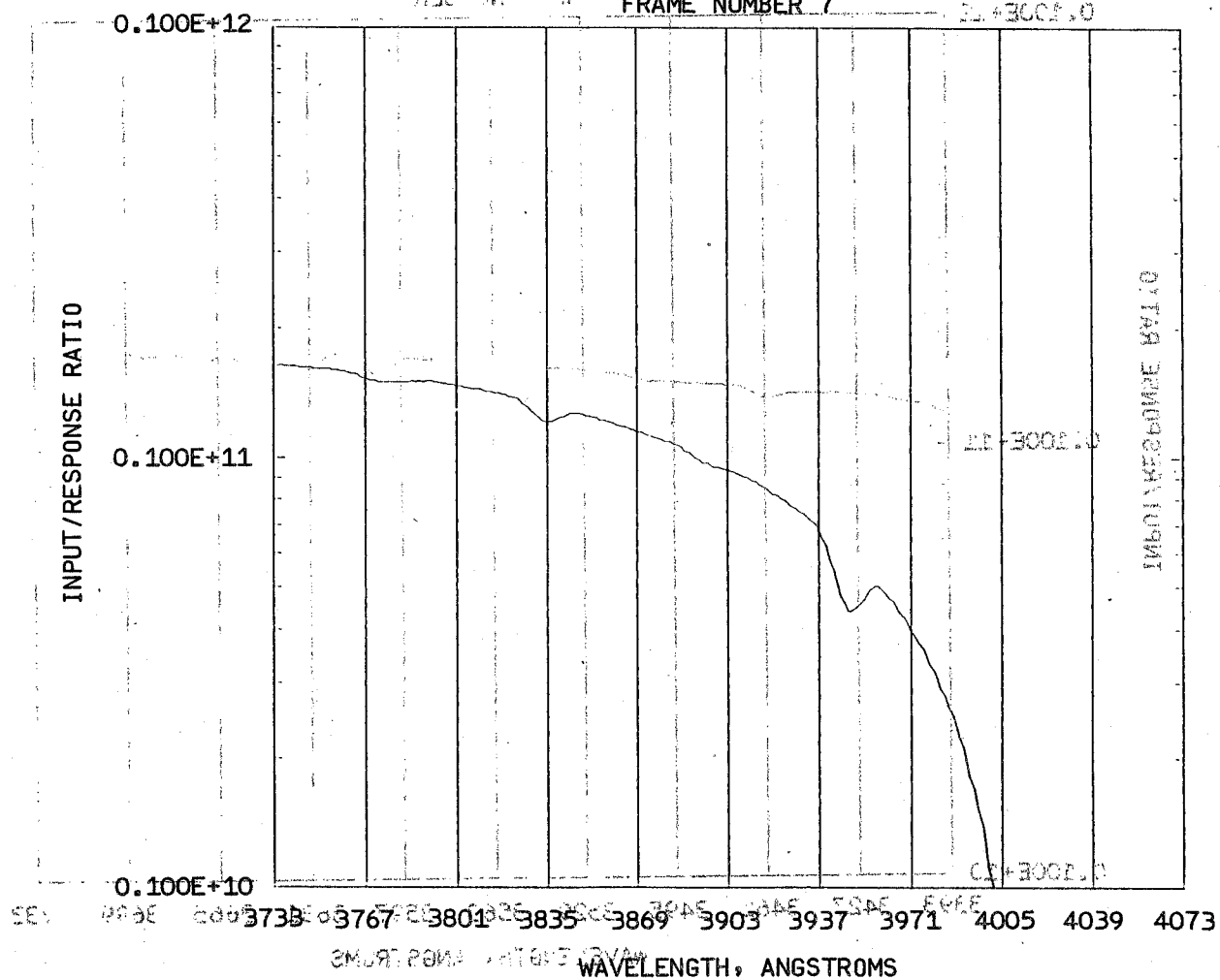


B6802-78

SEC 36

MURDAY 0802LX POSBUV/2783/243/15/53 MINI-ARG II EDK AL5083 VACUUM

832 4. 4F- FRAME NUMBER 7



A/N 3990

Figure 4-50 (cont.)



SECRET

RECEIVED JAN 11 1964

1000000	1000000	1000000	1000000
1000000	1000000	1000000	1000000
1000000	1000000	1000000	1000000
1000000	1000000	1000000	1000000
1000000	1000000	1000000	1000000

RECEIVED JAN 11 1964

RECEIVED JAN 11 1964

RECEIVED JAN 11 1964

RECEIVED JAN 11 1964

1000000	1000000	1000000	1000000
1000000	1000000	1000000	1000000
1000000	1000000	1000000	1000000
1000000	1000000	1000000	1000000
1000000	1000000	1000000	1000000

RECEIVED JAN 11 1964



Calibration errata

1. For day 217, lamp FEL 127, Mirror A, Old Al diffuser

<u>λ</u>	<u>Correct</u> <u>L_{dk}</u>	Incorrect	<u>Correction</u> <u>Factor</u>
		<u>L_{dk}</u> <u>used</u>	
312.5	0.219 E0	0.305 E0	0.718
379.0	0.129 E0	0.219 E0	0.589

This error causes the spline interpolation to go wild in the vicinity of these wavelengths in the sweep plots. The discrete mode print-outs are in error but the discrete mode plots are corrected.

2. The reflectance of the collimating mirrors was measured at an angle of incidence of 7.5° rather than 15° . The discrepancy turns out to be in the 1% range, within the error range of the measurement itself.

3. Calculations of E_{dk} & L_{dk} , Day 240, 244, Source D₂ 939.

Incorrect value $L_{dk} = .649E-2$ at 339nm was used. Correct value, $L_{dk} = .687E-2$ at 339 nm. This skewed the spline interpolation used in calculating nearby L_{dk} . Corrected values are:

<u>λ</u>	<u>L_{dk}</u>	DISCAL LC28	GDISCAL LC29
		240/14/22 <u>L_{dk}/C_p</u>	240/17/37 <u>L_{dk}/C_p</u>
312.5	.01000	.1290E10	.1290E10
317.5	.00945	.1297E10	.1295E10
331.2	.00774	.1042E10	.1040E10
339.8	.00687	.9219E9	.9221E9

DISCAL and GDISCAL plots have been corrected, computer printouts and sweep plots are incorrect.

